ANTI-PEPTIDE ANTIBODIES AS PROBES OF THE STRUCTURE, FUNCTION AND DISTRIBUTION OF CA^{2+} CHANNELS

By

KIERAN DAVID BRICKLEY B.Sc, M.Sc

A thesis submitted in fulfilment of the requirements
for the degree of
Doctor of Philosophy
in the
University of London

October 1993
The Royal Free Hospital School of Medicine
Rowland Hill Street
London NW3 2PF

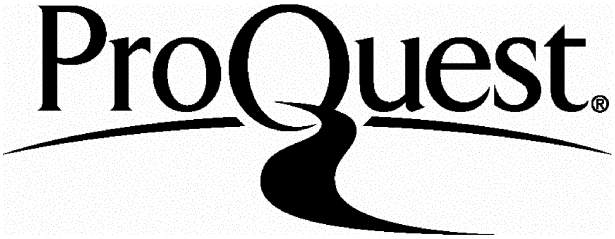

ABSTRACT

ANTI-PEPTIDE ANTIBODIES AS PROBES OF THE STRUCTURE, FUNCTION AND DISTRIBUTION OF CA^{2+} CHANNELS

BY

KIERAN DAVID BRICKLEY

Fifteen peptides were synthesized corresponding to sequences in the primary structure of the α_1 subunits of both the class A and class D rat brain, and of the α_1 and α_2 subunits of the rabbit skeletal muscle L-type Ca^{2+} channel. Conjugates of these peptides to various carrier proteins were used to produce polyclonal antibodies in rabbits. Each peptide-specific antibody was affinity purified and used to probe the structure, function and distribution of these channels. Nine of the antibodies identified (four strongly) their intact denatured polypeptide in t-tubules. The rat brain class A-specific antibody reacted strongly with a denatured polypeptide in skeletal muscle t-tubules, while only antibody N, raised against a sequence in α_2, bound to its denatured polypeptide in brain membranes. Eight antibodies bound (four strongly) to the L-type Ca^{2+} channel *in situ.* in rabbit, rat, mouse and human skeletal muscle. One antibody reacted strongly, and three weakly with the corresponding channel *in situ.* in cardiac muscle cryosections from rabbit, rat and pig. Nine of the antibodies recognized (five very clearly) the intact, native, L-type channel purified from rabbit skeletal muscle. None of these antibodies showed any inhibition of binding of nitrendipine to the L-type Ca^{2+} channel in t-tubule membranes.

The reactivity of the antibodies with the intact denatured channel polypeptides was examined in Western blots with rabbit and rat skeletal muscle t-tubules and brain membranes. *In situ.* identification of antibody binding was carried out using fluorescence immunocytochemistry in unfixed cryosections of skeletal muscle from rabbit, rat, mouse and human tissue and of cardiac muscle from rabbit, rat and pig. Antibody interaction with the native channel structure was studied by ELISA with the L-type channel following its purification from rabbit skeletal muscle. Inhibition of binding of either nitrendipine or D888 to the channel by the antibodies was assayed using radiolabelled ligand and t-tubule membranes which had been incubated with either test or control antibody.

These antibodies have been used to confirm the predicted high sequence homology between rabbit skeletal muscle L-type Ca^{2+} channel α subunits and those found in rabbit, rat, human and mouse skeletal muscle, and in rat and porcine cardiac muscle, whose sequences are unknown.The IS4 domain, and peptides located on predicted intracellular loops and in the C-terminal region appeared to be exposed in the native α_1 subunit. However, binding of dihydropyridines or phenylalkylamines to α_1 was not affected by antibodies bound to any of the exposed α_1 domains. Some ß-

sheet structure was revealed for a synthetic peptide, corresponding to the C-terminal α_1(1390-1437) domain, in aqueous buffer using FTIR spectroscopic studies. L-type Ca^{2+} α polypeptides were located primarily to the transverse-tubule system of both skeletal and cardiac muscle. The relative abundance of the channel α_2 subunit in rat brain membranes, was found to be not more than 10-30-fold less than that found in rat skeletal muscle transverse tubule membranes.

The observed exposure of the IS4 domain in native α_1 supports the model of the pore structure of voltage-gated ion channels, having both S2 and S4 as pore forming sequences, with the channel lined by the S5-S6 loop. Part of the loop between domain II and III in skeletal muscle α_1, which has a role in excitation-contraction coupling is possibly inaccessible to antibody *in situ.* but becomes exposed during channel purification. A polypeptide, possibly a neuronal-type channel subunit was identified in t-tubules by the rat brain class A-specific antibody.

ACKNOWLEDGEMENTS

I would like to thank my supervisor during the course of this work, Dr. Steve Baldwin for his guidance, assistance, encouragement and friendship. I also express my gratitude to Dr. Robert Norman (University of Leicester) for his advice during the project and for invaluable assistance with particular parts of the study including immunoblotting, membrane and channel purification and ligand binding studies. The assistance of Mr. Robert Leach (University of Leicester) and Miss Mary McKay (University of Leicester) with the above techniques is also gratefully acknowledged. Additionally, useful advice and discussion was forthcoming from Professor Dennis Wray and Dr. Gary Wilson (University of Leeds) at early stages in the project. Mass Spectrometry was kindly performed on the peptides by Dr. David Carter (School of Pharmacy) and Dr. Darryl Pappin (ICRF).

My thanks go to present and former members of the Departments of Biochemistry, Protein and Molecular Biology and Pharmacology at the Royal Free Hospital School of Medicine, particularly Dr Susan Brown, Dr. Nicholas Berrow, Dr. Anthony Davies. Mr. Bala Ramesh and Mrs. Jocelyn Baldwin for their help in establishing various techniques and to Mr. Richard Preston for preparing a number of diagrams for this manuscript. The competence in caring for the immunized rabbits, of the staff of the Comparative Biology Unit was invaluable. Finally I also wish to express my thanks to my wife Karen and my sister Carmel for their understanding and reliability.

I acknowledge the financial support of the Royal Free Hospital School of Medicine.

CONTENTS Page

LIST OF FIGURES

LIST OF TABLES

LIST OF ABBREVIATIONS

aa	amino acid
AEC	3-amino-9-ethyl-carbazole
BCG	Bacillus Calmette-Guerin
BSA	bovine serum albumin
BTA	benzothiazepine
C-terminal	carboxy-terminal
CaM	calmodulin
cAMP	cyclic adenosine monophosphate
CD	Circular Dichroism
cDNA	complementary DNA
ω-CgTx	ω-conotoxin GVIA
CHAPS	3-[(3-cholamidopropyl)-dimethylammonio]-1-propane-sulphonate
CTX	charybdotoxin
DCM	dichloromethane
DEAE	deoxyethylaminoethyl
dH_2O	distilled water
DHOBT	3,4-Dihydro-3-hydroxyl-4-oxo-1,2,3-benzotriazine
DHP	1,4 dihydropyridine
DMF	dimethylformamide
DPM	disintegrations per minute
DRG	dorsal root ganglion
DTNB	5,5'-dithio-bis(2-nitrobenzoic acid)
DTT	dithiothreitol
E-C coupling	excitation-contraction coupling
E-S coupling	excitation-secretion coupling
ECL	enhanced chemiluminescence
EDT	1,2-ethanedithiol

EGTA	ethylene glycol-bis(ß-aminoethyl ether)
E_{K+}	extracellular K^+ concentration
ELISA	enzyme-linked immunosorbent assay
EM	electron microscopy
E_{Na+}	extracellular Na^+ concentration
Fmoc	N^{α}-fluorenylmethoxycarbonyl-polyamide
FTIR	Fourier Transform Infrared
FTX	Funnel web spider toxin
GABA	γ-amino butyric acid
HBS	HEPES buffered saline
HEPES	N-(2-hydroxyethyl)piperazine-N'-(2-ethanesulphonic acid)
HOBT	1-hydroxybenzotriazole
IAA	iodoacetamide
IgG	immunoglobulin G
I_{K+}	intracellular K^+ concentration
I_{Na+}	intracellular Na^+ concentration
KLH	Keyhole limpet haemocyanin
MAb	monoclonal antibody
MBS	maleimidobenzoyl-*N*-hydroxysuccinimide ester
MDG	skeletal muscle dysgenic
MOPS	3-(N-Morpholino)propanesulphonic acid
M_r	apparent molecular mass
mRNA	messenger RNA
N-terminal	amino-terminal
NT	neurotransmitter
NTX	noxiustoxin
PAA	phenylalkylamine
PBS	phosphate buffered saline
PBSA-T	PBS (containing 0.02% (w/v) NaN_3 and 0.05% (v/v) Tween-20)

PEG	polyethylene glycol
pfp	pentafluorophenyl
PKA	protein kinase A
PKC	protein kinase C
PMFS	phenylmethylsulfonyl fluoride
PPD	purified protein derivative
α-ScTx	α scorpion toxin
SBTI	Soyabean trypsin inhibitor
SD	Standard deviation
SEM	Standard error of the mean
SDS/PAGE	sodium dodecylsulphate/polyacrylamide gel electrophoresis
Sh	Shaker
SR	sarcoplasmic reticulum
STX	saxitoxin
t-tubule	transverse tubule
TBS	Tris buffered saline
TBTU	2-(1H-Benzotriazole-1-yl)-1,1,3,3-tetramethyluronium tetrafluoroborate
TEA	tetraethylammonium
TEMED	N,N,N',N',tetramethylethylenediamine
TFA	trifluoroacetic acid
TGS	triglycerine sulphate
TID	3-(trifluoromethyl)-3-(m-iodophenyl)diazirine
Tris	tris(hydroxymethyl)aminomethane
TTBS	Tris buffered saline (containing 0.02% (v/v) Tween 20)
TTX	tetrodotoxin
WGA	wheat germ agglutinin
YHS	yellow excitation filter set

CHAPTER 1

1.1 GENERAL INTRODUCTION

1.1.1 Ion channels

Ion channels are proteins that form functional pores in membranes to allow ion flow. These channels, when open, mediate the rapid flux of ions across membranes, along their electrochemical gradients. In this way they control excitation, secretion and motility in eukaryotic cells, where they are widely distributed. These channels have been divided into a large number of classes according to their physiological and pharmacological properties. Different cells use different combinations of these channels for their specialized functions. In individual cells, membrane properties are controlled in a dynamic fashion by the differential expression of ion channels.

Each ion is present at different concentrations on either side of the cell membrane. The resting electrical potential across the membrane is largely determined by the unequal distribution of Na^+ and K^+ ions due to their active transport by the Na^+-K^+ Adenosine triphosphatase (ATPase) and the passive flux of K^+ ions through non-gated ion channels. When a channel allows an ion to cross the membrane, the net flux of that ion, into or out of the cell, is determined by the balance of two forces. One force is due to the concentration gradient of that ion across the membrane, with an ion passing through an open channel to the side of the membrane where the ion concentration is lower. The second force is electrical. A resting cell has a negative potential at the intracellular membrane face, relative to the outside. Thus when an ion channel opens, positive ions enter or negative ions leave the cell when their respective concentration gradients across the membrane are favourable and the selectivity of the channel allows. When these forces result in the net influx of positive ions the potential of the cell interior becomes more positive and the cell membrane is depolarized in this region. Conversely, efflux of positive, or influx of negative charges leads to membrane hyperpolarization.

A major role of ion channels, the generation of electrical signals, is carried out by two classes of channel. At chemical synapses, ligand-gated ion channels open in response to binding of specific ligands e.g. acetylcholine (ACh), glycine or γ-amino butyric acid (GABA). Following ACh receptor opening the ensuing influx of positively charged ions causes depolarization of the postsynaptic area of the cell. This depolarization in turn causes the opening (activation) of voltage-gated Na^+ channels in this area of the membrane initiating an action potential (see Section 1.2.1).

The voltage-gated ion channels have a role in controlling the resting potential of the membranes of both excitable and also many non-excitable cells, where they also mediate rapid changes in membrane ion permeability. Their ion conducting activities are sensitive to the voltage difference across the cell membrane and they are highly selective for a single species of ion. A single channel will conduct in the order of 10^7 ions per second. This ion conductance is controlled on the millisecond time scale by two separable processes, i.e. voltage-dependent activation and inactivation. The former controls the time and voltage-dependence of channel opening in response to changes in membrane potential. The latter controls the rate and extent of ion channel closure during a maintained depolarization. These two processes ensure rapid, transient activation of channels.

1.2 Role of voltage-gated channels in excitable cells

1.2.1 Na^+ channels

In the nervous system, ion channels are involved in sensory transduction and both propagation and processing of signals. In the excitable cells of this system, the rapid transmission of signals without significant attenuation along the extended processes of a neuron are due to action potentials, initiated by activation of the voltage-gated Na^+ channels present in an area of the cell membrane known as the axonal hillock. These action potentials result when a sufficient, transient depolarization of the membrane causes activation of voltage-dependent Na^+ channels,

which move from a resting (closed), to an activated (open) state. The latter state allows ions to flow through the channel and the resultant influx of positive charges causes further depolarization. This, in turn, causes more voltage-dependent Na^+ channels in this region of the membrane to open, with the greater influx of positive charge accelerating depolarization still further. Such local depolarization gives rise to the action potential.

The potential difference along the axon length, at each side of the membrane, then creates a current flow that causes the depolarization to spread from its initial site along the neuronal processes. The membrane depolarization activates more local Na^+ channels as it spreads along the length of the membrane. While this is taking place, membrane depolarization slowly inactivates the Na^+ channels, causing them to move from the open to a closed, inactivated state. As outlined in Section 1.2.2, the membrane is repolarized and then transiently hyperpolarized by K^+ channels. This hyperpolarization allows the Na^+ channels to recover from their inactivated state from which they re-enter the resting closed state. The channels can then be reactivated and a further action potential can be initiated.

1.2.2 K^+ channels

K^+ currents have been found in all cells which display action potentials mediated by Na^+ and Ca^{2+}, including neurones, secretory cells and skeletal, cardiac and smooth muscle. They vary widely in their kinetics, voltage-dependence, pharmacology and single channel behaviour. The resting membrane potential and the firing patterns, duration and threshold of the action potential in excitable cells are controlled by the particular types of K^+ channels present. These membranes typically contain three types of K^+ channel termed delayed-rectifier, fast-transient and Ca^{2+}-activated K^+ channels.

Delayed rectifier voltage-gated K^+ channels, first described in both the squid giant axon membrane (Hodgkin and Huxley, 1952b) and the frog node of Ranvier (Frankenhaeuser and Huxley, 1964), open shortly following membrane depolarization.

The resulting efflux of positive K^+ thus cause repolarization and subsequent hyperpolarization of this area of membrane. Thus, as the depolarizing pulse due to Na^+ channel activation moves along the membrane, repolarization occurs rapidly and the action potential is conducted along the entire length of the neuron. In this way, delayed-rectifier K^+ channels control the duration of the action potential of the membrane of most nerve and muscle cells.

A-type currents, which were first described in molluscan neurons (Hagiwara *et al.*, 1961; Connor and Stevens, 1971; Neher, 1971) are due to fast-transient K^+ channels. These rapidly open upon membrane depolarization ($<$100ms), and then become completely inactivated, with slow recovery. When open they oppose the effects of a depolarizing stimulus and hinder the triggering of action potentials, particularly by relatively weak depolarizations. In adult rat ventricular myocytes they also constitute the major outward K^+ current responsible for membrane repolarization (Josephson *et al.*, 1984). These channels ensure that the frequency of action potential firing reflects the intensity of the stimulation. The rate of firing is also regulated by the inward rectifier channel whose conductance increases upon hyperpolarization.

A sustained, strong depolarizing stimulus triggering many action potentials causes a build up of the cytoplasmic $[Ca^{2+}]$ to a high level. This is due to depolarization induced activation of voltage-dependent Ca^{2+} channels which mediate Ca^{2+} influx. Increased intracellular $[Ca^{2+}]$ in turn will activate Ca^{2+}-dependent K^+ channels. The resulting increased membrane permeability to K^+ makes the membrane harder to depolarize and thus increases the delay between each action potential. These K^+ currents are therefore involved in regulating the frequency of firing of the action potential e.g in bullfrog sympathetic cells (Pennefather *et al.*, 1985) and rat sympathetic neurons (Kawai and Watanabe, 1986). They provide a negative feedback for Ca^{2+} entry into secretory cells such as pancreatic ß-cells (Marty and Neher, 1982) chromaffin cells (Marty, 1981) and anterior pituitary cells (Wong *et al.*, 1982), where their activation causes closure of voltage-gated Ca^{2+} channels. These K^+ currents are responsible for terminating the plateau phase of the action potential in various cardiac cell types (Sanguinetti and Jurkiewicz, 1990).

1.2.3 Ca^{2+} channels

Four types of Ca^{2+} channel with distinguishable functional properties (discussed in more detail in Section 1.9.3) such as single-channel conductance, voltage- and time-dependent kinetics exist in vertebrate cells. These include the low, high and intermediate threshold voltage-activated T-, L- and N-type channels. The latter, along with a fourth P-type channel are found in neuronal cells, while T- and L-channels have been found in virtually all excitable cells. In cardiac cells, the cell membrane depolarization is maintained during a plateau phase due to inward movement of Ca^{2+} ions through voltage-sensitive Ca^{2+} channels, following the action potential. The Ca^{2+} ions entering the cells during this phase of the action potential serve as the primary intracellular second messenger for the electrical signals at the plasma membrane. In this way, Ca^{2+} channels primarily mediate their effects through the Ca^{2+} ions, rather than the amount of charge they conduct.

In mammalian systems, resting extracellular and cytosolic Na^+ levels, $[Na^+]_e$ and $[Na^+]_i$, respectively, are maintained at 145mM and 12mM, while those for K^+ are 4mM ($[K^+]_e$) and 139mM ($[K^+]_i$). The intracellular $[Ca^{2+}]$ is normally held within the much lower range 0.5-1.0μM, while the extracellular $[Ca^{2+}]$ is 1.8mM. Therefore, fluxes of Na^+ or K^+ through their activated voltage-dependent channels, while having a large effect on the membrane electrical properties, are too small to significantly alter their respective ion concentrations in the cytosol. However, because of the relatively low resting cytosolic levels of Ca^{2+}, the ion flux through voltage-gated Ca^{2+} channels, though being no larger in absolute terms, has a large effect on the intracellular $[Ca^{2+}]$. In this way, the Ca^{2+} channel provides the only known means of directly converting electrical signals into chemical changes inside excitable cells.

Hormone release from several secretory cells (Prentki and Matschinsky, 1987; Fitzpatrick *et al.*, 1988; Ma *et al.*, 1992) is known to be mediated by increases in the cytosolic $[Ca^{2+}]$ as a result of Ca^{2+} channel activation. Similarly, Ca^{2+} influx through Ca^{2+} channels in presynaptic membranes stimulates exocytotic release of the relevant neurotransmitter (NT) (Augustine et al., 1987). Skeletal and both smooth and cardiac

muscle contraction, which is initiated by a rise in the cytosolic [Ca^{2+}] from (0.5-1.0)μM to 1mM is also mediated via Ca^{2+} channels. However, this increase in $[Ca^{2+}]_i$ in skeletal muscle does not arise, as in cardiac and smooth muscle (Fabiato, 1985; Beuckelmann and Wier, 1988; Nabauer *et al.*, 1989), from Ca^{2+} entry via the Ca^{2+} channel (Armstrong *et al.*, 1972). It is released from intracellular stores, a process which is triggered by activation of the Ca^{2+} channel (discussed in more detail in Section 1.9.10).

1.3 Channel current measurement

The ionic currents through all channels in a cell can be measured in voltage-clamp studies. These involve impaling a cell with a microelectrode and then passing a current across the cell membrane between the microelectrode inside, and one outside the cell. By varying this current, the membrane potential can be changed rapidly to a predetermined level of depolarization. The voltage-gated channels open or close in response to the changes in membrane potential while the clamp prevents the changes in membrane current from influencing the membrane potential. In this way, the conductance of the membrane to different ions can be measured as a function of membrane potential.

The current through a single channel could not be measure using the voltage-clamp technique since the area of membrane examined is large, containing thousands of channels, randomly opening and closing. The patch-clamp method was developed to enable measurement of the current flowing through a single open channel (Hamill *et al.*, 1981; Sakmann and Neher, 1984). Instead of inserting a microelectrode into the cell, a micropipette was pressed onto the surface of the cell. This effectively electrically isolated a small area (1-10μm^2) of the membrane, reducing the intrinsic noise due to the large number of channels in the membrane. The seal between the patch pipette and the membrane was tightened by suction increasing the resistance between the inside and outside of the pipette, and dramatically lowering electronic

noise to such low levels that the picoampere currents flowing through single channels in the membrane could be measured directly. This was achieved by inserting a finer pipette into the patch pipette. Particular channels e.g. voltage-gated Ca^{2+} channels can be studied using this technique by selecting the solutions on both sides of the patch to contain ions that permeate these and not other membrane ion channels present. Thus, it has been possible to study the behaviour of individual channels with millisecond time resolution over many seconds or minutes, yielding insight into their function.

1.4 Electrical properties of channel

1.4.1 Activation

Voltage-clamp studies, where the membrane potential is the only parameter varied, showed that channel opening (activation) exhibits a very steep voltage dependence. Hodgkin and Huxley (1952b) predicted the existence of gating currents in cation channels due to the movement of charges intrinsic to the protein, upon channel activation. The existence of these gating currents was later physically demonstrated (Armstrong and Benzanilla, 1973) and the gating charge movement was shown to be confined to the membrane (Rojas and Keynes, 1975). It was thus proposed that the charge movement arises from three or four voltage-sensitive components (gating particles), subsequently shown to be intrinsic to the channel (for review see Hille, 1984). Since most of the drop in membrane potential occurs across the interior of the membrane, a region of low dielectric constant and high hydrophobicity, these charges would have to be located within the membrane, in order to perform their role in voltage sensing. It was proposed that a voltage change exerts an electrostatic force on the sensors leading to conformational changes within the channel protein which cause the channel to open.

Later, electrophysiological studies led to the prediction of a voltage sensor in

the form of a string of positive charges which may pair with negative charges in the membrane. The number of charges within a channel molecule that have to be translocated across the membrane as the channel opens (gating charge) was estimated, by examining voltage-dependence of channel activation, to be 4-6 for Na^+, K^+, and Ca^{2+} channels studied (Hodgkin and Huxley, 1952b; Almers, 1978; Hille 1984).

1.4.2 Inactivation

Some voltage-gated channels, opened in response to membrane depolarization, then move to an inactivated state. The time taken and conditions necessary for inactivation of the open channel vary for different channels. Some channels, e.g. a delayed rectifier K^+ channel found in skeletal muscle myotubes from *Drosophila* (Zagotta et al., 1988), stay open in certain membrane potential ranges and close at other potentials. Other channels inactivate with time, even when the membrane potential remains at a level which initially caused activation. Following inactivation, a channel has to return to the resting (closed) state before it can be reactivated.

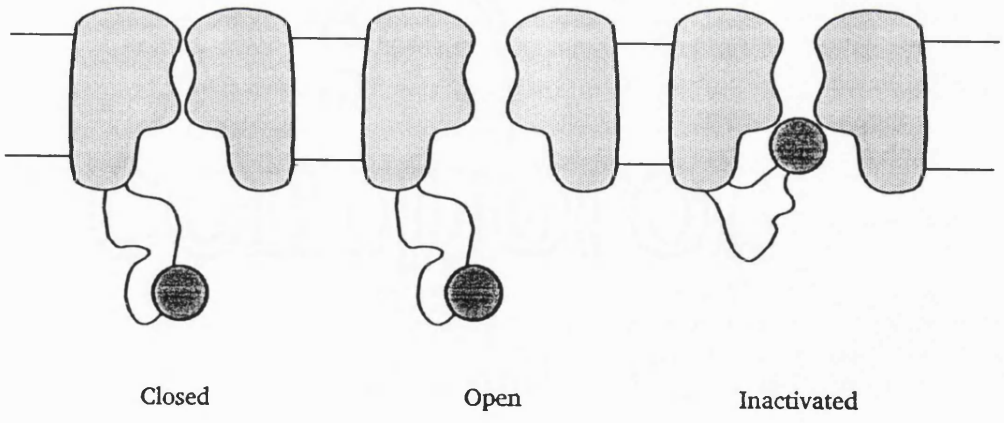

Fig. 1.1 Diagram of channel showing resting, activated and inactivated states.

The difference between the inactivated and resting states of the channel was demonstrated by measuring the movement of charges intrinsic to the channel under various conditions that affect Na^+ channel inactivation. Brief pulses that do not cause inactivation lead to a movement of an equal number of charges across the membrane in either direction on channel opening and closing. On channel inactivation the gating charges were seen to "immobilize" in the open state (Armstrong, 1981). Thus, the channel has to open before it can enter an inactivated state. Studies on single Na^+ channels have shown that they inactivate more readily when they are open (Aldrich and Stevens, 1983) although some may inactivate during the transition from closed to open state before reaching the open state.

1.5 Voltage-gated Na^+ channel structure and membrane arrangement

1.5.1 Identification of Na^+ channel polypeptides and elucidation of the α subunit primary structure

Initial information on the structure and function of voltage-gated ion channels was derived from the Na^+ channel, following its purification from various sources (review by Catterall. 1988). Experiments carried out following reconstitution of these preparations of defined polypeptide subunit composition, by incorporation into phospholipid vesicles, revealed that the protein components of the isolated channels were sufficient to mediate selective, neurotoxin-activated ion flux with the flux rate, ion selectivity and pharmacological properties expected of native Na^+ channels (Tamkun *et al.*, 1984; Kraner *et al.*, 1985; Duch & Levinson, 1987). Furthermore, the α subunit was found to contain most, if not all, of the functional domains of the channel (Tamkun *et al.*, 1984; Kraner *et al.*, 1985; Hartshorne *et al.*, 1985; Furman *et al.*, 1986; Duch and Levinson, 1987; Recio-Pinto *et al.*, 1987).

In 1984, Noda *et al.* deduced the entire amino acid sequence of the eel electroplax Na^+ channel via the cloning and sequencing of the channel complementary

DNA (cDNA). Expression of cDNA libraries prepared from eel electroplax messenger RNA (mRNA), were screened both with antibodies raised against the purified electroplax Na^+ channel α subunit and with oligonucleotides. The latter contained all possible cDNA sequences predicted from the partial amino acid sequence of a tryptic fragment of the channel and therefore recognized segments of the channel mRNA sequence. Three cDNA clones encoding different α subunits of the Na^+ channel from rat brain, defining the rat Na^+ channel subtypes I, II and III, were subsequently isolated by screening a rat cDNA library with cDNA probes encoding the electroplax polypeptide (Noda *et al.*, 1986a; Kayano *et al.*, 1988) or with antibodies against the purified protein (Auld *et al.*, 1985, 1988). Each of these rat brain cDNA's, as well as one from rat muscle (Trimmer *et al.*, 1989) encodes a polypeptide, known as the α subunit, consisting of at least 1,800 amino acid (aa) residues. These proteins closely resemble the eel electroplax α subunit, being made up of four internally homologous domains of 300-400 aa (denoted I to IV) that exhibit approximately 50% sequence identical or conserved residues. Each domain contains six predominantly hydrophobic segments (designated S1-S6), as predicted by a Kyte and Dolittle hydropathy plot (Kyte and Dolittle, 1982), comprising at least 19aa residues, which can potentially span the membrane.

mRNA transcribed from cDNA clones of α subunit of rat brain Na^+ channels II, III or, to a lesser extent, rat brain Na^+ channel I, is sufficient to induce functional Na^+ channels in *Xenopus* oocytes (Noda *et al.*, 1986b; Suzuki *et al.*, 1988; Auld *et al.*, 1988). The rate of inactivation as measured in voltage-clamp studies, however, is much slower compared with that of Na^+ channel induced by mRNA isolated from rat brain. Coinjection of low molecular weight mRNA from rat brain and mRNA from the rat brain Na^+ channel cDNA clone restores the normal inactivation kinetics (Auld *et al.*, 1988). This evidence indicates that whereas the ion channel itself is formed by the α polypeptide, the other subunits play important regulatory and stabilizing roles in the protein complex.

1.5.2 Orientation of the α polypeptide in the membrane

The glycosylated α polypeptide of the channel has been covalently labelled by TTX and both α and ß scorpion toxins (for review see Catterall, 1988). Because these toxins are known to act from outside the cell (reveiwed by Catterall, 1988), it follows that the α subunit must have extracellular domains. The observed phosphorylation of this polypeptide by adenosine 3',5'-monophosphate (cAMP)-dependent protein kinase in both intact cells and synaptosomes (Costa *et al.*, 1982; Costa and Catterall, 1984; Rossie and Catterall, 1987; Rossie *et al.*, 1987; Coombs *et al.*, 1988; Gordon *et al.*, 1988a) revealed that the polypeptide is also exposed to the cytosol. These findings led to the proposal that this is a transmembrane protein.

Based on the knowledge of Na^+ channel α subunit sequences, several models have been proposed for its structure (Noda *et al.*, 1984; Greenblatt *et al.*, 1985; Kosower, 1985; Noda *et al.*, 1986a; Catterall, 1986; Guy and Seetharamulu, 1986). Since the Na^+ channel contains four homologous domains (I-IV), most models postulate that each domain has an even number of transmembrane segments allowing for a cytoplasmic localization of both the carboxy (C-) and amino (N-) terminus and of the sequences between adjacent repeated domains. The four homologous domains of the Na^+ channel α subunit are predicted to form a square array in the membrane, surrounding a transmembrane pore.

Subsequently, the membrane orientation of the major hydrophilic segments of the Na^+ channel has been determined experimentally (Gordon *et al.*, 1987; Gordon *et al.*, 1988b; Barchi, 1988; Rossie *et al.*, 1987; Vassilev *et al.*, 1988; Nakayama *et al.*, 1993). Sequence-specific antibodies have been used to establish the cytoplasmic location both of the loop between homologous domains II and III and of the C- and N-termini of the channel (Gordon *et al.*, 1987; Gordon *et al.*, 1988b; Nakayama *et al.*, 1993). Five sites of cAMP-dependent phosphorylation have been located to the hydrophilic segment between homologous domains I and II of the rat brain Na^+ channel in intact neurons, defining this segment as intracellular (Rossie *et al.*, 1987; Rossie & Catterall, 1989), while two such sites were located to both the N- and C-

termini, respectively, of the eel electroplax channel (Emerick and Agnew, 1989). Phosphorylation of these sites can modulate the voltage dependence of closure of the channel by the inactivation gating segment between domains III and IV (see below). Observed modulation of Na^+ channel inactivation by intracellular perfusion of antibodies against the hydrophilic segment between homologous domains III and IV also reveals the intracellular orientation of this segment (Vassilev *et al.*, 1988; Vassilev *et al.*, 1988).

The α-scorpion toxin binding site, which is known to be extracellular has been shown to involve the glycosylated loop between the transmembrans domains IS5 and IS6, which contains seven possible sites of N-linked glycosylation (aa sequence Asn-X-Ser/Thr), as well as the corresponding loop in domain IV. This finding confirms the extracellular orientation of these regions of the α polypeptide (Tejedor and Catterall, 1988; Thomsen & Catterall, 1989). The formation of this receptor site by close apposition of segments in the S5-S6 loops of domains I and IV also supports the proposed tertiary model for the channel. A square arrangement of the four homologous domains would have domains I and IV side by side in the channel tertiary structure.

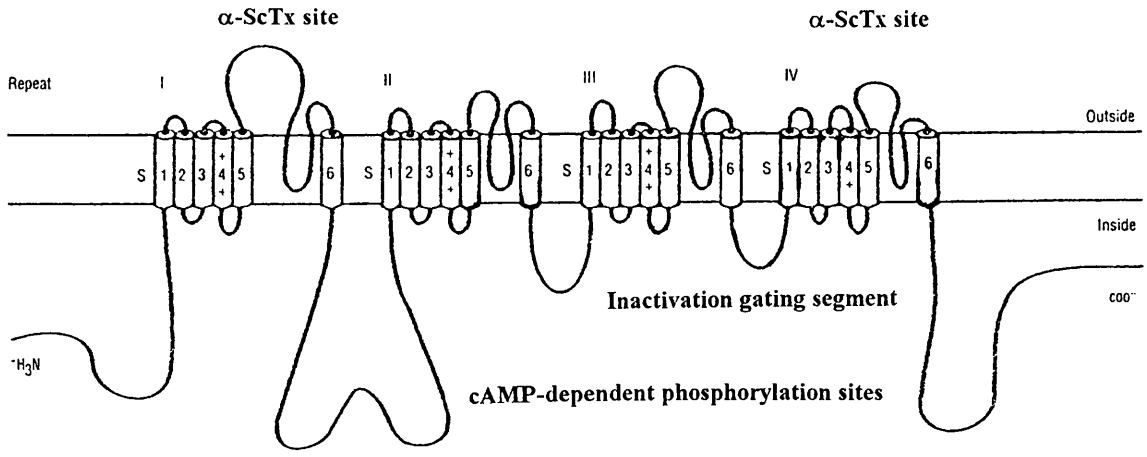

Fig. 1.2 Diagram of the proposed membrane arrangement of the Na^+ channel α subunit.

1.6. Voltage-gated K^+ channel structure and membrane arrangement

The *Drosophila* Shaker (Sh) locus was found to encodes 10 different Sh K^+ channel polypeptides (Tempel *et al.*, 1987; Schwarz *et al.*, 1988; Pongs *et al.*, 1988; Kamb *et al.*, 1988) that conduct a fast transient K^+ current (Timpe *et al.*, 1988a, 1988b; Iverson *et al.*, 1988). It was later discovered that distinct genes define four separate K^+ channel subfamilies in *Drosophila* designated Sh, Shab (924aa), Shal and Shaw (498aa) (Wei *et al.*, 1990; McCormack *et al.*, 1991).

Genes encoding K^+ channel polypeptides which resemble each of the *Drosophila* channel subfamilies have also been identified in both rat and mouse. These include several homologous rat K^+ channel proteins that are closely related to the *Drosophila* Sh polypeptide (Stuhmer *et al.*, 1988, 1989b; Betsholtz *et al.*, 1990; Grupe, A., 1991) and others which resemble those of *Drosophila* Shaw and have thus been termed Raw (Baumann, *et al.*, 1988; Yokoyama *et al.*, 1989; McCormack *et al.*, 1990b; Luneau *et al.*, 1991a, 1991b; Schroter *et al.*, 1991; Rettig *et al.*, 1992). Two Shab (Frech *et al.*, 1989; Hwang *et al.*, 1992) and one Shal homologue have also been isolated from rat cDNA libraries (Baldwin *et al.*, 1991; Roberds and Tamkum 1991). The Shab analogue DRK1, containing 853 aa, most resembles in its properties a classical delayed rectifier channel (Frech *et al.*, 1989). The mouse channels have properties which are identical to those of their equivalent rat channels (Grissmer *et al.*, 1990; Pak *et al.*, 1991; Ghanshani *et al.*, 1992).

Polypeptides from each of the four K^+ channel families, whose sequences are known, range in size from 428aa for a mouse inward rectifier to the 924aa *Drosophila* Shab. Their primary structure contains six or seven potential membrane spanning regions, including an S4 sequence (see Section 1.7.1). They thus resemble one of the repeated homologous domains of the Na^+ channel α subunit. It appears that individual K^+ channel polypeptides, resembling one quarter of the Na^+ channel, form as multimers, probably composed of four similar or identical subunits. This is supported by electrophysiological evidence that co-expression of different K^+ channel polypeptides produces heteromultimeric channels in heterologous expression systems

(Isacoff *et al.*, 1990; McCormack *et al.*, 1990a; Ruppersberg *et al.*, 1990; MacKinnon, 1991b). Additionally, more recent findings suggest the existence of heteromultimeric channels *in vivo*. These consist of observed immunoprecipitation of two mouse brain K^+ channel proteins by each of two antibodies which are known to be specific for just one of these proteins (Wang *et al.*, 1993), coupled with the identification of a rat brain A-type K^+ current combining features of two different channels (Sheng *et al.*, 1993).

1.7 Determination of functionally relevant regions of both Na^+ and K^+ channels

Identification of sites in the primary structure responsible for voltage-dependent activation and inactivation, selective ion conductance and modulation of the channel by toxins and drugs is central to understanding how voltage-gated channels function. These general properties of voltage-gated ion channel function are presumably conferred on these channels by the domains that are highly conserved among channel sequences; namely those contained in their core transmembrane regions (Schwarz *et al.*, 1988).

1.7.1 Domains involved in activation

The S4 region of each of the four homologous domains of both the Na^+ and K^+ channel contains a sequence of mainly hydrophobic residues with a basic (arginine or lysine) residue at every third or fourth position, which is highly conserved amongst Na^+ channels. These sequences which are postulated to form transmembrane helices having a row of positively charged residues spanning the membrane, were thus hypothesised to comprise the channel voltage sensors (see Section 1.4.1) (Noda *et al.*, 1984; Greenblatt et al., 1985; Guy and Seetharamulu, 1986). The voltage sensing function of S4 has been supported by site-directed mutagenesis experiments, which

show that neutralization of charged residues in the S4 segment of homologous domain I reduces channel gating charge (Stuhmer *et al.*, 1989a) and that alteration of hydrophobic residues in this sequence shifts the voltage dependence of channel activation markedly (Auld *et al.*, 1989). An antibody specific for part of the IS4 sequence of the eel α polypeptide shifted the steady state Na^+ current inactivation to more negative membrane potentials in rat neuronal channels (Meiri *et al.*, 1987).

Charged residues in K^+ channel S4 have also been shown, by site-directed mutagenesis to contribute to the voltage-dependent gating charge of the channel (Liman *et al.*, 1991; Lopez *et al.*, 1991; Logothetis *et al.*, 1992). The incremental reduction of S4 positive charge resulted in a corresponding decrease in the observed channel gating valence (Logothetis *et al.*, 1992). These findings, coupled with observed altered voltage-dependence properties as a result of mutations to the positive residues of S4 in the Sh channel (Papazian *et al.*, 1991), indicate a role for this domain in voltage-dependent K^+ channel activation.

1.7.2 Domains involved in inactivation

Fast inactivation of Na^+ and K^+ channels can be removed by treatment with proteases from the cytoplasmic side of the membrane (Armstrong *et al.*, 1973; Rojas and Rudy, 1976; Matterson and Carmeliet, 1988; Hoshi *et al.*, 1990), which suggests that fast inactivation involves parts of the channel exposed at the membrane intracellular face. The inactivation gate of the Na^+ channel has been located to the short intracellular IIIS6-IVS1 region of the α subunit, since an antibody specific for this domain delayed opening and prolonged open times of single channels during depolarizing test pulses, inhibiting Na^+ channel inactivation almost completely (Vassilev *et al.*, 1988; Vassilev *et al.*, 1989). Examination of the voltage-dependence of both the binding and effect of the antibody suggested that a conformational change involving this segment of the α subunit is required for fast inactivation of the channel and that this segment may fold into the channel structure to serve as the fast inactivation gate by blocking the pore of the Na^+ channel (Vassilev *et al.*, 1988).

Deletion or cleavage of the III-IV loop (Stuhmer *et al.*, 1989a), and phosphorylation of a serine residue in its sequence (West *et al.*, 1991), also slow channel inactivation. Studies of this region by Moorman *et al.*, (1990) suggested it also has in role in channel activation, suggesting structural interaction between inactivating domains and regions of the channel involved in activation.

The above findings support a 'ball-in-socket' model for voltage-gated channel inactivation, which has also been proposed for the K^+ channel (Hoshi *et al.*, 1990). In this model the inactivation gate consists of the III-IV loop of the Na^+ channel and of the N-terminus of the K^+ channel. These gates cause channel inactivation by physically plugging the channel pore, as a result of binding to a receptor site (the S4-S5 loop, for the latter channel), located at the cytoplasmic mouth of the pore.

Fast K^+ channel inactivation is mimicked by cytoplasmic application of pore blockers such as TEA or its analogues (Armstrong and Binstock, 1965; Armstrong, 1969; Choi *et al.*, 1991), suggesting that the process is achieved by the plugging of the channel pore by a cytoplasmic inactivation gate. The first 20 amino acids, including four basic residues, of Sh B channel were subsequently shown to be essential for the process of fast inactivation of Sh B (Hoshi *et al.*, 1990; Zagotta *et al.*, 1990) and also RCK1 and drk1 delayed rectifier type (Zagotta *et al.*, 1990; Isacoff *et al.*, 1991) channels. This domain forms the ball in the ball-in-socket i.e the inactivation gate.

The intracellular loop between S4 and S5 contains five residues, including a glutamate, which have been shown to be involved in fast inactivation (Isacoff *et al.*, 1991). These residues and their relative location to each other are conserved in most K^+ channels whose sequences are known. Their spacing in the primary structure, would allow them to align along one side of an α helical secondary structure in this domain. This raises the possibility that the S4-S5 loop is folded into a short helix which may be located at the cytoplasmic mouth of the pore where it interacts with the inactivation gate (Isacoff *et al.*, 1991). The sequence of a protein can be changed at one or more specific amino acid residues by altering one or more of the nucleotides in the DNA codons encoding these residues. Thus by altering the sequence of

expressed DNA a protein which is altered at a specific site can be expressed and its function compared to the normal protein. In this way, mutations of one of the residues in the S4-S5 loop which are known to be involved in inactivation, stabilized the inactivation state of Sh B suggesting that this residue is involved in destabilizing the fast-inactivation state of the channel (Isacoff *et al.*, 1991). Mutation of the equivalent residue in the drk1 channel (Frech *et al.*, 1989) similarly stabilized the channel inactivation which was induced by intracellular application of the Sh B N-terminal (20 amino acid) peptide (Isacoff *et al.*, 1991). This finding reveals that the receptor for the fast inactivation gate appears to be conserved in the drk1 channel, which only produces macroscopic currents which are slowly inactivating (Frech *et al.*, 1989; VanDongen *et al.*, 1990).

The slow inactivation of the drk1 channel can be delayed by deletions in either the channel amino or carboxy terminal region. However, deletion of hydrophilic sequences on both ends of the core region containing the S1-S6 segments, shows nearly wild-type levels of slow inactivation (VanDongen *et al.*, 1990). Thus slow inactivation appeared to involve sequences within the core region of the polypeptide, although its kinetic properties may be modified by hydrophilic sequences on either end of the core region. Consistent with this view, the difference in the rate of slow inactivation between the splice variants Sh A and B (Timpe *et al.*, 1988a, 1988b) can be attributed to a single hydrophobic residue in the S6 sequence (Hoshi *et al.*, 1991; Zagotta *et al.*, 1991). Although mutations have been found that alter primarily either fast or slow inactivation, these two processes appear to be coupled (Hoshi *et al.*, 1991; Isacoff *et al.*, 1991). The alanine-for-leucine mutation in drk1 that enhances the Shaker B peptide-induced fast inactivation also accelerates slow inactivation (Isacoff *et al.*, 1991). Similarly, many mutations of Shaker B that alter the stability of the fast inactivated state also affect the rate of slow inactivation (Hoshi *et al.*, 1991; Isacoff *et al.*, 1991).

1.7.3 Domains contributing to the pore structure

The similarity in primary structure between the K^+ channel and a single repeated domain of the Na^+ channel points to a membrane arrangement for the former polypeptide similar to that now established for the latter (see Section 1.5.3). Domains of these channels involved in function have been determined (see Section 1.7). However, an understanding of the tertiary structure of these channels is essential in elucidating channel structure-function relationships. In this regard, recent studies have allowed the proposal of the tertiary structure of the channel pore.

The binding domains for K^+ channel-specific drugs and toxins that block ionic currents, have been located to the S5-S6 loop (MacKinnon and Miller, 1989; Yellen *et al.*, 1991; Hartmann *et al.*, 1991; Choi *et al.*, 1991). Residues at either end of this loop bind charybdotoxin (CTX) and external TEA (MacKinnon and Miller, 1989; Miller 1990; MacKinnon and Yellen, 1990; MacKinnon *et al.*, 1990; MacKinnon 1991a) and thus appear to be located at the mouth of the pore. Within this loop are located two clusters of predominantly negatively charged amino acids in both the Na^+ and K^+ channel α polypeptides. Negatively charged amino acid residues in this region, termed the SS1-SS2 region, of the S5-S6 loop in each of the four domains of the Na^+ channel, have been shown to constitute part of the binding domain for the channel blockers TTX and STX and to also be involved in ion conductance, interacting directly with the pathway for ions permeating the open channel (Noda *et al.*, 1989; Pusch *et al.*, 1991; Terlau *et al.*, 1991; Backx *et al.*, 1992; Chen *et al.*, 1992; Heinemann *et al.*, 1992). The K^+ channel equivalent of the SS1-SS2 domain, the 20aa H5 sequence, appears also to contain residues that interact with permeant ions (Hartmann *et al.*, 1991; Yool and Schwarz, 1991) as well as with both internal and external TEA (Hartmann *et al.*, 1991; Yellen *et al.*, 1991).

Backx *et al.*, (1992) located the TTX binding site in the Na^+ channel domain I approximately 20% down the membrane electrical field. More recently, the region between the S5 and S6 sequences of both domains III and IV, has been shown to form part of the TTX binding domain (Nakayama *et al.*, 1992a). The internal TEA

blockade of each of the four K^+ channel families shows a voltage dependence, which indicates that the internal TEA-binding site is located about 20% into the membrane electric field (Kirsch *et al.*, 1991; Taglialatela, *et al.*, 1992). This evidence suggests that the S5-S6 loops regions of both channels are located in the pore region of the channel with the H5 and SS1-SS2 regions lining at least some of the channel pore.

1.8 Channel tertiary structure/function relationships

In light of the finding discussed in Section 1.7.3, Sato and Matsumoto (1992) have proposed a model for Na^+ channel tertiary structure with the S5-S6 region playing a role in activation gating, voltage sensing and ion selectivity. In their model (See Fig. 1.3), this S5-S6 region in each homologous domain loops from the outside into the membrane, in the resting state, as far as the location of negatively charged residues on the S2 sequence, some way into the membrane interior, and back out again. The negatively charged loop is stabilized by the positively charged residues on the S4 segment of the same homologous domain. S2 and S4 contribute to the structure of a guiding pore for the loop, with the loop acting as voltage sensor. The four S5-S6 loops collectively form the internal structure of the pore.

If the tip of each loop comprises the negatively charged SS1-SS2 domain, they can sense depolarizing changes in membrane potential which cause the loop to slide further down into the S4-S2 pore along the plane of orientation of the positive charges on the S4 segment. Amino acids residues having opposing charges may thus continue to interact. This movement of a nett negative charge perpendicular to the membrane towards its intracellular face, rather than the movement of positive charges in the opposite direction, constitutes the gating current in this model. The model is compatible with the finding that the S5-S6 loop lines the pore, but also proposes that S5-S6 and not S4 is the membrane voltage sensor; S4 has a role in stabilizing the charged sensor in the membrane in the resting, activating, activated and inactivated states.

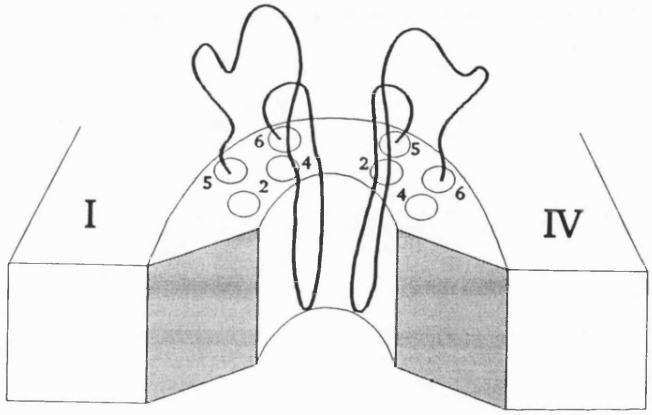

Fig. 1.3 Diagram of a cutaway section of the Na^+ channel showing the pore structure proposed by Sato and Matsumoto (1992).

Durell and Guy (1992) have proposed an atomic scale model for the K^+ channel pore region, with the outer, larger than the inner half of the pore (see Fig. 1.4). The ion selective H5 region having ß barrel secondary structure, spans the outer half of the membrane. During activation the S4 region rotates and moves perpendicular to the plane of the membrane towards the membrane exterior. This results in a conformational change in which the S4-S5 loops move from blocking the pore at the intracellular entrance to forming part of the lining of the inner portion of the pore. This model also encompasses the, previously proposed, 'ball-in-socket' model for channel inactivation (Hoshi *et al.*, 1990), in which the K^+ channel N-terminus causes channel inactivation by physically plugging the channel pore, as a result of its binding to the S4-S5 loop which is located at the cytoplasmic mouth of the pore.

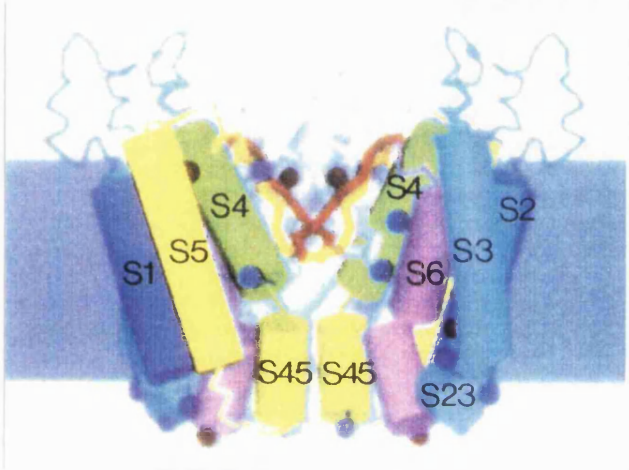

Fig. 1.4 Model of the arrangement of the K^+ channel in the membrane proposed by Durell and Guy (1992).

1.9 Voltage-gated Ca^{2+} channels

1.9.1 Discovery of Ca^{2+} channels

In a number of excitable tissues, it was shown that the action potential was produced by an increase in the conductance of the membrane to Na^+ followed by an increase to K^+ (Hodgkin and Huxley, 1952a). However, in certain other tissues, such as crustacean muscle fibres, capable of generating long-lasting action potentials in the absence of external Na^+ (Fatt and Katz, 1953; Fatt and Ginsborg, 1958), the active inward current was subsequently found to be carried by Ca^{2+} instead of Na^+ (Fatt and Ginsborg, 1958; Hagiwara and Naka, 1964), constituting the first evidence for a channel specific for Ca^{2+}.

Thus, evidence began emerging in the early 1960s, that several excitable cells had both a Na^+ and a Ca^{2+} system. In the frog cardiac ventricle, it had been shown

that the rapid initial rise of the action potential was due to an increase in conductance to Na^+ (Brady and Woodbury, 1960). However, the size of the action potential in this preparation did not obey the Nernst relation (Coraboeuf and Otsuka, 1956), leading Orkand and Niedergerke (1964) to suggest that Ca^{2+} ions were involved in the genesis of its slow phase. Hagiwara and Nakajima (1965) later showed that there were two different ionic systems involved in the inward carriage of currents. Later, *Aplysia* neurones were also shown to have both Na^+ and Ca^{2+} systems (Geduldig and Gruener, 1970).

During muscle activity, a significant increase in Ca^{2+} uptake in frog skeletal muscle was observed (Bianchi and Shanes, 1959). A Ca^{2+} dependent action potential in frog twitch muscle fibres was described following block of the delayed K^+ current with tetraethylammonium (TEA) and removal of the chloride shunt by using an impermeant anion (Beaty and Stefani, 1976). Under these conditions a slow inward current mainly carried by, and dependent on, extracellular Ca^{2+} ions was discovered (Sanchez and Stefani, 1978). Since the current was also unaffected by removal of external Na^+ or by TTX, it was proposed to enter via a specific channel.

Such channels for calcium had been described in heart muscle (Reuter, 1968; Vassort *et al.*, 1969; Reuter and Scholz, 1977), barnacle muscle cells (Hagiwara *et al.*, 1969; Keynes, 1973), frog slow muscle fibres (Stefani and Uchitel, 1976) and in nonexcitable cells such as tunicate egg (Okamoto *et al.*, 1976) and later lymphocytes (Fukushima and Hagiwara, 1983), sperm (Kazazoglou *et al.*, 1985) and neutrophils (von Tscharner *et al.*, 1986). Calcium channels are now known to be present in muscle, neuronal and secretory cells (Tsien *et al.*, 1988).

1.9.2 Classes of calcium channels

Voltage-dependent Ca^{2+} channels open in response to an appropriate membrane depolarization. The existence of distinct low- and high-threshold (T- and L-type) Ca^{2+} channels in vertebrate cells was first shown by action potential recordings from guinea pig central neurons (Llinas and Yarom, 1981; Jahnsen and

Llinas, 1984). Subsequent studies have led to the identification of at least four classes of voltage-dependent Ca^{2+} channel, namely, L-, T-, N- and P-type, in vertebrate cells. Such identification was assisted by the availability of potent activators and inhibitors of the channel, since the different channel types show different sensitivities to these synthetic compounds and natural toxins. These channels could also be distinguished on the basis of functional properties such as single-channel conductance, voltage- and time-dependent kinetics, and cellular distribution.

1.9.2.1 L-type channel

L-type channels are found in virtually all excitable tissue representing the major pathway for Ca^{2+} entry in cardiac and smooth muscle and helping to control transmitter release from endocrine cells and some neuronal cell preparations. These high-threshold 1.4-dihydropyridine- (DHP)-sensitive channels were initially described in various cardiac cells including guinea pig ventricle, dog and frog atrial, and rabbit sinoatrial cells and in various neuronal cells (review by Bean, 1989). They showed single channel conductances of 15-25pS (cardiac cells) and 20pS and 27-28pS, respectively, in chick sensory and both rat and frog sympathetic neurons, with 100mM Ba^{2+} as charge carrier. A Ca^{2+} channel with similar properties has also been described in a variety of smooth muscle cells from mammalian arteries, veins and aortic muscle (Bean, 1989).

Isoforms of this channel, termed the "high threshold", "slow" or L-type (long lasting) Ca^{2+} channel exist, since skeletal muscle L-type differs from the channel responsible for cardiac and smooth muscle and for the neuronal L-type Ca^{2+} current in that it inactivates more than an order of magnitude more slowly (for reviews see, Bean, 1989; Hess, 1990; Tsien and Tsien, 1990). These L-type channels show similar sensitivity to DHP and phenylalkylamine (PAA) antagonists (McCleskey, 1985) and are each potentiated by ß-adrenergic agonists and internal cAMP (Arreola *et al.*, 1987).

1.9.2.2 T-type channel

A second type of channel was also observed in the cardiac cells examined above, having a small single channel conductance of 8pS, in 100mm Ba^{2+}, which was activated by small depolarizations and inactivated rapidly. A Ca^{2+} channel with similar properties was also described in the smooth muscle cells studied above, and in sensory neurons (Nowycky *et al.*, 1985; Fox *et al.*, 1987a). The latter had a single channel conductance of 8pS in 110mM Ba^{2+} and were unaffected by either DHP's (Boll and Lux, 1985; Nowycky *et al.*, 1985; Fox *et al.*, 1987b) or the PAA, verapamil (Boll and Lux, 1985; Fedulova *et al.*, 1985). This was termed the "low threshold", "fast" or T-type (transient) Ca^{2+} channel.

This channel was recognized to comprise the minor component of Ca^{2+} current in skeletal muscle (Arreola *et al.*, 1987; Cota and Stefani, 1986; Garcia and Stefani, 1987), being potentiated by adrenergic stimulation but insensitive to DHP (Arreola *et al.*, 1987). Unlike the cardiac and smooth muscle channel it did not inactivate over several seconds (Cota and Stefani, 1986), indicating that subtypes of this channel also exist.

1.9.2.3 N-type channel

A third type of channel observed in studies on neurons (Carbone and Lux, 1987; Swandulla and Armstrong, 1988) showed a single channel conductance of intermediate size, 13pS, in 110mM Ba^{2+}, which activated at potentials more positive than T-type and more negative than L-type channels. It inactivated more slowly than the former and faster than the latter channel type and was termed the N-type (neuronal) channel. It was identified as a DHP-insensitive current, having conductance of 11-15pS (in 110mM Ba^{2+}) in sympathetic neurons (Hirning *et al.*, 1988; Lipscombe *et al.*, 1988) and as a high-threshold activating channel in chick DRG neurons, in single channel and whole cell recordings experiments (Nowycky *et al.*, 1985; Fox *et al.*, 1987a, 1987b; Hirning *et al.*, 1988).

ω-conotoxin GVIA (ω-CgTx), subsequently demonstrated to interact with a single class of binding sites in chick and rat brain synaptosomes with a K_d of 0.8-2 pM (Barhanin *et al.*, 1988), is known to cause persistent and direct inhibition of N-type Ca^{2+} channels in vertebrate neurons (McCleskey *et al.*, 1987; Kasai *et al.*, 1987). A ω-CgTx-sensitive and DHP-insensitive Ca^{2+} current was expressed in *Xenopus* oocytes injected with mRNA from *Torpedo californica* electric lobe (Umbach and Gundersen, 1987), while more recently, the cloning and functional expression of human neuronal N-type Ca^{2+} channel, which is irreversibly blocked by ω-CgTx, has been achieved (Williams *et al.*, 1992a).

1.9.2.4 P-type channel

Funnel web spider toxin (FTX), a purified Ca^{2+} channel-blocking polyamine fraction (0.2-0.4kD) derived from the venom of the funnel web spider, was shown to block dendritic spiking (Sugimori and Llinas., 1987) in Purkinje cells. It also blocked Ca^{2+}-dependent spikes in Purkinje cells and synaptic transmission in squid giant synapses, without affecting the presynaptic action potential (Llinas *et al.*, 1989). Voltage clamp experiments showed that these effects resulted from blockade of presynaptic inward Ca^{2+} current and consequent NT release.

This channel was isolated from both guinea pig cerebellum and squid optic lobe by affinity chromatography on an FTX column. Patch clamp studies of these channels revealed a 10-12pS conductance, using 80mM Ba^{2+}, and a 5-8pS conductance in 100mM Ca^{2+} for the cerebellar channel, while the squid optic lobe channel showed a higher conductance in Ba^{2+}. Both channels were blocked by FTX, Cd^{2+} and Co^{2+} but were unaffected by either ω-CgTx or DHP (Llinas *et al.*, 1989). The voltage and time dependence of the currents were comparable to those from current clamp experiments on the dendrites of Purkinje cells (Llinas and Sugimori, 1980). This fourth, previously undefined, Ca^{2+} channel in mammalian neurons and squid presynaptic terminal membranes, was designated P-type (Purkinje).

Table 1.1 Table of physiological and pharmacological properties of Ca^{2+} channel types.

Channel class	Voltage dependence of activation	Open time	Inhibitors
T	Low	Short	
L	High	Long	DHP, PAA, BTA
N	Intermediate	Long	ω-CgTx
P	Intermediate	n.d.	FTX, Aga-IVA

1.9.3 Ca^{2+} channel antagonists

L-type Ca^{2+} channels can be blocked by binding a heterologous group of drugs, collectively known as "Ca^{2+} channel antagonists", which can be divided into several different classes according to their molecular structures. Verapamil, a PAA, identified by Fleckenstein in 1963, diminished contractile force, without a major change in the action potential and also decreased Ca^{2+}-dependent high-energy phosphate utilization and extra-oxygen consumption of cardiac muscle (effects which were removed by increasing [Ca^{2+}] in the extracellular medium), giving rise to the term "Ca^{2+} antagonist" (Fleckenstein, 1964). Later it was shown that these compounds inhibit Ca^{2+} entry into cells via the L-type Ca^{2+} channel (Fleckenstein, 1967) and they are now described by the terms Ca^{2+} channel antagonists, inhibitors or blockers. In 1969, Fleckenstein showed that the DHP, nifedipine, similarly inhibited Ca^{2+} channel function, with the benzothiazepine (BTA), diltiazem, later identified as an inhibitor by Nakajima *et al.* (1975).

Skeletal, cardiac and smooth muscle and also neuronal L-type channels are now known to show a similar sensitivity to several DHP's and also to the PAA, D600 (McCleskey, 1985). The list of classes of drugs which act as calcium channel inhibitors has subsequently grown to include among others, the

diphenylbutylpiperidines (Galizzi *et al.*, 1986), 1,3-diphosphonates (Rossier *et al.*, 1989) and aminoalkynyldithianes (Adams *et al.*, 1991). Because of their inhibitory effects on L-type Ca^{2+} channel activity in both cardiac and smooth muscle, these Ca^{2+} channel blockers are currently amongst the most prescribed drugs in cardiovascular disease, treating hypertension, stable and unstable angina, and myocardial infarction.

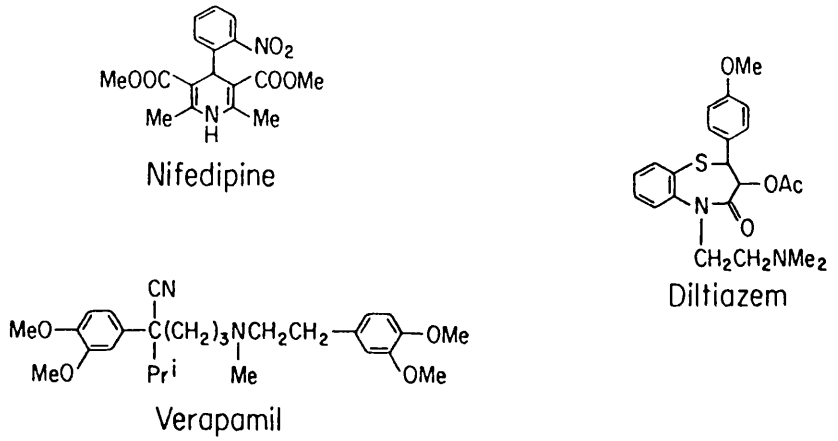

Fig. 1.5 Diagram of molecular structure of drugs from the DHP, PAA and BTA classes.

Although no known antagonist completely blocks the L-type Ca^{2+} channel, some are extremely potent. The DHP's have been shown to block the channel in the concentration range 10^{-9}-10^{-7}M (Fosset *et al.*, 1983). High affinity binding of [^{3}H]nitrendipine to its receptor has been observed with a dissociation constant for the complex formed in brain, cardiac and smooth muscle tissue in the range 0.05-1nM, while this value is in the range 1.4-4.0μM for antagonists from other classes including the PAA, verapamil (Fosset *et al.*, 1983). These ligands appear to bind more tightly to an inactivated state of the channel favoured by depolarization (Sanguinetti and Kass, 1984; Bean, 1984; Hosey and Lazdunski, 1988). This high affinity binding was found to be Ca^{2+} dependent (Sanguinetti and Kass, 1984) although very low levels, of the order of 1μM Ca^{2+}, were enough to allow full demonstration of binding. Binding was noncompetitively inhibited by divalent cations like Ni^{2+}, Co^{2+} and Mg^{2+} (Fosset *et al.*, 1983). Ca^{2+} binding to high, or Mg^{2+}

binding to low, affinity sites on the extracellular side of both skeletal and cardiac muscle Ca^{2+} channel apparently allosterically regulates DHP binding (Ebata *et al.*, 1990; Staudinger *et al.*, 1991), while binding of BTA (Knaus *et al.*, 1992) and PAA (Schneider *et al.*, 1991; Knaus *et al.*, 1992) is inhibited by Ca^{2+}.

The functional significance of the [^{3}H]DHP-labelled site is indicated by a correlation in the order of the potency of DHP Ca^{2+} antagonists in inhibiting [^{3}H]DHP binding with their inhibition of smooth muscle contraction (Belleman *et al.*, 1983; Bolger *et al.*, 1983). A significant correlation between the negative inotropic effects of verapamil and its analogues in heart and their ability to inhibit [^{3}H]D888 binding has been observed (Goll *et al.*, 1986). Similarly, a functional correlation for drugs known to interact with the [^{3}H]diltiazem binding site within the Ca^{2+} channel and their allosteric modulation of [^{3}H]nitrendipine binding has been demonstrated recently with respect to their inhibition of spontaneous myogenic activity in rat portal vein (Schoemaker *et al.*, 1987).

The distinct sites of interaction of DHP (Bolger *et al.*, 1982; Ehrlert *et al.*, 1982; Ferry and Glossmann, 1982; Murphy *et al.*, 1983; Fosset *et al.*, 1983; Boles *et al.*, 1984), PAA (Goll *et al.*, 1984; Galizzi *et al.*, 1984) and BTA (Balwierczak *et al.*, 1987; Schoemaker *et al.*, 1987) antagonists with the α_1 subunit show pharmacological specificity. These three binding sites, which appear to be present in a 1:1:1 stoichiometry (Galizzi *et al.*, 1986; Barhanin *et al.*, 1987) interact allosterically with each other (Schoemaker and Langer, 1989; Murphy and Tuana, 1990). The binding of [^{3}H]nitrendipine has been shown to be inhibited uncompetitively by the PAA verapamil (Ehrlert *et al.*, 1982; Ferry and Glossmann, 1982; Murphy *et al.*, 1983; Boles *et al.*, 1984), while stimulated at physiological temperature and inhibited at low temperature by diltiazem (De Pover *et al.*, 1982; Boles *et al.*, 1984). Competitive studies of verapamil and diltiazem indicated that the effects of these two drugs on [^{3}H]nitrendipine binding are mutually exclusive (Boles *et al.*, 1984). Thus, the DHP binding site is allosterically affected by spatially related binding sites for PAA and BTA.

Diltiazem and verapamil or desmethoxyverapamil have been shown, by direct

measurements of specific binding, to bind to two distinct sites both in t-tubules (Glossmann *et al.*, 1985) and in cardiac plasma membranes (Garcia *et al.*, 1986), that have negative allosteric interactions. Binding of diltiazem enhanced the binding of DHP's and slowed their dissociation through allosteric interactions, while verapamil decreased DHP binding and allosterically enhanced its dissociation (Glossmann *et al.*, 1985). The binding of the PAA (-)-desmethoxyverapamil to t-tubules was seen to be inhibited in a mixed noncompetitive fashion by the BTA, d-cis-diltiazem and the DHP, (+)-PN200-110 (Goll *et al.*, 1984), while (+)-PN200-110 inhibits binding of a fluorescently labelled PAA, DMBODIPY-PAA to purified Ca^{2+} channels (Knaus *et al.*, 1992).

1.9.4 Ca^{2+} channel-specific neurotoxins

A peptide, ω-CgTx, consisting of 27aa, isolated from the venom of the fish-hunting marine snail *Conus geographus* (Olivera *et al.*, 1984; 1985), has been demonstrated to cause irreversible, persistent and direct inhibition of N-type (McCleskey *et al.*, 1987; Kasai *et al.*, 1987) Ca^{2+} channels in vertebrate neurons. Reversible block of a subclass of N-type channels has now also been reported (Plummer *et al.*, 1989). This toxin also blocked L-type Ca^{2+} channels in vertebrate neurons but had no effect on these channels in smooth, cardiac or skeletal muscle or on neuronal T-type channels (McCleskey *et al.*, 1987). The toxin was shown to interact with a single class of binding sites in chick and rat brain synaptosomes with a K_d of 0.8-2 pM (Barhanin *et al.*, 1988). The site of toxin binding on neuronal L-type channels is distinct from the DHP binding domain (Abe *et al.*, 1986; Cruz and Olivera, 1986; Rivier *et al.*, 1987) and it binds and inhibits channels with picomolar-nanomolar affinity (Reynolds *et al.*, 1986; Cruz and Olivera, 1986; Rivier *et al.*, 1987).

Along with the polyamine fraction, P-type currents are also blocked by a number of toxin of a second class from funnel web spider venom, the peptide ω-agatoxins (I-IV) (Llinas *et al.*, 1989; Regan *et al.*, 1991; Regan, 1991; Mintz *et al.*,

1992). The most potent of these is ω-aga-IIIA which preferentially blocks P-type channels, (as does ω-aga-IIA), and also inhibits synaptosomal N-type neuronal Ca^{2+} channels, several times more potently than ω-CgTx. Type II and type III, but not type I toxin, shares a common binding domain with ω-CgTx in these channels (Venema *et al.*, 1992). ω-aga-IIIA selectively blocks L-type channels in myocardial cells (Cohen *et al.*, 1992) and inhibits L-type channels of cardiac muscle and L- and N-type currents of sensory neurons (Mintz *et al.*, 1991). This toxin was later found to block P-type Ca^{2+} channels potently in rat Purkinje neurons and to selectively block P-type channels over the N- and L-type channels in dorsal root ganglion (DRG) neurons (Mintz *et al.*, 1992). ω-aga-IVA was seen to be a potent inhibitor of Ca^{2+} entry into rat brain synaptosomes (Llinas *et al.*, 1989) and of high-threshold P-type Ca^{2+} currents in rat Purkinje neurons which are resistant to ω-CgTx and DHP (Llinas *et al.*, 1989; Regan *et al.*, 1991; Regan, 1991).

1.9.5 Purification and characterization of Ca^{2+} channels

1.9.5.1 Skeletal muscle channel

The availability of [^{3}H]nitrendipine as a probe for the Ca^{2+} channel allowed its first reported purification to be carried out by Curtis and Catterall, in 1984, using rabbit skeletal muscle t-tubules, solubilized in digitonin. Later the DHP probe (+)[^{3}H]PN200-110 was employed by the same group (Curtis and Catterall, 1985) and others (Borsotto *et al.*, 1984; Flockerzi *et al.*, 1986b; Striessnig *et al.*, 1986), and also the labelled DHP drugs [^{3}H]azidopine (Striessnig *et al.*, 1986), [^{3}H]nimodipine (Kanngiesser *et al.*, 1988) and the PAA (-)[^{3}H]azidopamil (Hosey *et al.*, 1987), in further reported purifications of this DHP receptor.

The initial reported 330-fold purification of this DHP receptor was achieved by sedimentation through sucrose density gradients, followed by ion-exchange chromatography using a deoxyethylaminoethyl (DEAE)-Sephadex column and affinity

chromatography on a WGA-Sepharose column. Sodium dodecylsulphate/ polyacrylamide gel electrophoresis (SDS/PAGE), under nonreducing conditions, revealed the presence of at least three channel polypeptide components designated α, ß and γ, having M_r values, 167,000, 54,000 and 30,000 (Curtis & Catterall, 1984). Upon reduction, the α band was converted into two clearly resolved components with apparent molecular masses of 175,000 and 143,000. These were subsequently shown to be two distinct channel subunits, now designated α_1 and α_2, having similar sizes but very different properties (Takahashi *et al.*, 1987). α_2, γ and two other polypeptides at 24,000-27,000 (δ), are glycosylated, with α_2 and γ having core polypeptide size of 105,000 and 20,000, respectively (Burgess and Norman, 1989; Catterall *et al.*, 1989). δ, which appears under reducing conditions and is detectible by silver staining following SDS/PAGE, is now known to be derived from α_2 (De Jongh *et al.*, 1990). Only the α_1 and γ polypeptides were prominently labelled with the hydrophobic probe [^{125}I]-3-(trifluoromethyl)-3-(m-iodophenyl)diazirine ([^{125}I]-TID), identifying them as the principal transmembrane components in the purified Ca^{2+} channel complex (Catterall *et al.*, 1989).

1.9.5.2 Brain and Cardiac channel

Solubilized skeletal and smooth muscle, heart and brain DHP receptor complexes, and brain ω-CgTx-receptor complex had similar sedimentation coefficient of 19-20S, in sucrose density gradients, indicating that they have similar sizes (Curtis and Catterall, 1983; Catterall *et al.*, 1989; Rosenberg *et al.*, 1989). The solubilized DHP receptor from skeletal muscle and brain also contained binding sites for the PAA, verapamil and the BTA, diltiazem, and were seen to be specifically adsorbed to and eluted from lectin affinity columns (Curtis and Catterall, 1983, 1984; Glossmann and Ferry, 1983; Borsotto *et al.*, 1984) indicating the presence of at least one channel glycoprotein.

1.9.5.2.1 Cardiac

The cardiac DHP receptor, of much lower membrane abundance than its skeletal muscle counterpart (Fosset *et al.*, 1983; Glossmann *et al.*, 1983), has been purified, from bovine (Schneider and Hofmann, 1988), porcine (Haase *et al.*, 1991; Tokumaru *et al.*, 1992) and chick (Cooper *et al.*, 1987; Chang and Hosey., 1988) cardiac membranes. The channel comprised of two large polypeptides of similar size and electrophoretic behaviour to the skeletal muscle channel α_1 and α_2 subunits, having M_r values in the range 185-195,000 and 140-155,000, under reducing, and 185-195,000 and 174-180,000, under nonreducing conditions, respectively. Polypeptides were observed in some purifications, upon reduction of the smaller channel polypeptide, having M_r values 29-32,000 (Cooper *et al.*, 1987) and 20,000 (Tokumaru *et al.*, 1992), while 50, and 30,000 polypeptides copurified with the larger subunit (Haase *et al.*, 1991). The DHP receptor was shown to be contained in the larger polypeptide (Ferry *et al.*, 1987), which was found to be structurally and immunologically distinct from the skeletal muscle α_1 subunit (Takahashi and Catterall, 1987a; Chang and Hosey, 1988). The smaller polypeptide showed immunological cross-reactivity with skeletal muscle preparations, indicating that these α_2 polypeptides are structurally similar.

1.9.5.2.2 Brain

Brain Ca^{2+} channels have also shown reactivity with anti-skeletal muscle α_2/δ antibodies (Takahashi and Catterall., 1987b; Hayakawa *et al.*, 1990; Tokumaru *et al.*, 1992). In one of these studies, the polypeptide, immunoprecipited from solubilized rat brain synaptic plasma membranes, was also electrophoretically similar to skeletal muscle channel α_2, having M_r values of 169,000, following SDS/PAGE under non-reducing conditions, and of 140,000, under reducing conditions (Takahashi and Catterall., 1987b). These studies revealed the presence of an α_1/α_2 brain channel complex, while rabbit brain DHP-sensitive Ca^{2+} channel was shown to consist of α_1,

α_2/δ and ß polypeptides having apparent molecular mass, following SDS/PAGE, of 166,000, 166,000 and 57,000, respectively, under non-reducing, and of 175,000, 142,000 and 57,000, under reducing conditions (Ahlijanian *et al.*, 1990).

The ω-CgTx-receptor, purified to apparent homogeneity from rat forebrain, comprised two large 230,000 and 140,000 subunits along with 110, 70 and 60,000 polypeptides, as determined by SDS/PAGE, under reducing conditions (McEnery *et al.*, 1991). An ^{125}I-ω-CgTx binding brain complex consisting of five polypeptides with similar M_r values, had previously been shown to react with antibodies which recognize the α_2 and ß subunits of the skeletal muscle DHP receptor and the cardiac Ca^{2+} channel α_1. These antibodies recognized the 140,000, both the 60 and 70,000, and the 230,000 M_r value components, respectively (Sakamoto and Campbell, 1991a, 1991b). Thus, as expected, both brain N-type, ω-CgTx-sensitive (Ahlijanian *et al.*, 1991; Pragnell *et al.*, 1991) and L-type, DHP-sensitive (Ahlijanian *et al.*, 1990) Ca^{2+} channels are multisubunit proteins containing polypeptides resembling those designated α_1, α_2 and ß in muscle L-type channel isoforms.

1.9.6 Functional studies of purified channel

Functional reconstitution of L-type Ca^{2+} channel activity following purification has been demonstrated (Curtis and Catterall, 1986; Flockerzi *et al.*, 1986a; Smith *et al.*, 1987; Talvenheimo *et al.*, 1987; Hymel *et al.*, 1988; Horne *et al.*, 1988), revealing a single channel conductance, sensitive to activation by BAY K 8644 and inhibition by Ca^{2+} channel antagonists, of 20pS in 90mM Ba^{2+}, while phosphorylation of the channel by cAMP-dependent protein kinase increased the probability of channel opening (Curtis and Catterall, 1986; Flockerzi *et al.*, 1986a; Hymel *et al.*, 1988). Skeletal and cardiac muscle α_1 subunits have been seen to be basally phosphorylated on cAMP-dependent phosphorylation sites and are phosphorylated in response to the presence of cAMP-dependent protein kinase or increased intracellular cAMP, stimulating DHP-sensitive Ba^{2+} currents (Lai *et al.*, 1990; Yoshida *et al.*, 1992). Phosphorylation of the channel ß subunit by protein kinase A (PKA) has also been

observed (Nunoki *et al.*, 1989; Chang *et al.*, 1991) to stimulate Ca^{2+} uptake. α_1 is preferentially targeted by PKA in intact muscle (Mundina-Weilenmann *et al.*, 1991), and is also phosphorylated to a 2-5-fold greater extent than ß by PKA, protein kinase C (PKC) and calmodulin (CaM) protein kinase, with phosphorylation by both PKA and PKC causing channel activation in purified t-tubule membranes (Chang *et al.*, 1991).

1.9.7 Elucidation of the primary structure of Ca^{2+} channel subunits by cDNA cloning

1.9.7.1 α_1 subunit

The primary structure of the α_1 subunit of the DHP receptor from rabbit skeletal muscle was deduced, subsequent to its purification, by cDNA cloning and sequencing (Tanabe *et al.*, 1987), revealing a polypeptide containing 1,873 aa residues. The polypeptide is approx 30% identical to the voltage-dependent Na^+ channel in its amino acid sequence and so has been proposed to possess the same putative transmembrane topology. In particular, the protein has four homologous domains each with six putative membrane-spanning segments, with the fourth transmembrane region in each domain containing an arginine or lysine residue at every third or fourth position. Subsequently, the sequence of the α_1 subunit of the rabbit cardiac muscle L-type Ca^{2+} channel isoform was deduced (Mikami *et al.*, 1989). It is homologous to the skeletal muscle α_1 sequence but, consisting of 2,171 aa, has longer N- and C-terminal segments. Primary structures for α_1 polypeptides from rabbit lung (Biel *et al.*, 1990) and brain (Mori *et al.*, 1991; Niidome *et al.*, 1992; Fujita *et al.*, 1993) have more recently been reported.

Following the elucidation of the two rabbit muscle α_1 sequences, Snutch *et al.* (1990) isolated and characterized several rat brain Ca^{2+} channel cDNA's. They were grouped into four different classes (A, B, C and D) according to distinct hybridization

patterns with rat brain mRNA's of (8.3 and 8.8)kb, 10kb, (8.0 and 12)kb and finally 9.5kb, respectively, in Northern blots. Members of the four classes of cDNA were also shown to hybridize to unique patterns of rat genomic DNA in Southern blots, suggesting that each of the four classes of cDNA is encoded by a distinct gene or gene family. The expression of at least four different Ca^{2+} channel genes in rat brain was therefore confirmed by the finding that cDNA's that were assigned to a particular class through Northern analysis, also showed a similar banding pattern to genomic DNA in Southern blots and by the partial amino acid sequences of the products of DNA from each class, derived from DNA sequencing.

Full length cDNA's encoding rat brain Ca^{2+} channels of each of these four classes have now been isolated and characterized (Starr *et al.*, 1991; Snutch *et al.*, 1991; Hui *et al.*, 1991; Dubel *et al.*, 1992), along with cDNA encoding a class E channel (Soong *et al.*, 1993). Class A and B clones are homologous to each other but are less closely related to the skeletal and cardiac clones (33% identical for A) than C and D. The two class C α_1 polypeptides are 95% identical to both the rabbit heart and lung and 70% homologous to the skeletal muscle α_1 subunit. D class α_1 subunits show 71% and 76% similarity to the skeletal and cardiac muscle protein, respectively. Class E polypeptide is most closely related to class A and class B, with which it has 54% identity. The other Ca^{2+} channel α_1 subunits sequences determined to date are from mouse brain (Ma *et al.*, 1992), rat aorta (Koch *et al.*, 1990), carp skeletal muscle (Grabner *et al.*, 1991) and human (Seino *et al.*, 1992) and hamster (Yaney *et al.*, 1992) pancreatic ß cell, along with both human neuronal L-type (Williams *et al.*, 1992a) and N-type (Williams *et al.*, 1992b) α_1 polypeptides.

These polypeptides (aligned in Fig. 3.1) range in size between 1634 aa (rat brain D-type) and 2336 aa (rat brain B-type) and 2339 aa (human neuronal 1B-1). They all have the same pattern of putative transmembrane segments and notably, the S4 segment is highly conserved between α_1 polypeptides and in each of the four homologous regions of individual channel α_1 subunits.

1.9.7.2 Minor subunits

1.9.7.2.1 Skeletal muscle L-type channel subunits

Studies of the biochemical properties and functional reconstitution of purified skeletal muscle Ca^{2+} channels (Catterall *et al.*, 1988; Glossmann and Striessnig, 1990; Hosey and Lazdunski, 1988; Campbell *et al.*, 1988; Hofmann *et al.*, 1988; Vaghy *et al.*, 1988) have pointed to a complex multisubunit structure for this protein (Takahashi *et al.*, 1987). Combinations of protein chemistry and cDNA cloning experiments have defined the primary structures of the remaining four subunits α_2, ß, γ and δ of the skeletal muscle L-type Ca^{2+} channel (Ellis *et al.*, 1988; Ruth *et al.*, 1989; Bosse *et al.*, 1990; Jay *et al.*, 1990; De Jongh *et al.*, 1990). Points of interaction between subunits are not known, but specific association of the α_1, α_2/δ, ß subunits as a complex is supported by copurification (Curtis and Catterall, 1984; Takahashi *et al.*, 1987; Catterall *et al.*, 1988; Glossmann and Striessnig, 1990; Hosey and Lazdunski, 1988; Campbell *et al.*, 1988; Hofmann *et al.*, 1988; Vaghy *et al.*, 1988) and by coimmunoprecipitation with antibodies directed against each of the individual subunits (Takahashi *et al.*, 1987; Leung *et al.*, 1987, 1988; Sharp and Campbell, 1989; Ahlijanian *et al.*, 1990).

1.9.7.2.2 α_2 and δ subunits

The skeletal muscle L-type channel α_2/δ polypeptide was seen to have immunological and electrophoretic properties similar to polypeptides present in both brain (Takahashi and Catterall., 1987b; Sakamoto and Campbell, 1991a) and cardiac (Schmid *et al.*, 1986a, 1986b; Vandaele *et al.*, 1987) preparations. As outlined above (Section 1.9.5), this polypeptide has been identified in various preparations as a component of M_r 167,000 (skeletal muscle), 169,000 (brain) and 170,000-180,000 (cardiac muscle), under nonreducing conditions. The reduction in M_r of this polypeptide to 143,000 (skeletal muscle) and 140,000 (cardiac and brain) coupled

with the appearance of peptides of M_r 20,000-32,000 (Cooper *et al.*, 1987; Tokumaru *et al.*, 1992) in cardiac, and 24-27,000 (Curtis and Catterall, 1984) in skeletal muscle preparations, under reducing conditions, indicates the existence of an α_2/δ complex in all three tissue types.

The mRNA transcript that encodes α_2 was later shown to be present in all tissues expressing Ca^{2+} channels (Ellis *et al.*, 1988). Subsequently, it was observed that skeletal muscle α_2 and δ are derived from the same primary transcript, with δ arising, as a result of proteolysis, from the C-terminal end of the α_2/δ polypeptide (De Jongh *et al.*, 1990). The cDNA sequences of α_2/δ polypeptides from human neuronal tissue (Williams *et al.*, 1992a), rat brain (Kim *et al.*, 1992) and rabbit skeletal muscle (Ellis *et al.*, 1988) have now been deduced. Both brain and muscle polypeptide isoforms are produced by alternative splicing of a single primary transcript (Ellis *et al.*, 1988; Kim *et al.*, 1992). The cloned rat brain and skeletal muscle polypeptides contain 51 non-identical amino acids, while the human neuronal and rat brain isoforms, contain just 43 non-identical amino acids. It thus appears that α_2 subunits expressed in various tissues are highly similar.

α_2 was predicted to contain two, and δ, a single membrane spanning domain (Ellis *et al.*, 1988). However, a reduction in the quantity of α_2 in a microsomal membrane preparation was observed, following extraction of the membranes at pH 11, under reducing conditions (Jay *et al.*, 1991). These conditions have been seen to cause solubilization of peripheral, but not integral erythrocyte membrane proteins (Steck and Yu, 1973). Therefore, the above finding, coupled with observed glycosylation of α_2 (Burgess and Norman, 1989; Catterall *et al.*, 1989), suggest that this polypeptide is extracellular being anchored to the membrane via disulfide interaction with δ, which has a single membrane spanning domain.

1.9.7.2.3 ß subunit

The M_r values for purified ß polypeptides reveal a similar size for the skeletal (53,000) and cardiac (50,000) muscle isoforms, with a larger ß subunit associated

with both the DHP (57,000) and ω-CgTx (60 and 70,000) receptors from brain. The latter subunit is immunologically similar to that found in skeletal muscle (Sakamoto and Campbell, 1991a, 1991b). Using the skeletal muscle ß subunit as probe in Northern blots, a cross-hydridizing species was detected in brain poly(A)$^+$ RNA but not heart (Ruth *et al.*, 1989; Kim *et al.*, 1990b).

To date, the amino acid sequences of fifteen ß polypeptide isoforms have been determined, including one from both rabbit (Ruth *et al.*, 1989) and human (Powers *et al.*, 1992) skeletal muscle. The human skeletal muscle cDNA encodes a protein of 523 aa which is 97% identical to the rabbit skeletal muscle ß subunit. A further three human ß subunit cDNA's have been isolated from a human hippocampal cDNA library (Powers *et al.*, 1992; Williams *et al.*, 1992a) and four rat brain ß isoforms, namely, rtß$_{1b}$ (Pragnell *et al.*, 1991), rtß$_2$ (also present in rat heart) (Perez-Reyes *et al.*, 1992), rtß$_3$ (Castellano *et al.*, 1993a) and rtß$_4$ (Castellano *et al.*, 1993b), consisting 597, 604, 484 and 519 amino acids, respectively, have now also been cloned. cDNA encoding three distinct ß polypeptides from both rabbit (Hullin *et al.*, 1992) and human (Collin *et al.*, 1993) heart have also been isolated. Rabbit CaB2a (identical to rtß$_2$) and CaB2b are splicing products from a common primary transcript (CaB2). CaB2 is predominantly expressed in heart, aorta and brain, whereas CaB3 is most abundant in brain but also present in aorta, trachea, lung, heart and skeletal muscle, as revealed by Northern blot analysis. An alignment of known amino acid sequences (not shown) has illustrated the high degree of sequence similarity amongst these ß polypeptides, which are predicted to have an intracellular location.

1.9.7.2.4 γ subunit

Northern blot analysis indicates that this skeletal muscle γ subunit is only expressed in skeletal muscle, and possibly in lung (Jay *et al.*, 1990; Bosse *et al.*, 1990). A single reported cardiac channel purification has revealed a 30kDa band following SDS/PAGE (Haase *et al.*, 1992). Interestingly, skeletal muscle γ subunit has recently been shown to determine the inactivation properties of cardiac α_1

polypeptide expressed in *Xenopus* oocytes, irrespective of the combination of other subunits present (Singer *et al.*, 1991). It is therfore likely that a γ polypeptide is necessary for normal cardiac channel function.

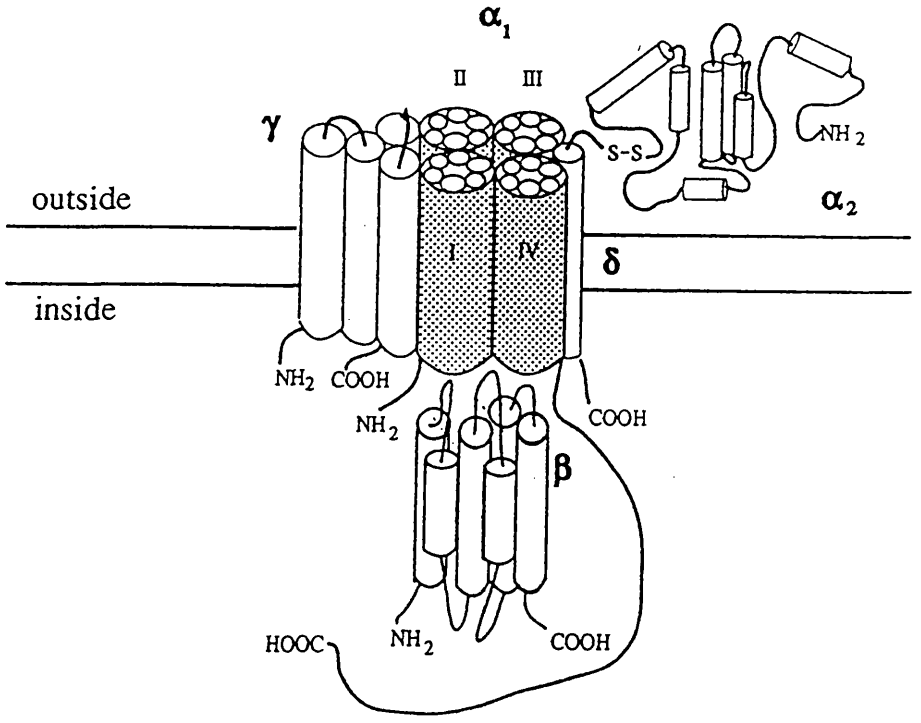

Fig. 1.6 Proposed model for the arrangement of the skeletal muscle L-type channel in the membrane.

1.9.8 Role of the individual subunits in Ca^{2+} channel function

1.9.8.1 Location of inhibitor binding sites

The α_1 polypeptide of the purified channel complex is now known to bind the Ca^{2+} channel antagonists. It was identified as the receptor for DHP binding, by photoincorporation of [^{3}H]azidopine and (+)-PN200-110, into membranes and isolated channel from both skeletal (Striessnig *et al.*, 1986; Galizzi *et al.*, 1986; Vaghy *et al.*, 1987; Sharp *et al.*, 1987) and cardiac (Ferry *et al.*, 1987; Vaghy *et al.*, 1987; Tokumaru *et al.*, 1992) muscle. These studies revealed DHP binding in a channel component of M_r value 155-179,000 and M_r 165-195,000, in the respective

tissues. Incorporation of PAA's (Galizzi *et al.*, 1986; Striessnig *et al.*, 1987; Vaghy *et al.*, 1987; Hosey *et al.*, 1987) and of the BTA's d-cis [^{3}H]diltiazem and (+)-cis-azidodiltiazem (Hosey *et al.*, 1987; Striessnig *et al.*, 1990) into the same skeletal muscle polypeptide has also been observed. In guinea-pig hippocampal membranes, [^{3}H]azidopine and [N-methyl-^{3}H]LU49888 were seen to photoincorporate into a 195 kDa protein component (Striessnig *et al.*, 1988).

Because these classes of antagonist have such a profound effect on channel function localization of their binding domains in the α_1 subunit, was undertaken. The PAA's D600 (methoxyverapamil) and D890 (a quaternary derivative) have both been shown to bind at the intracellular surface of the channel in guinea pig myocytes and cat ventricular trabeculae (Hescheler *et al.*, 1982). Subsequently, Ebata *et al.*, (1990) only observed Ca^{2+}-, Mg^{2+}- and chelator-dependent binding of the DHP PN200-110 to right-side-out skeletal muscle microsome vesicles. Similarly, DHP derivatives amlodipine and SDZ 207-180, which are charged and membrane-impermeable caused voltage-dependent block of Ca^{2+} channels on extracellular, but not on intracellular application (Kass *et al.*, 1991). More recently, a membrane-impermeable BTA ligand has been reported to bind to an extracellular domain in the L-type Ca^{2+} channel (Hering *et al.*, 1993). These studies revealed an extracellular orientation for both the DHP and BTA sites, while PAA ligands were seen to bind cytoplasmically.

A theoretical study of the precise location of the DHP binding site suggested it may be on the S4 putative voltage sensor, as the molecule shows high affinity for the inactivated state, leading to the proposal that DHP's may dock between Arg^{531} and Arg^{534} in the IIS4 putative transmembrane helix (Langs *et al.*, 1990b). Direct evidence for the location of the binding site was subsequently obtained by isolating and sequencing radiolabelled peptide fragments obtained from the purified α_1 subunit following its covalent labelling with [^{3}H]nitrendipine or [^{3}H]azidopine (Regulla *et al.*, 1991). This approach indicated that the sites of labelling lay in a region between residues 1390 and 1437 of the channel protein. This region which lies just beyond the C-terminus of the last putative transmembrane helix of the protein (IVS6), is highly conserved among α_1 subunits sequenced to date. It also contains a putative Ca^{2+}-

binding domain (residues 1410-1437) which is predicted to form an EF hand structure, according to the Tufty-Kretsinger test (Babitch *et al.*, 1990). However, since it is predicted to lie on the cytoplasmic surface of the membrane, its labelling by DHP's, which act at the extracellular side of the membrane, is surprising.

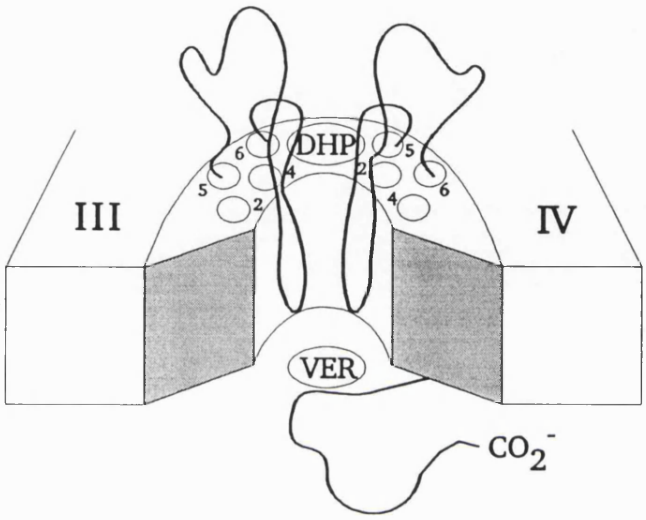

Fig. 1.7 Diagram of putative arrangement of the Ca^{2+} channel pore structure showing the proposed sites of both DHP and PAA (verapamil) binding.

A pattern of labelling more consistent with the site of action of DHP's was subsequently obtained by using site-specific anti-peptide antibodies to immunoprecipitate labelled fragments of the protein (Nakayama *et al.*, 1991). By these means sites of labelling by [^{3}H]diazipine were located both in the predicted loop linking transmembrane helices IIIS5 and IIIS6, and in transmembrane helix IVS6. A similar pattern of labelling was seen for [^{3}H]azidopine, while [^{3}H](+)-PN200-110 labelled primarily IIIS6 and IVS6 (Striessnig *et al.*, 1991). It therefore seems likely that the binding site is formed by close apposition of the predicted extracellular loop between IIIS5 and IIIS6, and the extracellular end of helix IVS6. The binding site probably involves primarily helices IIIS6 and IVS6, while the IIIS5-IIIS6 loop may interact with the long side chain of some DHP's such as azidopine.

Using the PAA receptor selective ([N-methyl-^{3}H] LU49888), the site of PAA binding was similarly, previously located to a domain of the channel including IVS6

and eight residues at both its intracellular and extracellular ends. Since the PAA receptor site is only accessible to the cytoplasmic side of the membrane, this study located the binding site of the label at the intracellular end of IVS6 and its adjacent amino acid residues (Striessnig *et al.*, 1990b). This domain is situated close to the highly conserved α_1(1390-1437) region with its proposed Ca^{2+}-binding domain.

The physical localization of the regions in the primary structure of α_1 involved in the binding of BTA antagonists, ω-CgTx, polyamines and ω-agatoxins have not been achieved to date.

1.9.8.2 Probing subunit function via expression

cDNA's, or the corresponding mRNA's encoding muscle L-type Ca^{2+} channel α_1 subunits can direct expression of functional voltage-gated Ca^{2+} channels in recipient *Xenopus* oocytes or mammalian L cells (Mikami *et al.*, 1989; Perez-Reyes *et al.*, 1989), and can restore both Ca^{2+} currents and E-C coupling in myocytes from mice having the muscular dysgenesis mutation, which disrupts the endogenous α_1 gene (Tanabe *et al.*, 1988). mRNA encoding the α_1 polypeptides from both rabbit lung (Biel *et al.*, 1990) and brain (Mori *et al.*, 1991) and rat aorta (Itagaki *et al.*, 1992) have also produced functional Ca^{2+} channels in *Xenopus* oocytes. However, the amount of current and the number of high affinity binding sites for DHP's produced by expression of the rabbit muscle α_1 subunit isoforms in these cells are very low, while activation kinetics are 100 times slower than expected for skeletal muscle Ca^{2+} channel currents (Lacerda *et al.*, 1991), and inactivation is also delayed at the depolarizing test potential (Kim *et al.*, 1990b). The time course and voltage-dependence of Ca^{2+} channel gating also differs sharply from those observed in the native channels. The currents obtained on expression of brain α_1 polypeptide is similarly low, unless it is coexpressed with α_2/δ and ß subunits from skeletal muscle (Mori *et al.*, 1991). Similarly, the expression of the α_1 polypeptide from both the DHP- and ω-CgTx-sensitive human neuronal L-type channel in oocytes, and N-type channel in HEK293 cells, failed to produce a functional channel, unless both the α_2/δ

and ß neuronal polypeptides were simultaneously expressed (Williams *et al.*, 1992a, 1992b).

1.9.8.2.1 α_2/δ subunit

Coexpression of skeletal muscle α_2/δ complex was found in separate studies to substantially increase both the amount and amplitude of Ca^{2+} current in oocytes expressing the cardiac or aorta α_1 subunit (Mikami *et al.*, 1989; Singer *et al.*, 1991; Itagaki *et al.*, 1992) and to accelerate activation of the expressed channel such that its kinetics resembled those characteristic of the native channel (Singer *et al.*, 1991). The combination of both the α_2/δ and ß subunits, but neither subunit alone, shifted the voltage-dependence of Ca^{2+} channel activation, seen with the expressed α_1 subunit, to more negative membrane potentials and strongly accelerated the current decay (Singer *et al.*, 1991). The currents obtained in oocytes, following expression of rabbit lung α_1 (Biel *et al.*, 1990), and upon injection of mRNA for the brain DHP-insensitive Ca^{2+} channel α_1 subunit (Mori *et al.*, 1991), were both enhanced by the presence of skeletal muscle α_2, without alteration of kinetics. It thus appears that α_2/δ is necessary for both normal expression and stability of α_1.

1.9.8.2.2 ß subunit

Many studies have shown that coexpression of the Ca^{2+} channel ß subunit has profound effects on the channel properties of α_1 subunits expressed in a variety of systems. A chief observation was that of increased functional expression of α_1 in the presence of ß. Skeletal muscle ß enhanced expression of aortic and cardiac α_1 polypeptide in *Xenopus* oocytes (Singer *et al.*, 1991; Wei *et al.*, 1991; Itigaki *et al.*, 1992) and of skeletal muscle α_1 in L cells (Varadi *et al.*, 1991), while cardiac α_1 expression in oocytes was also enhanced by three distinct cardiac ß polypeptides (Hullin *et al.*, 1992) and also a brain ß subunit (Perez-Reyes *et al.*, 1992). Similarly, the current induced in oocytes by DHP-insensitive Ca^{2+} channel α_1 subunit mRNA

was increased by two orders of magnitude by coinjection of skeletal muscle ß subunit (Mori *et al.*, 1991). Interestingly, expression of both a DHP- and ω-CgTx-sensitive L-type and an N-type ω-CgTx-sensitive Ca^{2+} current were completely dependent on coexpression of the human neuronal β subunit (Williams *et al.*, 1992a, 1992b).

Skeletal muscle ß subunit causes normalization of activation kinetics of expressed skeletal muscle α_1 subunit in L cells (Lacerda *et al.*, 1991). Cardiac α_1 expressed in oocytes was influenced differently by various ß isoforms. Skeletal muscle ß accelerated activation and shifted its voltage dependence to slightly more negative membrane potentials, with the latter effect enhanced by presence of α_2/δ (Singer *et al.*, 1991; Wei *et al.*, 1991; Itigaki *et al.*, 1992). Coexpression with two cardiac ß subunits accelerated channel activation kinetics, while in one case reducing α_1 sensitivity to the activator Bay K 8644 (Hullin *et al.*, 1992). A brain ß subunit caused a large increase in the peak inward current due to cardiac α_1, accelerated the channel activation kinetics and shifted the current-voltage relationship to hyperpolarizing potentials (Perez-Reyes *et al.*, 1992). In addition, when coexpressed with the ß subunit, the channel activity was found to become sensitive to cAMP. Injection of the latter into the *Xenopus* oocytes used for expression of cardiac or vascular smooth muscle Ca^{2+} channel α_1 polypeptide caused doubling of the channel current only when skeletal muscle ß polypeptide was coexpressed (Klockner *et al.*, 1992).

1.9.8.2.3 γ subunit

The skeletal muscle γ subunit has only modest effects on the expression and kinetics of the skeletal muscle α_1 subunit in L cells (Varadi *et al.*, 1991), while this γ subunit does not enhance the expression of either cardiac or brain α_1 polypeptide (Mikami *et al.*, 1989; Mori *et al.*, 1991). However, one study has revealed kinetic effects of γ, with the inactivation of currents induced by cardiac α_1 in *Xenopus* oocytes accelerated, and the voltage sensitivity of their inactivation moved to more negative membrane potentials, upon coexpression with γ; while γ determined the

inactivation properties, irrespective of the combination of other subunits present (Singer *et al.*, 1991). In this study, coexpression of all subunits was required for the cardiac Ca^{2+} channel to generate Ca^{2+} currents with a normal time course and voltage dependence (Singer *et al.*, 1991). Thus this subunit appears to have a modulatory role in channel inactivation.

The results described above show that, with the exception of γ alone, coexpression of the subunits, previously identified as components of the oligomeric Ca^{2+} channel complex, greatly enhances efficient expression of Ca^{2+} channels with normal physiological properties. The α_2/δ and β subunits interact with α_1 subunit from either cardiac or skeletal muscle to increase its expression and to restore some aspect of normal channel function. This indicates that there is direct interaction between the α_1 subunit and these subunits, which modifies the expression and functional properties of α_1. Moreover, coexpression of all subunits is required for the cardiac Ca^{2+} channel to generate Ca^{2+} currents with a normal time course and voltage dependence (Singer *et al.*, 1991). However, the rabbit brain and both human neuronal channels studied appear to function as an α_1, α_2, ß complex.

Each individual subunit has a different functional effect on skeletal muscle α_1 subunits expressed in L cells compared to cardiac α_1 subunits expressed in *Xenopus* oocytes (Singer *et al.*, 1991; Varadi *et al.*, 1991; Lacerda *et al.*, 1991; Wei *et al.*, 1991). It thus seems likely that these auxiliary subunits are not direct functional participants in voltage-dependent gating and ion conductance. Their probable role in the channel complex is to stabilize the α_1 subunit native structure, providing it with an appropriate environment in which to function while possibly modulating its function.

1.9.9 Role of Ca^{2+} channels in E-S and E-C coupling

1.9.9.1 E-S coupling

The key step in E-S coupling in presynaptic nerve terminals, the influx of Ca^{2+} through voltage-sensitive Ca^{2+} channels (Augustine *et al.*, 1987), is the trigger for the release of NT's from the nerve terminals (Katz, 1969; Llinas, 1991). The evoked release of NT in sympathetic neurons is known to be dependent on Ca^{2+} influx through the N-type channel (Hirning *et al.*, 1988), while the release of substance P from DRG neurons (Perney *et al.*, 1986; Cazalis *et al.*, 1987) and of catecholamines from chromaffin cells (Cena *et al.*, 1983) is mediated by L-type channel activation. N-type channels have also been observed to have a predominant role in presynaptic Ca^{2+} channels at amphibian (Kerr and Yoshikami, 1984), reptilian (Lindgren and Moore, 1989) and avian synapses (Rivier *et al.*, 1987; Venema *et al.*, 1992).

However, in mammalian systems, Ca^{2+} entry, neurosecretion and synaptic transmission were seen to be, at most, only partially mediated by either L- or N-type channels (Reynolds *et al.*, 1986; Horne and Kemp, 1991; Turner and Goldin, 1989; Mintz *et al.*, 1992), suggesting that the exocytotic Ca^{2+} channel at mammalian synapses is of a different subtype. More recently, P-type channels have been reported to mediate presynaptic Ca^{2+} influx and NT release in mouse neuromuscular junction and rat brain synaptosomes (Uchitel *et al.*, 1992; Mintz *et al.*, 1992), while FTX, a P-type specific blocker, was shown to be effective in blocking Ca^{2+} conductance and synaptic transmission at the squid giant synapse (Llinas *et al.*, 1989). [^{3}H]Glutamate release from rat brain synaptosomes has also been shown to be mediated by P-type channels (Turner *et al.*, 1992).

1.9.9.2 E-C coupling

As mentioned in Section 1.2.3, the mechanism by which the Ca^{2+} channel mediates E-C coupling differs between skeletal and both cardiac and smooth muscle. In cardiac and smooth muscle cells, muscle contraction was blocked on incubation of the tissue in Ca^{2+}-free medium (Fabiato, 1985; Beuckelmann and Wier, 1988; Nabauer *et al.*, 1989) indicating that Ca^{2+} entry via the L-type Ca^{2+} channel is an essential trigger for contraction. In skeletal muscle, however, depolarization of the t-tubule membrane (see Fig. 1.7, overleaf) is sufficient to initiate contraction without entry of extracellular Ca^{2+} (Armstrong *et al.*, 1972).

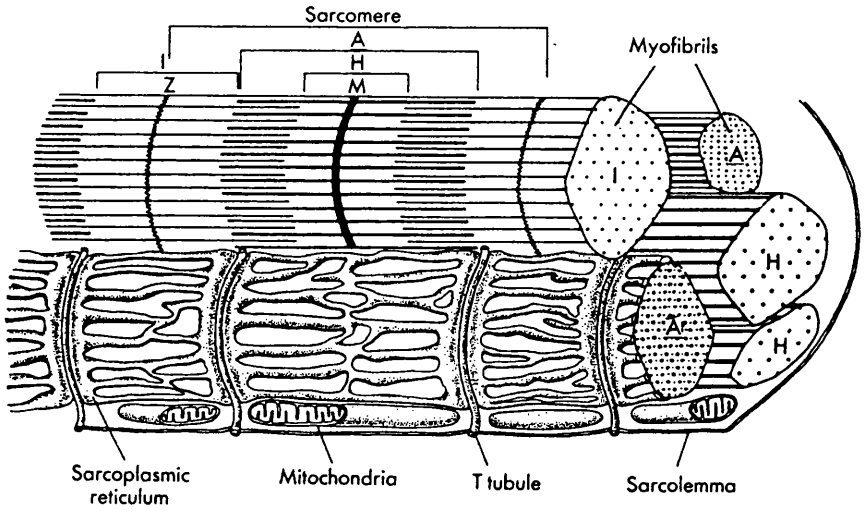

Fig. 1.8 Diagram of the architecture of a skeletal muscle cell

Much evidence has now accumulated for the direct involvement of the L-type Ca^{2+} channel in E-C coupling, acting, in the skeletal muscle t-tubule membrane, as a voltage sensor. Rios and Brum (1987) observed that, although the entry of extracellular Ca^{2+} into skeletal muscle fibres was not required for E-C coupling, both contraction of skeletal muscle and transmembrane movement of gating charge for E-C coupling were reduced by DHP's and PAA's. Another study showed that both the voltage dependence of activation of the L-type Ca^{2+} channel, and of activation of

contraction required the same range of membrane potentials, while both systems appeared to have receptors for the four classes of Ca^{2+} channel antagonists, with their relative effects on both systems being voltage-dependent (Romey *et al.*, 1988). Subsequently, E-C coupling, intramembranous current (charge movement) and slow Ca^{2+} currents, which are absent in dysgenic muscle cells, were seen to be restored by expression of the skeletal muscle L-type Ca^{2+} channel $\alpha 1$ subunit (Tanabe *et al.*, 1988; Adams *et al.*, 1990). The expression of cardiac muscle Ca^{2+} channels in the same cells produces L-type Ca^{2+} current and cardiac type E-C coupling (Tanabe *et al.*, 1990a). Later, expression of various chimaeric channel α_1 subunit cDNA's in dysgenic myotubes revealed that the loop between homologous domains II and III of the skeletal muscle α_1 polypeptide is directly involved in skeletal E-C coupling and thus, in the mechanism of function of the voltage sensor (Tanabe *et al.*, 1990b).

The mechanism by which the electrical stimulus is converted into muscle contraction is currently understood to occur as follows. Depolarization of the presynaptic membrane of the neuromuscular junction causes release of ACh which in turn initiates an action potential in the postsynaptic (muscle) membrane via activation of ACh receptors. In cardiac muscle, Ca^{2+} channels open in response to depolarization of the cell membrane and the ensuing influx of Ca^{2+} immediately signals the cell to contract. In skeletal muscle, following the depolarization of the muscle plasmalemma, the action potential is conducted along the t-tubule system. The L-type channels which are clustered in the t-tubule membranes, at the regularly spaced triads, function in physically communicating this depolarization directly to the ryanodine receptors (calcium release channels) in the terminal cisternae of the sarcoplasmic reticulum (SR), which are also located at the triad junction. This causes the ryanodine receptors to open, releasing Ca^{2+} into the sarcolemma, which in turn signals contraction. Depolarization-induced Ca^{2+} release from SR in isolated triads has been previously shown to be controlled by the attached t-tubule (Ikemoto *et al.*, 1984) and inhibition of the slow phase of the depolarization-induced release of Ca^{2+} from SR, has been observed by DHP's (Ohkusa *et al.*, 1991a) and also by an antibody raised against the α_1 subunit of the Ca^{2+} channel (Ohkusa *et al.*, 1990),

supporting the view that this function is mediated by the L-type channel.

1.9.9.3 Ca^{2+} channel as skeletal muscle voltage sensor

Two size forms of the Ca^{2+} channel α_1 subunit have been identified in purified preparations of skeletal muscle channel, t-tubules membranes and intact skeletal muscle cells in culture (De Jongh *et al.*, 1989; Lai *et al.*, 1990). The larger, previously undescribed, 212kDa form corresponds to the predicted size for the full length product of the sequenced α_1 subunit cDNA and constitutes less than 10% of expressed α_1 in skeletal muscle (De Jongh *et al.*, 1989, 1991). The 175kDa polypeptide corresponds to the α_1 subunit obtained in purifications of the channel, and is derived from the 212kDa polypeptide by the proteolytic cleavage of its C-terminus between amino acid residues 1685 and 1699 (De Jongh *et al.*, 1991). Only about 5% of skeletal muscle DHP receptor sites in muscle fibres or purified preparations (about the percentage of channels present in the 212kDa form) have been seen to function as active Ca^{2+} channels (Schwartz *et al.*, 1985; Curtis and Catterall, 1986). It was thus hypothesised, that the full-length form of α_1 is specialized for Ca^{2+} conductance while the truncated 175kDa α1 subunit no longer functions as an ion channel, following cleavage of its C-terminus, subsequently having the role of voltage sensor in E-C coupling (De Jongh *et al.*, 1989). This proposal was supported by the fact that three consensus sites for cAMP-dependent phosphorylation, a process which activates the Ca^{2+} conductance mediated by the skeletal muscle Ca^{2+} channel (Arreola *et al.*, 1987; Flockerzi *et al.*, 1986a; Hymel *et al.*, 1988; Nunoki *et al.*, 1989), are missing from this smaller polypeptide. However, the truncated polypeptide has recently been shown to have both voltage sensing and ion channel activity (Gutierrez *et al.*, 1991; Ma *et al.*, 1991; Beam *et al.*, 1992).

Protein-protein interactions between the voltage sensor and the ryanodine receptor may serve to transmit the effect of depolarization across the triad junction. However, the fact that it had not been possible to recombine these proteins, although they have been isolated for several years suggested the involvement of at least a third

protein in their interaction (Caswell and Brandt, 1989). A candidate for this role has now been suggested in the 95kDa protein called triadin, initially described by Kim *et al.*, (1990a), which is known to be a major constituent of the triad junction, binding both the Ca^{2+} channel and the Ca^{2+} release channel (Brandt *et al.*, 1990; Kim *et al.*, 1990a). It is an intrinsic protein of the terminal cisternae of the SR, where it exists in the form of a homopolymer of variable size, with a distribution and content approximately the same as those of the Ca^{2+} release channel (Caswell *et al.*, 1991). Recently, a monoclonal antibody (MAb) directed against triadin was shown to have an inhibitory effect on the slow phase of depolarization-induced Ca^{2+} release from SR (Brandt *et al.*, 1992). Since a similar effect was previously observed with both DHP's and a MAb directed against the Ca^{2+} channel α_1 subunit (Ohkusa *et al.*, 1990, Ohkusa *et al.*, 1991a) this points to a role for triadin in the Ca^{2+} channel mediated t-tubule to SR communication and therefore in the mechanism of E-C coupling in skeletal muscle. MAb's directed against a 28kDa protein of the t-tubule inhibited the fast phase (Ohkusa *et al.*, 1991b), while nifedipine and a MAb directed against the Ca^{2+} channel α_1 subunit both inhibited the slow phase of depolarization induced Ca^{2+} release from SR (Ohkusa *et al.*, 1990), suggesting that the DHP receptor and the 28kDa protein are involved in two distinguishable signal transduction pathways.

If triadin interacts physically with the skeletal muscle Ca^{2+} channel, the localization of this site of interaction is important in understanding the mechanism of E-C coupling. A likely candidate is one of the large intracellular loops of the channel, possibly the IIS6-IIIS1 loop, previously shown to be essential for skeletal type E-C coupling (Tanabe *et al.*, 1990).

1.10 Aims of the work described in this thesis

The aim of the study was to exploit the sequence information that became available from cDNA cloning, on the subunits of the skeletal muscle and brain class A and D Ca^{2+} channels, to make specific site-directed antibodies as tools to investigate these proteins.

Therefore, the initial requirement was to produce peptide-specific antibodies that would recognize the channel proteins, both specifically and in their native form, and which could therefore be used as probes of the primary structure and distribution of the L-type channel. To this end the occurrence and distribution of individual Ca^{2+} channel types in skeletal and cardiac muscle, and the similarities and differences in both the skeletal (rat, rabbit, human, mouse) and cardiac (rabbit and rat) L-type Ca^{2+} channel of these different mammalian species were to be examined by exploiting the specificity of the anti-peptide antibodies.

The involvement of various regions of the skeletal muscle channel in the interaction between DHP and PAA ligands and the channel was also to be examined, by investigating the effect of the presence of these antibodies on ligand binding. Additionally, it was proposed to examine the secondary structure of a domain of protein implicated in Ca^{2+} and antagonist binding, following the synthesis of this part of the channel sequence.

CHAPTER 2

MATERIALS AND METHODS

2.1 Materials

All reagents were obtained from British Drug Houses Ltd. except where otherwise stated and were of analar or higher grade. All aqueous solutions and buffers were made up in double-distilled or milliQ water. Rabbits were obtained from Gorseside Farm, Northchurch, Berkhamsted, Hertfordshire HP4 1LP, mice from Bantin and Kingman Ltd., Tealings Park, Eastwick Rd., Harlow CM20 2QR, Essex and Sprague-Dawley rats were bred at the Comparative Biology Unit, Royal Free Hospital School of Medicine. Radiochemicals were purchased from Amersham.

2.2 Peptide Synthesis

2.2.1 Continuous Flow Synthesis

Short peptides (12-21 residues) were synthesized using the solid phase N^{α}-fluorenylmethoxycarbonyl-polyamide (Fmoc-polyamide) method with N^{α}-Fmoc-amino acid pentafluorophenyl (pfp) esters (Atherton and Sheppard, 1985). Continuous-flow synthesis was carried out on a Polyamide-Kieselguhr (Pepsyn KA) resin (MilliGen/Biosearch) (1g) using a Cambridge Research Biochemicals Pepsynthesizer, with dimethylformamide (DMF) as solvent. The resin, consisting of a polydimethylacrylamide gel held within the pores of an inert macroporous rigid kieselguhr matrix containing an acid-labile 4-hydroxymethylphenoxyacetyl-norleucyl derivative, was purchased with the first amino acid, cysteine, attached. Peptides, thus synthesised, had a *C*-terminal cysteine residue to facilitate coupling to a carrier protein.

Prior to each coupling step, the N^{α}-Fmoc protecting group was removed by

a 10 min. incubation with DMF containing 20% (v/v) piperidine (Aldrich), a weak base. After this deprotection step the resin was washed for 10 min. with DMF. The next amino acid was then coupled by recirculation of the corresponding N^{α}-Fmoc-amino acid pfp ester (Milligen/Biosearch) (3-fold molar excess over free amino groups) through the resin column for 60 min. in the presence of the catalyst 1-hydroxybenzotriazole (HOBT) (Fluka). Following the coupling step the resin was again washed for 10 min. in DMF.

Each peptide was cleaved from the resin support, and side-chain protecting groups removed, using a 95%(v/v) trifluoroacetic acid (TFA) (Fluka) solution in distilled H_2O (dH_2O), containing 2.5% (v/v) 1,2-ethanedithiol (EDT) (Fluka) and 2.5% (w/v) phenol as free radical scavengers (100ml). The time allowed for cleavage was normally at least 90 min. For peptides containing arginine residues having a 4-methoxy-2,3,6-trimethylbenzenesulfonyl side-chain protecting group, cleavage times were extended to 6h per arginine residue. Following cleavage, the peptide solution was filtered to remove the resin particles and then TFA and most of the scavenger molecules were removed by rotary evaporation at 30°C under vacuum. Residual scavengers and the products of the side-chain protecting groups were then removed by precipitation of the peptide from diethylether (80ml), followed by two washes of the precipitate with diethylether (80ml). The resultant peptides were then dried under vacuum and stored dry at -20°C.

2.2.2 Batch Method Synthesis

Batch method synthesis was carried out on a number of the short peptides (those designated H, I, K and O, see Section 3.3.1), essentially as described by Atherton and Sheppard (1985), in a sintered glass funnel using the same resin as for continous flow synthesis, but employing N_2 gas agitation. The same amino acid deprotection and resin washing conditions as described above were used, but the length of the coupling step was shortened to 30 min.

2.2.3 Automatic Peptide Synthesis

The longer 48 residue peptide (designated J, see Section 3.3.1), was synthesised using a PS3 automatic peptide synthesiser (Protein Technologies Inc.). It was sythesized on a 4(2'4'-dimethoxyphenyl-Fmoc-aminomethyl)p-phenoxy resin (0.45g) (Novabiochem) having a substitution ratio of 0.19 mmol/g. The deprotection and washing conditions were the same as for shorter peptides. However, the amino acids were coupled as symmetric anhydrides, using a 3-fold molar excess of N^{α}-Fmoc-amino acid (Novabiochem) and 4.5-fold molar excess of 2-(1H-Benzotriazole-1-yl)-1,1,3,3-tetramethyluronium tetrafluoroborate (TBTU) (Novabiochem) in the presence of 3,4-Dihydro-3-hydroxyl-4-oxo-1,2,3-benzotriazine (DHOBT) (Fluka) and 0.1M 4-methylmorpholine (Fluka) in DMF. The first 18 coupling steps were 20 min. long, while coupling time for the remainder was extended to 40 min. Following synthesis the N-terminus of the resin-bound peptide was acetylated in the presence of acetic anhydride and triethylamine in DMF.

The resin-bound peptide was washed in dichloromethane (DCM) (20ml) twice in a sintered glass funnel and the peptide was then removed by incubation in 3% (v/v) TFA in DCM (100ml) for 70 min. After removal of DCM by rotary evaporation side chain protecting groups were cleaved from the peptide by incubation with 100ml 95% (v/v) TFA in dH_2O, containing 2.5% (v/v) EDT, 2% (w/v) phenol and 0.1% (w/v) indole (Sigma) for 150 min. The peptide was then precipitated in a large excess of ice-cold diethylether (250ml) and separated from TFA and scavengers by centrifugation. The peptide was washed a further two times in diethylether (80ml) before freeze-drying from aqueous solution and subsequent storage at -20°C.

2.3 Peptide characterization and purification

The purity of each short peptide and also of peptide J, both before and following purification, as outlined below, was assessed by reverse phase HPLC using a 90 min. gradient of 5-40% (v/v) acetonitrile in 0.1% (v/v) aqueous TFA at a flow rate of 1 ml/min. on a 300A pore-size, C_{18} column (Aquapore RP-300) attached to a Varian 500 liquid chromatograph. Peptide samples of 50-100μg were loaded and the chromatogram obtained by the absorption at 220nm of the eluate. A sample of peptide J was purified using HPLC under similar conditions as for characterization. Material eluted in each of the three major peaks was collected and freeze dried.

The purity of both crude and purified peptide J was also examined by tricine-SDS/PAGE according to the method of Schagger and Von Jagow (1987). Samples and standards were solubilized in a sample buffer containing 50mM Tris-HCl, pH 6.8, 4% (w/v) SDS, 12% (v/v) glycerol and 2% (w/v) dithiothreitol (DTT) (Sigma). Aliquots of sample (10-50μl), containing 10-50μg protein, were loaded onto 1.5mm slab gels consisting of separating gel (length 7cm), overlaid with 3cm of spacer gel and 2cm of stacking gel. Separating and spacer gels consisted of [15.5% (w/v) acrylamide, 1% (w/v) bisacrylamide, 13.3% (w/v) glycerol] and [9.7% (w/v) acrylamide, 0.3% (w/v) bisacrylamide], respectively, while the stacking gel contained [3.84% (w/v) acrylamide, 0.12% (w/v) bisacrylamide] each made up in 1M Tris-HCl, pH 8.45 containing 0.1% (w/v) SDS. Gels were run at 30V (constant voltage) for 2h. and then at 95V (constant voltage) for 16h. They were subsequently fixed in 10%(v/v) acetic acid, 25% (v/v) isopropanol for 2h. and then stained in 10%(v/v) acetic acid, 25% (v/v) isopropanol, 0.025% (w/v) Coomassie Brilliant Blue R-250 (Sigma) for 8h. Destaining was carried out initially in 10%(v/v) acetic acid, 25% (v/v) isopropanol, 0.0025% (w/v) Coomassie blue R-250 for 8h and continued in several changes of 10% (v/v) acetic acid.

The amino acid composition of each peptide was determined using a 4151 Alpha Plus amino acid analyzer (LKB), following hydrolysis in 6M HCl containing 0.04% (v/v) 2-mercaptoethanol and 0.1% (w/v) phenol for 24h at 110°C. The

molecular mass of peptides A, B, C, D, E, F, G, L, M and N was determined by matrix assisted Fast Atom Bombardment Mass Spectrometry, using a Vacuum Generator ZAB-SE Mass Spectrometer in the Department of Pharmaceutical Chemistry at The School of Pharmacy, Brunswick Square, London WC1. The matrix consisted of thioglycerol, glycerol and TFA. The molecular mass of peptides H, I, J, K and O was determined by matrix assisted Laser Desorption Mass Spectrometry, using a Kratos KOMPACT MALDI III mass spectrometer in the Protein Sequencing Laboratory at the Imperial Cancer Research Fund, Lincoln's Inn Fields, London WC2. Samples (pmolar quantities) were deposited individually onto disposable sample slides in sinapinic acid. The slide was inserted into a system drying unit, mounted on a probe and drawn into the vacuum system where the sample was ionized by fifty laser shots from a 337nm Nitrogen source, giving ionization at different locations along the sample.

2.4 Studies of peptide secondary structure

2.4.1 Fourier Transform Infrared (FTIR) Spectroscopy

Peptide samples (5mg) were prepared for secondary structure analysis by dissolving in 10mM HEPES/Tris, pH 7.4 at 20°C (0.5ml). Samples were then divided into two equal aliquots prior to dialysis of one versus 10mM HEPES/Tris, 2.5mM EGTA, pH 7.4 (2l) and of the other against 10mM HEPES/Tris, 20mM $CaCl_2$, pH 7.4 (2l) for 16h. Subsequently, samples were dialysed against the same buffers made up in D_2O (Sigma) (20ml) for 8h. at 20°C. Insoluble material was removed by centrifugation at 3,000g for 5 min. and an FTIR spectrum obtained of the supernatant using a Perkin-Elmer Model 1750 Infrared Fourier Transform Spectrometer equipped with a TGS detector. A Perkin-Elmer model 7300 data station was used for data acquisition, storage and analysis. Briefly, samples (volumes up to 50μl) were placed in a thermostatted Beckman FH-01 CFT microcell fitted with CaF_3 windows. The sample compartment was continuously purged with dry air to eliminate

absorption by water vapour in the spectral region of interest. Spectral conditions were as follows: 200 scans; spectral resolution 4cm^{-1}; sample thickness of 50μm using a Teflon spacer; sample temperature 20°C.

2.4.2 Circular Dichroism (CD) Spectroscopy

Peptide sample (1mg) was prepared for CD spectroscopy in the same way as for FTIR spectroscopy with the following modifications. Peptide was prepared at a concentration of 2mg/ml while dialysis against D_2O was omitted. CD spectra were obtained using a Jasco J600 CD spectrometer with a 0.02 cm pathlength cell.

2.5 Membrane and receptor preparations

2.5.1 T-Tubule membrane preparation

Hind-leg skeletal muscle (300g) was quickly cut into small pieces ($<1cm^3$) immediately following removal from freshly killed rats or rabbits. Hind leg muscle (300g) that had been previously removed and stored at -70°C was chopped while thawing. All remaining steps in the procedure were carried out at 0-4°C, after the method of Rosemblatt *et al.* (1981). The muscle was homogenized by five 20s bursts in a Waring blender, with 30s breaks between each burst, following the addition of 1.1l of homogenizing buffer consisting of [40mM 3-(NMorpholino)propanesulphonic acid (MOPS) (Sigma), 0.3M sucrose pH 7.4 at 4°C].

Homogenate was sedimented at 3,000g for 20 min. The top layer, consisting of fat, and the pellet were discarded, and 2M NaOH (5ml) added to the supernant to maintain the pH above 7.0. The supernatant was then sedimented at 10,000g for 20min. The volume of the resultant supernatant volume was next measured, and sufficient KCl added to adjust the concentration to 0.5M. After 15 min. at 4°C, the solution was sedimented at 13,000g for 4h. The supernatant was discarded, the pellets

resuspended in homogenizing buffer (30ml) and the membranes washed free of KCl at 100,000g for 30 min. Aliquots (5ml) of the resuspended pellet (total volume 30ml) were then overlaid onto each of six tubes containing 15ml 0.9M sucrose, 40mM MOPS, pH 7.4. The t-tubule membranes were subsequently isolated from the interface between the two sucrose layers following centrifugation at 100,000g for 16h. and were diluted 1:4 in 40mM MOPS, pH 7.4. Following resuspension in a glass/teflon homogenizer, the membranes were collected by centrifugation at 100,000g for 30 min. The pellet was suspended to 1.5ml in homogenizing buffer, aliquoted, frozen in liquid N_2 and stored at -70°C. Protein concentration was determined using the method of Lowry *et al.* (1951), as described in Section 2.9.1. Typical yields were 20-30 mg t-tubule membrane protein per 300g tissue.

2.5.2 Preparation of skeletal muscle microsomes

All steps were carried out at 0-4°C after the method of Flockerzi *et al.*, (1986b) and all solutions contained the following protease inhibitor cocktail: 0.1mM phenylmethylsulfonyl fluoride (PMFS), 1mM iodoacetamide (IAA), 1mM benzamidine, 1mM 1,10 phenanthroline, 1μg/ml leupeptin, 10μg/ml Soybean trypsin inhibitor (SBTI), 1μg/ml antipain and 1.5μM pepstatin A (all purchased from Sigma). Microsomal membranes were prepared from fresh rabbit hind-leg skeletal muscle. Muscle (70g) was minced and added to 3.5% (w/v) buffer A [(20mM MOPS, pH 7.4, 0.3M sucrose, 10mM ethylene glycol-bis(ß-aminoethyl ether) N,N,N',N'-tetraacetic acid (EGTA)]. The muscle was homogenized in a Waring blender for six 5s periods at low speed, then another six 5s bursts at high speed.

The homogenate was sedimented at 3,000g for 10 min. to remove fat and connective tissue, and the supernatant retained. The pellets were rehomogenized in 3 vol. buffer A and sedimented as before. Both supernatants were combined, the pH checked, solid KCl added to give a final concentration of 0.5M and the supernatant stirred on ice for 15min. Mitochondria were removed by sedimentation at 7,000g for 10min. and the supernatant was spun at 100,000g for 30 min. The microsomal pellet

was resuspended in buffer A (50ml) using 6 to 7 up-down strokes of a Potter-Elvejhem homogenizer, diluted to 250ml and re-sedimented at 100,000g for 40min. The sedimented membranes were then resuspended in buffer B (10mM HEPES-Tris, pH 7.4; 185mM KCl; 1.5mM $CaCl_2$) (50ml), to give a final protein concentration of 15-30mg/ml.

Protein content was approximated by measuring absorbance at 280 and 260 nm of an aliquot (10μl) in 2% (w/v) SDS and later more accurately determined using the method of Lowry *et al.* (1951) (Section 2.9.1). Typical yields were 24mg/g muscle. Microsomes were immediately taken for solubilization and purification of the DHP receptor (Section 2.7.3) and for the assay of [^{3}H](+)-PN200-110 binding sites (Section 2.8.2). The remainder were aliquoted and frozen in liquid N_2 in 1ml volumes and stored at -70°C.

2.5.3 Purification of the skeletal muscle DHP receptor

All stages of the procedure were carried out at 0-4°C under dim light and all buffers included the following protease inhibitors, 0.1mM PMSF, 1mM IAA, 1mM benzamidine, 10μg/ml SBTI, 1mM 1,10 phenanthroline, 1μg/ml leupeptin, 1μg/ml antipain and 1.5μM pepstatin A.

Fresh skeletal muscle microsomes (200mg) were incubated with 2.2 nM (+)[^{3}H]PN200-110 in buffer B (above) at a protein concentration of 2 mg/ml for 1h. An aliquot (1ml) of the incubation mixture was taken and unlabelled nitrendipine (10μl) was added giving 1μM final concentration. This aliquot was used in the calculation of nonspecific binding. Following incubation, the labelled membranes were sedimented by centrifugation at 160,000g for 30 min. The specifically labelled membranes were resuspended in buffer B (100ml), containing 1% (w/v) digitonin (Sigma), in a Potter-Elvejhem homogenizer using 12-15 gentle down-up strokes. The non-specifically labelled membranes were resuspended in the same buffer (1ml) by passing the membranes several times through a 21 gauge hypodermic needle. The solubilization mixtures were kept on ice for 45 min. with occasional gentle agitation.

Insoluble material was sedimented by centrifugation at 160,000g for 30 min. after which aliquots were taken from both specifically and non-specifically labelled membrane samples for calculation of total and protein-bound radioactivity.

The soluble supernatant was immediately loaded onto a 10ml column of Wheat Germ Agglutinin (WGA)-Sepharose 6MB (Sigma) equilibrated in 10mM N-(2-hydroxyethyl)piperazine-N'-(2-ethanesulphonic acid) /tris (hydroxymethyl) aminomethane (HEPES-Tris), pH 7.4, containing 1.5mM $CaCl_2$ and 0.1% (w/v) digitonin. The column was then washed with 10mM HEPES-Tris, pH 7.4, containing 1.5mM $CaCl_2$, 0.5M sucrose, 150mM NaCl and 0.1% (w/v) digitonin (25ml) to remove non-specifically bound material and finally the DHP receptor was eluted in 10mM HEPES-Tris, pH 7.4, containing 1.5mM $CaCl_2$, 0.1% (w/v) digitonin and 0.3M *N*-acetylglucosamine (Sigma).

Approximately 1.8ml fractions were collected and their protein content determined according to the method of Lowry *et al.* (1951), as described in Section 2.9.1. The PEG assay described by Curtis and Catterall (1983) was employed in order to locate the purified DHP receptor. Aliquots (100μl) of the fractions, and of supernatant samples retained for determination of total and nonspecifically bound [^{3}H](+)PN200-110 (200μl), were first mixed with 1.8 ml binding medium (100mM HEPES, 125mM choline chloride (Sigma), 5.5mM KCl, 5.4mM glucose, 1.5mM $CaCl_2$, pH 7.4) at 4°C and then newborn calf serum (100μl) added. Ice cold 30%(w/v) aqueous PEG (av. M_r. 8,000) (BDH) (1.2ml) was added and the mixture kept on ice for 15 min. to precipitate soluble protein. The latter was then removed by filtration through GF/C filters (Whatman) presoaked and washed in wash buffer [100mM HEPES, 8.5% PEG, pH 7.4]. Filters were placed in scintillation vials and 4ml of Optiscint "T" (LKB, U.K.) was added. The vials were capped, shaken and left to equilibrate for at least an hour.

2.5.4 Preparation of rat whole brain and cerebellar membranes

Brains from six freshly killed rats were dissected and the remaining steps of the procedure were carried out at 4°C, essentially as outlined by Catterall *et al.* (1979). Visible white matter was removed in homogenizing buffer (0.32M sucrose, 5mM sodium phosphate, pH 7.4, containing 5mM benzamidine, 5mM DTT, 0.1% (w/v) SBTI, 100μM PMSF, 50μM leupeptin and 1% (v/v) aprotinin (Sigma). Brains were minced in buffer (20ml) prior to the addition of a further 20ml of buffer before homogenization in a teflon/glass homogenizer (10 passes). Homogenate was sedimented at 1,000g for 10 min. and the supernatant stored at 4°C. The pellet was resuspended in homogenization buffer (30ml) and rehomogenized. Following resedimentation, as above, the pellet was discarded and both supernatants combined. The P2 membrane fraction was then sedimented at 20,000g for 50 min., resuspended in homogenization buffer and stored at -70°C. Lysed "P2" fraction was obtained by homogenization of the P2 fraction in 5mM HEPES, pH 8.0, followed by centrifugation at 100,000g for 30 min. The membranes were resuspended in 5mM HEPES, pH 8.0, frozen in liquid N_2 and stored at -70°C.

2.6 Production and characterization of antibodies

2.6.1 Production of antiserum

Prior to use for antiserum production each peptide was coupled to a carrier protein, either Keyhole limpet haemocyanin (KLH) (Sigma), ovalbumin (Sigma) or purified protein derivative (PPD) from *Mycobacterium tuberculosis* (Cambridge Research Biochemicals) using maleimidobenzoyl-*N*-hydroxysulphosuccinimide ester (sulpho-MBS) (Pierce), essentially as described by LaRochelle et al. (1985). Antisera against the peptide conjugates were then raised in female New Zealand White or Half-Lop rabbits, as follows. KLH-peptide and ovalbumin-peptide conjugates (266μg) in 0.4 ml 10 mM sodium phosphate, 145 mM NaCl, pH 7.2 (PBS), were first

emulsified with 0.8 ml complete Freund's adjuvant (Sigma) and then 0.9 ml of emulsion was injected into the hind leg muscle. An additional ("booster") injection of antigen (100μg) in 0.9 ml emulsion with incomplete Freund's adjuvant (Sigma) was administered subcutaneously, after 4 weeks, and subsequently at intervals of not less than 6 weeks. The animals were bled from the ear vein (30ml) two weeks after each boost and subsequently at four week intervals. Control sera were obtained from the rabbits prior to the first injection.

When PPD-peptide conjugates were employed, all injections of antigen were made subcutaneously using emulsions of incomplete Freund's adjuvant. The animals were first immunized, subcutaneously, with *Bacillus* Calmette-Guerin (BCG) vaccine obtained from a Tuberculin PPD kit (Cambridge Research Biochemicals) and conjugates were administered 2 weeks later, and subsequently at 6 week intervals. The rabbits were bled two weeks after each antigen injection and subsequently at four week intervals. The blood was allowed to clot in glass tubes for 16h. at 4°C. Both red and white blood cells were removed by sedimentation at 1,000g for 10 min. and the serum aspirated. Antisera were then treated at 56°C for 30 min. to inactivate complement and subsequently stored at -70°C.

2.6.2 Affinity purification of antibodies

Peptide-specific antibodies were purified from crude serum by chromatography on columns containing immobilized peptides. The latter were prepared by reaction of peptide with either tresyl-activated Sepharose 4B (Pharmacia), Sulfolink gel (Pierce) or triazine-activated Agarose 4XL (Affinity Chromatography Ltd.). The former matrix consisted of Sepharose, containing tresyl groups which are replaced by peptide, while the latter two matrices contained, respectively, iodoacetyl groups, which react with peptide sulphydryl groups, and triazine groups which react with peptide amines. Peptides (2mg) were immobilized on these matrices according to the manufacturer's instructions, and the resultant columns (1.5ml) were stored in buffer containing 0.02% (w/v) sodium azide (Sigma) at 4°C.

For purification of antibody, serum samples (3 - 10 ml) diluted two-fold in PBS were repeatedly passed through the relevant peptide column for 2h. The column was then washed with 10mM sodium phosphate, 800mM NaCl, pH 7.2 to remove nonspecifically-bound protein. Bound IgG was then eluted with either 0.2 M glycine/HCl buffer, pH 2.4 or 50 mM diethylamine/HCl buffer (Sigma), pH 11.3. The eluate was rapidly neutralized by addition of 150 mM sodium phosphate buffer, pH 10.0 or 4.0 respectively. In some cases antibodies were eluted in 5M $MgCl_2$, followed immediately by 10-fold dilution in dH_2O. Following elution, purified antibodies were dialysed overnight in PBS (4l). All the above steps were carried out at 4°C. Purified antibodies were concentrated to a volume of 1-2ml, depending on the initial serum volume, using Centricon 30 concentrators (Amicon) and stored at -70°C. Protein content was later determined by the method of Lowry et al. (1951).

2.6.3 Enzyme-linked Immunosorbent Assay (ELISA)

The abilities of antisera and affinity-purified antibodies to recognise synthetic peptides were assessed by ELISA essentially as described by Davies *et al.* (1987), with the following modifications. Briefly, Maxisorp microtiter plates (Nunc) were coated with 20ng peptide per well, by incubation with a peptide solution in 50mM sodium carbonate buffer, pH 9.6. Plates were then blocked by incubation with 5% (w/v) non-fat milk powder in PBSA-T [PBS containing 0.02% (w/v) NaN_3 and 0.05% (v/v) Tween 20 (Bio-Rad)]. The blocked plates were then incubated overnight with serial dilutions of antisera diluted in antibody buffer [PBSA-T containing 1% (w/v) milk powder]. After washing, the plates were incubated for 2h with goat anti-rabbit IgG conjugated to alkaline phosphatase (Bio-Rad) diluted 1/500 in antibody buffer. Bound antibody was then detected by the addition of p-nitrophenyl phosphate (Sigma), which yielded yellow p-nitrophenol upon hydrolysis. The latter was quantified by its absorbance at 405nm. All the above steps were carried out at 20°C.

The ability of antisera and purified antibodies to recognise the intact channel protein was also studied using ELISA, with the following modifications. Maxisorp

microtiter plates were coated with purified rabbit skeletal muscle DHP-receptor by incubation overnight at 4°C with a solution of purified Ca^{2+} channel in PBS containing 0.0025% (w/v) digitonin 140ng/well). Since the specific activity of the purified DHP receptor was 0.9 nmoles DHP binding sites / mg protein each well contained 126 fmoles DHP binding sites. The remaining steps were carried out at 20°C, as outlined for the peptide ELISA, except that the incubation of the receptor with primary antibody was for four hours with serial dilutions of pre-immune and immune serum from each animal, or with equivalent amounts of test and control antibodies.

2.6.4 Western blotting

The protein components of t-tubule membranes from both rat and rabbit and of purified DHP receptor from rabbit skeletal muscle and from partially purified rat brain membranes (P2 fraction), prepared as described in Sections 2.7.1, 2.7.3 and 2.7.4, along with high molecular weight markers (Bio Rad) were separated either on sodium dodecyl sulphate (SDS) polyacrylamide (4-12)% gels (length 12cm) at 50V constant voltage over 16h or on SDS polyacrylamide (4-12)% minigels (length 6cm) at 50 mA constant current for 90 min. The proteins and markers separated on the large gels were electrotransferred onto nitrocellulose paper (Sartorius) in 25mM Tris, 192mM glycine, pH 8.7, containing 1% (v/v) methanol, by wet blotting at 80V constant voltage for 2.5h. Protein transfer from the minigels onto ProBlott membranes was by semi-dry blotting in 20mM Tris, 150mM glycine, pH 8.5, containing 20% (v/v) methanol, at 1.5 mA/cm^2 for 90 min. (Applied Biosystems). Markers transferred to nitrocellulose were stained in 0.1% (w/v) Amido Black (Sigma) in 25% (v/v) isopropanol (BDH) and 10% (v/v) acetic acid for 5 min. and destained in 10% (v/v) acetic acid. Markers on ProBlott membranes were stained using 0.5%(w/v) Coomassie Brilliant Blue G (Sigma) in 7% (v/v) acetic acid (BDH) for 20 min. and destained using 100% methanol.

To prevent nonspecific binding of antibodies, nitrocellulose blots were blocked

with 5% (w/v) non-fat milk powder in 20mM Tris, 500mM NaCl, pH 7.5, containing 0.02% (v/v) Tween-20 (TTBS). Incubation of the nitrocellulose blots with primary antibodies was then performed for 16h. at 4°C in antibody buffer [TTBS containing 1% (w/v) non-fat milk powder]. Antisera were routinely used at a dilution of 1/500, whereas purified antibodies were used at 10μg/ml. Incubation with secondary antibody (biotinylated whole anti-rabbit IgG, raised in donkey, Amersham) diluted 1/500 in antibody buffer was for 60 min. at 20°C, followed by streptavidin/biotin-horse radish peroxidase complex (Amersham), diluted 1/400 in antibody buffer, for 30 min. at 20°C. The nitrocellulose was given three 10 min. washes with TTBS before and after each incubation. Bound antibody was detected using an enhanced chemiluminescence (ECL) kit (Amersham) according to the manufacturer's instructions.

To prevent nonspecific binding of antibodies to Problott membranes, these were incubated in 3% (w/v) bovine serum albumin (BSA) (ICN) in TTBS for 2h. at 20°C. Primary antibodies were diluted, as outlined for nitrocellulose blotting, in antibody buffer [3% (w/v) BSA, 0.5% (w/v) ovalbumin, 10% (v/v) goat serum (Sigma), 0.5% (v/v) Nonidet P40 (NP40) (Sigma) in TBS], prior to incubation with the membranes for 16h. at 20°C. The blots were then incubated for 3h. at 20°C in antibody buffer containing a 1/500 dilution of secondary antibody, which consisted of a horseradish peroxidase conjugate of goat anti-rabbit IgG (Bio-Rad). The blocking and antibody incubation steps were followed by three 10 min. washes in 0.5% (v/v) NP40 in TBS. Finally, bound antibody was detected by incubation for 5 min. with an aqueous solution of 0.0125% (w/v) 3-amino-9-ethyl-carbazole (AEC) (Sigma), 0.03% (v/v) H_2O_2 (Sigma), and 0.05% (v/v) Tween-20 in 0.05M sodium acetate, pH 5.2.

2.7 Immunocytochemistry

2.7.1 Preparation of brain and muscle sections

Both rabbit and rat biceps and cardiac ventricle muscle, and mouse triceps muscles were removed and pieces, approximately 4 mm^3, were mounted in OCT compound (Tissue-Tek) containing 10.24% (w/w) polyvinyl alcohol and 4.26% (w/w) polyethylene glycol (PEG) on cork, prior to rapid freezing in isopentane at -56°C. These frozen tissue samples were stored at -70°C over moist paper. Cryostat muscle sections (12-16μm thick) were cut using a stainless steel knife at -30°C and collected on glass slides which had been freshly coated with a solution of 0.5% (w/v) pig skin gelatin (Sigma) and 0.05% (w/v) $Cr_2(SO_4)_3.K_2SO_4.24H_2O$ (chrome alum.) (Aldrich Chemical Co. Ltd.). Sections were air dried for 20 min. at 20°C before storage at -20°C. Human muscle sections were obtained from the Department of Neurological Science, Royal Free Hospital School of Medicine, already frozen following mounting and drying on coated glass slides, as described above.

2.7.2 Immunostaining of muscle sections

Muscle sections were thawed for 20 min. at 20°C and washed by immersion in PBS (80ml) for 10 min. In early experiments the sections were blocked for 60 min. with 10% (v/v) swine serum in PBS, but this stage was subsequently omitted as it was found to have no significant effect on the quality of antibody staining obtained. Control rabbit IgG (Sigma) and purified anti-peptide antibodies (0.033mg protein/ml) in PBS were incubated with the sections for 3.5h at 20°C. The sections were then incubated in the dark for 60 min. at 20°C with a 1/40 dilution in PBS of swine anti-rabbit second antibody, conjugated to rhodamine (Dako). After each incubation the sections were washed by immersing the slides in PBS (80ml) in five consecutive beakers for 3 min. each. The sections were finally mounted for viewing in Citifluor (Citifluor Ltd.) under glass coverslips No.1 (Chance Propper Ltd.).

Antibodies that did not yield sufficiently intense staining using the above procedure had their staining enhanced in the following way. Primary and control antibodies and the secondary antibody, consisting of donkey anti-rabbit IgG conjugated to biotin (Amersham), were diluted and incubated with the relevant muscle sections as described above. The bound second antibody was subsequently labelled by incubation, in the dark, with streptavidin conjugated to Texas Red (Amersham), diluted 1/40 in PBS. Sections were washed following each incubation step and mounted for viewing, as described above.

2.7.3 Fluorescence microscopy of stained sections

Bound antibody was detected in muscle sections, stained as outlined above, using an MRC-600 Confocal Microscope (Imaging System) (Bio Rad Ltd.). The light source consisted of an air cooled Argon Ion laser. The excitation wavelength was selected at 568nm using an excitor filter, while emitted light of wavelength 585nm was detected having passed through a YHS filter. Using the operating software the fixed specimen was scanned and a series of images collected from sections at 2μm intervals in the vertical plane of the tissue section. The images were collected onto a Winchester (hard) disc and were transferred to a Panasonic Optical Disk (Matsushita Electric Industrial Co. Ltd.) for storage. For presentation the images in the series were later superimposed on one another prior to photographing on 400 ASA print film (Kodak) using a Nikon F301 camera.

2.8 Drug binding studies

2.8.1 Equilibrium binding of (+)-[^{3}H]PN200-110 to skeletal muscle microsomes

Skeletal muscle microsomes were incubated in 20mM Tris-HCl, pH 7.5, at a protein concentration of 0.66 mg/ml with 0.086-2.4nM (+)-[^{3}H]PN200-110 for 60 min. at 4°C. Nonspecific binding was determined with a 1,000-fold excess of unlabelled nitrendipine (1μM). Total binding was measured by filtering duplicate 400μl volumes from each reaction tube on Whatman GF/B glassfibre filters under reduced pressure, using a Millipore filtration apparatus. Filters were washed once before, and twice after, filtration with 20mM Tris-HCl, pH 7.5 (3ml), to remove free ligand and then placed in scintillation vials containing 4ml of Optiscint "T" (LKB, U.K.). Disintegrations per minute (DPM) were counted following equilibration for one hour. Free ligand concentrations were calculated by counting DPM from aliquots of each reaction mixture in 3ml of Optiphase "X" (LKB, U.K.).

2.8.2 Equilibrium binding of [^{3}H]nitrendipine and [^{3}H]D888 to t-tubule membranes.

T-tubule membranes were incubated at a protein concentration of 0.1mg/ml in either, 20mM Tris-HCl, pH 7.5 with 0.25-7.2nM (+)-[^{3}H]nitrendipine for 60 min. at 4°C or 0.1M Tris-HCl, pH 7.5 with 0.5-14.4nM (+)-[^{3}H]D888 for 2h. at 20°C. Nonspecific binding was determined in the respective assays in the presence of a 1000-fold excess of nitrendipine (1μM) and verapamil (1μM). For both assays, total binding was measured by filtering duplicate 400μl volumes from each reaction tube on Whatman GF/B glassfibre filters under reduced pressure using a Millipore filtration apparatus. Filters were washed once before, and twice after, filtration with 8ml of incubation buffer, 0.1mM Tris-HCl, pH 7.5 (nitrendipine assay) and 0.1M Tris-HCl, pH 7.5 (D888 assay), to remove soluble material. The counting procedure

for both bound and free ligand concentrations were as outlined in Section 2.8.1.

2.8.3 Fitration assay of [^{3}H]nitrendipine and [^{3}H]D888 binding to t-tubules in the presence of antibody.

For single-point assays, duplicate samples of relevant quantities of both control and purified anti-peptide antibody, or of pre-immune and immune serum, having total protein content in the range 5 to 500 μg, were incubated with t-tubule membranes (65μg protein) for 16h. at 4°C, in either 20mM Tris-HCl, pH 8.0 (nitrendipine assay) or 0.1M Tris-HCl, pH 8.0 (D888 assay) in a total volume of 0.5ml. The membranes were then incubated with an equal volume either of [^{3}H]nitrendipine in 20 mM Tris-HCl, pH 8.0 at a final concentration of 2.7nM, for 2h. at 4°C, or of [^{3}H]D888 in 0.1M Tris-HCl, pH 8.0 at a final concentration of 5.4nM for 3h. at 20°C. Non-specific binding was determined for nitrendipine, in the presence of a 370-fold excess of unlabelled nitrendipine (1μM) and for D888 in the presence of a 3,700-fold excess of verapamil (200μM) verapamil.

Bound ligand in each sample was determined following filtration of duplicate volumes of 400μl on Whatman GF/B glassfibre filters, while free ligand concentrations were calculated from aliquots of each reaction mixture, as outlined in Section 2.8.1.

2.9 Lowry assay for protein

Reagent solution [2% (w/v) Na_2CO_3 in 0.1M NaOH, containing 0.5% (w/v) SDS, 0.01% (w/v) $CuSO_4.5H_2O$ and 0.02% (w/v) Na,K,tartrate] was made up immediately prior to use. Protein standards and samples (200μl) diluted, as appropriate, in distilled H_2O were incubated, following mixing, with 1ml aliquots of reagent solution for 20 min. at 20°C, followed by incubation with a 1/2 dilution of Folin-Ciocalteau reagent in distilled H_2O (100μl) for 30 min. at 20°C. Absorbance at 750nm was determined for each sample and the resultant standard curve obtained

for protein content (0-50μg) was used to determine sample protein concentrations.

2.10 Assay for sulfhydryl groups

This assay was carried out after the method of Ellman, (1959). Samples were diluted as appropriate and 330μl added to tubes containing 100mM sodium phosphate buffer, pH 7.5 (600μl) and 10mM 5,5'-dithio-bis(2-nitrobenzoic acid) (DTNB) (65μl). Following mixing and incubation at 20°C for 10 min. the absorbance of each reaction solution was measured at 412nm. The extinction coefficient for the chromophore at 412nm is 14,100 M^{-1}. A concentration of 5 x 10^{-5} M chromophore thus yields an absorbance of 0.705. Hence the concentration of free sulphydryl groups is given the following equation.

[Free sulfhydryl groups] = 0.05M x A_{412} / 0.705 x sample vol.

2.11 SDS/PAGE with Coomassie Blue staining

SDS/PAGE was performed according to the method of Laemmli (1970), using 1.5mm-thick 10 and 12% slab gels. All materials were 'Electran' grade or electrophoresis purity reagents from Bio-Rad.

Protein samples were solubilized in a sample buffer [50mM Tris-HCl, pH 6.8, 1mM EDTA, 2% (w/v) SDS, 4mM DTT, 10% (v/v) glycerol, 0.012% (w/v) pyronin Y] and heated to 95°C for 5 min. Aliquots of the protein samples (10-50μl) containing 10-50μg protein were separated in each lane of a 10cm separating gel (10 or 12% acrylamide/0.27 or 0.32% bisacrylamide in a buffer of 375mM Tris-HCl, pH 8.8 plus 0.1% SDS, polymerized by 0.1% (w/v) ammonium persulphate and 0.016% (v/v) tetramethylethylenediamine (TEMED). In order to achieve such separation, protein samples were loaded into individual wells of a 2cm stacking gel (3% acrylamide/0.08% bisacrylamide in a buffer of 125mM Tris/HCl, pH 6.8, containing

0.1% (w/v) SDS, polymerized by 0.1% (w/v) ammonium persulphate and 0.05% (v/v) TEMED) which had been overlaid on the separating gel. Molecular weight markers used consisted of a low molecular weight range preparation (M_r range 14,400-97,400) (Bio-Rad). The electrode buffer comprised 25mM Tris, 190mM glycine and 0.1% (w/v) SDS, pH 8.3. Electrophoresis was performed at 12mA (constant current) over 14h. using a Protean Mk I electrophoresis cell (Bio-Rad) and an EPS 500/400 power supply (Pharmacia). The gels were run until the pyronin Y marker had migrated to within 0.5cm of the end of the gel.

For Coomassie blue staining of the proteins, the gels were soaked for 2h in 10% (v/v) acetic acid, 25% (v/v) isopropanol, soaked for 8h in 10% (v/v) acetic acid, 25% (v/v) isopropanol, 0.025% (w/v) Coomassie Brilliant Blue R-250, followed by 12h. 10% (v/v) acetic acid, 10% (v/v) isopropanol, 0.0025% (w/v) Coomassie Brilliant Blue R-250 and destained in 10% (v/v) acetic acid.

CHAPTER 3

SYNTHESIS AND CHARACTERIZATION OF CALCIUM CHANNEL PEPTIDES

3.1 GENERAL INTRODUCTION

3.1.1 Rationale for the use of the anti-peptide antibody approach in the study of the Ca^{2+} channel

Antibodies provide an alternative means to protein-chemical and physical methods in the study of both the structure and function of membrane proteins. Both polyclonal and monoclonal antibodies raised using the intact protein as immunogen have been used successfully to study a variety of membrane proteins. Antibodies raised using the intact L-type channel from rabbit skeletal muscle or its various subunits have proved useful in the identification and purification of Ca^{2+} channels from a variety of sources (Takahashi and Catterall, 1987; Sakamoto and Campbell, 1991b; Tokumaru *et al.*, 1992). They have also been very useful for investigating the tissue distribution and intracellular localization of Ca^{2+} channels, using immunocytochemical techniques (Jorgensen *et al.*, 1989; Yuan *et al.*, 1990; Flucher *et al.*, 1990; Flucher *et al.*, 1991a, 1991b; Chin *et al.*, 1992). The availability of antibodies raised in this fashion has facilitated the examination of changes in levels of channel expression during tissue development (Morton and Froehner, 1989).

Ca^{2+} channels in general, with the exception of the skeletal muscle L-type channel, are very low abundance components of the membranes of most tissues. This has made purification of the channels from virtually all sources except skeletal muscle very difficult, with the yields of purified protein obtained being extremely low. Various monoclonal (Leung *et al.*, 1987; Morton and Froehner, 1987; Norman *et al.*, 1987; Hayakawa *et al.*, 1990) and polyclonal (Takahashi and Catterall, 1987) antibodies which recognize channel polypeptides have been produced, using the intact,

purified rabbit skeletal muscle L-type, and more recently the purified rat brain P-type channel (Cherksey *et al.*, 1991), as immunogen. This approach is, conceivably, also possible for the other channel types, whose purification protocols have recently been reported, namely, cardiac L-type and brain N-type, despite their 100-fold, or more, lower abundance in their respective membranes, compared to the t-tubule L-type channel (Tokumaru *et al.*, 1992; Takahashi and Catterall, 1987). However, for channel types of such low abundance, isolation of the channel prior to its use as immunogen is very difficult.

Alignment of all the currently available amino acid sequences for Ca^{2+} channel α_1, α_2 and δ subunits (see Fig. 3.1), and also of the ß and γ subunits (not shown), reveals the existence of regions both of identity and of very strong similarity between the subunits associated with the various channel classes found in different tissues. Thus, antibodies raised using either a purified whole channel protein or an intact purified subunit as immunogen may react with some or with all related Ca^{2+} channel proteins. While this phenomenon has proved useful e.g. in the purification of both the brain N-type and cardiac L-type channels (Takahashi and Catterall, 1987; Tokumaru *et al.*, 1992), investigations of channel distribution require antibodies which are specific for single channel classes. The existence of four homologous domains within the channel α_1 subunit also means that it is theoretically possible even for some monoclonal antibodies to bind to more than one site in a single α_1 subunit. Thus, the main limitation of this approach is the difficulty in producing antibodies against certain purified channel subtypes, coupled with the possible lack of specificity of the resultant antibodies either for their particular channel subtypes or for particular regions/domains in the channel tertiary structure.

As described above, there are a number of problems associated with the use of intact Ca^{2+} channel proteins as immunogens. However, it has been known for a number of years that antibodies capable of recognizing an intact protein can also be produced by using short synthetic peptide immunogens which correspond in sequence to particular regions of that protein. Production of such antibodies is known to be most readily achieved by immunization with synthetic peptides bound to carrier

proteins, using protocols such as those outlined in Section 2.4.1. Use of this anti-peptide antibody approach offers a number of advantages in the study of Ca^{2+} channels. This is due to the site-directed nature and pre-determined specificity of anti-peptide antibodies, features that distinguish them from antibodies produced by other procedures (reviewed by Lerner, 1982, 1984). By careful selection of the peptide sequences used as immunogens, it should be possible to raise antibodies that are specific not only for a single region in a protein containing multiple homologous domains, but also that do not recognize other, homologous proteins. Such antibodies are potentially more useful as probes than those raised using the whole protein as antigen, e.g. for studying the distribution of channel polypeptides and the membrane orientation of segments of their primary structure. For these reasons, and also because of the lack of availability of purified rat brain class A and D channels, the anti-peptide antibody approach was adopted for the present study, in order to probe channel structure, function and distribution.

3.1.2 Theoretical considerations

Antibodies bind to proteins via interaction between functional binding sites or paratopes on the immunoglobulin molecule and antigenic determinants or epitopes on the antigen. Thus, an epitope is that part of an antigen, in this case a protein, which is recognized by an antibody. Antibodies bind to the surface of proteins and so the epitopes of native proteins consist of residues exposed at the surface. Two general types of epitope exist, namely continuous and discontinuous. The former consist of a single set of residues that are contiguous in the protein sequence, while the latter is made up of a number of residues which are not contiguous in the sequence but are brought together by the folding of the polypeptide chain or by the closeness of two separate peptide chains.

Any linear peptide fragment which reacts with antibodies raised using the intact protein denotes a continuous epitope. However, the linear peptide may not represent the complete structure of the corresponding epitope in the protein. The

peptide may constitute only a part of a large discontinuous epitope but nevertheless react with antibodies specific for that epitope. The reactivity of continuous epitopes with anti-protein antibodies depends on the peptide's ability to assume the correct conformation, and it is likely that not all of its amino acid residues will make contact with the antibody.

In an attempt to produce anti-peptide antibodies which are cross-reactive with the native protein of interest, methods have been developed which claim to predict the position of continuous epitopes and thus, of suitable immunogenic sequences in a protein. Such sequences, consisting mostly of residues exposed on the protein surface, tend to be hydrophilic and accessible, while possessing relatively high segmental mobility and relatively little secondary structure compared to the rest of the protein. Attempts have been made to correlate the generation of anti-peptide antibodies, capable of recognizing native proteins, with a variety of factors including secondary structure (Chou and Fasman, 1978; Garnier *et al.*, 1978; Niman *et al.*, 1983; Dyson *et al.*, 1985, 1988; Wright *et al.*, 1988), atomic (segmental) mobility (Artymiuk *et al.*, 1979; Moore and Williams 1980, Williams and Moore, 1985; Lerner, 1984; Westhof *et al.*, 1984; Tainer *et al.*, 1984, 1985; Hirayama *et al.*, 1985; Karplus and Schulz, 1985) and sequence accessibility/polarity (Hopp and Woods, 1981; Hopp, 1985; Stevens, 1986). However, in a review of over 100 peptides studied, Palfreyman *et al.*, (1984) failed to assign statistical significance to any of the predictive algorithms used. Instead, they concluded that the success rate (antibodies produced that recognize the native protein) could be maximized simply by choosing a peptide length of at least 10 residues, of which a significant number are hydrophilic. The generation of antibodies to terminal sequences was successful in all cases, and this has been attributed to greater conformational freedom within these sequences (Walter, 1986).

3.1.3 Specific application of antibodies in the study of membrane proteins, in particular channels

The usefulness and limitations of antibodies raised against intact proteins have been outlined above. In this section examples are given of studies, mainly on channels, which have required site-directed anti-peptide antibodies. These studies include establishing the membrane orientation of various segments of primary structure of the Na^+ channels α polypeptide (Meiri *et al.*, 1987; Gordon *et al.*, 1987a, 1988a, 1988b; Tejedor and Catterall, 1988; Vassilev *et al.*, 1988, 1989; Nakayama *et al.*, 1993) and investigating the function and role of specific regions of the channel via inhibition/stimulation of an activity e.g. channel opening/closing (Meiri *et al.*, 1987; Gordon *et al.*, 1988b; Vassilev *et al.*, 1988, 1989). Sites of ligand binding and phosphorylation have also been located, thus identifying functionally important sites, by examining effects on binding of site-specific antibodies (Thomsen and Catterall, 1989; Nakayama *et al.*, 1992b). 'Active sites' of ligand binding and phosphorylation have also been located by using anti-peptide antibodies to identify peptides in digests either of prelabelled Na^+ channel α polypeptide (Rossie *et al.*, 1987; Tejedor & Catterall, 1988; Rossie and Catterall, 1989; Nakayama *et al.*, 1992a) or of Ca^{2+} channel α_1 subunit photolabelled with inhibitors (Striessnig *et al.*, 1990b, 1991; Nakayama *et al.*, 1991).

3.1.3.1 Purification and elucidation of functional roles

Antibodies have been used in several studies for the purification of Ca^{2+} channels and their subunits. For example, affinity chromatography using a monoclonal antibody recognizing the rabbit skeletal muscle L-type Ca^{2+} channel α_2/δ subunit has facilitated a rapid purification of porcine cardiac channel (Tokumaru *et al.*, 1992). A single iodinated brain Ca^{2+} channel subunit was purified from solubilized synaptosomal proteins by immunoprecipitation, using a polyclonal antibody raised against the purified rabbit skeletal muscle channel. This allowed its

electrophoretic similarity to the skeletal muscle α_2 polypeptide and thus the presence of both Ca^{2+} channel α_1 and α_2 polypeptides in the brain to be established (Takahashi and Catterall, 1987). Immunological, and therefore structural, similarities between rabbit skeletal muscle channel subunits and those present in other muscle types or other tissues e.g. rabbit brain DHP- and CgTx-sensitive channel ß polypeptide (Sakamoto and Campbell, 1991b), have been revealed by observed immunoprecipition of these polypeptides, using both monoclonal and polyclonal antibodies specific for the rabbit skeletal muscle subunits.

Immunoprecipitation has also been used to demonstrate that the separate subunits of the channel complex are integral, stoichiometric components of the complex, not just co-purifying contaminants. For example, immunoprecipitation of whole rabbit skeletal muscle Ca^{2+} channel, along with immunoblotting, using a monoclonal antibody raised against the 52kDa ß subunit of this protein has shown this subunit to be an integral part of the purified DHP receptor (Leung *et al.*, 1988). Similarly, anti-α_1 and anti-α_2 polyclonal antibodies have immunoprecipitated an $\alpha_1,\alpha_2,ß,\gamma,\delta$ complex from both digitonin- and CHAPS- solubilized rabbit skeletal muscle t-tubule membranes (Takahashi *et al.*, 1987). The comparative study of both chick cardiac and skeletal muscle L-type channel subunits was also enabled by the immunoprecipitation of [^{3}H]PN200-110-labelled Ca^{2+} channel from their digitonin-solubilized membranes by Yoshida *et al.*, (1990) using a monoclonal antibody.

3.1.3.2 Tissue distribution and developmental changes (immunocytochemistry as a complement to in situ hybridization)

Various studies have employed immunofluorescence and immunogold labelling techniques to localize proteins in different tissues using either monoclonal and polyclonal antibodies, raised using intact polypeptides as immunogen or peptide-specific antibodies. The distribution of L-type Ca^{2+} channel α_1 and α_2 subunits in fixed and embedded rat skeletal muscle sections (Flucher *et al.*, 1990), and of its α_1

and γ subunits in cryosections of both fixed and unfixed rabbit skeletal muscle (Jorgensen *et al.*, 1989) has been established using monoclonal antibodies, raised against the Ca^{2+} channel α_1/α_2 subunit complex (in the former study) and against both the α_1 and γ polypeptides, in the latter study. More recently DHP-sensitive Ca^{2+} channel α_1 subunits have been similarly localized in fixed rat brain sections using an antibody raised against a peptide sequence found in both class C and class D neuronal L-type calcium channels (Chin *et al.*, 1992).

Various other localization studies of the α_1 and α_2 polypeptides have yielded information on the expression and interaction of these polypeptides in developing muscle. Morton and Froehner (1989) used monoclonal antibodies recognizing these two polypeptides to show that they are differentially expressed, during development, in rat skeletal muscle. Levels of α_1 are quite low during the first 10 days after birth and then rise dramatically, reaching levels approaching those found in adult muscle by day 20. On the other hand, α_2 is present in substantial amounts at birth and increases only slightly with development. Immunofluorescence labelling using monoclonal antibodies revealed that while in normal muscle both Ca^{2+} channel α_1 and α_2 subunits appear to be located in clusters along the t-tubules, in muscle from skeletal muscle dysgenic (MDG) mice, where no α_1 polypeptide was detected, α_2 was distributed abnormally (Flucher *et al.*, 1991a), leading to the suggestion that α_2 requires the presence of α_1 for its localization to the t-tubule triads.

3.1.3.3 Membrane Topology

Information on the arrangement of proteins in the membrane has been obtained using monoclonal antibodies raised using the whole protein as immunogen. However, it is first necessary to establish the antibody binding site. Such antibodies recognizing domains in the IS5-IS6 loop of the Na^+ channel helped to identify the part of the extracellular site of interaction of α-Scorpion toxin with the channel (Thomsen and Catterall, 1989).

However, the production of antibodies to synthetic peptides has enabled the

transmembrane topology of membrane proteins to be studied in more detail. Vectorial binding studies using these site-specific, membrane-impermeable probes offers a means to assess protein structure predictions based on sequence data. Several studies have employed such an approach including investigations of the lactose permease of *E. coli* (Seckler *et al.*, 1983, 1986; Carrasco *et al.*, 1986), the nicotinic acetylcholine receptor (Ratnam *et al.*, 1986), the bovine heart ADP/ATP carrier (Brandolin *et al.*, 1989), the melibiose/Na^+ symporter of *E. coli* (Botfield and Wilson, 1989), the hamster $ß_2$-adrenergic receptor (Wang *et al.*, 1989) and synaptophysin, a major integral membrane protein of small synaptic vesicles (Johnston *et al.*, 1989). Antibodies raised against specific peptide sequences from the human erythrocyte glucose transporter have been used to probe the membrane topology of this protein by assigning either intra- or extracellular orientation to the binding site for each particular antibody on the protein in "inside-out" or "right-side-out" erythrocyte membranes vesicles (Davies *et al.*, 1987, 1990).

With regard to ion channels, findings from various studies using anti-peptide antibodies (discussed in Section 1.5.2), and in one case also monoclonal antibodies, have allowed the membrane orientation of all the major hydrophilic segments in the primary structure of the α subunit of the Na^+ channel to be determined (Meiri *et al.*, 1987; Gordon *et al.*, 1987a, 1988a, 1988b; Tejedor & Caterall, 1988; Vassilev *et al.*, 1988, 1989; Thomsen and Catterall, 1989; Nakayama *et al.*, 1993).

3.1.3.4 Structure and function

The latter studies also helped to identify functionally relevant regions of the Na^+ channel such as the binding site for α-Scorpion toxin (Tejedor & Caterall, 1988; Thomsen and Catterall, 1989) and sites of cAMP-dependent phosphorylation which are known to modulate the voltage dependence of closure of the channel by the inactivation gating segment (Rossie *et al.*, 1987; Rossie and Catterall, 1989). Localization of these sites was achieved by identifying the labelled peptides obtained following CNBr digestion of the labelled channel, by immunoprecipitation, using

peptide-specific antibodies. More recently, the same experimental approach has facilitated the determination of the binding domain of a photoactivable TTX derivative (TTX[^{3}H]enDTB) to the electroplax Na^+ channel (Nakayama *et al.*, 1992a) and of particular sites of phosphorylation on the α polypeptide of the rat brain Na^+ channel (Nakayama *et al.*, 1992b).

In the case of the Ca^{2+} channel α_1 subunit, the functionally important binding sites for Ca^{2+} channel antagonists of the PAA (Striessnig *et al.*, 1990b) and DHP (Striessnig *et al.*, 1991; Nakayama *et al.*, 1991) classes have similarly been identified following immunoprecipitation of photolabelled, proteolytic fragments using peptide-specific antibodies (discussed in Section 6.1.2). Immunoblotting and immunoprecipitation of the skeletal muscle L-type Ca^{2+} channel α_1 subunit using several peptide-specific antibodies has also allowed the location of the C-terminus of the truncated polypeptide to between amino acid residues 1685 and 1699 (De Jongh *et al.*, 1991).

Subsequently, studies using anti-peptide antibodies have yielded valuable information on structure/function relationships of the Na^+ channel (Meiri *et al.*, 1987; Gordon *et al.*, 1988b; Vassilev *et al.*, 1988, 1989). Na^+ channel inactivation was modulated by intracellular perfusion with antibodies against the hydrophilic segment between homologous domains III and IV of the α subunit (Gordon *et al.*, 1988b; Vassilev *et al.*, 1988, 1989). Antibodies directed against this segment caused delayed opening and prolonged open times of single channels during depolarizing test pulses, inhibiting Na^+ channel inactivation almost completely (Vassilev *et al.*, 1988; Vassilev *et al.*, 1989). The observed voltage-dependence both of the binding and of the effect of the antibody indicated that its intracellular antigenic site was rendered inaccessible by inactivation. These studies reveal that a conformational change involving this segment in the III-IV loop of the Na^+ channel α subunit is required for fast inactivation of the channel and suggest that this segment may be the fast inactivation gate of the Na^+ channel. The segment appears to fold into the channel structure to serve as the inactivation gate by blocking the pore, thus becoming inaccessible to antibody binding (Vassilev *et al.*, 1988, 1989). Antibodies recognizing the IS4

segment of eel Na^+ channel caused channel activation to become less sensitive to membane voltage, while antibodies recognizing a peptide in the C-terminal region of the α polypeptide had the opposite effect, rendering activation more sensitive to membrane voltage (Meiri *et al.*, 1987).

3.2 INTRODUCTION TO PRESENT STUDY

3.2.1 Choice of regions of the channel subunit sequences used for production of anti-peptide antibodies

As well as utilizing the antibodies to achieve the aims of this study (outlined in Section 1.10), it was intended to supply a number of the antibodies, recognizing proposed functionally important regions of the channel, for a study involving electrophysiological investigation of their effect on the function of the Ca^{2+} channel in mouse neuroblastoma x rat glioma NG108-15 cells. With this in mind, the criterion for selection of many of the peptides was their location in regions of the channel which were suspected to have a role in either channel activation (peptides B, C and G) or inactivation (peptide E and L), or to be involved in functionally-important activities such as the binding of Ca^{2+} or ligands (peptides J and K) and channel phosphorylation (peptide N). For distributional studies, it was necessary to identify peptides whose sequences were specific to channels of a given class (peptides H and I, which are class A and D specific, respectively). A further polypeptide, J, corresponding to a region which is highly conserved between all channels sequenced to date, containing a putative EF hand, Ca^{2+}-binding domain which has proposed α-helical structure, was also selected for synthesis for the purpose of investigating its secondary structure.

An EF hand (see Fig. 3.1) is a helix-loop-helix supersecondary structure which has now been observed in several soluble Ca^{2+}-chelating proteins including parvalbumin, troponin C and calmodulin (Kretsinger and Nockolds, 1973; Moews and

Kretsinger, 1975; Hertzberg and James, 1985; Babu *et al.*, 1985; Babu *et al.*, 1988). X-ray crystallographic analysis of parvalbumin showed it to consist of six helices, A and B, C and D, and E and F separated by loops containing 12 aa, many of which are acidic and are involved in Ca^{2+} coordination. (Kretsinger and Nockolds, 1973; Moews and Kretsinger, 1975). The helices are oriented approximately perpendicular to each other with the C-D and E-F loops each binding one Ca^{2+}. The E helix, EF loop and F helix resemble the extended forefinger, clenched middle finger and extended thumb of a right hand and this is the structural motif referred to as the EF-hand.

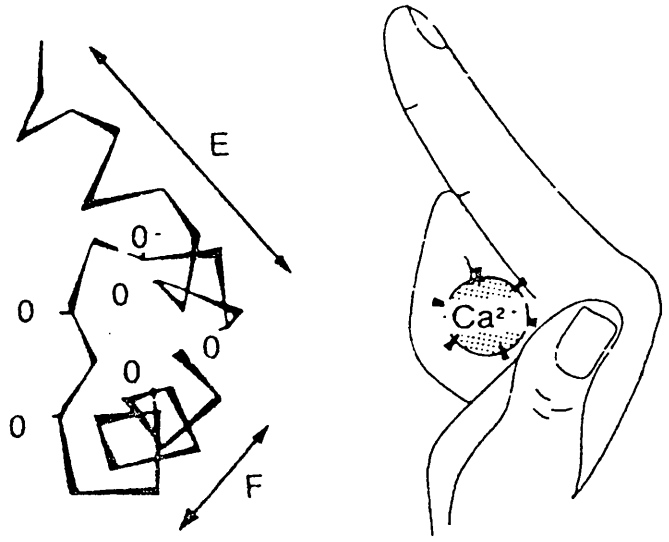

Fig. 3.1 Model of the structure of an EF-hand domain.

Later x-ray diffraction revealed four Ca^{2+} binding domains of the EF-hand (helix-loop-helix) type in both troponin C (Hertzberg and James, 1985) and calmodulin (Babu *et al.*, 1985; Babu *et al.*, 1988). All the studies were carried out on Ca^{2+}-loaded structures. Spectroscopic techniques, including CD (Closset and Gerday, 1975) and FTIR (Haris *et al.*, 1987; Trewhella *et al.*, 1989) have also

revealed a predominately α helical structure for EF-hand proteins in the presence of Ca^{2+}, while Ca^{2+} removal leads to an observable decrease in the apparent α helical content of the proteins.

Peptides sequences were selected from regions of the protein predicted to be accessible on the channel surface. The latter was done following comparison of the polypeptides sequences from different channels (see Figs. 3.2 and 3.3). The presence of insertions or deletions and of predominantly hydrophilic amino acid residues at particular sites is known to be a good predictor of surface probability, with interaction between these residues and the polar environment stabilizing the protein. There are three main reasons for the prerequisite of surface accessibility of peptide used to produce antibody probes. Firstly, only antibodies raised against surface sequences on a protein will in turn react with the intact protein in its native conformation. Secondly, the size of the response elicited by a synthetic peptide appears to be directly related to its hydrophilicity. This seems likely to be due to hydrophilic peptides remaining accessible in the polar environment on the surface of the carrier protein, following immunization, thereby being presented to the immune system of the animal concerned. Finally, such peptides, being highly soluble in aqueous buffer are easy to handle for characterization purposes as well as for conjugation to carrier protein, prior to use for antibody production.

The precise peptide sequence selected for synthesis in each case, with the exception of the 48 amino acid residue polypeptide to be used in secondary structure analysis, contained at least 12 and not more than 21 amino acid residues, a significant number of which were hydrophilic. As discussed above, such short peptides are likely to generate a good anti-peptide response.

As is evident in Fig. 3.2, all the known α_1 polypeptides possess a high degree of amino acid sequence similarity in their proposed membrane spanning domains, while the sequences diversify in the smaller exofacial loops and to a greater extent in the larger intracellular domains, particularly the loop between IIS6 and IIIS1, and the C-terminal region. However, the cytoplasmic sequence adjacent to the IVS6 segment is highly conserved in all the channel sequences published to date.

Fig. 3.2 ALIGNMENT OF CALCIUM CHANNEL SEQUENCES

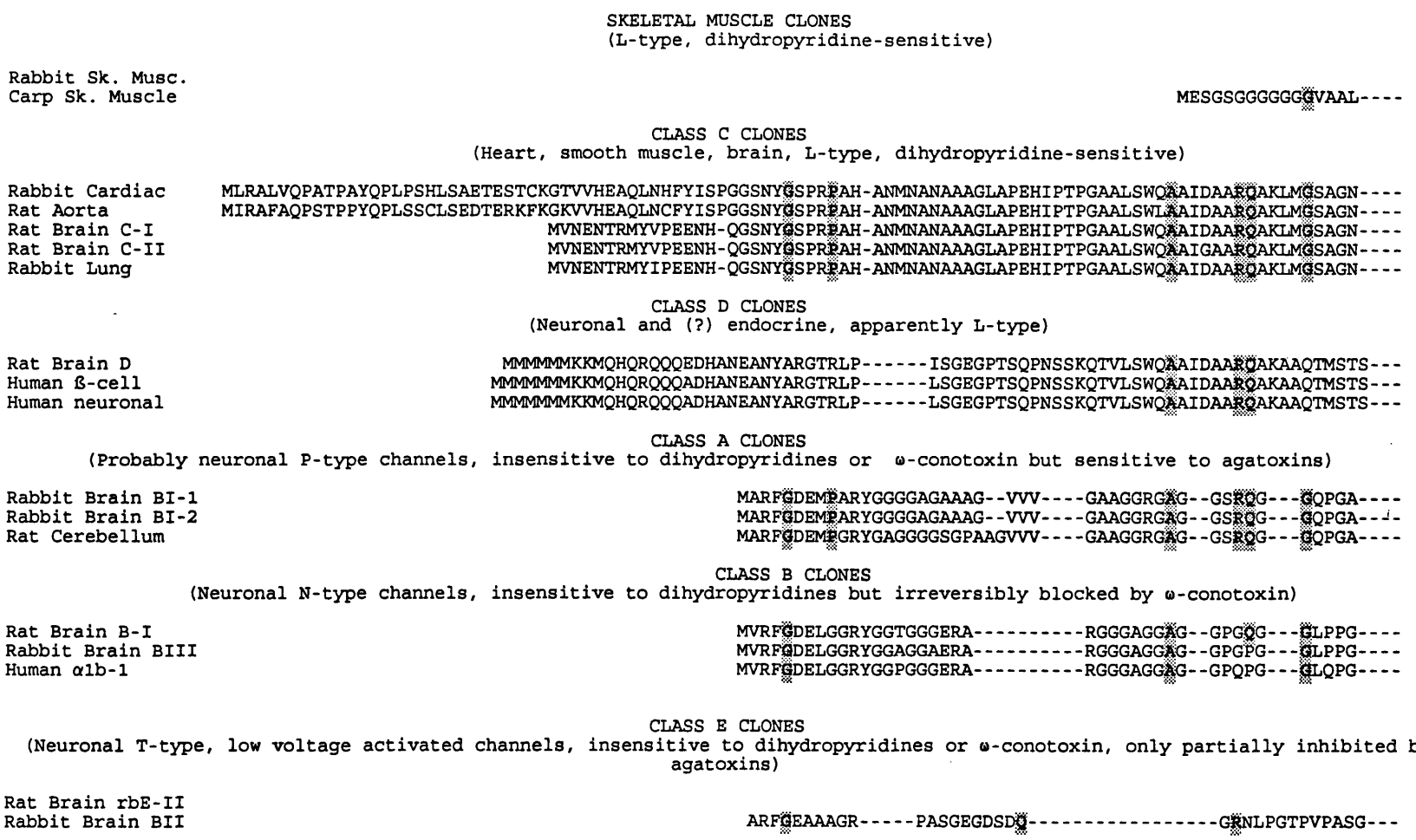

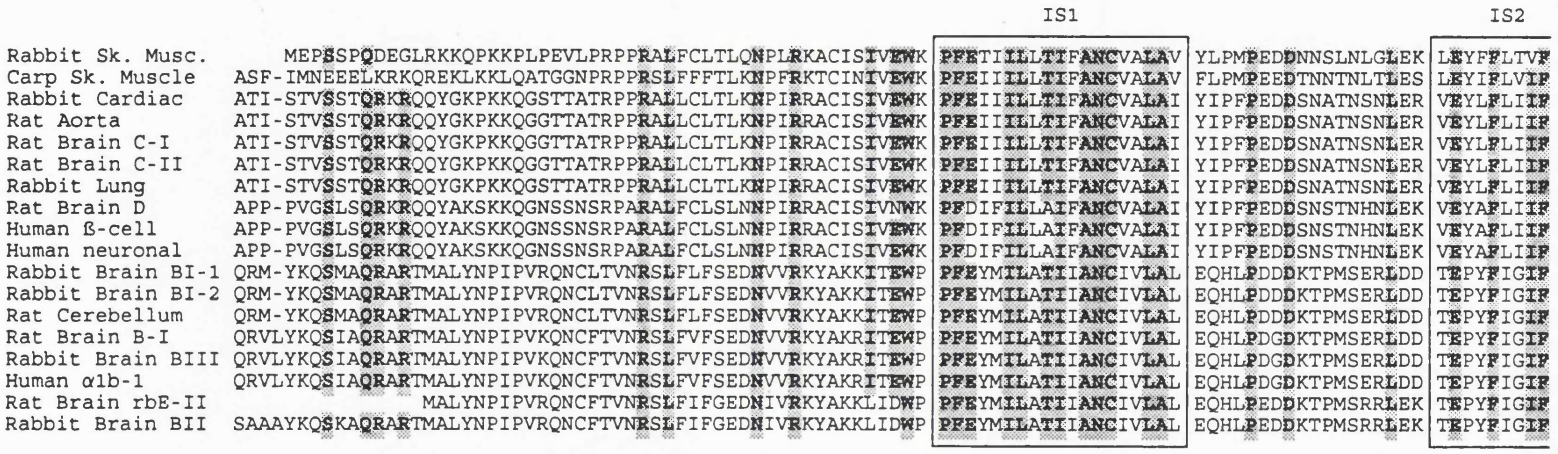
IS1
IS2
Rabbit Sk. Musc.
Carp Sk. Muscle
Rabbit Cardiac
Rat Aorta
Rat Brain C-I
Rat Brain C-II
Rabbit Lung
Rat Brain D
Human ß-cell
Human neuronal
Rabbit Brain BI-1
Rabbit Brain BI-2
Rat Cerebellum
Rat Brain B-I
Rabbit Brain BIII
Human α1b-1
Rat Brain rbE-II
Rabbit Brain BII

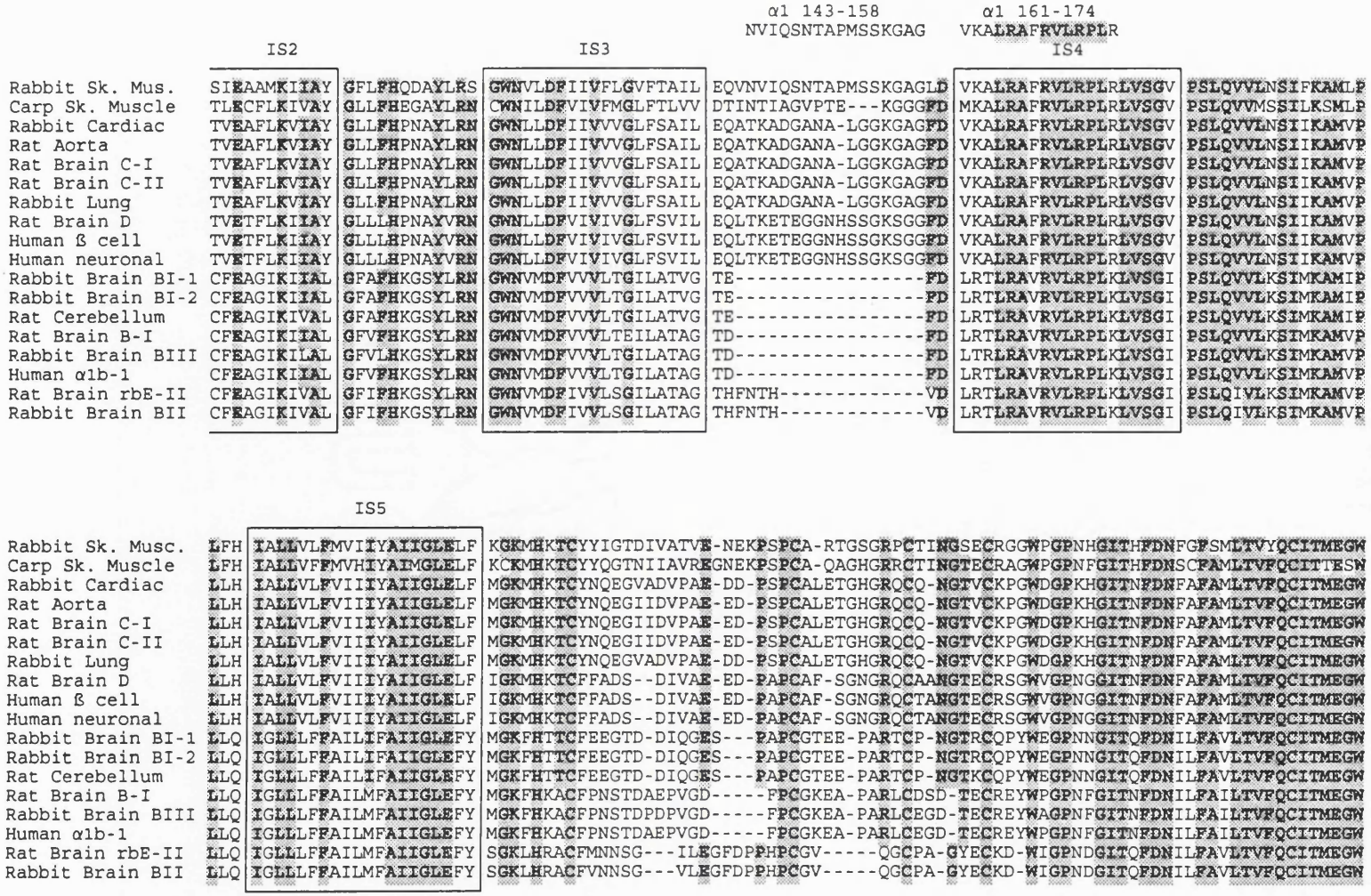
α1 143-158
NVIQSNTAPMSSKGAG
α1 161-174
VKALRAFRVLRPLR
IS2
IS3
IS4
IS5
Rabbit Sk. Mus.
Carp Sk. Muscle
Rabbit Cardiac
Rat Aorta
Rat Brain C-I
Rat Brain C-II
Rabbit Lung
Rat Brain D
Human ß cell
Human neuronal
Rabbit Brain BI-1
Rabbit Brain BI-2
Rat Cerebellum
Rat Brain B-I
Rabbit Brain BIII
Human α1b-1
Rat Brain rbE-II
Rabbit Brain BII
Rabbit Sk. Musc.
Carp Sk. Muscle
Rabbit Cardiac
Rat Aorta
Rat Brain C-I
Rat Brain C-II
Rabbit Lung
Rat Brain D
Human ß cell
Human neuronal
Rabbit Brain BI-1
Rabbit Brain BI-2
Rat Cerebellum
Rat Brain B-I
Rabbit Brain BIII
Human α1b-1
Rat Brain rbE-II
Rabbit Brain BII

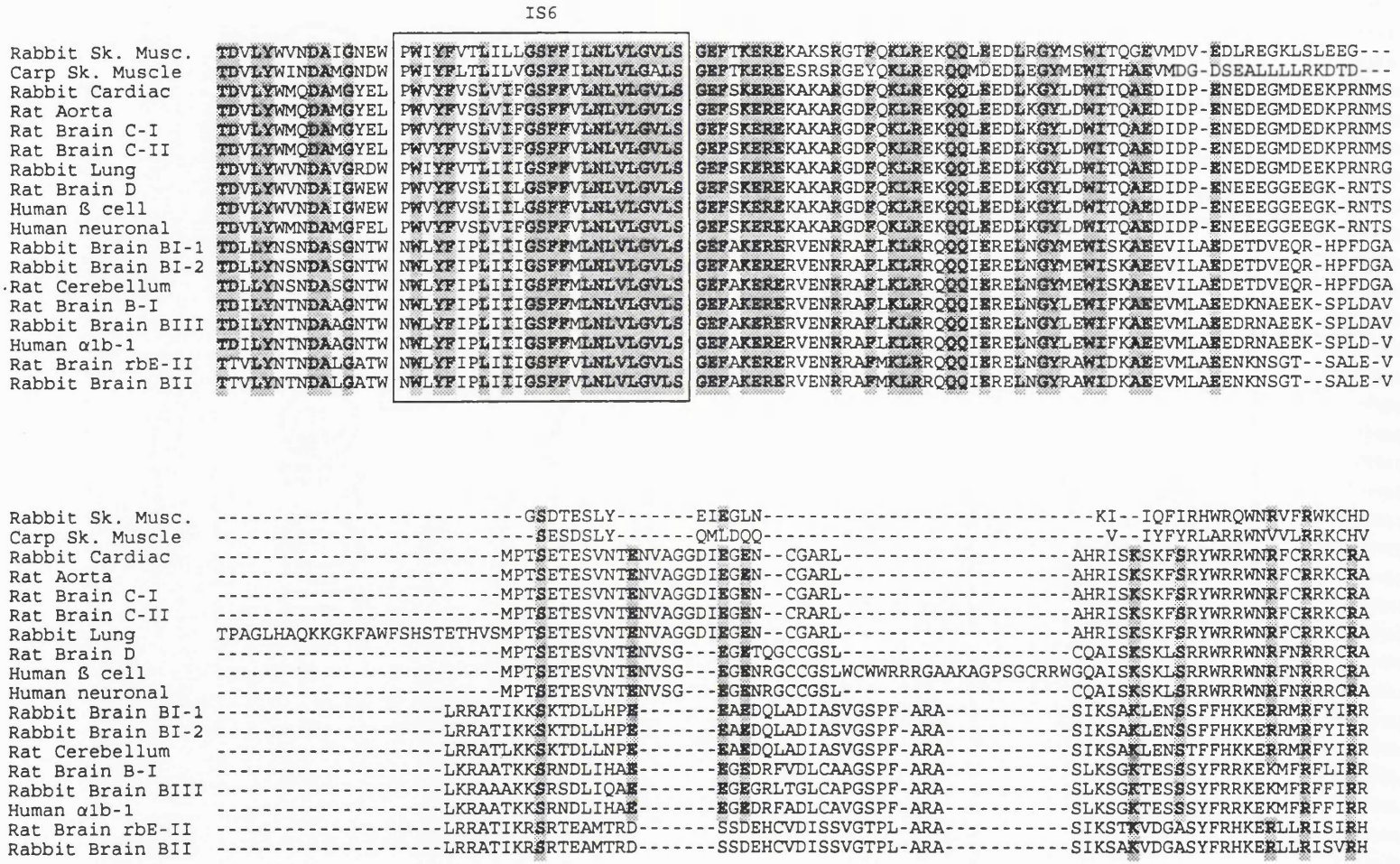
IS6
Rabbit Sk. Musc.
Carp Sk. Muscle
Rabbit Cardiac
Rat Aorta
Rat Brain C-I
Rat Brain C-II
Rabbit Lung
Rat Brain D
Human ß cell
Human neuronal
Rabbit Brain BI-1
Rabbit Brain BI-2
Rat Cerebellum
Rat Brain B-I
Rabbit Brain BIII
Human α1b-1
Rat Brain rbE-II
Rabbit Brain BII

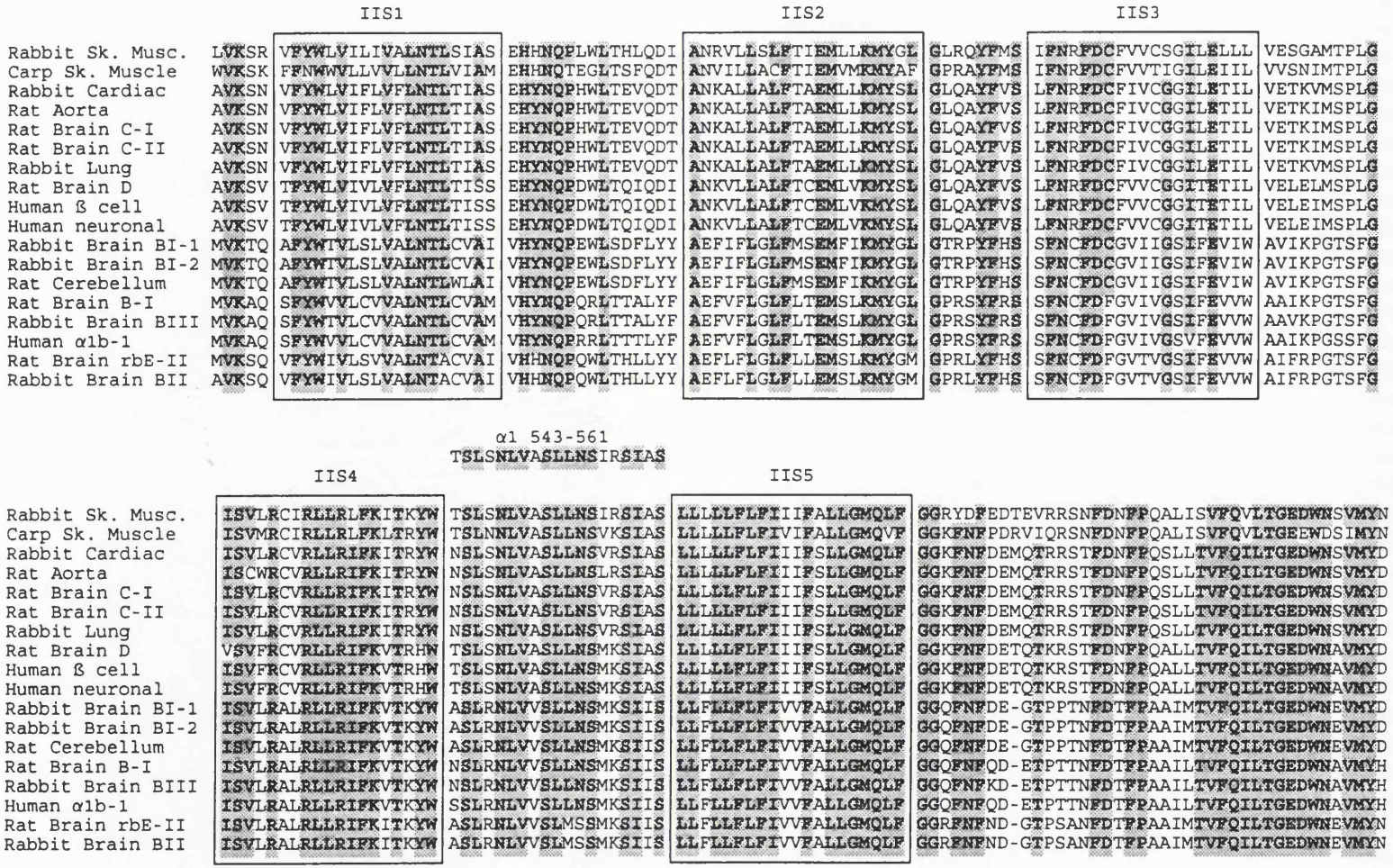
IIS1
IIS2
IIS3
Rabbit Sk. Musc.
Carp Sk. Muscle
Rabbit Cardiac
Rat Aorta
Rat Brain C-I
Rat Brain C-II
Rabbit Lung
Rat Brain D
Human ß cell
Human neuronal
Rabbit Brain BI-1
Rabbit Brain BI-2
Rat Cerebellum
Rat Brain B-I
Rabbit Brain BIII
Human α1b-1
Rat Brain rbE-II
Rabbit Brain BII
α1 543-561
TSLSNLVASLLNSIRSIAS
IIS4
IIS5

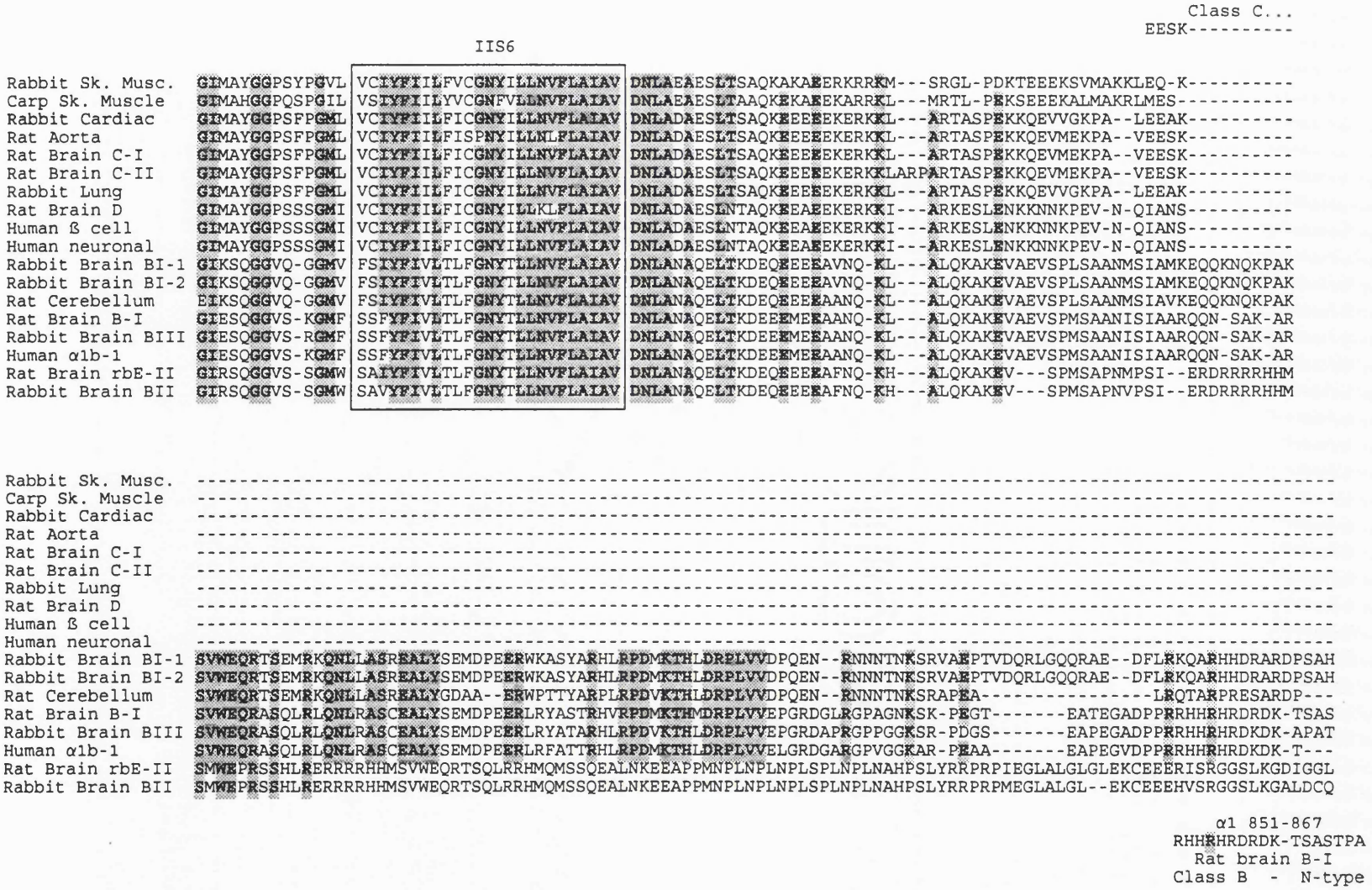
Class C...
EESK----------
IIS6
Rabbit Sk. Musc.
Carp Sk. Muscle
Rabbit Cardiac
Rat Aorta
Rat Brain C-I
Rat Brain C-II
Rabbit Lung
Rat Brain D
Human ß cell
Human neuronal
Rabbit Brain BI-1
Rabbit Brain BI-2
Rat Cerebellum
Rat Brain B-I
Rabbit Brain BIII
Human α1b-1
Rat Brain rbE-II
Rabbit Brain BII
α1 851-867
RHHRHRDRDK-TSASTPA
Rat brain B-I
Class B - N-type

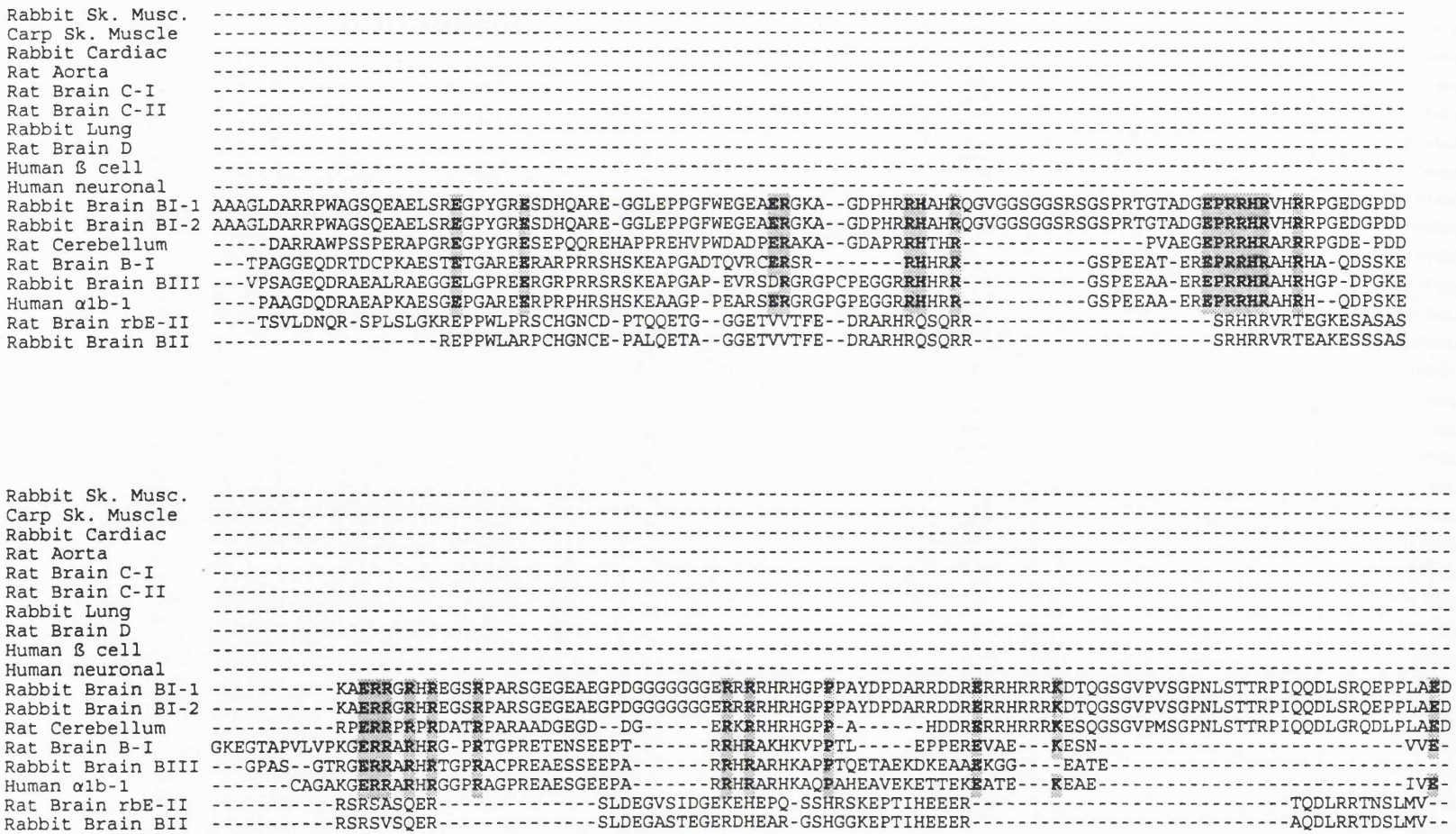
Rabbit Sk. Musc.
Carp Sk. Muscle
Rabbit Cardiac
Rat Aorta
Rat Brain C-I
Rat Brain C-II
Rabbit Lung
Rat Brain D
Human ß cell
Human neuronal
Rabbit Brain BI-1
Rabbit Brain BI-2
Rat Cerebellum
Rat Brain B-I
Rabbit Brain BIII
Human α1b-1
Rat Brain rbE-II
Rabbit Brain BII

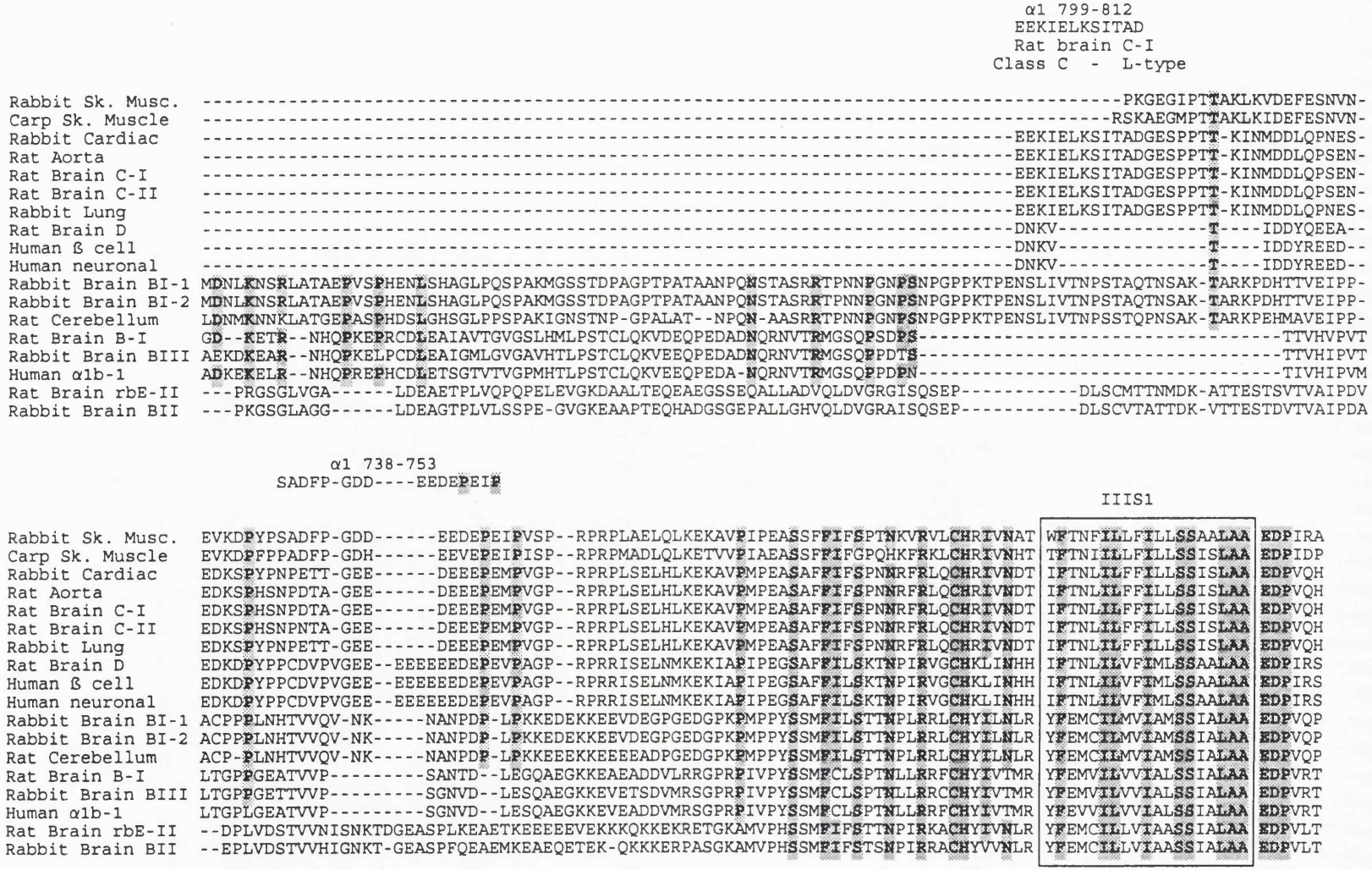
α1 799-812
EEKIELKSITAD
Rat brain C-I
Class C - L-type
α1 738-753
SADFP-GDD----EEDEPEIP
IIIS1
Rabbit Sk. Musc.
Carp Sk. Muscle
Rabbit Cardiac
Rat Aorta
Rat Brain C-I
Rat Brain C-II
Rabbit Lung
Rat Brain D
Human ß cell
Human neuronal
Rabbit Brain BI-1
Rabbit Brain BI-2
Rat Cerebellum
Rat Brain B-I
Rabbit Brain BIII
Human α1b-1
Rat Brain rbE-II
Rabbit Brain BII

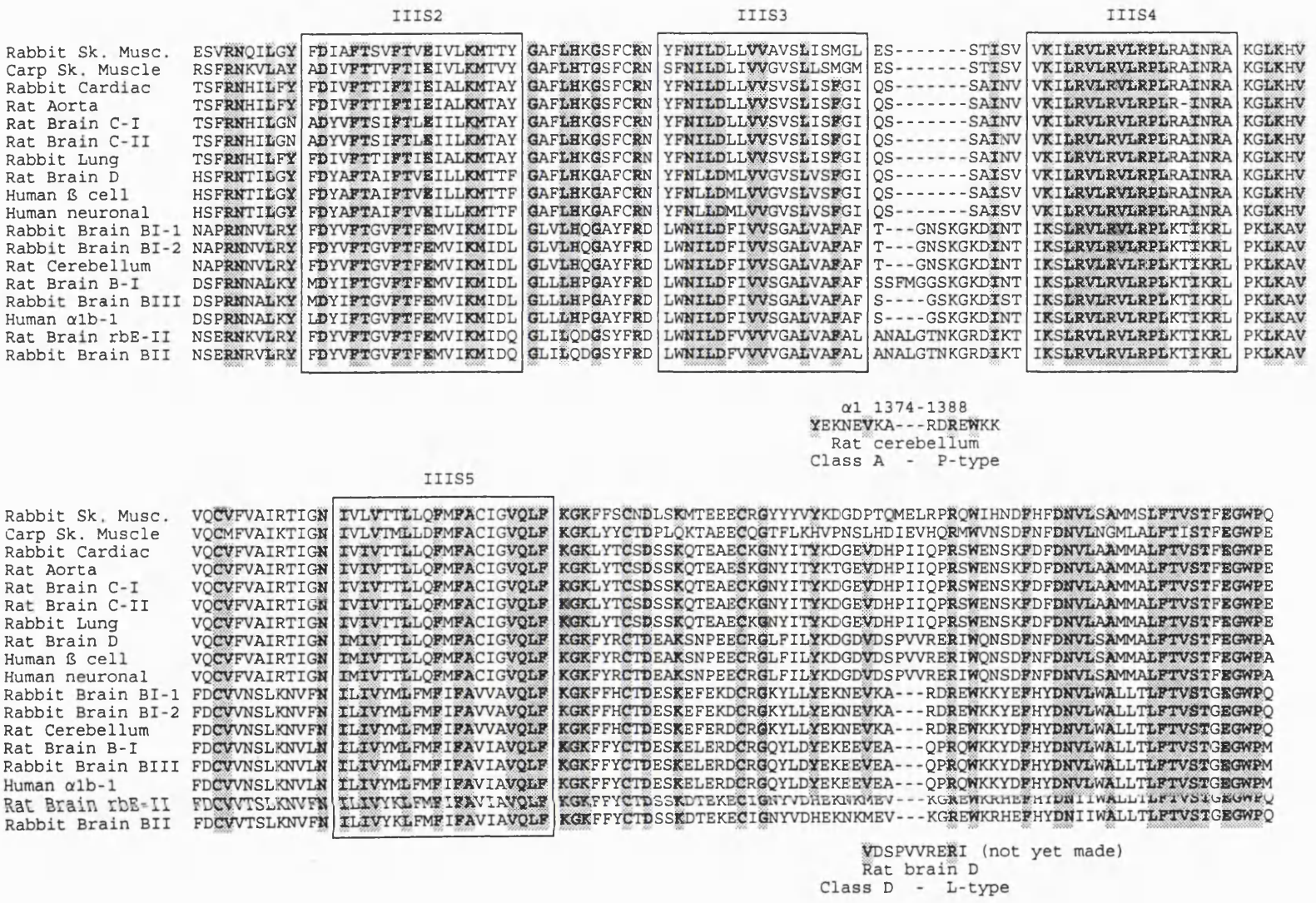
IIIS2
IIIS3
IIIS4
Rabbit Sk. Musc.
Carp Sk. Muscle
Rabbit Cardiac
Rat Aorta
Rat Brain C-I
Rat Brain C-II
Rabbit Lung
Rat Brain D
Human ß cell
Human neuronal
Rabbit Brain BI-1
Rabbit Brain BI-2
Rat Cerebellum
Rat Brain B-I
Rabbit Brain BIII
Human α1b-1
Rat Brain rbE-II
Rabbit Brain BII
α1 1374-1388
YEKNEVKA---RDREWKK
Rat cerebellum
Class A - P-type
IIIS5
VDSPVVRERI (not yet made)
Rat brain D
Class D - L-type

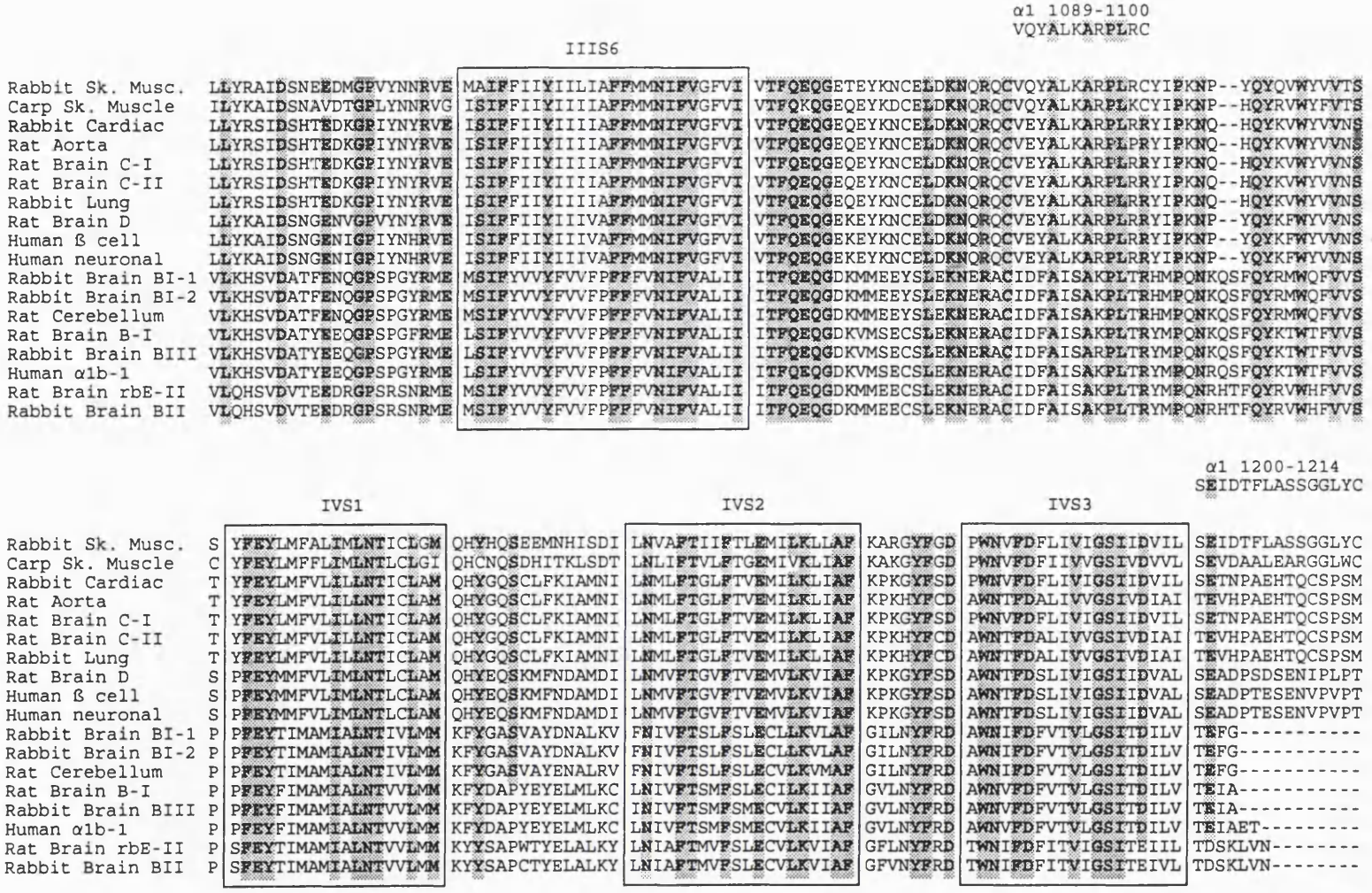
α1 1089-1100
VQYALKARPLRC
IIIS6
Rabbit Sk. Musc. LLYRAIDSNEEDMGPVYNNRVE MAIFFIIYIILIAFFMMNIFVGFVI VTFQEQGETEYKNCELDKNQRQCVQYALKARPLRCYIPKNP--YQYQVWYVVTS
Carp Sk. Muscle ILYKAIDSNAVDTGPLYNNRVG ISIFFIIYIIIIAFFMMNIFVGFVI VTFQKQGEQEYKDCELDKNQRQCVQYALKARPLKCYIPKNP--HQYRVWYFVTS
Rabbit Cardiac LLYRSIDSHTEDKGPIYNYRVE ISIFFIIYIIIIAFFMMNIFVGFVI VTFQEQGEQEYKNCELDKNQRQCVEYALKARPLRRYIPKNQ--HQYKVWYVVNS
Rat Aorta LLYRSIDSHTEDKGPIYNYRVE ISIFFIIYIIIIAFFMMNIFVGFVI VTFQEQGEQEYKNCELDKNQRQCVEYALKARPLPRYIPKNQ--HQYKVWYVVNS
Rat Brain C-I LLYRSIDSHTEDKGPIYNYRVE ISIFFIIYIIIIAFFMMNIFVGFVI VTFQEQGEQEYKNCELDKNQRQCVEYALKARPLRRYIPKNQ--HQYKVWYVVNS
Rat Brain C-II LLYRSIDSHTEDKGPIYNYRVE ISIFFIIYIIIIAFFMMNIFVGFVI VTFQEQGEQEYKNCELDKNQRQCVEYALKARPLRRYIPKNQ--HQYKVWYVVNS
Rabbit Lung LLYRSIDSHTEDKGPIYNYRVE ISIFFIIYIIIIAFFMMNIFVGFVI VTFQEQGEQEYKNCELDKNQRQCVEYALKARPLRRYIPKNQ--HQYKVWYVVNS
Rat Brain D LLYKAIDSNGENVGPVYNYRVE ISIFFIIYIIIVAFFMMNIFVGFVI VTFQEQGEKEYKNCELDKNQRQCVEYALKARPLRRYIPKNP--YQYKFWYVVNS
Human ß cell LLYKAIDSNGENIGPIYNHRVE ISIFFIIYIIIVAFFMMNIFVGFVI VTFQEQGEKEYKNCELDKNQRQCVEYALKARPLRRYIPKNP--YQYKFWYVVNS
Human neuronal LLYKAIDSNGENIGPIYNHRVE ISIFFIIYIIIVAFFMMNIFVGFVI VTFQEQGEKEYKNCELDKNQRQCVEYALKARPLRRYIPKNP--YQYKFWYVVNS
Rabbit Brain BI-1 VLKHSVDATFENQGPSPGYRME MSIFYVVYFVVFPFFFVNIFVALII ITFQEQGDKMMEEYSLEKNERACIDFAISAKPLTRHMPQNKQSFQYRMWQFVVS
Rabbit Brain BI-2 VLKHSVDATFENQGPSPGYRME MSIFYVVYFVVFPFFFVNIFVALII ITFQEQGDKMMEEYSLEKNERACIDFAISAKPLTRHMPQNKQSFQYRMWQFVVS
Rat Cerebellum VLKHSVDATFENQGPSPGYRME MSIFYVVYFVVFPFFFVNIFVALII ITFQEQGDKMMEEYSLEKNERACIDFAISAKPLTRHMPQNKQSFQYRMWQFVVS
Rat Brain B-I VLKHSVDATYEEQGPSPGFRME LSIFYVVYFVVFPFFFVNIFVALII ITFQEQGDKVMSECSLEKNERACIDFAISAKPLTRYMPQNKQSFQYKTWTFVVS
Rabbit Brain BIII VLKHSVDATYEEQGPSPGYRME LSIFYVVYFVVFPFFFVNIFVALII ITFQEQGDKVMSECSLEKNERACIDFAISARPLTRYMPQNKQSFQYKTWTFVVS
Human α1b-1 VLKHSVDATYEEQGPSPGYRME LSIFYVVYFVVFPFFFVNIFVALII ITFQEQGDKVMSECSLEKNERACIDFAISAKPLTRYMPQNRQSFQYKTWTFVVS
Rat Brain rbE-II VLQHSVDVTEEDRGPSRSNRME MSIFYVVYFVVFPFFFVNIFVALII ITFQEQGDKMMEECSLEKNERACIDFAISAKPLTRYMPQNRHTFQYRVWHFVVS
Rabbit Brain BII VLQHSVDVTEEDRGPSRSNRME MSIFYVVYFVVFPFFFVNIFVALII ITFQEQGDKMMEECSLEKNERACIDFAISAKPLTRYMPQNRHTFQYRVWHFVVS
α1 1200-1214
SEIDTFLASSGGLYC
IVS1
IVS2
IVS3
Rabbit Sk. Musc. S YFEYLMFALIMLNTICLGM QHYHQSEEMNHISDI LNVAFTIIFTLEMILKLLAF KARGYFGD PWNVFDFLIVIGSIIDVIL SEIDTFLASSGGLYC
Carp Sk. Muscle C YFEYLMFFLIMLNTLCLGI QHCNQSDHITKLSDT LNLIFTVLFTGEMIVKLIAF KAKGYFGD PWNVFDFIIVVGSIVDVVL SEVDAALEARGGLWC
Rabbit Cardiac T YFEYLMFVLILLNTICLAM QHYGQSCLFKIAMNI LNMLFTGLFTVEMILKLIAF KPKGYFSD PWNVFDFLIVIGSIIDVIL SETNPAEHTQCSPSM
Rat Aorta T YFEYLMFVLILLNTICLAM QHYGQSCLFKIAMNI LNMLFTGLFTVEMILKLIAF KPKHYFCD AWNTFDALIVVGSIVDIAI TEVHPAEHTQCSPSM
Rat Brain C-I T YFEYLMFVLILLNTICLAM QHYGQSCLFKIAMNI LNMLFTGLFTVEMILKLIAF KPKGYFSD PWNVFDFLIVIGSIIDVIL SETNPAEHTQCSPSM
Rat Brain C-II T YFEYLMFVLILLNTICLAM QHYGQSCLFKIAMNI LNMLFTGLFTVEMILKLIAF KPKHYFCD AWNTFDALIVVGSIVDIAI TEVHPAEHTQCSPSM
Rabbit Lung T YFEYLMFVLILLNTICLAM QHYGQSCLFKIAMNI LNMLFTGLFTVEMILKLIAF KPKHYFCD AWNTFDALIVVGSIVDIAI TEVHPAEHTQCSPSM
Rat Brain D S PFEYMMFVLIMLNTLCLAM QHYEQSKMFNDAMDI LNMVFTGVFTVEMVLKVIAF KPKGYFSD AWNTFDSLIVIGSIIDVAL SEADPSDSENIPLPT
Human ß cell S PFEYMMFVLIMLNTLCLAM QHYEQSKMFNDAMDI LNMVFTGVFTVEMVLKVIAF KPKGYFSD AWNTFDSLIVIGSIIDVAL SEADPTESENVPVPT
Human neuronal S PFEYMMFVLIMLNTLCLAM QHYEQSKMFNDAMDI LNMVFTGVFTVEMVLKVIAF KPKGYFSD AWNTFDSLIVIGSIIDVAL SEADPTESENVPVPT
Rabbit Brain BI-1 P PFEYTIMAMIALNTIVLMM KFYGASVAYDNALKV FNIVFTSLFSLECLLKVLAF GILNYFRD AWNIFDFVTVLGSITDILV TEFG----------
Rabbit Brain BI-2 P PFEYTIMAMIALNTIVLMM KFYGASVAYDNALKV FNIVFTSLFSLECLLKVLAF GILNYFRD AWNIFDFVTVLGSITDILV TEFG----------
Rat Cerebellum P PFEYTIMAMIALNTIVLMM KFYGASVAYENALRV FNIVFTSLFSLECVLKVMAF GILNYFRD AWNIFDFVTVLGSITDILV TEFG----------
Rat Brain B-I P PFEYFIMAMIALNTVVLMM KFYDAPYEYELMLKC LNIVFTSMFSLECILKIIAF GVLNYFRD AWNVFDFVTVLGSITDILV TEIA----------
Rabbit Brain BIII P PFEYFIMAMIALNTVVLMM KFYDAPYEYELMLKC INIVFTSMFSMECVLKIIAF GVLNYFRD AWNVFDFVTVLGSITDILV TEIA----------
Human α1b-1 P PFEYFIMAMIALNTVVLMM KFYDAPYEYELMLKC LNIVFTSMFSMECVLKIIAF GVLNYFRD AWNVFDFVTVLGSITDILV TEIAET---------
Rat Brain rbE-II P SFEYTIMAMIALNTVVLMM KYYSAPWTYELALKY LNIAFTMVFSLECVLKVIAF GFLNYFRD TWNIFDFITVIGSITEIIL TDSKLVN--------
Rabbit Brain BII P SFEYTIMAMIALNTVVLMM KYYSAPCTYELALKY LNIAFTMVFSLECVLKVIAF GFVNYFRD TWNIFDFITVIGSITEIVL TDSKLVN--------

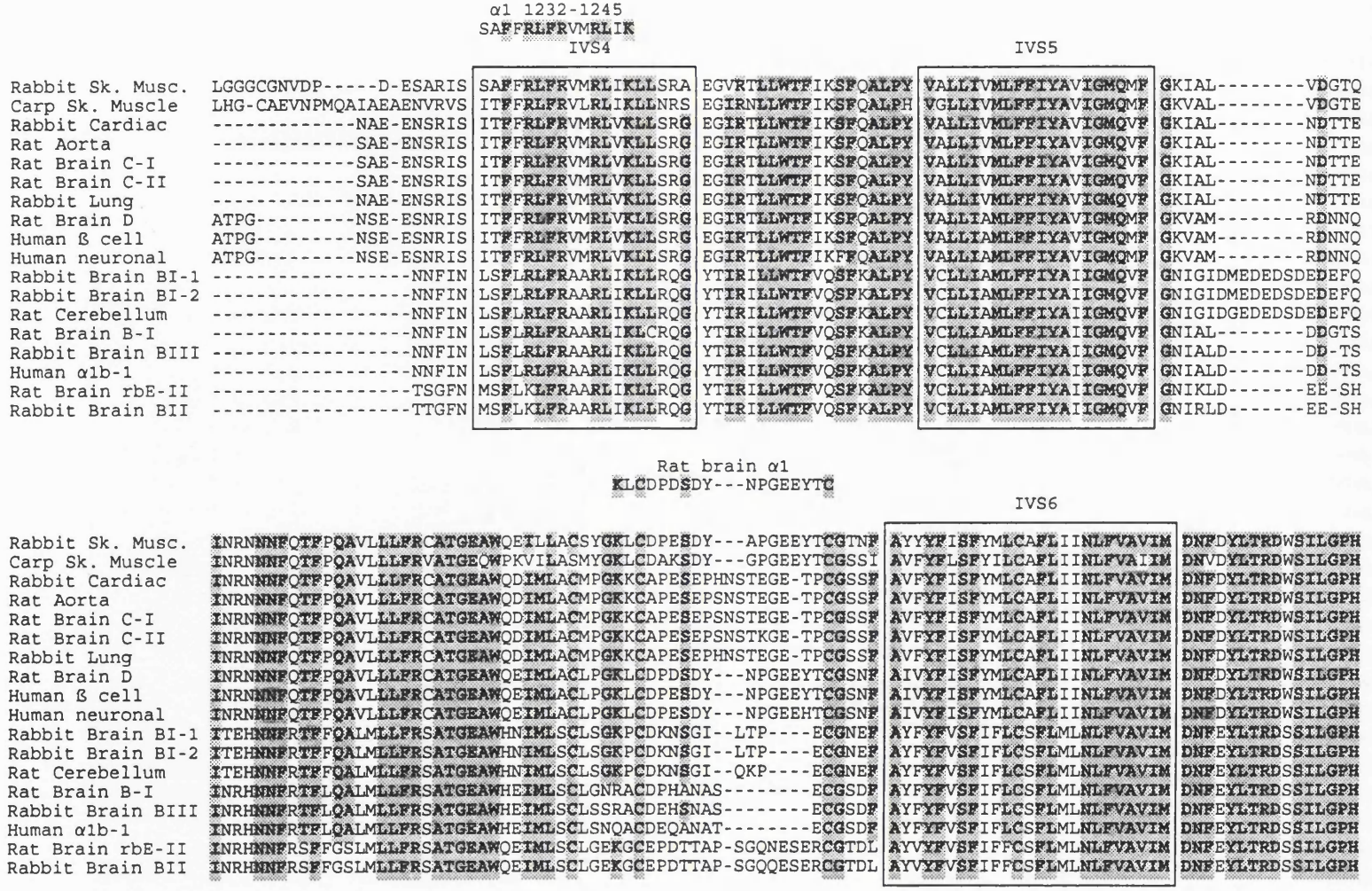
α1 1232-1245
IVS4
IVS5
Rat brain α1
IVS6
Rabbit Sk. Musc.
Carp Sk. Muscle
Rabbit Cardiac
Rat Aorta
Rat Brain C-I
Rat Brain C-II
Rabbit Lung
Rat Brain D
Human ß cell
Human neuronal
Rabbit Brain BI-1
Rabbit Brain BI-2
Rat Cerebellum
Rat Brain B-I
Rabbit Brain BIII
Human α1b-1
Rat Brain rbE-II
Rabbit Brain BII


α1 1399-1418
LDEFKAIWAEYDPEAKGRIK
Rabbit Sk. Musc.
Carp Sk. Muscle
Rabbit Cardiac
Rat Aorta
Rat Brain C-I
Rat Brain C-II
Rabbit Lung
Rat Brain D
Human ß cell
Human neuronal
Rabbit Brain BI-1
Rabbit Brain BI-2
Rat Cerebellum
Rat Brain B-I
Rabbit Brain BIII
Human α1b-1
Rat Brain rbE-II
Rabbit Brain BII
α1 1555-1569
IQAGLRTIEEEAAPE
Rabbit Sk. Musc.
Carp Sk. Muscle
Rabbit Cardiac
Rat Aorta
Rat Brain C-I
Rat Brain C-II
Rabbit Lung
Rat Brain D
Human ß cell
Human neuronal
Rabbit Brain BI-1
Rabbit Brain BI-2
Rat Cerebellum
Rat Brain B-I
Rabbit Brain BIII
Human α1b-1
Rat Brain rbE-II
Rabbit Brain BII

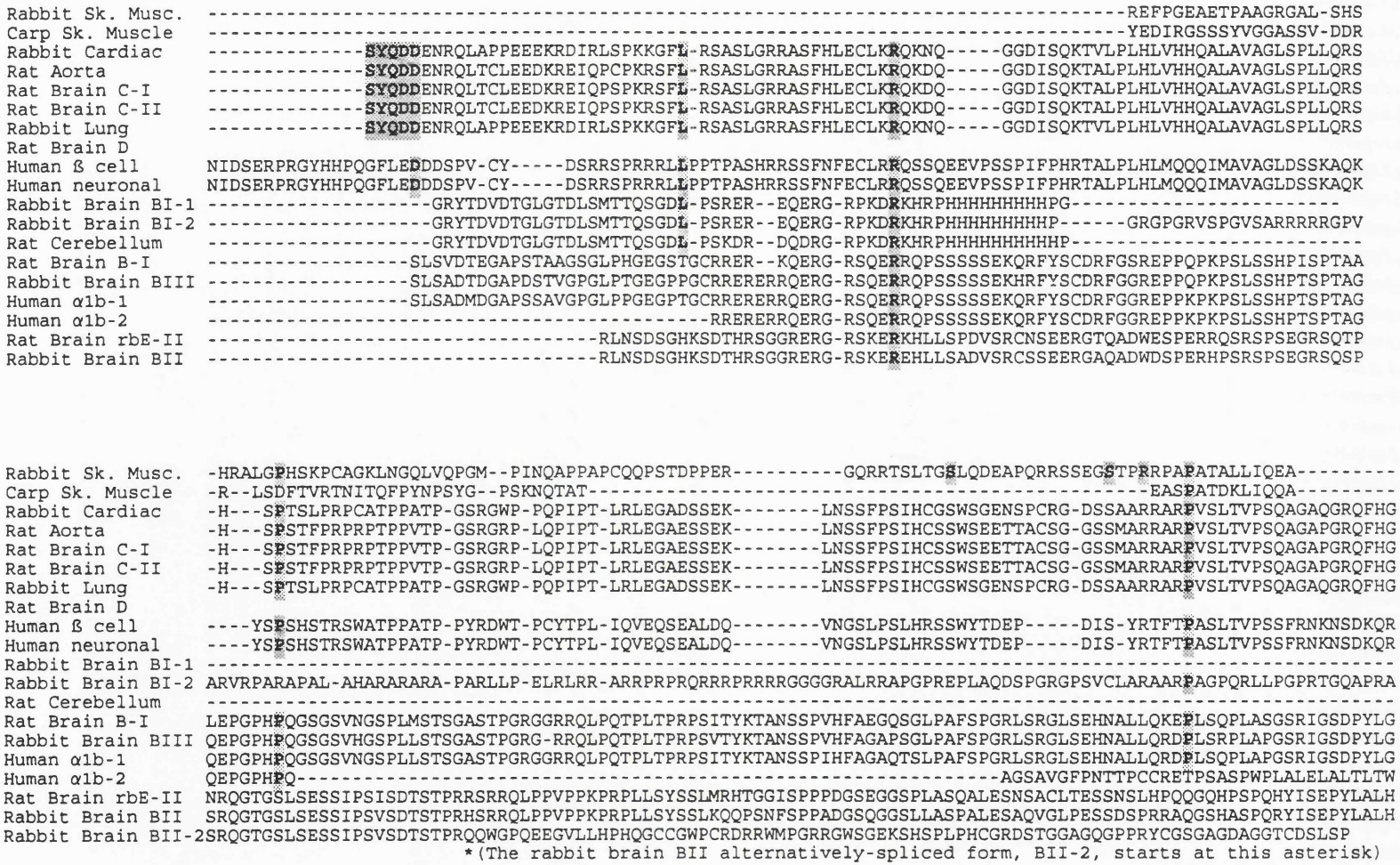
Rabbit Sk. Musc.
Carp Sk. Muscle
Rabbit Cardiac
Rat Aorta
Rat Brain C-I
Rat Brain C-II
Rabbit Lung
Rat Brain D
Human ß cell
Human neuronal
Rabbit Brain BI-1
Rabbit Brain BI-2
Rat Cerebellum
Rat Brain B-I
Rabbit Brain BIII
Human α1b-1
Human α1b-2
Rat Brain rbE-II
Rabbit Brain BII
Rabbit Sk. Musc.
Carp Sk. Muscle
Rabbit Cardiac
Rat Aorta
Rat Brain C-I
Rat Brain C-II
Rabbit Lung
Rat Brain D
Human ß cell
Human neuronal
Rabbit Brain BI-1
Rabbit Brain BI-2
Rat Cerebellum
Rat Brain B-I
Rabbit Brain BIII
Human α1b-1
Human α1b-2
Rat Brain rbE-II
Rabbit Brain BII
Rabbit Brain BII-2
*(The rabbit brain BII alternatively-spliced form, BII-2, starts at this asterisk)

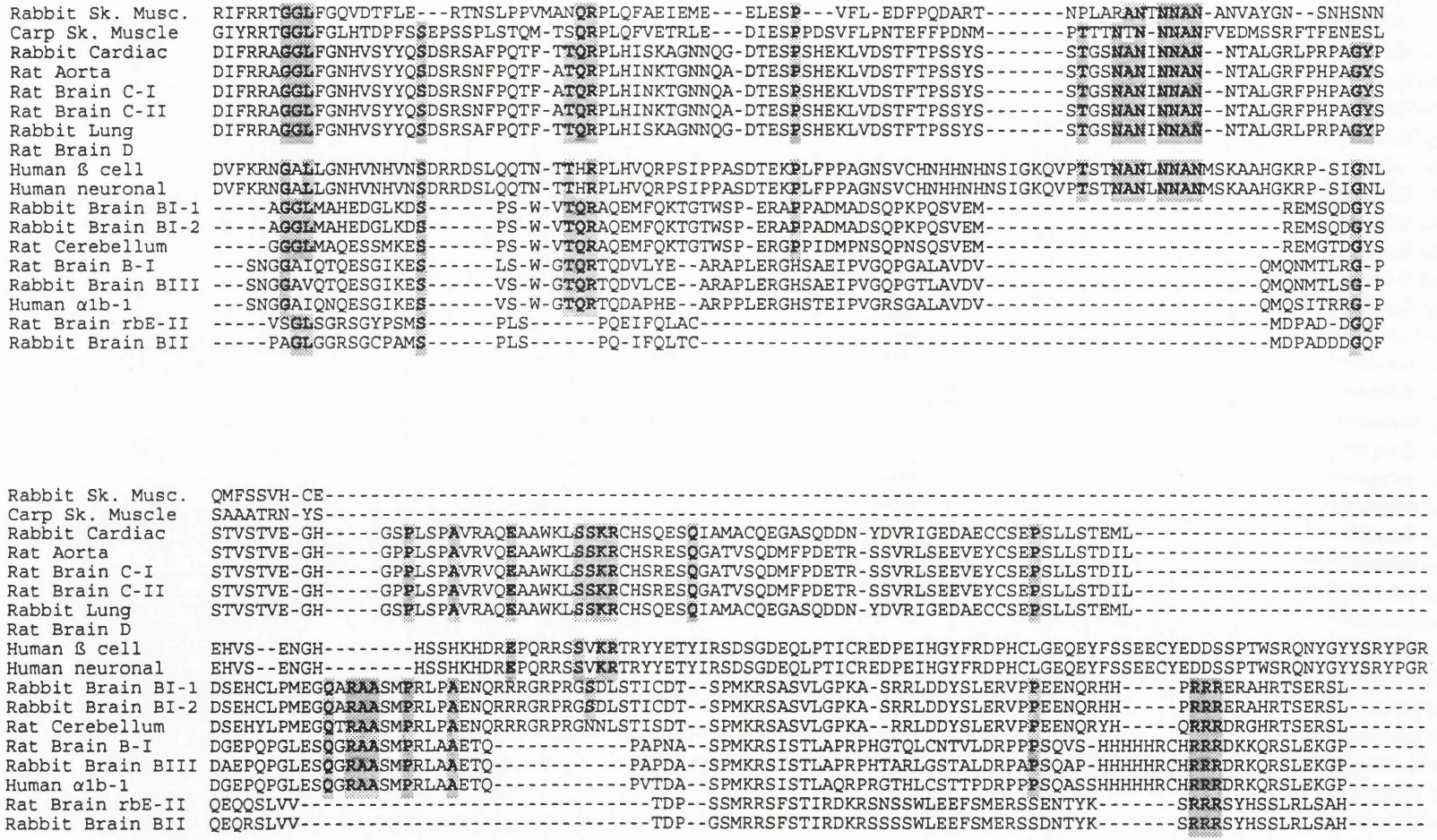
Rabbit Sk. Musc.
Carp Sk. Muscle
Rabbit Cardiac
Rat Aorta
Rat Brain C-I
Rat Brain C-II
Rabbit Lung
Rat Brain D
Human ß cell
Human neuronal
Rabbit Brain BI-1
Rabbit Brain BI-2
Rat Cerebellum
Rat Brain B-I
Rabbit Brain BIII
Human α1b-1
Rat Brain rbE-II
Rabbit Brain BII


Rabbit Sk. Musc. ----------LVRGGLDTLAADAGFVTATSQALADACQMEP-EEVEVAATEL-LK--ARESVQG--MASVP--GSLSRRS------SLGSLD
Carp Sk. Muscle ----------LRDGGLDSLAEDPKFVSVTRKELAEAINIGM-EDMEGMAQGI-VN---RQSGKV--TKRRKRRPIPVPPG----------
Rabbit Cardiac SAS----------SLVEAVLISEGLGQFAQDPKFIEVTTQELADACDLTI-EEMENAADDI-LSGGARQSPNGTLLPFVNRRDPGRDRAGQNEQDASGACA
Rat Aorta SAS----------SLVEAVLISEGLGQFAQDPKFIEVTTQELADACDMTI-EEMENAADNI-LSGGAQQSPNGTLLPFVNCRDPGQDRAVVPEDESCVYAL
Rat Brain C-I SAS----------SLVEAVLISEGLGQFAQDPKFIEVTTQELADACDMTI-EEMENAADNI-LSGGAQQSPNGTLLPFVNCRDPGQDRAVVPEDESCVYAL
Rat Brain C-II SAS----------SLVEAVLISEGLGQFAQDPNFIEVTTQELADACDMTI-EEMENAADNI-LSGGAQQSPNGTLLPFVNCRDPGQDRAVVPEDESCVYAL
Rabbit Lung SAS----------SLVEAVLISEGLGQFAQDPKFIEVTTQELADACDLTI-EEMENAADDI-LSGGARQSPNGTLLPFVNRRDPGRDRAGQNEQDASGACA
Rat Brain D
Human ß cell SAD----------SLVEAVLISEGLGRYARDPKFVSATKHEIADACDLTI-DEMESAASTL-LNGNVRPRANGDVGPLSHRQDYELQDFGPGY---S-DEE
Human neuronal SAD----------SLVEAVLISEGLGRYARDPKFVSATKHEIADACDLTI-DEMESAASTL-LNGNVRPRANGDVGPLSHRQDYELQDFGPGY---S-DEE
Rabbit Brain BI-1 ----------PAAADKERYGPQDRPDHGHGRARARDQRWSRSPSEGREHTTHRQ
Rabbit Brain BI-2 RLPQKPARSVQRERRGLV-LSPPPPPPGELAPRAHPARTPRPGPGDSRSRRGGRRWTASAGKG--GGGPRASAPSP
Rat Cerebellum ----------PAP-DRERYA-QERPDTGRARARE--QRWSRSPSEGREHATHRQ
Rat Brain B-I QRLDSEASAHNLPEDTLTFEEAVATNSGRSSRTSYVSSLTSQSHPLRRVPNGYHCTLGLSTGVRARHSYHHPDQDHWC
Rabbit Brain BIII QRLDSEAPARALPEDAPAFEETAASNSGRSSRTSYVSSLTSQPPPLRRVPNGYHCTLGLGGGGRARRGCHHPDRDRRC
Human α1b-1 QRLDSEASVHALPEDTLTFEEAVATNSGRSSRTSYVSSLTSQSHPLRRVPNGYHCTLGLSSGGRARHSYHHPDQDHWC
Human α1b-2 GSVWTVRPLSTPCLRTRSLSRRLWPPTRAAPPGLPTCPP
Rat Brain rbE-II EDSHASDCGEEETLTFEAAVATSLGRSNTIGSAPPLRHSWQMPNGHYRRRRLGGLGLAMMCGAVSDLLSDTEEDDKC
Rabbit Brain BII EDSHASDCGEEETLTFEAAVATSLGRSNTIGSAPPLRHSWQMPNGHYRRRR-GGPGAGALCGAVGDLLSDTEE-DKC
Rabbit Brain BII-2
Rabbit Sk. Musc. QVQG-SQETLIPPRP
Carp Sk. Muscle ----TKSTKPKENTSAV
Rabbit Cardiac PGCGQSEEALADRRAGVSSL
Rat Aorta GR-GRSEEALPDSRSYVSNL
Rat Brain C-I GR-GQSEEALPDSRSYVSNL
Rat Brain C-II GR-GRSEEALPDSRSYVSNL
Rabbit Lung PGCGQSEEALADRRAGVSSL
Rat Brain D
Human ß cell PDPGRDEEDLADEMICITTL
Human neuronal PDPGRDEEDLADEMICITTL
Rabbit Brain BI-1
Rabbit Brain BI-2
Rat Cerebellum
Rat Brain B-I
Rabbit Brain BIII
Human α1b-1
Human α1b-2
Rat Brain rbE-II
Rabbit Brain BII
Rabbit Brain BII-2

Source of sequence information

SKELETAL MUSCLE CLONES:

RABDHPR.PEP: Source: Rabbit Skeletal Muscle.
Reference: Tanabe *et al.* (1987) Nature **328**, 313-318.

CYICCA1.PEP: Source: Carp Skeletal Muscle.
Reference: Grabner *et al.* (1991) Proc. Natl. Acad. Sci. USA **88**, 727-731.

CLASS C CLONES:

RABCACHA.PEP: Source: Rabbit Cardiac Muscle.
Reference: Mikami *et al.* (1989) Nature **340**, 230-233.

RATVDCCA.PEP: Source: Rat Aorta.
Reference: Koch *et al.* (1990) J. Biol. Chem. **265**, 17786-17791.

RATRBC1.PEP: Source: Rat Brain C-I.
Reference: Snutch *et al.* (1991) Neuron **7**, 45-47.

RATRBC2.PEP: Source: Rat Brain C-II.
Reference: Snutch *et al.* (1991) Neuron **7**, 45-47.

RABCACBR.PEP: Source: Rabbit Smooth Muscle (Lung).
Reference: Biel *et al.* (1990) FEBS Lett. **269**, 409-412.

CLASS D CLONES:

RATRBC.PEP: Source: Rat Brain D
Reference: Hui *et al.* (1991) Neuron **7**, 35-44.

No file Source: Human pancreatic ß-cell.
Reference : Seino *et al.* (1992) Proc. Natl. Acad. Sci. USA **89**, 584-588.
(But resembles class C clones at *C*-terminus).

No file Source: Human neuronal
Reference: Williams *et al.* (1992) Neuron **8**, 71-84.
(Almost identical to the ß-cell sequence)

CLASS A CLONES:

RABCCBI1.PEP: Source: Rabbit Brain BI-1.
Reference: Mori *et al.* (1991) Nature **350**, 398-402.

RABCCBI2.PEP: Source: Rabbit Brain BI-2.
Reference: Mori *et al.* (1991) Nature **350**, 398-402.

RATBCCA.PEP: Source: Rat Brain (Cerebellum).
Reference: Starr *et al.* (1991) Proc. Natl. Acad. Sci. USA **88**, 5621-5625.

CLASS B CLONES:

OMEGASCC.PEP: Source: Rat Brain rbB-I
Reference: Dubel *et al.* (1992) Proc. Natl. Acad. Sci. USA **89**, 5058-5062.

No file: Source: Rabbit Brain BIII
Reference: Fujita *et al.* (1993) Neuron **10**, 585-598 (refid# 4267).

No file: Source: Human Brain α1b-1 and α1b-2
Reference: Williams *et al.* (1992) Science **257**, 389-395.

CLASS E CLONES

No file: Source: Rat Brain rbE-II
Reference: Soong *et al.* (1993) Science **260**, 1133-1136 (refid# 4358)
GenBank accession number L15453

No file: Source: Rabbit Brain BII
Reference: Niidome *et al.* (1992) FEBS Lett **308**, 7-13 (refid# 4359)

Fig. 3.3 ALIGNMENT OF CALCIUM CHANNEL α2 SUBUNIT SEQUENCES

α2 1-15
EPFPSAVTIKSWVDK

```
Rabbit sk. muscle MAAGRPLAWTLTLWQAWLILTGPSSEEPFPSAVTIKSWVDKMQEDLVTLAKTASGVHQLVDIYEKYQDLYTVEPNNARQLVEIAARDIEKLLSNRSKALVRLAL
Rat brain         MAAGCLLALTLTLFQSWL--TGPSSEEPFPSPVTIKSWVDKMQEDLVTLAKTASGVTQLADIYEKYQDLYTVEPNNARQLVEIAARDIEKLLSNRSKALVRLAM
Human neuronal    MAAGCLLALTLTLFQSLL--IGPSSEEPFPYAVTIKSWVDKMQEDLVTLAKTASGNNQLVEIYEKYQDLYTVEPNNARQLVEIAARDIEKALSNRSKALVSLAL

                  (Proposed signal sequence)

Rabbit sk. muscle EAEKVQAAHQWREDFASNEVVYYNAKDDLDPEKNDSEPGSQRIKPVFIDDANFRRQVSYQHAAVHIPTDIYEGSTIVLNELNWTSALDDVFKKNREEDPSLLWQ
Rat brain         EAEKVQAAHQWREDFASNEVVYYNAKDDLDPERNESEPGSQRIKPVFIEDANFGRQISYQHAAVHIPTDIYEGSTIVLNELNWTSALDEVFKRNRDEDPTLLWQ
Human neuronal    EAEKVQAAHQWREDFAVNEVVYYNAKDDLDPEKNDSEPGSQRIKPVKIEDANFGRQISYQHAAVHIPTDIYEGSTILLNELNWTSALDEVFKKNREEDPSLLWQ

Rabbit sk. muscle VFGSATGLARYYPASPWVDNSRTPNKIDLYDVRRRPWYIQGAASPKDMLILVDVSGSVSGLTLKLIRTSVSEMLETLSDDDFVNVASFNSNAQDVSCFQHLVQA
Rat brain         VF-AADRLARYYPASPWVDNSRTPNKIDLYDVRRRPWYIQGAASPKDMLILVDVSGSVSGLTLKLIRTSVSEMLETLSDDDFVNVASFNSNAQDVSCFQHLVQA
Human neuronal    VFGSATGLARYYPASPWVDNSRTPNKIDLYDVRRRPWYIQGAASPKDMLILVDVSGSVSGLTVKLIRTSVSEMLETLSDDDFVNVASFNSNALDVSCFQHLVQA

Rabbit sk. muscle NVRNKKVLKDAVNNITAKGITDYKKGFSFAFEQLLNYNVSRANCNKIIMLFTDGGEERAQEIFAKYNKDKKVRVFTFSVGQHNYDRGPIQWMACENKGYYYEIP
Rat brain         NVRNKKVLKDAVNNITAKGITDYKKGFTFAFEQLLNYNVSRANCNKIIMLFTDGGEERAQEIFAKYNKDKKVRVFTFSVGQHNYDRGPIQWMACENKGYYYEIP
Human neuronal    NVRNKKVLKDAVNNITAKKITDYKKGFSFAFEQLLNYNVSRANCNKIILLFTDGGEERAQEIFNKYNKDKKVRVFRFSIGQHNYERGPIQWMACENKGYYYEIP

                                                                                                    α2 469-483
                                                                                                    SLEDIKRLTPRFTLC

Rabbit sk. muscle SIGAIRINTQEYLDVLGRPMVLAGDKAKQVQ WTNVYLDALELGLVITGTLPVFNI TGQFENKTNLKNQLILGVMGVDVSLEDIKRLTPRFTLCPNGYYFAID
Rat brain         SIGAIRINTQEYLDVLGRPMVLAGDKAKQVQ WTNVYLDALELGLVITGTLPVFNV TGQSENKTNLKNQLILGVMGVDVSLEDIKRLTPRFTLCPNGYYFAID
Human neuronal    SIGAKRINTQEYLDVLGRPMVLAGDKAKQVQ WTNVYLDALELGLVITGTLPVFNI TGQFENKTNSKNQLILGVMGVDVSLEDIKRLTPRFTLCPRGYYFAID

Rabbit sk. muscle PNGYVLLHPNLQPKPIGVGIPTINLRKRRPNVQNPKSQEPVTLDFLDAELENDIKVEIRNKMIDGESGEKTFRTLVKSQDERYIDKGNRTYTWTPVNGTDYSSL
Rat brain         PNGYVLLHPNLQPK----------NPKSQEPVTLDFLDAELENDIKVEIRNKMIDGESGEKTFRTLVKSQDERYIDKGNRTYTWTPVNGTDYRYL
Human neuronal    PNGYVLLHPNLQPK----------NPKSQEPVTLDFLDAELENDIKVEIRNKMIDGESGEKTFRTLVKSQDERYIDKGNRTYTWTPVNGTGY-SL

Rabbit sk. muscle ALVLPTYSFYYIKAKIEETITQARY-------SETLKPDNFEESGYTFLAPRDYCSDLKPSDNNTEFLLNFNEFIDRKTPNNPSCNTDLINRVLLDAGFTNELV
Rat brain         ALVLPTYSFYYIKAKIEETITQARSKKGKMKDSETLKPDNFEESGYTFIAPREYCNDLKPSDNNTEFLLNFNEFIDRKTPNNPSCNTDLINRILLDAGFTNELV
Human neuronal    ALVLPTYSFYYIKAKLEETITQARSKKGKMKDSETLKPDNFEESGYTFIAPRDYCNDLKISDNNTEFLLNFNEFIDRKTPNNPSCNADLINRVLLDAGFTNELV

Rabbit sk. muscle QNYWSKQKNIKGVKARFVVTDGGITRVYPKEAGENWQENPETYEDSFYKRSLDNDNYVFTAPYFNKSGPGAYESGIMVSKAVEIYIQGKLLKPAVVGIKIDVNS
Rat brain         QNYWSKQKNIKGVKARFVVTDGGITRVYPKEAGENWQENPETYEDSFYKRSLDNDNYVFTAPYFNKSGPGAYESGIMVSKAVELYIQGKLLKPAVVGIKIDVNS
Human neuronal    QNYWSKQKNIKGVKARFVVTDGGITRVYPKEAGENWQENPETYEDSFYKRSLDNDNYVFTAPYFNKSGPGAYESGIMVSKAVEIYIQGKLLKPAVVGIKIDVNS

Rabbit sk. muscle WIENFTKTSIRDPCAGPVCDCKRNSDVMDCVILDDGGFLLMANHDDYTNQIGRFFGEIDPSLMRHLVNISVYAFNKSYDYQSVCEPGAAPKQGAGHR SAYVPS
Rat brain         WIENFTKTSIRDPCAGPVCDCKRNSDVMDCVILDDGGFLLMANHDDYTNQIGRFFGEIDPRMMRHLVNISLYAFNKSYDYQSVCDPGAAPKQGAGHR SAYVPS
Human neuronal    WIENFTKTSIRDPCAGPVCDCKRNSDVMDCVILDDGGFLLMANHDDYTNQIGRFFGEIDPSLMRHLVNISVYAFNKSYDYQSVCEPGAAPKQGAGHR SAYVPS
```

δ 1-17
EA ADMEEDDFTASMSKQSC

```
Rabbit sk. muscle IADILQIGWWATAAAWSIL QQFLLSLTFPRLLEA ADMEEDDFTASMSKQSCITEQTQYFFDNDTKSFSGVLDCGNCSRIFHVEKLMNTNLIFIMVESKGTCP
Rat brain         ITDILQIGWWATAAAWSIL QQLLLSLTFPRLLEA VEMEEDDFTASLSKQSCITEQTQYFFKNDTKSFSGLLDCGNCSRIFHVEKLMNTNLVFIMVESKGTCP
Human neuronal    VADILQIGWWATAAAWSIL QQFLLSLTFPRLLEA VEMEDDDFTASLSKQSCITEQTQYFFDNDSKSFSGVLDCGNCSRIFHGEKLMNTNLIFIMVESKGTCP
```

*N-terminus of δ-subunit

```
Rabbit sk. muscle CDTRLLIQAEQTSDGPDPCDMVKQPRYRKGPDVCFDNNVLEDYTDCGGVSGL NPSLWSIIGIQFVLLWLVSGS RHCLL
Rat brain         CDTRLLMQAEQTSDGPDPCDMVKQPRYRKGPDVCFDNNVLEDYTDCGGVSGL NPSLWSIFGLQFILLWLVSGS RHYLW
Human neuronal    CDTRLLIQAEQTSDGPNPCDMVKQPRYRKGPDVCFDNNVLEDYTDCGGVSGL NPSLWYIIGIQFLLLWLVSGS THRLL
```


Source of sequence information

Rabbit skeletal muscle	Ellis *et al.* (1988) Science **241**, 1661-1664 (refid# 1690)
Rat brain	Kim *et al.* (1992) Proc. Natl. Acad. Sci. USA **89**, 3251-3255 (refid# 3050)
Human neuronal	Williams *et al.* (1992) Neuron **8**, 71-84

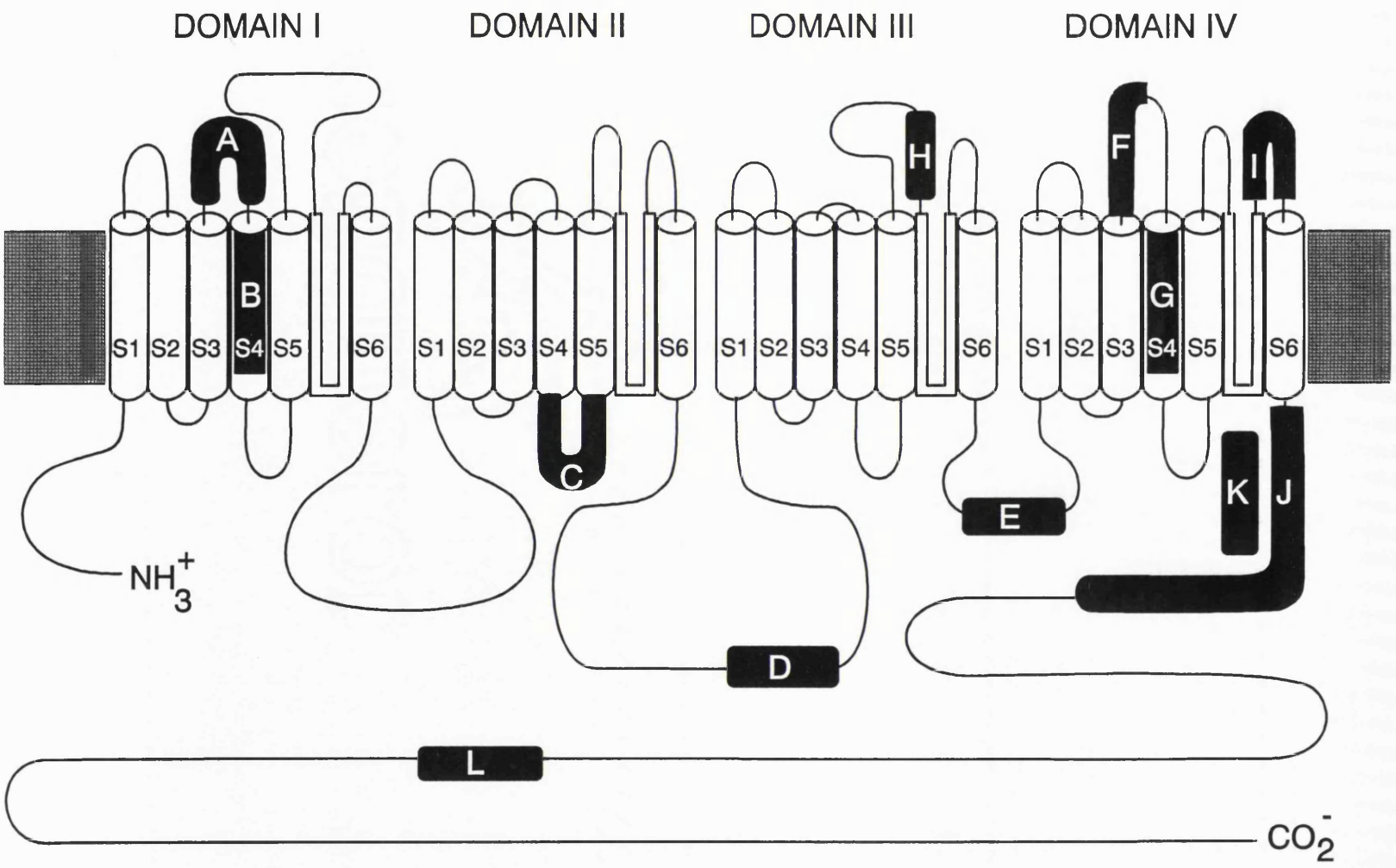
DOMAIN I
DOMAIN II
DOMAIN III
DOMAIN IV
A
B
C
D
E
F
G
H
I
J
K
L
S1
S2
S3
S4
S5
S6
NH_3^+
CO_2^-

Fig. 3.4 (overleaf) Diagram of the proposed membrane orientation of a generic α_1 subunit showing the location of peptides chosen for synthesis. All peptides correspond to sequences in the primary structure of the rabbit skeletal muscle L-type polypeptide, with the exception of H (rat cerebellar class A) and I (rat neuronal L-type, class D).

Peptide A	α_1(143-158)	NVIQSNTAPMSSKGAGC
Peptide B	α_1(161-174)	VKALRAFRVLRPLRCG
Peptide C	α_1(543-561)	TSLSNLVASLLNSIRSIASC
Peptide D	α_1(738-753)	SADFPGDDEEDEPEIPC
Peptide E	α_1(1089-1100)	VQYALKARPLRC
Peptide F	α_1(1200-1214)	SEIDTFLASSGGLYC
Peptide G	α_1(1232-1245)	SAFFRLFRVMRLIKCG
Peptide H	α_1(1374-1387)	YEKNEVKARDREWKYC
Peptide I	α_1(1459-1475)	KLCDPDSDYNPGEEYTC
Peptide J	α_1(1390-1437)	DWSILGPHHLDEFKAIWAEYDPEAK GRIKHLDVVTLLRRIQPPLGFGK
Peptide K	α_1(1399-1418)	LDEFKAIWAEYDPEAKGRIKC
Peptide L	α_1(1555-1569)	IQAGLRTIEEEAAPEC

Peptides on extracellular loops

Both peptides A and F, predicted to be exofacial, contain a significant number of hydrophilic amino acids (Tanabe *et al.*, 1987). A corresponds to an inserted loop relative to the Na^+ channel in the IS3-IS4 loop (Noda *et al.*, 1984) while F corresponds to the N-terminal 15 amino acid residues in the IVS3-IVS4 loop. If channel activation is indeed dependent on movement of either or both IS4 and IVS4 in the membrane, then it may also require movement of and/or a conformational change in the predicted exofacial loops containing these peptide sequences.

Brain channel class-specific peptides

Peptides H and I correspond to predicted extracellular hydrophilic sequences located respectively on the IIIS5-IIIS6 loop of the rat brain class A (Starr *et al.*, 1991) and the IVS5-IVS6 loop of the rat brain class D channels (Hui *et al.*, 1991). H is N-terminal, and I is C-terminal to the SS1-SS2 domains of their loops, which are proposed to form part of the channel pore region (see Section 1.7.3). Therefore both sequences are predicted to be exposed at the channel surface probably close to the pore entrance. The amino acid sequence of H is found only in the rat brain class A polypeptide amongst all of the α_1 sequences currently known, while the sequence of I is specific, in rat brain, for the class D polypeptide (see Fig. 3.2). However, it is identical to a corresponding sequence in the rabbit skeletal muscle L-type channel, at 12 of its 14 residues.

Transmembrane peptides

Peptides B and G are located in the predominantly hydrophobic, functionally-important, putative voltage sensor S4 regions of homologous domains I and IV, respectively (see Section 1.7.1). At first sight these regions seem likely to be inaccessible in the membrane, while the synthetic peptides are fairly hydrophobic and

thus not likely to be immunogenic. However, an antibody was previously raised against a 14aa peptide corresponding to the middle region of the IS4 domain of the eel Na^+ channel α polypeptide. Upon its application to the external face of rat DRG cells, Na^+ current inactivation was seen to be shifted to more negative potentials in both slow and fast channels (Meiri *et al.*, 1987). An increased rate of slow current inactivation was also observed. These functional effects of the antibody indicate that it recognises the peptide in the intact protein, and thus that the IS4 region must be exposed, at least in part, at the extracellular face of the membrane in one or more conformational states of the channel. On the other hand, Nakayama *et al.*, (1992a) found that antibodies recognizing a peptide corresponding to the IVS4 domain of the eel electroplax Na^+ channel failed to interact with this region either in the intact channel in the native or denatured (following SDS-PAGE) states, but did react with channel fragments following lysyl endoproteinase digestion.

Peptides on intracellular loops

Peptides C, D and E are located on three of the largest intracellular loops of the polypeptide. Peptide C corresponds to the entire loop between IIS4 and IIS5, while peptides D and E are hydophilic and predicted to be highly antigenic sequences in the loops connecting homologous domains II and III, and III and IV, respectively. Each of these regions is suspected either to have a role in channel function (activation/inactivation) or to be involved in possibly functionally-important Ca^{2+} binding. The domain corresponding to peptide C, resembles a leucine zipper motif (Landschultz *et al.*, 1988) and is in close proximity to the proposed voltage sensing IIS4 domain. It is possible that it undergoes conformational change due to movement of the IIS4 domain during channel activation/inactivation. The sequence of E corresponds in its location in the channel sequence to a region in the Na^+ channel proposed to be involved in channel inactivation (Vassilev *et al.*, 1988; 1989). Antibodies recognizing this region of the rat brain type II Na^+ channel slowed channel inactivation. Peptide D contains a sequence between residues 740 and 752

that resembles the EF hand domains found in Ca^{2+} binding proteins (see Section 3.3.2), suggesting the presence of a possible Ca^{2+} binding site. The II-III loop where this domain is located has been shown to be necessary for skeletal type E-C (Tanabe *et al.*, 1990b).

Intracellular C-terminal peptides

As revealed in Fig. 3.2 the region of the protein which includes peptide J is largely conserved in all Ca^{2+} channels whose sequences are known (Tanabe *et al.*, 1987; Mikami *et al.*, 1989; Koch *et al.*, 1990; Biel *et al.*, 1990; Grabner *et al.*, 1991; Hui *et al.*, 1991; Mori *et al.*, 1991; Snutch *et al.*, 1991; Starr *et al.*, 1991; Dubel *et al.*, 1992; Ma *et al.*, 1992; Niidome et al., 1992; Seino *et al.*, 1992; Williams *et al.*, 1992a, 1992b; Fujita *et al.*, 1993; Horne *et al.*, 1993; Soong *et al.*, 1993), indicating a possible role in channel function. Peptide J was synthesized primarily, in order to study the secondary structure of the Ca^{2+} channel α_1 polypeptide in that particular region, using FTIR and CD spectrometry. Several such synthetic protein domains have previously been shown to have stable secondary structures in solution. For example, a synthetic 32 amino acid peptide from a cloned K^+ channel was shown to possess 57% α helical secondary structure in methanol using CD (Ben-Efraim *et al.*, 1993). This peptide contained a hydrophobic, 22 amino acid, putative α helical transmembrane segment. A peptide corresponding to the H5 region of the K^+ channel, previously synthesized as outlined in Section 2.2.3, was shown using both FTIR and CD to possess α helical structure in lyso phosphatidyl choline micelles and dimyristoyl phosphatidyl choline bilayers (Haris *et al.*, 1993). Whether or not these peptide domains in the native channel have the same secondary structure as the synthetic peptide in such solutions, is not known. However, whole proteins similarly synthesized, such as the 140 amino acid Interleukin-3 (Clark-Lewis *et al.*, 1986), have been shown to have the same biological activity as the native protein. This implies that a synthetic polypeptide can possess the same conformation as the native protein.

FTIR is an established technique for studying the secondary structure of proteins in solution (reviewed by Haris and Chapman, 1992). Protein secondary structures are stabilized by hydrogen bonding between amide hydrogen and carbonyl oxygen atoms, which vary in strength with their secondary structure. The H-bond strength inversely affects the strength of the C=O bond. The amount of energy needed to stretch the C=O bond will determine the position of the amide I absorbance band, which arises from C=O stretch, in an FTIR spectrum of a protein. This position can thus be used to deduce the protein secondary structure e.g. presence of α-helix causes absorbance in the range (1648-1656)cm^{-1}.

The polypeptide synthesized corresponds to α_1(1390-1437) in the rabbit skeletal muscle protein. This largely hydrophilic, cytoplasmic region, located C-terminal to the IVS6 region, contains a sequence resembling, in part, the EF-hand domains (Ca^{2+}-binding sites) that are found in Ca^{2+}-binding proteins (Tufty and Kretsingher, 1975). The domain corresponding to peptide J may also have a role in ligand-binding. While the site of PAA binding has been identified in close proximity N-terminal this region, one report has suggested a role for this part of the protein in DHP binding, although other workers have identified a DHP site on the other side of the membrane (discussed in Section 1.9.8.1). Specific antibodies against this region might allow these disparate findings to be further investigated. The folding of this polypeptide appears to be important in channel function, particularly inactivation (Meiri *et al.*, 1987).

Peptide K corresponds to the most highly conserved and hydrophilic part of the longer peptide J, consisting of the N-terminal 18 residues of the EF hand domain. Since Ca^{2+}-binding is known to regulate both DHP-, and PAA-binding to the channel, this proposed Ca^{2+}-binding site may have a functional role in the latter. Specific antibodies against this region might allow the findings on the domains for DHP and PAA binding to be further investigated.

Peptide L corresponds to a hydrophilic segment located approximately midway between the IVS6 domain and the C-terminus of the 212kDa α_1 polypeptide. Antibodies against a region of the eel Na^+ channel, corresponding to the sequence

between residues 1558-1566 contained in peptide L, have been reported to shift the Na^+ channel inactivation curve to more positive potentials (Meiri *et al.*, 1987).

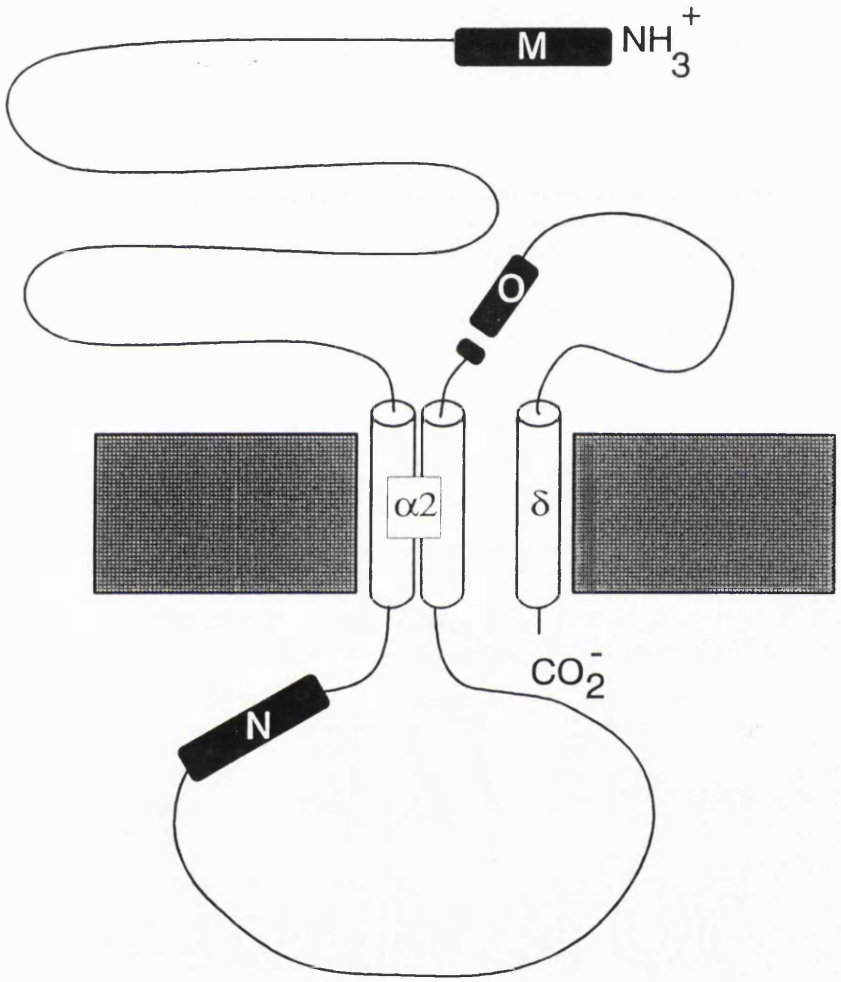

Fig. 3.5 Diagram of the proposed membrane orientation of both the α_2 and δ subunits showing the location of each peptide chosen for synthesis.

Peptide M	α_2(1-15)	EPFPSAVTIKSWVDKC
Peptide N	α_2(469-483)	SLEDIKRLTPRFTLC
Peptide O	α_2(933-934)	EA-
	δ(1-17)	ADMEDDDFTASMSKQSC

Peptides corresponding to regions of both α_2 and δ

The N-terminal hydrophilic peptides M and O, located in the α_2 and δ polypeptides, respectively, both have proposed exofacial membrane orientation. Peptide N, corresponds to a hydrophilic region containing a proposed site of phosphorylation by cAMP-dependent protein kinase, which may be relevant to channel activation and/or inactivation. Ellis *et al.*, (1988) proposed that this peptide is located on an intracellular loop between putative membrane spanning domains I and II. However, an exofacial localization of this peptide sequence would support the proposal that α_2 is an entirely extracellular polypeptide.

3.3 RESULTS

3.3.1 Characterization of the short peptides synthesised for use as immunogens

As described above, a total of 14 short peptides corresponding to various parts of the α_1, α_2 and δ subunits were synthesized by either the continuous flow or batch methods, detailed in Section 2.2. The yields obtained in the synthesis of each peptide are listed in Table 3.1. These are given as a percentage of the theoretical maximum mass of peptide that can be obtained given the amount of solid support used, along with its known amino acid substitution ratio, and the calculated maximum amount of each amino acid residue that could couple in each step. The lowest yield obtained for the synthesis of the short peptides produced was 57%, and the more typical yields were 80-90% of theoretical (Table 3.1). Purity of the peptides was assessed by amino acid analysis, yielding the results shown in Table 3.2. In all cases the measured composition closely resembled that predicted from the sequence. Fast Atom Bombardment or Laser Desorption Mass Spectrometry carried out on individual

Table 3.1 Table of values for both the expected and measured mass, the measured % yield and the % purity, estimated from the HPLC chromatogram, of each peptide synthesized.

Peptide	Yield %	Expected Mass g/mole	Measured Mass g/mole	Purity %
A	93	1664	1664	82
B	93	1854	1854	90
C	95	2049	2049	95
D	78	1863	1863	70
E	92	1416	1416	80
F	66	1561	1561	80
G	61	1945	1945	85
H	91	2118	2118	62
I	62	1949	1949	92
J	16	5603	5603	64
K	57	2482	2482	62
L	79	1728	1728	86
M	78	1805	1805	90
N	89	1792	1792	85
O	76	2079	2079	75

Table 3.2 Table of expected and measured amino acid composition of each peptide synthesized. The letter in the first row of each column denotes the peptide represented by that column, while the letter in the first column of each row denotes the amino acid represented by that row. The expected content of each amino acid is given on the left of each box, while the number on the right gives the amount determined using amino acid analysis, as described in Section 2.3.

	A	B	C	D	E	F	G	H	I	J	K	L	M	N	O
A	2 2.0	2 1.7	2 2.0	1 0.8	2 1.6	1 1.0	1 1.0	1 1.0		3 3.2	3 3.1	3 2.9	1 1.0		3 3.3
C	1 n.d	1 n.d	1 0.8	1 n.d	1 n.d	1 n.d	1 n.d	1 0.8	2 1.4		1 n.d	1 n.d	1 n.d	1 n.d	1 n.d
Asx	2 2.5		2 1.9	4 4.3		1 0.7		2 2.4	4 4.4	4 3.5	2 1.7		1 1.1	1 0.9	4 4.2
Glx	1 1.1			4 3.1	1 1.1	1 1.0		3 3.4	2 2.2	4 4.0	3 3.3	5 5.4	1 1.0	1 1.0	3 4.1
F		1 0.8		1 0.9		1 1.2	3 3.0			2 2.2	1 0.8		1 1.3	1 1.1	1 1.1
G	2 2.1	1 1.0		1 0.7		2 2.1	1 1.1		1 1.0	4 4.4	1 1.0	1 1.0			
H										3 1.7					
I	1 0.7		2 1.8	1 1.1		1 0.8	1 1.0			4 3.4	2 2.1	2 1.6	1 1.2	1 1.2	
K	1 1.0	1 0.8			1 0.9		1 1.0	3 2.8	1	4 3.7	3 2.8		2 2.1	1 1.2	1 1.2
L		3 3.2	4 4.2		2 2.2	2 1.9	2 2.2		1 1.0	6 6.7	1 1.2	1 1.0		3 2.9	
M	1 1.0						1 0.9								2 2.4
P	1 1.3	1 1.0		3 n.d	1 n.d				2 2.0	4 4.0	1 1.2	1 1.3	2 2.3	1 n.d	
R		4 3.9	1 1.0		2 1.6		3 2.9	2 2.0		3 3.2	1 1.1	1 1.0		2 2.1	
S	3 3.6		6 5.4	1 0.4		3 2.1	1 0.8		1 0.9	1 0.7			2 1.6	1 0.8	3 1.2
T	1 1.0		1 0.8			1 0.8			1 1.1	1 1.2		1 0.9	1 0.9	2 2.0	1 0.7
V	1 0.7	2 2.1	1 0.9		1 1.4		1 1.0	1 0.9		2 1.6			2 2.2		
W								1 n.d.		2 n.d.	1 n.d.		1 n.d.		
Y					1 0.8	1 1.1		2 1.7	2 1.9	1 1.0	1 1.0				

synthetic peptide samples revealed the presence in each synthetic sample of quasi-molecular ions of equivalent mass to the appropriate peptide species. However, in some samples, the existence of molecules having molecular mass different from that of the synthetic peptide was observed. In the case of the synthetic peptide H, a single additional molecule was identified in the sample having a molecular mass of 2330g/mole, 212g/mole greater than the calculated value for synthetic peptide H. The mass spectra for peptides K and O revealed the presence of molecules in these samples having molecular mass smaller than that of the peptide. The difference between the measured molecular mass of these species and the synthetic peptide was 92g/mole and 278g/mole for the former and 94g/mole and 228g/mole for the latter.

Reverse-phase HPLC analysis of each peptide, as described in Section 2.3, revealed the presence of a single major peak in the chromatogram. A typical result is illustrated for peptide M in Fig. 3.6. Estimation of the purity of the peptides was

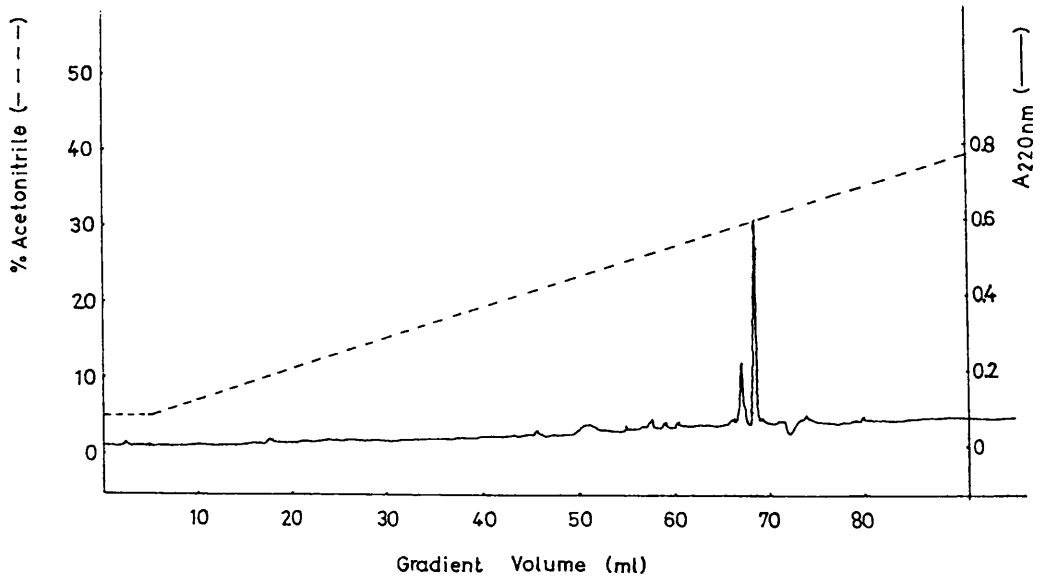

Fig. 3.6 HPLC chromatogram obtained from the absorption at 220nm of the eluate in a 5-40% (v/v) acetonitrile gradient in 0.1% (v/v) TFA at a flow rate of 1ml/min. from a 300A pore-size, C_{18} column following loading of 50μg of peptide M.

made by comparing the area under the peak with the total area of the absorbance trace yielded by gradient elution of the HPLC column. As illustrated in Table 3.1, peptide purities estimated by this procedure were typically >70%. In the case of peptides H,

K, and D multiple minor peaks were also observed in the absorbance trace which account for their lower apparent purity.

3.3.2 Characterization of the large peptide synthesised for the study of its secondary structure

In contrast to the results obtained with the synthesis of the small peptides (12-21 residues) produced for use as immunogens, a much lower yield (16%) of the 48 residue polypeptide J was obtained. HPLC revealed that the peptide was reasonably pure, the major peak corresponding to about 55% of the total area of the chromatogram (Fig. 3.7). Similarly, amino acid analysis revealed a composition close to that predicted (see Table 3.2), while a species with molecular mass identical to that expected was detected by Laser Desorption mass spectrometry (Table 3.1). However, the latter technique demonstrated the presence in the crude synthetic peptide sample of a number of molecules which were smaller than the synthetic peptide. The discrepancy in size between the three apparently most abundant of these species and the synthetic peptide were 64g/mole, 214g/mole and 424g/mole.

Tricine-SDS/PAGE of the crude synthetic peptide revealed the presence of a band with a mobility corresponding to the expected M_r of approximately 5,600 (Fig. 3.9). A sole additional band of apparent M_r 8,000 was observed which contained not more than 5% of the peptide material. A sample of the crude peptide was subjected to preparative HPLC, using the same conditions as for its analysis. The major peak and both minor peaks (see Fig. 3.7) in the eluate were collected, freeze-dried and the former subjected to analytical HPLC (see Fig. 3.8). This revealed that almost all of the minor contaminating peaks had been removed. Upon tricine gel electrophoresis of the material from each of the three peaks (Fig. 3.7), the major peak was seen to contain solely the peptide material of apparent M_r 5,600, while the composition of both of the minor peaks resembled that of the crude polypeptide (Fig. 3.9). However, the amino acid composition of the two minor peaks was identical to that in the major peak (results not shown).

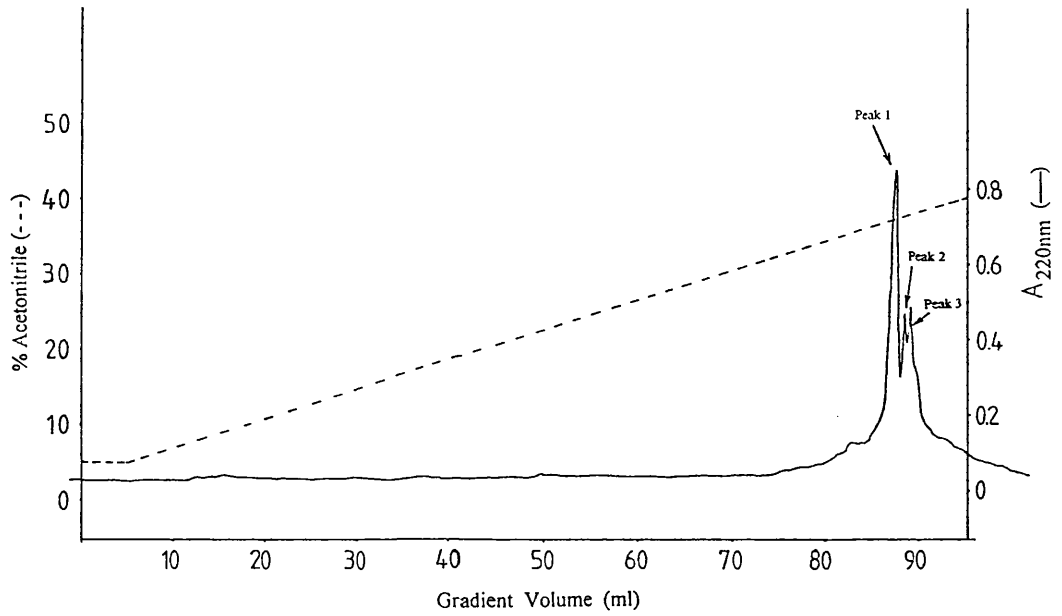

Fig. 3.7 HPLC chromatogram obtained from the absorption at 220nm of the eluate in a 5-40% (v/v) acetonitrile gradient in 0.1% (v/v) TFA at a flow rate of 1ml/min. from a 300A pore-size, C_{18} column following loading of 80μg of peptide J.

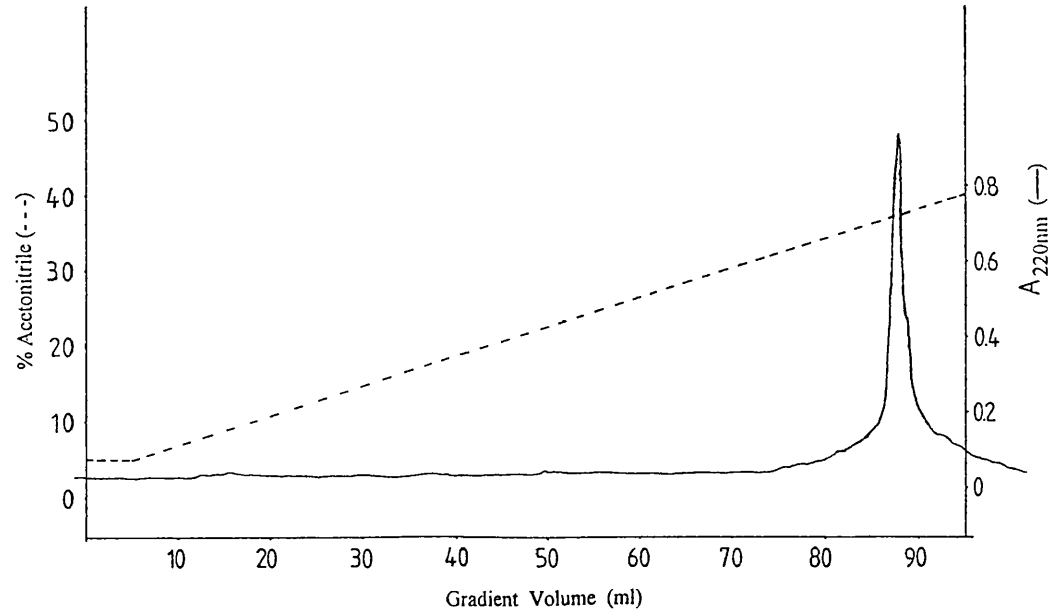

Fig. 3.8 HPLC chromatogram obtained from the absorption at 220nm of the eluate in a 5-40% (v/v) acetonitrile gradient in 0.1% (v/v) TFA at a flow rate of 1ml/min. from a 300A pore-size, C_{18} column following loading of 50μg of peptide J. The peptide had previously been freeze dried following isolation in the major peak, following preparative HPLC under the same condition as used for analysis of crude peptide J (see Fig 3.7).

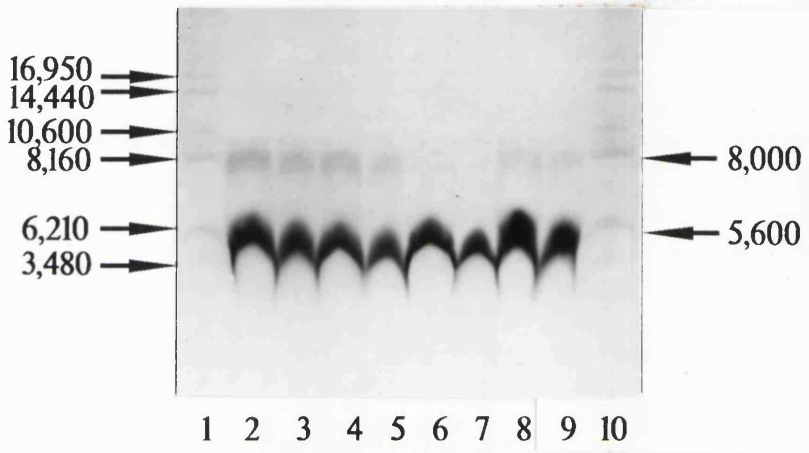

Fig. 3.9 Tricine SDS polyacrylamide gel of crude peptide J and of peptide material isolated from the three major peaks observed in the HPLC chromatogram of crude peptide J (see Fig. 3.7) electrophoresed at 30V for 2h. and 95V for 16h. The separating and spacer gels contained 15.5% (w/v) acrylamide, 1% (w/v) bisacrylamide, 13.5% (w/v) glycerol and 9.7% (w/v)acrylamide, 0.3% (w/v) bisacrylamide, respectively. Samples were loaded as follows; low molecular weight standards (Sigma), (lanes 1 and 10), crude peptide J, 30 and 60μg (lanes 2 and 3, respectively), purified peptide J 30 and 60μg (lanes 4 and 5, respectively), peak 1 material (see Fig. 3.7), 30 and 60μg (lanes 6 and 7, respectively) and peak 3 material (see Fig. 3.7), 30 and 60μg (lanes 8 and 9, respectively).

3.3.3 Secondary structure studies of polypeptide J

Figures 3.10 and 3.11 show the FTIR spectra for polypeptide J prepared as described in Section 2.4, in both the presence and absence, respectively, of 20mM Ca^{2+}. These spectra contain predominant bands of similar intensity at around 1620cm^{-1} and 1682cm^{-1} revealing the presence of intermolecular ß-sheet secondary structure, revealing some aggregation of the polypeptide material. A band at 1637cm^{-1} revealing the presence in the polypeptide of typical ß-sheet structure was more intense in the presence of Ca^{2+}.

This study was repeated. However, this time the peptide was first dissolved in 6M Urea, which causes protein unfolding or denaturation, and then dialysed against 10mM HEPES, pH 7.4 in H_2O, as before. It was hoped that the slow dialysis from 6M Urea would encourage the peptide to fold up into a conformation resembling that found in the intact native protein, without the problems of aggregation observed in the first study. Following dialysis against 10mM HEPES in D_2O, in both the presence and absence of Ca^{2+}, the spectra obtained for the peptide were similar to those obtained in the first study revealing predominant bands at around 1620cm^{-1}, 1637cm^{-1} and 1682cm^{-1} (results not shown). Initially the polypeptide was observed to dissolve easily to a concentration of 5mg/ml in the aqueous buffer in preparation for the structural studies. However, the presence of traces of scavengers (EDT and phenol) and particularly TFA was undesirable. The latter is known to confer α helical structure on proteins which are normally ß sheet. Therefore dialysis of the polypeptide for 24h was carried out prior to structural studies. It is thus apparent that the polypeptide was soluble at the high concentrations (5mg/ml) but aggregated to some extent following dialysis at the concentrations required to obtain secondary structure information using FTIR.

In an attempt to circumvent problems of peptide aggregation, the peptide was also examined by CD spectroscopy because this technique requires only 1/5 of the concentration of peptide needed for analysis by FTIR. Thus, the presence of α-helical secondary structure was also investigated by obtaining CD spectra, using a sample

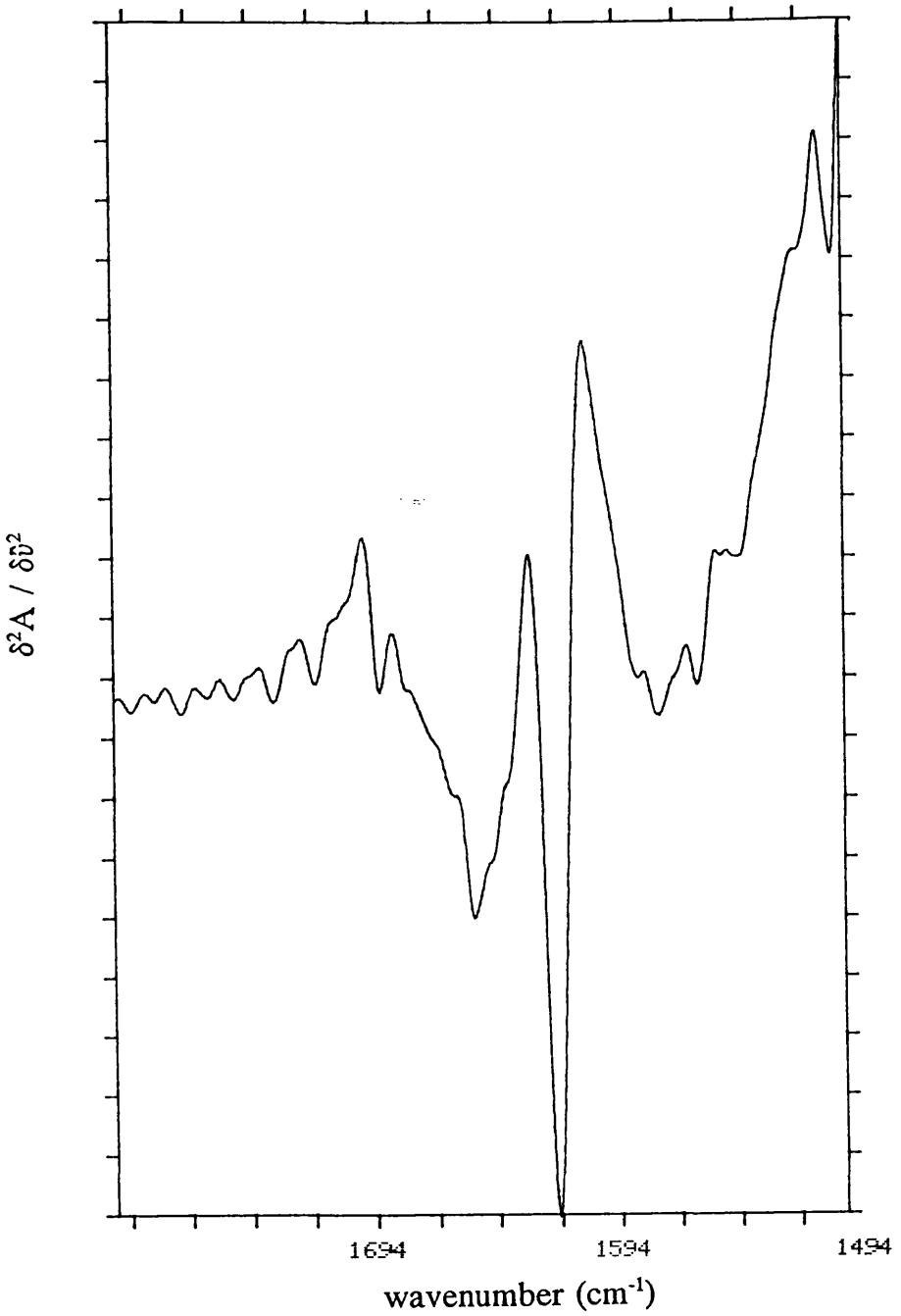

Fig. 3.10 FTIR spectrum for a solution of peptide J in 10mM HEPES/Tris, 20mM $CaCl_2$, pH 7.4 made up in D_2O. The peptide was treated prior to analysis by dialysis of a 250μl of a 10mg/ml solution versus 10mM HEPES/Tris, 20mM $CaCl_2$, pH 7.4 (2l) for 24h, prior to dialysis versus this buffer in D_2O (20ml) for 8h. The spectrum was obtained using a Perkin-Elmer Model 1750 Infrared Fourier Transform Spectrometer equipped with a TGS detector. Briefly, samples (volumes up to 50μl) were placed in a thermostatted Beckman FH-01 CFT microcell fitted with CaF_3 windows. Spectral conditions were as follows: 200 scans; spectral resolution 4cm^{-1}; sample thickness of 50μm using a Teflon spacer; sample temperature 20°C.

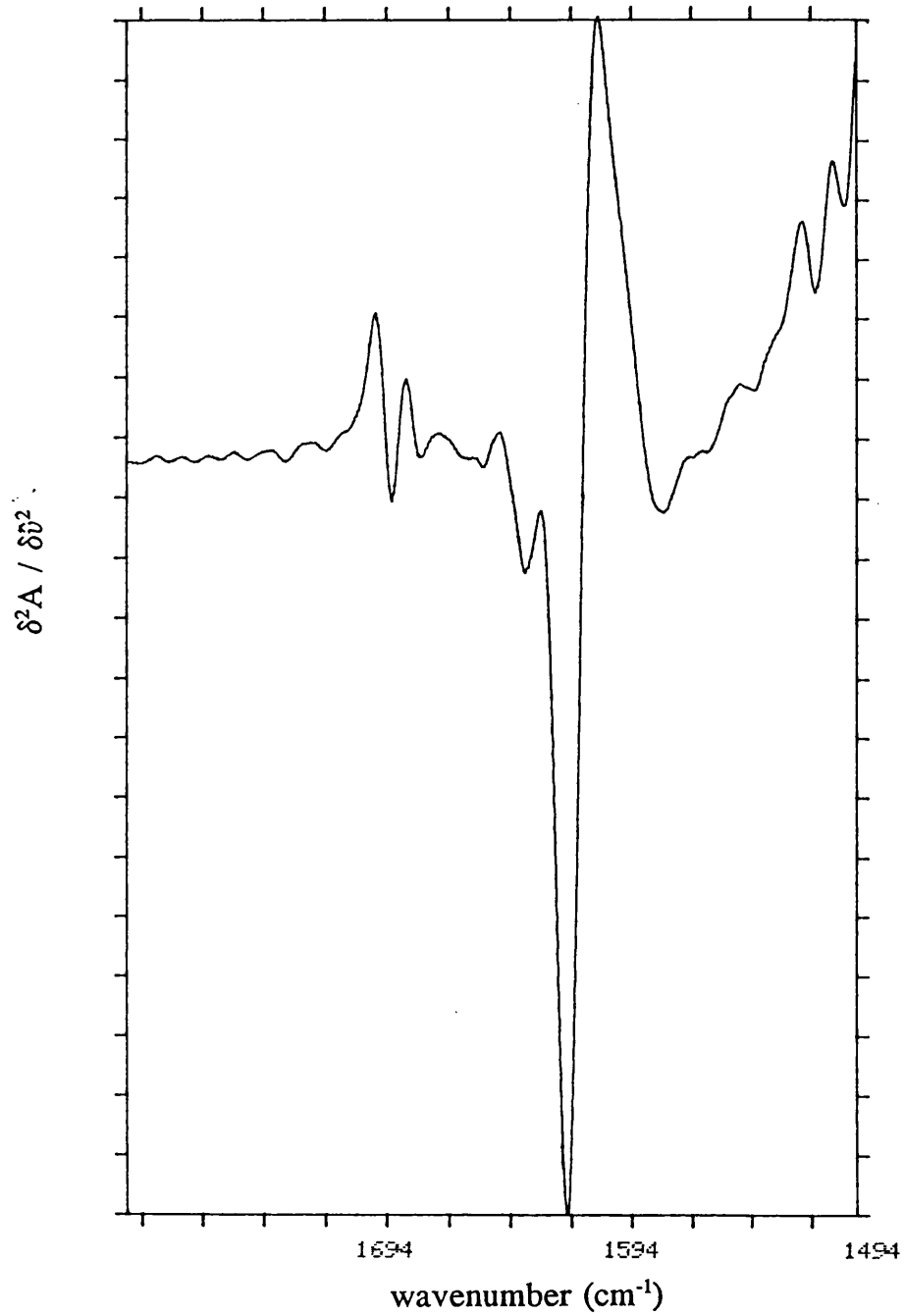

Fig. 3.11 FTIR spectrum for a solution of peptide J in 10mM HEPES/Tris, 5mM EGTA, pH 7.4 made up in D_2O. The peptide was treated prior to analysis by dialysis of a 250μl of a 10mg/ml solution versus 10mM HEPES/Tris, 5mM EGTA, pH 7.4 (2l) for 24h, prior to dialysis versus this buffer in D_2O (20ml) for 8h. The spectrum was obtained using a Perkin-Elmer Model 1750 Infrared Fourier Transform Spectrometer equipped with a TGS detector. Briefly, samples (volumes up to 50μl) were placed in a thermostatted Beckman FH-01 CFT microcell fitted with CaF_3 windows. Spectral conditions were as follows: 200 scans; spectral resolution 4cm^{-1}; sample thickness of 50μm using a Teflon spacer; sample temperature 20°C.

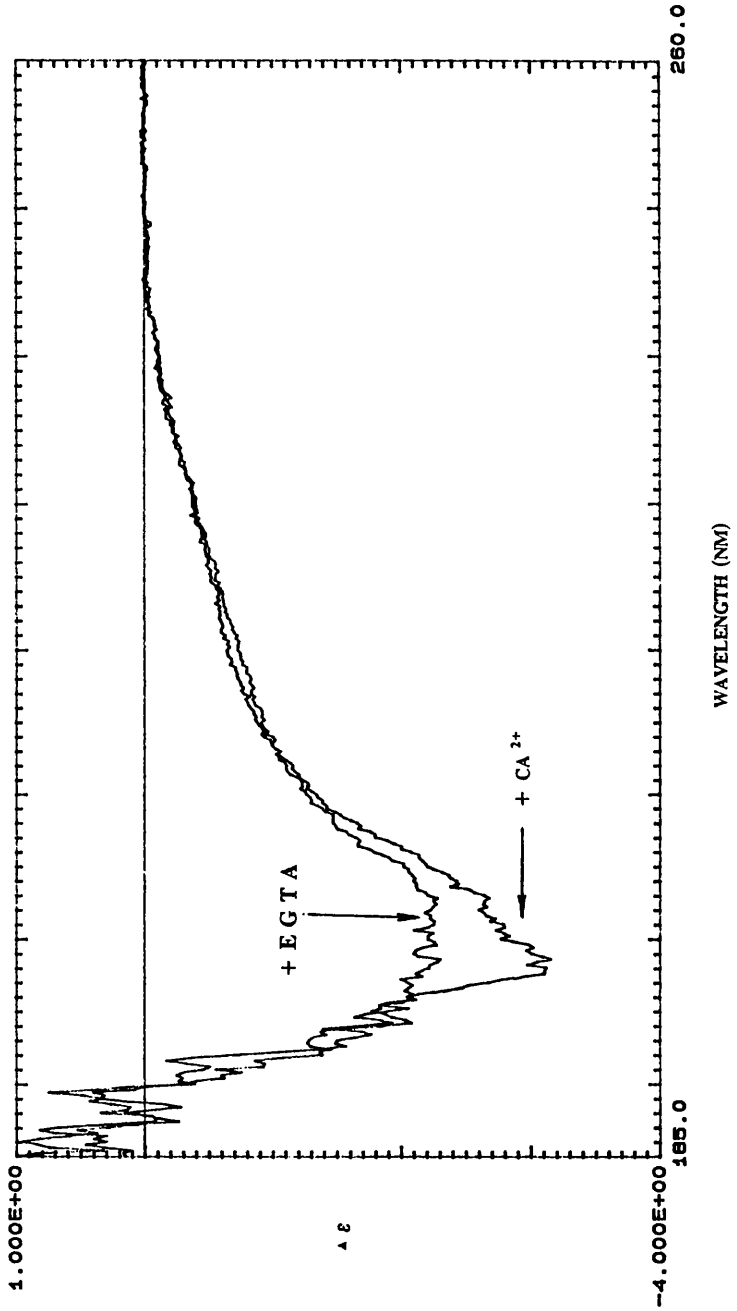

Fig. 3.12 CD spectra for a solutions of peptide J in 10mM HEPES/Tris, 20mM $CaCl_2$, pH 7.4 and 10mM HEPES/Tris, 2.5mM EGTA, pH 7.4. The peptide was treated prior to analysis by dialysis of a 250μl of aliquots (250μl) of 2mg/ml solution versus 10mM HEPES/Tris, 20mM $CaCl_2$, pH 7.4 (2l) or 10mM HEPES/Tris, 5mM EGTA, pH 7.4 (2l) for 24h. The spectrum was obtained using a Jasco J600 CD spectrometer with a 0.02 cm pathlength.

concentration of 2mg/ml. Samples were prepared as outlined in Section 2.4. In both the presence or absence of Ca^{2+}, no α-helical secondary structure was seen, since there is no absorbance at 220nm in the CD spectra (Fig. 3.12). The revealed absorbance of rotating light at 197nm indicates a random coil conformation for the polypeptide. However, the noise level in the traces again indicates some polypeptide aggregation.

3.4 DISCUSSION

3.4.1 Characterization of the synthetic peptides

The yields obtained for the synthesis of each of the smaller synthetic peptides produced compares favourably with those reported in the literature for the Fmoc polyamide procedure (reviewed by Fields and Noble, 1990). The much lower yield obtained for polypeptide J, is also similar to yields of polypeptides of similar sizes synthesised using the Fmoc polyamide procedure (see Fields and Noble, 1990).

In all cases measured amino acid composition of the peptides closely resembled that predicted from the sequence, suggesting that the addition of a three-fold molar excess of amino acid at each coupling step was sufficient to ensure saturation of coupling sites on the growing peptide, and that each deprotection step had proceeded to completion. However, because the accuracy with which amino acid compositions can be determined is fairly low (typically $\pm$ 10% for each type of amino acid) it was desirable to use additional, complementary methods to assess peptide purity. The presence within the synthetic product of molecules with mass identical to that predicted from the amino acid sequence is a very good indication of the success both of the synthetic procedure and of successful removal of side-chain protecting groups without damage to the peptide. Samples of each of the smaller peptides were therefore subjected to Fast Atom Bombardment mass spectrometry,

while it was necessary to analyze all peptides, with the exception of peptide C, whose estimated molecular mass was greater than 2,000g/mole using Laser Desorption mass spectrometry.

In each peptide sample a quasi-molecular ions of expected mass was obtained, suggesting the presence of the appropriate peptide species in the synthetic products. However additional species were detected in peptide samples H, J, K and O. In synthetic peptide sample H a molecule having molecular mass 212g/mole larger than the synthetic peptide was present. Since the size difference is equivalent to the molecular mass of a single Mtr side-chain protecting group for arginine residues, the larger species apparently represents peptide H with a single Mtr group still attached to one of its two arginine residues. It is known that Mtr protecting groups are difficult to remove from peptide molecules and it is recommended to allowed peptide containing Mtr groups four hours for deprotection in 95%(v/v) TFA for each Mtr group in the peptide. This advice was adhered to in the case of peptide H. Species smaller than the required synthetic peptide were identified in samples of peptides J, K and O. These are most likely to result from the lack of complete coupling of an amino acid during at least one of the coupling steps. This is known to be a particular problem with large peptides such as peptide J (48 residues), contributing to their lower % yield (see Fields and Noble, 1990). Interestingly, peptides K (21 residues) and O (19 residues) are also comparatively large. Unfortunately, the size of the peaks in the mass spectra cannot be taken as a measure of the relative abundance of the corresponding molecules and so the abundance of the peptide of correct mass in each synthetic sample cannot be measured by this technique. Therefore in addition each peptide was subjected to analysis by reverse-phase HPLC, as described in Section 2.3. In all cases a single major peak was seen, a typical result being illustrated for peptide M in Fig. 3.6. The presence of multiple minor peaks for some of the peptides, such as peptide H, K or D, which accounts for their lower apparent purity, may in fact be a result of partial oxidation of sulphur-containing amino acids. This is known to be a particular problem with cysteine-containing peptides. Similarly, partial failure to remove protecting groups from some residues, particularly arginine,

is known to result in the appearance of multiple peaks on HPLC. This can explain the presence of one of the minor peak in the trace for peptide H. Minor peaks in samples of peptides J, K and O may be due to the presence of peptides containing deletions of one or more amino acid in the sequence. However, the abundance of these peptide species in synthetic samples K and O appear to be much lower than those for the peptide which has the correct sequence.

Similar peptide purities of >80% were previously obtained in a study of the glucose transporter (Davies, 1990b). In this glucose transporter study, analysis of significant minor peaks (>5% of total peak area) observed in the HPLC profile for a particular peptide showed amino acid compositions very similar to the main peak. This suggested that these minor peaks represent either oxidized/dimeric peptides or peptides whose amino acid side chain protecting groups have not been fully removed under the deprotection conditions used. It was subsequently shown that immunization with crude peptide resulted in generation of antibodies that reacted with the native protein (Davies, 1990b). Given the presence of products of the correct molecular mass, as indicated by either FAB or Laser Desorption mass spectrometry, the purity of all our peptides was judged sufficiently high for their use as immunogens without further purification.

The mass spectrum and HPLC profile for samples of the crude synthetic polypeptide J, synthesized for structural studies raised doubts about the sample having the purity required for these studies. Additional information on the size and composition of the synthetic sample was sought using the tricine-SDS/PAGE system, which is capable of resolving polypeptides of low M_r. Upon tricine gel electrophoresis of the material from each of the three peaks obtained during HPLC of the crude peptide, the major peak was seen to contain only peptide material of apparent M_r 5,500, while the composition of both of the minor peaks resembled that of the crude polypeptide, apparently containing traces of a polypeptide of apparent M_r 8,000 (Fig. 3.9). However, the amino acid composition of the two minor peaks was identical to that in the major peak (results not shown). In an attempt to purify the peptide, to remove this contaminant of large apparent M_r, a sample of the peptide was subjected

to preparative HPLC, using the same conditions as for its analysis. The major peak and both minor peaks (see Fig. 3.7) in the eluate were collected, freeze-dried and the former subjected to analytical HPLC (see Fig. 3.8). This revealed that almost all of the minor contaminating peaks had been removed.

The nature and origin of the apparently larger peptide therefore remains obscure, although since conformers of a single polypeptide species, with very different electrophoretic mobility, are commonly seen in the analysis of membrane proteins by SDS-PAGE, it is possible that the two bands seen on gels may represent such conformers. This seems likely in view of the fact that the material in both bands coelute on the shallow reverse-phase gradient. The minor peaks in the HPLC profile probably arise from polypeptides containing unremoved amino acid side chain protecting groups and peptide material containing deletions in the intended amino acid sequence of the polypeptide. However, preparative HPLC removed much of this contamination, yielding purified polypeptide for use in structural studies and antibody production.

3.4.2 Secondary structure of polypeptide J

In the FTIR spectra of polypeptide J in the presence and absence of 20mM Ca^{2+} predominant bands of similar intensity at around 1620cm^{-1} and 1682cm^{-1} reveal the presence of intermolecular ß-sheet secondary structure, while the band at 1637cm^{-1} reveals that the polypeptide contains typical ß-sheet secondary structure (reviewed by Haris and Chapman, 1992). Since the bands at 1620cm^{-1} and 1682cm^{-1} are normally characteristic of aggregated/denatured proteins and polypeptides it seems that there is some aggregation of the polypeptide samples examined in these studies (5mg/ml). The band at 1637cm^{-1} is more intense in the presence of Ca^{2+}, indicating that Ca^{2+} may have an effect on the protein structure. It could be preventing a certain amount of aggregation of polypeptide allowing more of the polypeptide to adopt normal ß sheet structure. However, the greater amount of ß-sheet structure evident when Ca^{2+}

is present may indeed be due to Ca^{2+} binding to the polypeptide and conferring on it a change in its secondary structure. No absorbance due to α-helical structure is evident in either spectrum.

Denaturation of the polypeptide in 6M Urea, followed by dialysis against 10mM HEPES, pH 7.4 in H_2O, did not appear to eliminate the problems of aggregation observed in the first study. The problem appears to be one of solubility of the peptide at the high concentrations (5mg/ml) required to obtain secondary structure information using FTIR. It appears that the polypeptide aggregates as a result of being in solution at a concentration of 5mg/ml for 24h or possibly due to the removal of TFA. The latter seems more likely since the noise level in the CD spectra for the polypeptide following dialysis at a concentration of 2mg/ml for 24h also revealed some peptide aggregation.

It thus appears that this polypeptide posesses some random coil and ß sheet secondary structure. However, no α helical content was observed. The latter finding is contrary to prediction from its amino acid sequence, while the presence of some random coil was expected. In the FTIR studies the presence of Ca^{2+}, which may bind to the polypeptide, could possibly be affecting the polypeptide conformation. However, it is most likely that its presence is preventing some aggregation of the peptide molecules.

CHAPTER 4

ANTIBODY PRODUCTION, PURIFICATION AND CHARACTERIZATION

4.1 INTRODUCTION

4.1.1 Antiserum production

All anti-peptide antibodies were produced in rabbits following the procedures outlined in Section 2.6.1. In most cases an initial immunization with a water in oil emulsion of peptide conjugated to carrier protein in Freund's complete adjuvant and subsequent booster injections of water in oil emulsions of peptide conjugate in Freund's incomplete adjuvant were administered. This method has been widely employed to produce anti-peptide antibodies to study membrane proteins (for a review see White, 1976).

In order to elicit an immune response in the animal to peptides in the size range of those synthesized for this study it is necessary to conjugate the peptides, to a much larger carrier protein, prior to their use as immunogens. There are a number of reasons for this. Firstly, in small size range 12-36 residues, closely related peptide sequences exist in the animals normally used for antiserum production and so the peptide alone will not be recognized as foreign. These small peptides also may lack a defined structure, which is necessary for their recognition as antigens. Finally peptide-conjugates are less prone than peptides to rapid degradation in the tissue and circulation of the immunized animal, where they must remain relatively intact in order to elicit an immune response.

4.1.2 Immunization procedures

In this study, KLH was initially used as a carrier protein for peptides. This protein is frequently used as an antigen carrier for polyclonal antibody production. However, this very large protein is only sparingly soluble in aqueous buffer, therefore producing a relatively small amount of soluble peptide conjugate. Bovine serum albumin and ovalbumin, which are highly soluble proteins, have also frequently been used by many researchers as an antigen carrier. Immunization using peptides coupled to ovalbumin was also carried out, as for KLH conjugates, according to the protocol for antiserum production outlined in Section 2.6.1. Immunization in this way elicits an antibody response to both the peptide and also the carrier protein.

Purified protein derivative (PPD) which consists of heat inactivated protein derived from *Mycobacterium tuberculosis*, has also been found to be highly effective when used as a carrier protein in the production of anti-peptide antibodies. This protein, whose major component has an M_r value of 10kD, is more soluble in aqueous buffer than KLH, easily reaching the dissolved concentration required for coupling with the peptide (5mg/ml) (Lachmann *et al.*, 1986). It has the added advantage that when used as an antigen carrier, as outlined in Section 2.6.1, PPD has not been observed to elicit an immune response to itself. Peptides, B and G, corresponding to the less apparently immunogenic domains IS4 and IVS4, respectively, were coupled to PPD prior to immunization following the protocol outlined in Section 2.6.1. These PPD-peptide conjugates were thus predicted to elicit production solely of anti-peptide antibodies.

Rabbits are used in the production of polyclonal antiserum for many reasons including relative cost, ease of maintenance, robustness in the face of extensive immunization, size (large enough to yield 15-20ml serum per month) and ease of bleeding. The New Zealand White strain, which has been used extensively for producing polyclonal antisera, was used at the outset of this project. However, Half-Lop rabbits, which appear to have stronger immune responses to administered antigens were subsequently employed in antibody production.

4.1.3 Monitoring antibody production

4.1.3.1 Reaction with peptide

The titre of peptide-specific antibodies produced in serum was monitored by examining the reactivity of serial dilutions of serum with the peptide antigen using ELISA, as outlined in Section 2.6.3. The estimated relative binding of the serum to the microtiter wells coated with the relevant peptide is then plotted against the dilution of serum in the wells. Comparison of anti-peptide titres of different antisera can be made by comparing the respective estimated dilutions at which the binding of the serum to the antigen is equivalent to half its maximum value. Thus those antisera which react with the peptide with half maximum efficiency at comparatively high dilutions strongly recognize their peptide antigen.

Those antibodies produced using a peptide coupled to any carrier protein, with the exception of PPD, which react with the peptide in ELISA, may be elicited entirely by a region or regions in the peptide, or by domains on both the peptide and the carrier protein. Additionally, the synthetic peptide resembles, but is not structurally identical to, its corresponding domain in the intact, native or denatured protein. Thus, it is clear that strong recognition of peptide in ELISA, by an antibody, does not necessarily imply strong recognition of the intact protein.

4.1.3.2 Reaction with intact polypeptide

While being useful in detecting recognition of its antigen, knowledge of peptide recognition is of little value in characterizing an anti-peptide antibody to be used to probe an intact protein. The majority of antibodies produced by the rabbit in response to a peptide probably recognize the exposed N-terminal end of the peptide. For peptides which are located within rather than at either end of a polypeptide sequence, it is those antibodies produced which recognize the middle of the peptide that are likely to react with the peptide sequence in the intact protein. Thus, prior to

their use in probing structure, function or distribution of their relevant channel subunits, it was necessary to determine whether the antibodies would react with their respective peptides in these channel polypeptides.

The reactivity of antipeptide antibodies with their specific peptide sequences in the intact protein in the denatured state was examined using the technique of Western blotting, as described in Section 2.6.4. This standard method used to characterize antibodies demonstrates their recognition of proteins in the denatured state. However, the native and denatured forms of the same protein differ immunogenically. This is due to the fact that regions/domains of a polypeptide which are inaccessible to antibody when the protein is in its native conformation become exposed upon denaturation. Similarly all discontinuous, and probably almost all continuous native epitopes are lost or altered. Therefore recognition of a denatured protein by an antibody does not imply that the antibody will also bind to the protein in its native conformation and similarly antibodies may react with a polypeptide when it is in its native, but not in a denatured, state.

As discussed in Section 1.9.9.3, the rabbit skeletal muscle L-type channel α_1 subunit is processed following synthesis, leading to the appearance of two polypeptides having M_r values of 212,000 and 173,000, as revealed upon SDS/PAGE of the purified DHP receptor. The truncated polypeptide is now known to be functional as both voltage sensor and channel (Gutierrez *et al.*, 1991; Ma *et al.*, 1991; Beam *et al.*, 1992), but the loss of three potential sites of phosphorylation due to proteolysis may have regulatory significance. In order to investigate whether or not this proteolytic modification of α_1 was a more general phenomenon, it was important to examine t-tubule membranes from rat skeletal muscle (mouse and human t-tubules were not available in large enough quantities) in parallel with those obtained from rabbit. This was done by probing for the presence of the two size-forms of the α_1 subunit using Western blotting with those antibodies already known to recognize the denatured channel α_1 subunit from rabbit muscle.

4.1.4 Antibody purification

Because of the relatively high ratio of serum protein to peptide-specific antibody found in all antisera, most studies have used affinity purified anti-peptide antibodies as probes for membrane protein structure and function. Affinity purification removes non-specific antibodies, some of which recognize the carrier protein, along with other serum proteins, particularly rabbit serum albumin. Some of these proteins e.g. non-specific IgG and serum albumin, are much more concentrated in serum than the peptide-specific antibodies. Thus purification removes the possibility of a nonspecific effect due to the presence of these proteins, when these antibodies are subsequently used as probes.

In this study, peptide-specific antibodies were purified from serum prior to their use in structural, functional and localization studies. Anti-peptide antibodies were isolated from serum by affinity chromatography using a column containing immobilized peptide. Initial purifications involved isolation of serum IgG, using AffiGel-Blue gel (Bio-Rad) prior to affinity purification. This step was included to avoid the addition of crude serum, containing proteases, to the Sepharose affinity column. Subsequently, this initial step was omitted and crude serum diluted 1/2 in PBS buffer was recirculated through the affinity column. Most peptides were coupled to the column material, either Tresyl-activated Sepharose 4B or Sulfolink coupling gel, via their C-terminal or, in one case, an N-terminal cysteinyl residue. Polypeptide J which did not contain a cysteine residue was coupled via the ϵ-amino group on the lysine residues to a Triazine-activated Agarose 4XL column. Peptide I was similarly coupled to this column material via its N-terminal lysine residue. Following serum recirculation, non-specifically bound material was eluted from the column using 10mM sodium phosphate, 800mM NaCl, pH 7.25. Peptide-specific IgG was then eluted using either 5M $MgCl_2$ followed by 1/10 dilution in distilled water or either 50mM diethylamine, pH 11.3 or 0.2M glycine/HCl, pH 2.4 followed by rapid neutralization. In each case the eluate was then dialyzed against PBS.

4.2 RESULTS

4.2.1 Reaction with synthetic peptide

Figs. 4.1-4.17 show plots of A_{405} versus serum dilution obtained in ELISA versus the immunizing peptide for serum from rabbits immunized with conjugates of the synthetic peptides. In each of these plots, the error bars representing the standard deviation (SD) from the mean A_{405} value at each serum dilution are within the data point symbol. Significant reactivity of each antiserum with its relevant peptide is revealed in these plots, while recognition of the peptide by preimmune serum from each of the immunuzed rabbits was low (see Figs. 4.1-4.17). These plots also reveal removal of the majority of the reactivity of each antiserum with its peptide antigen following its recirculation through a column containing the peptide. A comparison of the estimated dilution at which the binding of each serum sample to the antigen, both prior to and following recirculation on the peptide column, is half the maximum value is shown in Table 1. These dilution values indicate that for most antisera at least 90% of the apparent recognition of peptide observed in ELISA was removed by the column containing the relevant immobilized peptide. The remaining antisera B, C, D, E and G showed estimated reductions of peptide recognition following recirculation of 83%, 75%, 50%, 80% and 50%, respectively.

The reactivity of each antiserum with a peptide different from the one against which the serum was raised was examined. Figs. 4.18 shows that antisera obtained from rabbits immunized with conjugates of peptides E and L do not react with peptide C any more strongly than preimmune serum from the rabbit immunized with peptide C (Fig. 4.2). Similarly, antisera produced in rabbits following immunization with conjugates of peptides E and F, and of peptides C and N, show comparably poor recognition, respectively, of peptides D (Fig. 4.19) and M (Fig. 4.20). In each of these assays serum from the rabbit immunized with the peptide used to coat the plate shows reactivity with its peptide which is comparable to that previously observed (see Figs. 4.2, 4.8 and 4.15). Similar to Figs 4.1-4.17, the error bars representing the

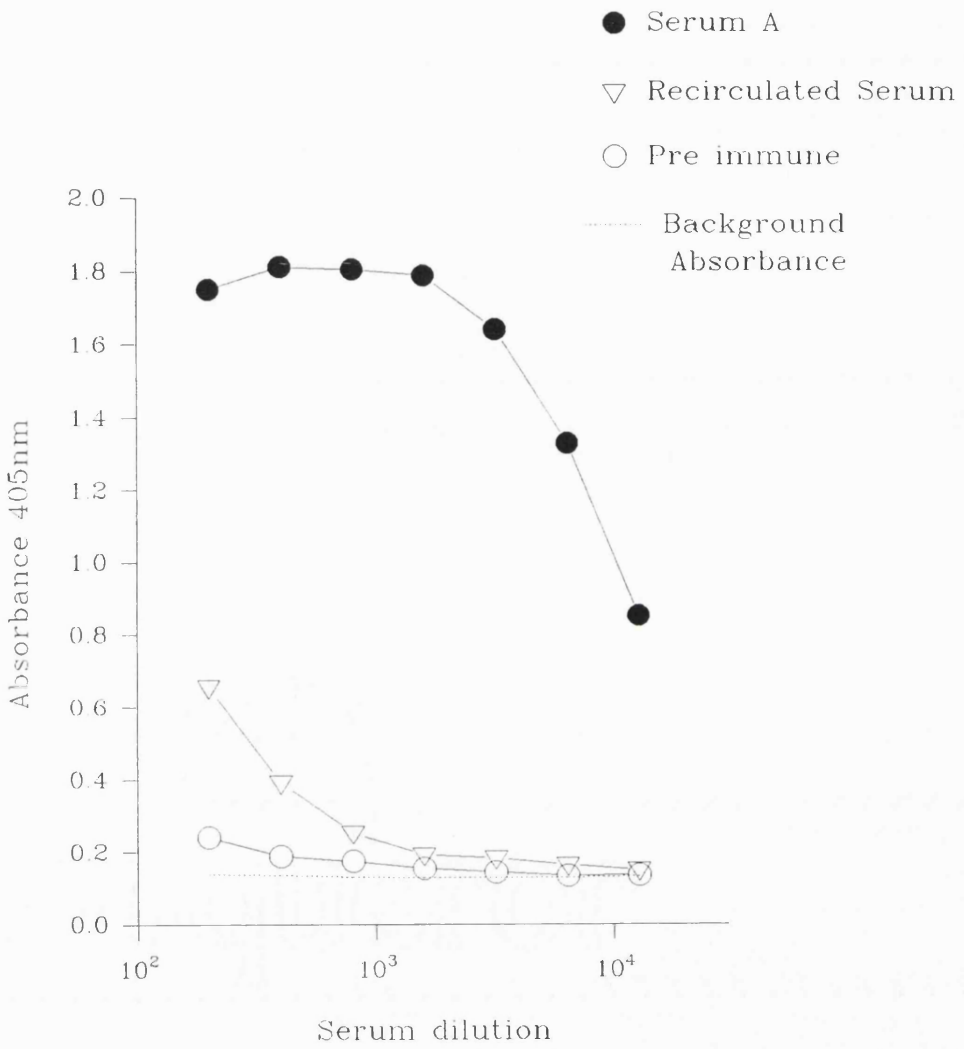

Fig. 4.1 Plot of A_{405} versus serum dilution for preimmune serum, antiserum and recirculated antiserum obtained from NZW rabbit no. 1285 which was immunization using a KLH-conjugate of peptide A. The background absorbance is also indicated in the plot. The serum was recirculated through a column to which peptide A had been bound. The plate was coated with peptide A and blocked and incubatated with both primary and secondary antibody, as outlined in 2.6.3. Bound antibody was detected by the addition of p-nitrophenyl phosphate (Sigma), which yielded yellow p-nitrophenol upon hydrolysis. The latter was quantified by its absorbance at 405nm. Serum dilutions were assayed in triplicate. The error bars representing the SD value for each data point are smaller than the radius of the data point symbols.

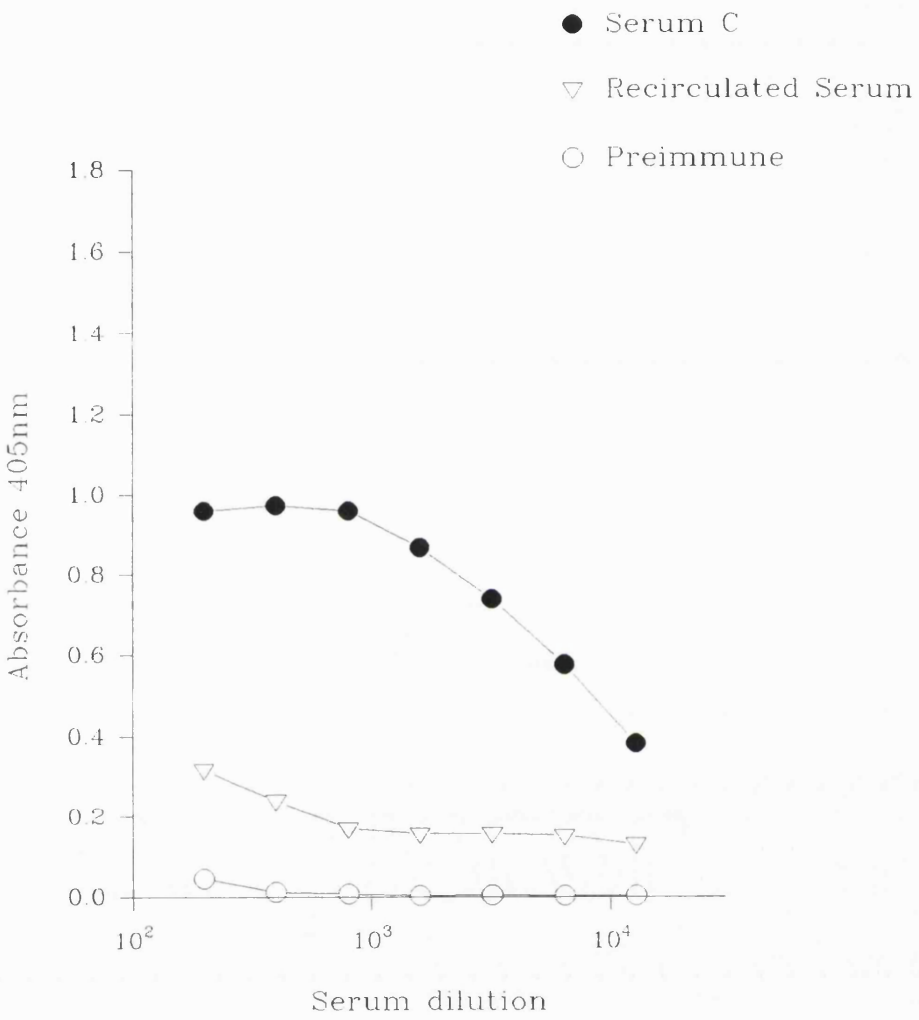

Fig. 4.2 Plot of A_{405} versus serum dilution for preimmune serum, antiserum and recirculated antiserum obtained from Half-Lop rabbit no. 1753 which was immunization using a KLH-conjugate of peptide C. All of the A_{405} values shown have been corrected for background absorbance. The serum was recirculated through a column to which peptide C had been bound. The assay was carried out, using a plate coated with peptide C, as outlined in the legend for Fig. 4.1. Serum dilutions were assayed in triplicate. The error bars representing the SD value for each data point are smaller than the radius of the data point symbols.

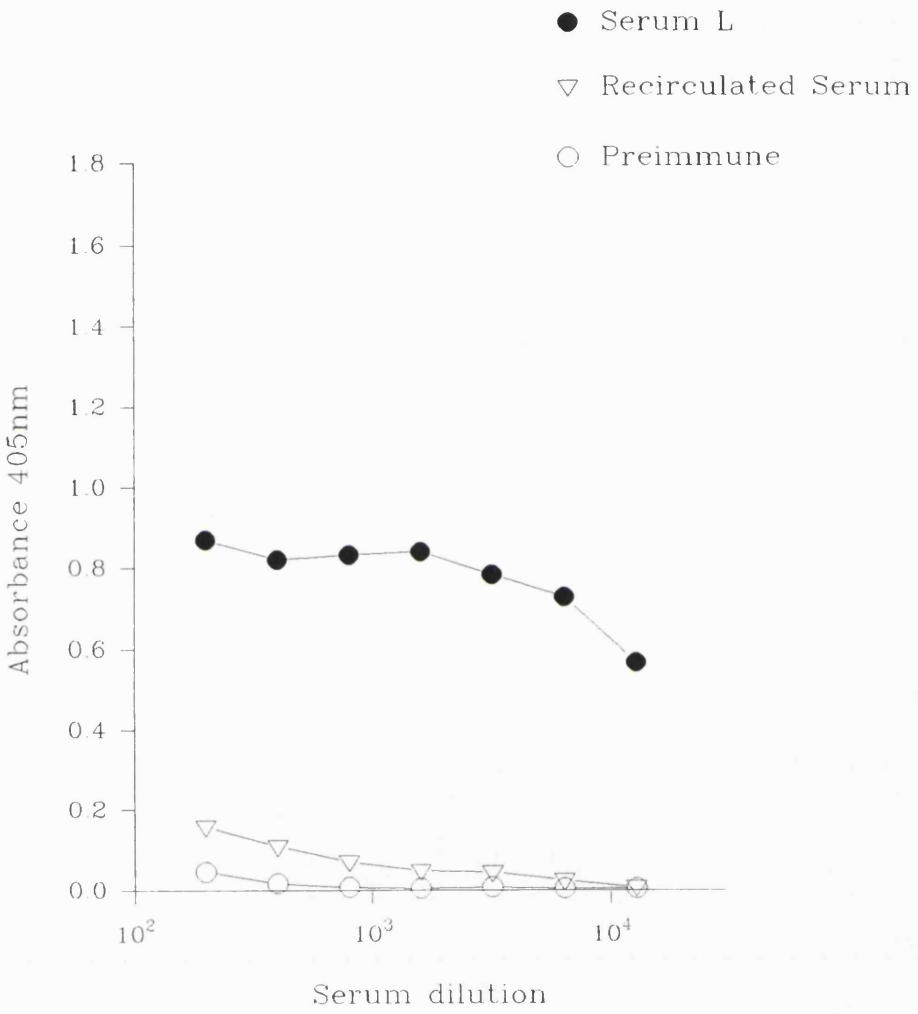

Fig. 4.3 Plot of A_{405} versus serum dilution for preimmune serum, antiserum and recirculated antiserum obtained from Half-Lop rabbit no. 1752 which was immunization using a KLH-conjugate of peptide L. All of the A_{405} values shown have been corrected for background absorbance. The serum was recirculated through a column to which peptide L had been bound. The assay was carried out, using a plate coated with peptide L, as outlined in the legend for Fig. 4.1. Serum dilutions were assayed in triplicate. The error bars representing the SD value for each data point are smaller than the radius of the data point symbols.

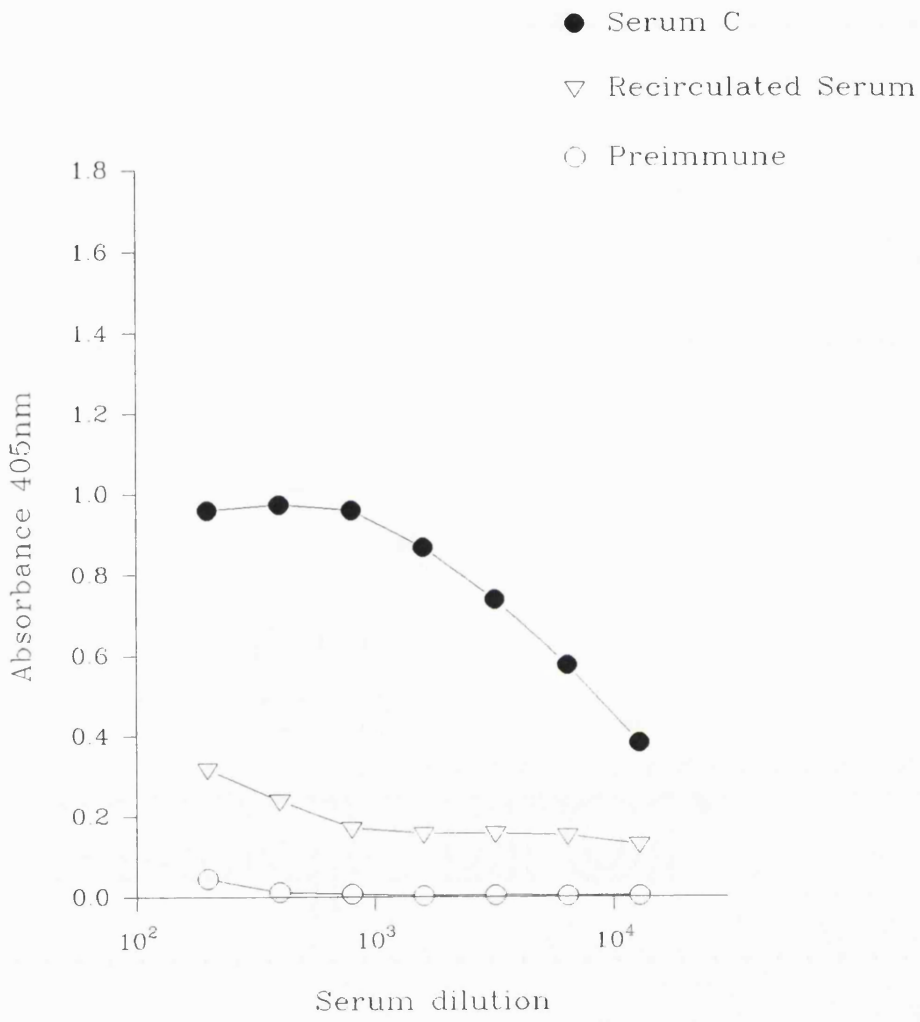

Fig. 4.4 Plot of A_{405} versus serum dilution for preimmune serum, antiserum and recirculated antiserum obtained from NZW rabbit no. 1642 which was immunization using a KLH-conjugate of peptide M. All of the A_{405} values shown have been corrected for background absorbance. The serum was recirculated through a column to which peptide M had been bound. The assay was carried out, using a plate coated with peptide M, as outlined in the legend for Fig. 4.1. Serum dilutions were assayed in triplicate. The error bars representing the SD value for each data point are smaller than the radius of the data point symbols.

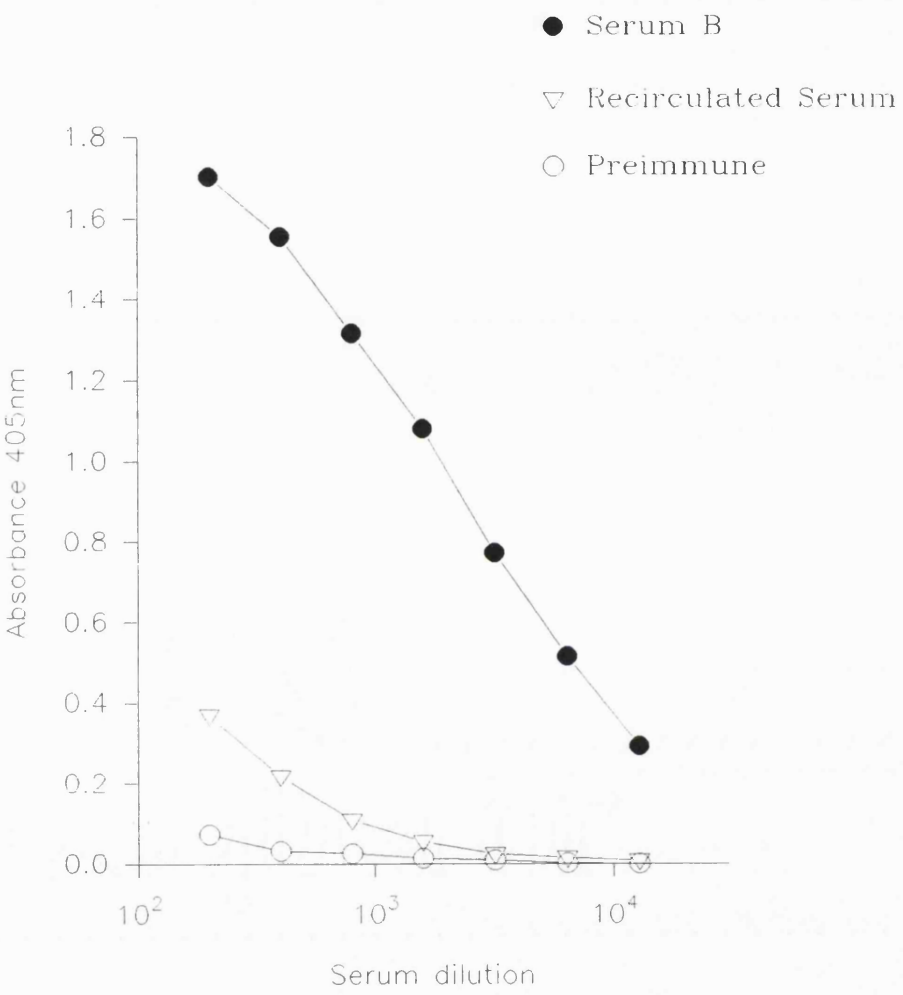

Fig. 4.5 Plot of A_{405} versus serum dilution for preimmune serum, antiserum and recirculated antiserum obtained from NZW rabbit no. 1501 which was immunization using a PPD-conjugate of peptide B. All of the A_{405} values shown have been corrected for background absorbance. The serum was recirculated through a column to which peptide B had been bound. The assay was carried out, using a plate coated with peptide B, as outlined in the legend for Fig. 4.1. Serum dilutions were assayed in triplicate. The error bars representing the SD value for each data point are smaller than the radius of the data point symbols.

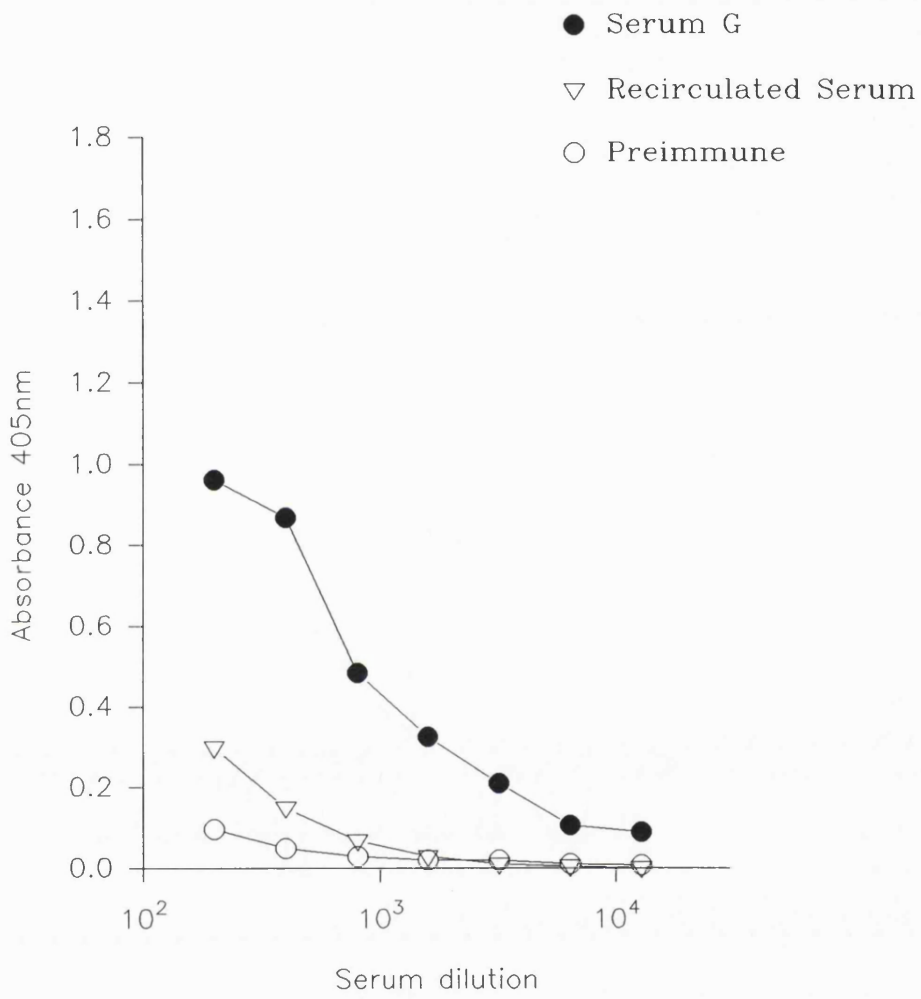

Fig. 4.6 Plot of A_{405} versus serum dilution for preimmune serum, antiserum and recirculated antiserum obtained from NZW rabbit no. 1502 which was immunization using a PPD-conjugate of peptide G. All of the A_{405} values shown have been corrected for background absorbance. The serum was recirculated through a column to which peptide G had been bound. The assay was carried out, using a plate coated with peptide G, as outlined in the legend for Fig. 4.1. Serum dilutions were assayed in triplicate. The error bars representing the SD value for each data point are smaller than the radius of the data point symbols.

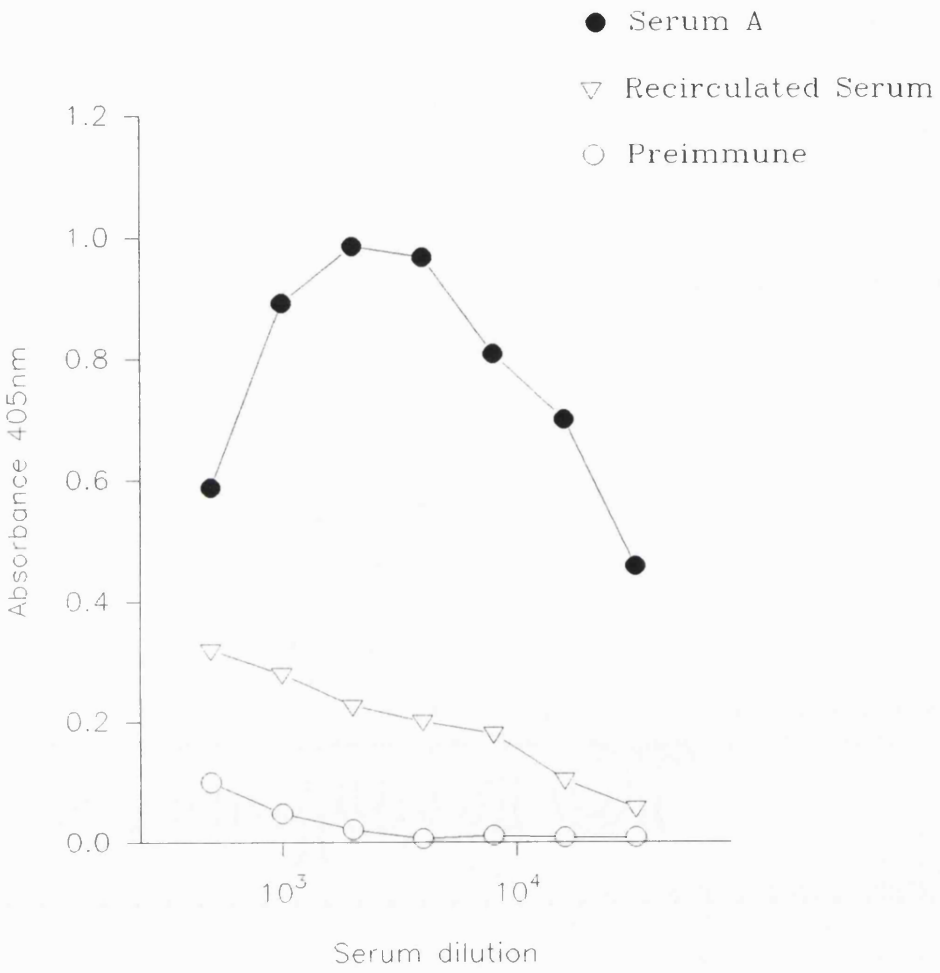

Fig. 4.7 Plot of A_{405} versus serum dilution for preimmune serum, antiserum and recirculated antiserum obtained from Half-Lop rabbit no. 1866 which was immunization using an ovalbumin-conjugate of peptide A. All of the A_{405} values shown have been corrected for background absorbance. The serum was recirculated through a column to which peptide A had been bound. The assay was carried out, using a plate coated with peptide A, as outlined in the legend for Fig. 4.1. Serum dilutions were assayed in triplicate. The error bars representing the SD value for each data point are smaller than the radius of the data point symbols.

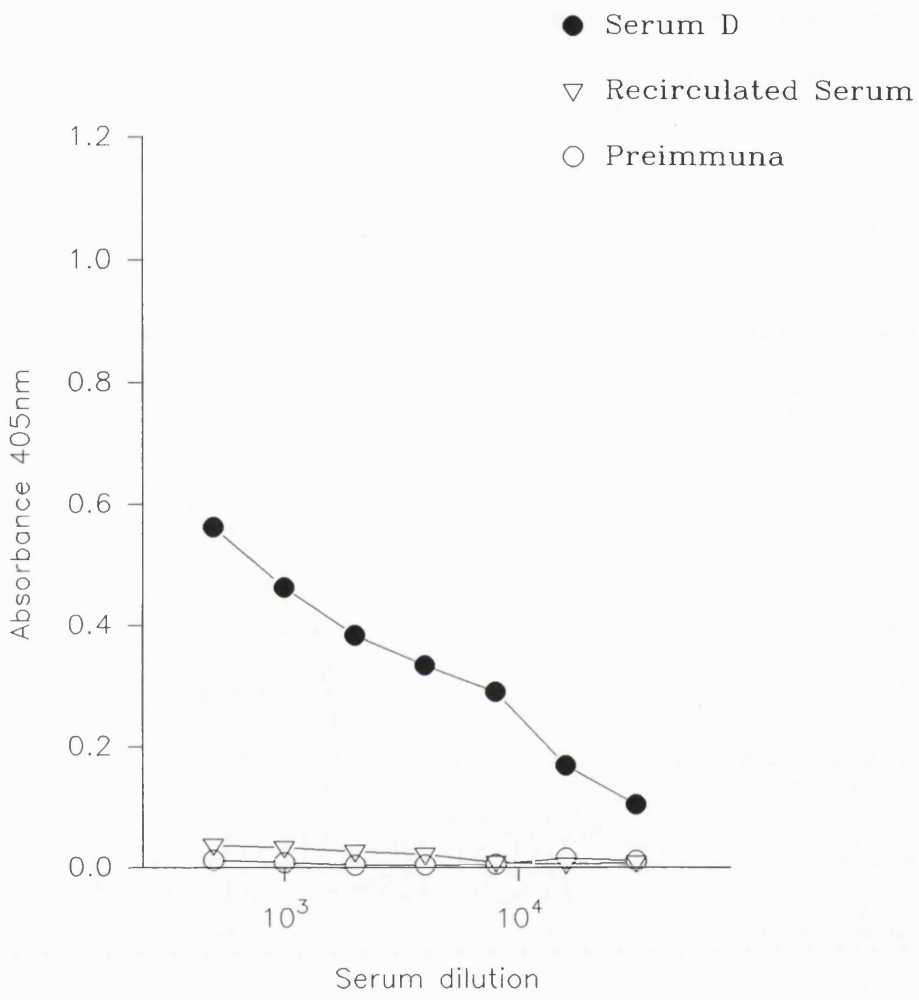

Fig. 4.8 Plot of A_{405} versus serum dilution for preimmune serum, antiserum and recirculated antiserum obtained from Half-Lop rabbit no. 1804 which was immunization using an ovalbumin-conjugate of peptide D. All of the A_{405} values shown have been corrected for background absorbance. The serum was recirculated through a column to which peptide D had been bound. The assay was carried out, using a plate coated with peptide D, as outlined in the legend for Fig. 4.1. Serum dilutions were assayed in triplicate. The error bars representing the SD value for each data point are smaller than the radius of the data point symbols.

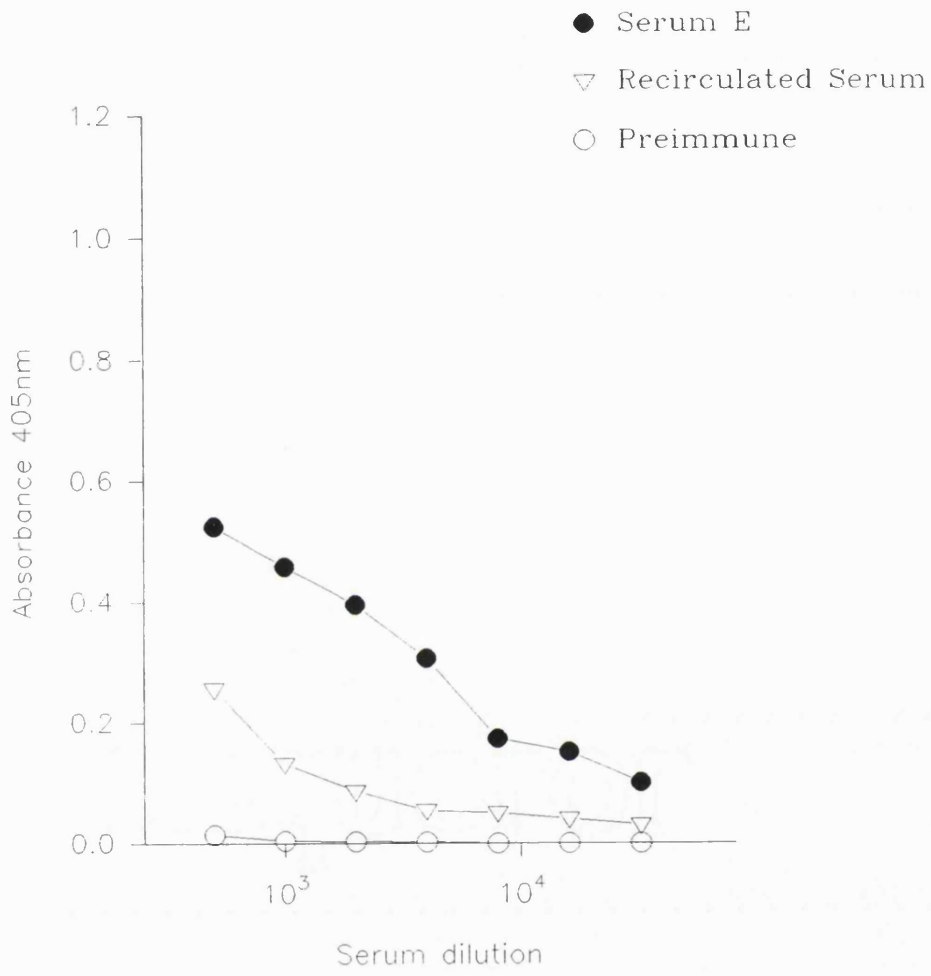

Fig. 4.9 Plot of A_{405} versus serum dilution for preimmune serum, antiserum and recirculated antiserum obtained from Half-Lop rabbit no. 1805 which was immunization using an ovalbumin-conjugate of peptide E. All of the A_{405} values shown have been corrected for background absorbance. The serum was recirculated through a column to which peptide E had been bound. The assay was carried out, using a plate coated with peptide E, as outlined in the legend for Fig. 4.1. Serum dilutions were assayed in triplicate. The error bars representing the SD value for each data point are smaller than the radius of the data point symbols.

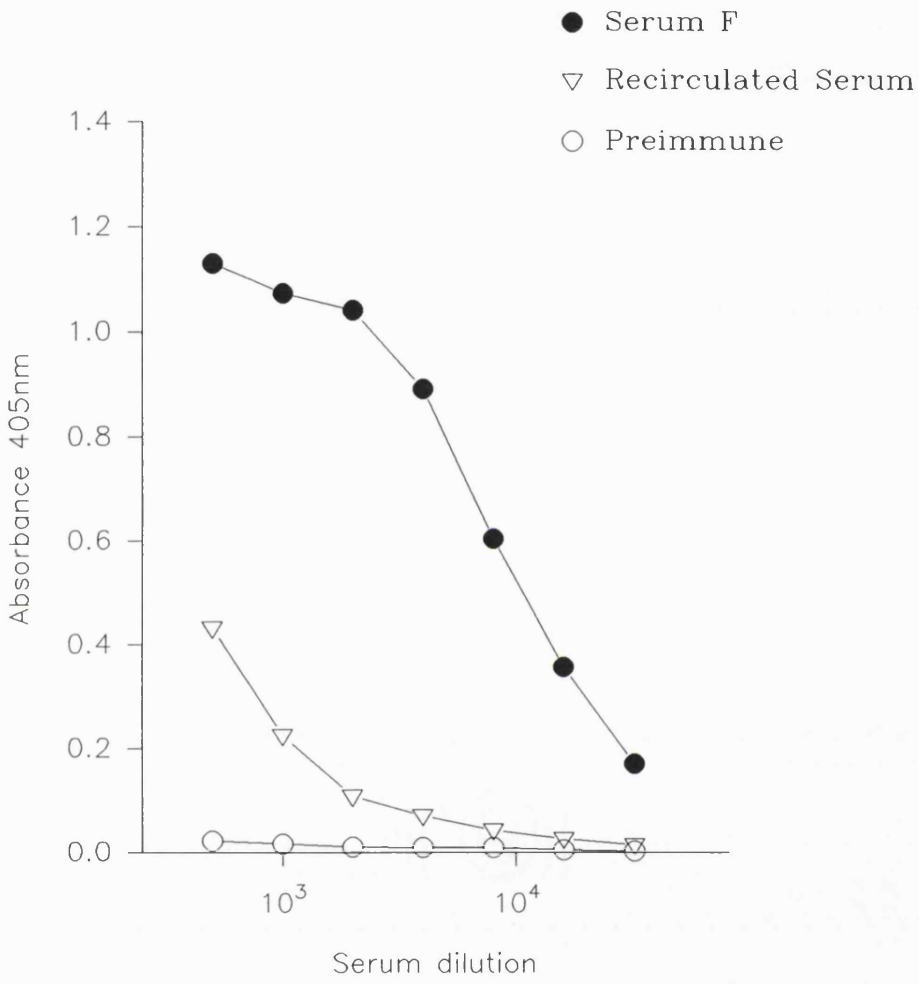

Fig. 4.10 Plot of A_{405} versus serum dilution for preimmune serum, antiserum and recirculated antiserum obtained from Half-Lop rabbit no. 1971 which was immunization using an ovalbumin-conjugate of peptide F. All of the A_{405} values shown have been corrected for background absorbance. The serum was recirculated through a column to which peptide F had been bound. The assay was carried out, using a plate coated with peptide F, as outlined in the legend for Fig. 4.1. Serum dilutions were assayed in triplicate. The error bars representing the SD value for each data point are smaller than the radius of the data point symbols.

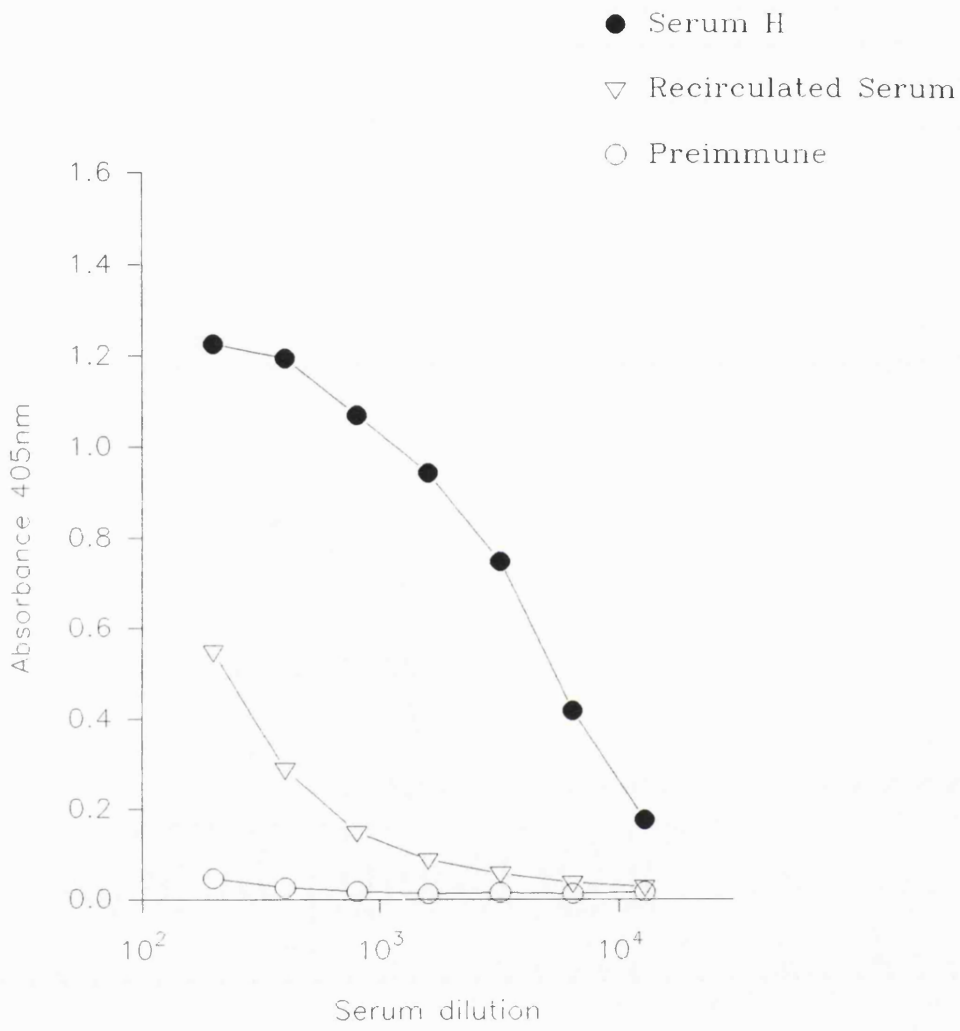

Fig. 4.11 Plot of A_{405} versus serum dilution for preimmune serum, antiserum and recirculated antiserum obtained from Half-Lop rabbit no. 2307 which was immunization using an ovalbumin-conjugate of peptide H. All of the A_{405} values shown have been corrected for background absorbance. The serum was recirculated through a column to which peptide H had been bound. The assay was carried out, using a plate coated with peptide H, as outlined in the legend for Fig. 4.1. Serum dilutions were assayed in triplicate. The error bars representing the SD value for each data point are smaller than the radius of the data point symbols.

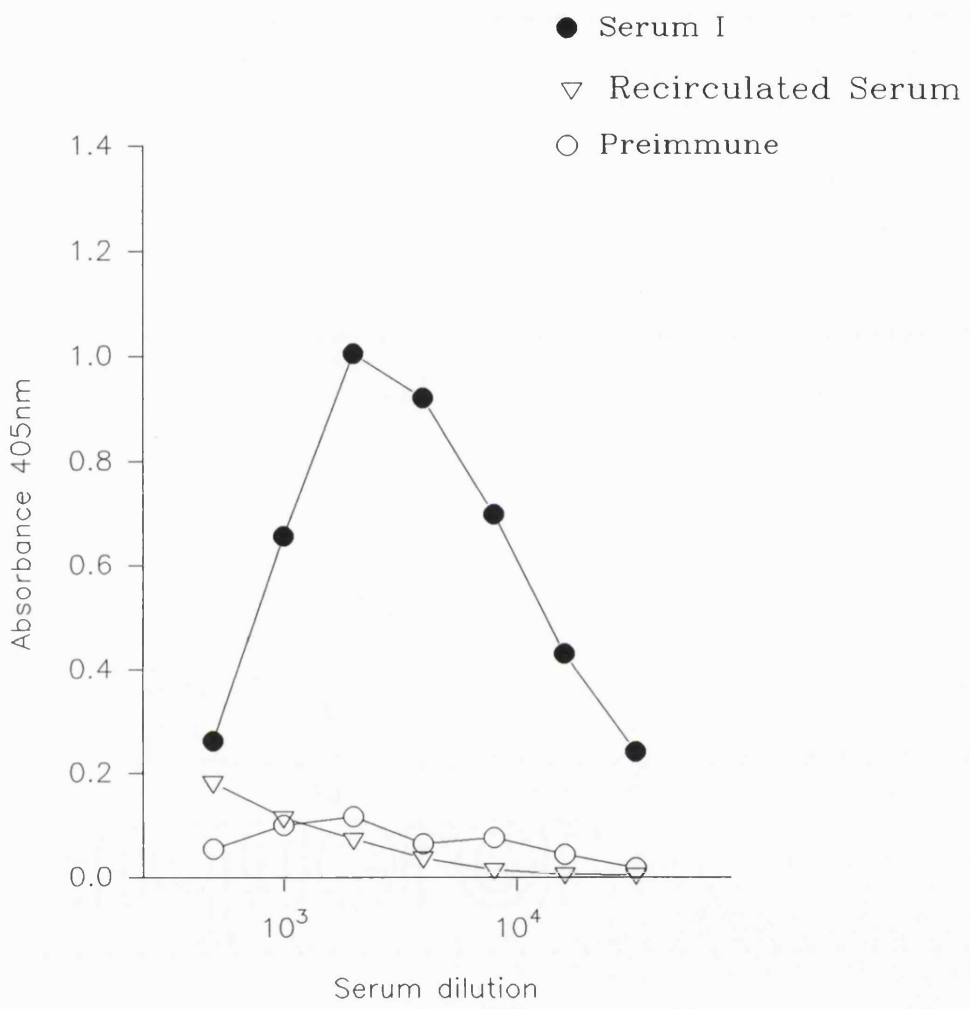

Fig. 4.12 Plot of A_{405} versus serum dilution for preimmune serum, antiserum and recirculated antiserum obtained from Half-Lop rabbit no. 2079 which was immunization using an ovalbumin-conjugate of peptide I. All of the A_{405} values shown have been corrected for background absorbance. The serum was recirculated through a column to which peptide I had been bound. The assay was carried out, using a plate coated with peptide I, as outlined in the legend for Fig. 4.1. Serum dilutions were assayed in triplicate. The error bars representing the SD value for each data point are smaller than the radius of the data point symbols.

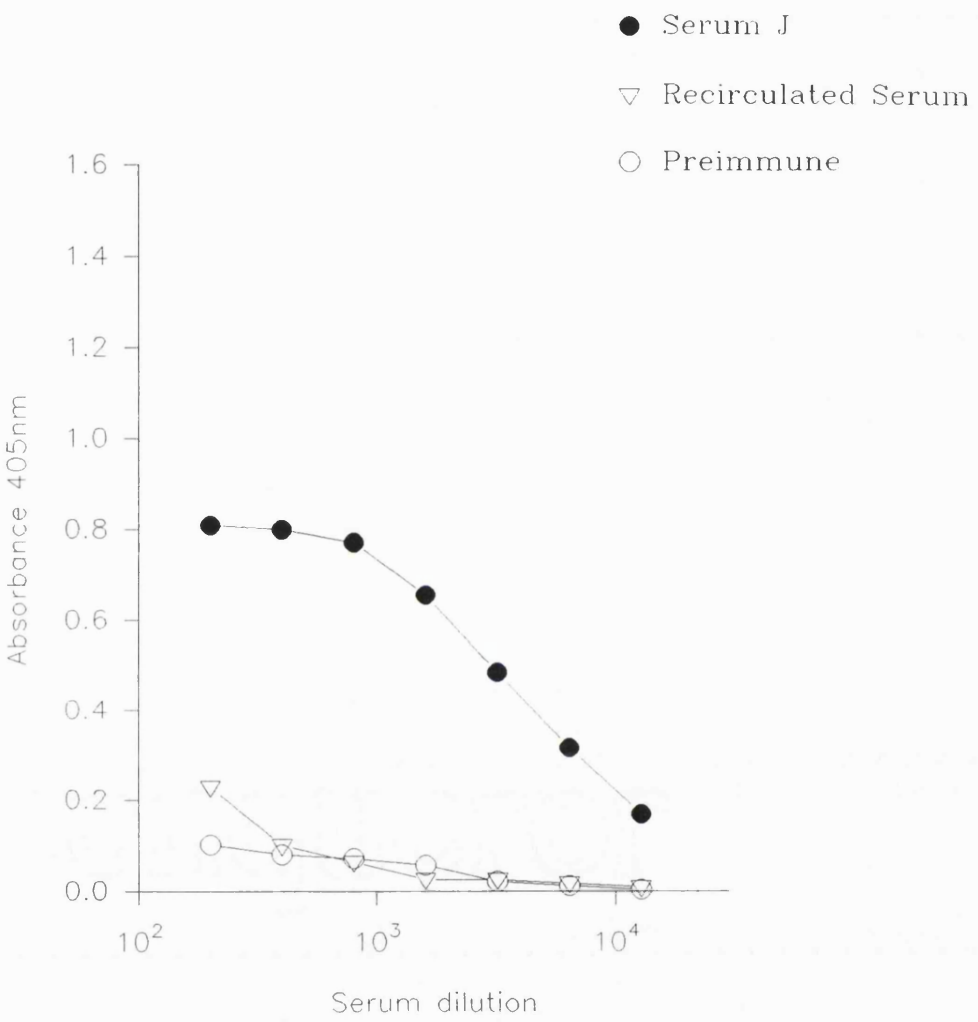

Fig. 4.13 Plot of A_{405} versus serum dilution for preimmune serum, antiserum and recirculated antiserum obtained from Half-Lop rabbit no. 2192 which was immunization using an ovalbumin-conjugate of peptide J. All of the A_{405} values shown have been corrected for background absorbance. The serum was recirculated through a column to which peptide J had been bound. The assay was carried out, using a plate coated with peptide J, as outlined in the legend for Fig. 4.1. Serum dilutions were assayed in triplicate. The error bars representing the SD value for each data point are smaller than the radius of the data point symbols.

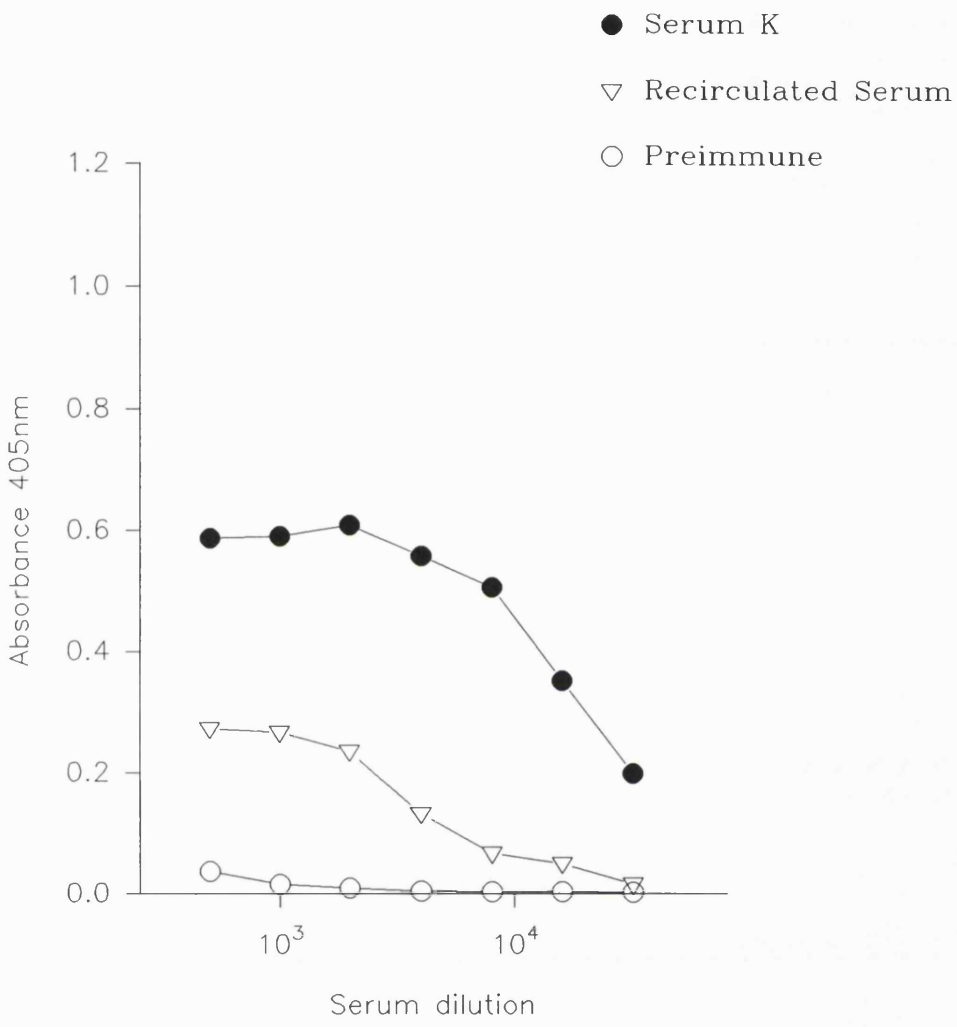

Fig. 4.14 Plot of A_{405} versus serum dilution for preimmune serum, antiserum and recirculated antiserum obtained from Half-Lop rabbit no. 2077 which was immunization using an ovalbumin-conjugate of peptide K. All of the A_{405} values shown have been corrected for background absorbance. The serum was recirculated through a column to which peptide K had been bound. The assay was carried out, using a plate coated with peptide K, as outlined in the legend for Fig. 4.1. Serum dilutions were assayed in triplicate. The error bars representing the SD value for each data point are smaller than the radius of the data point symbols.

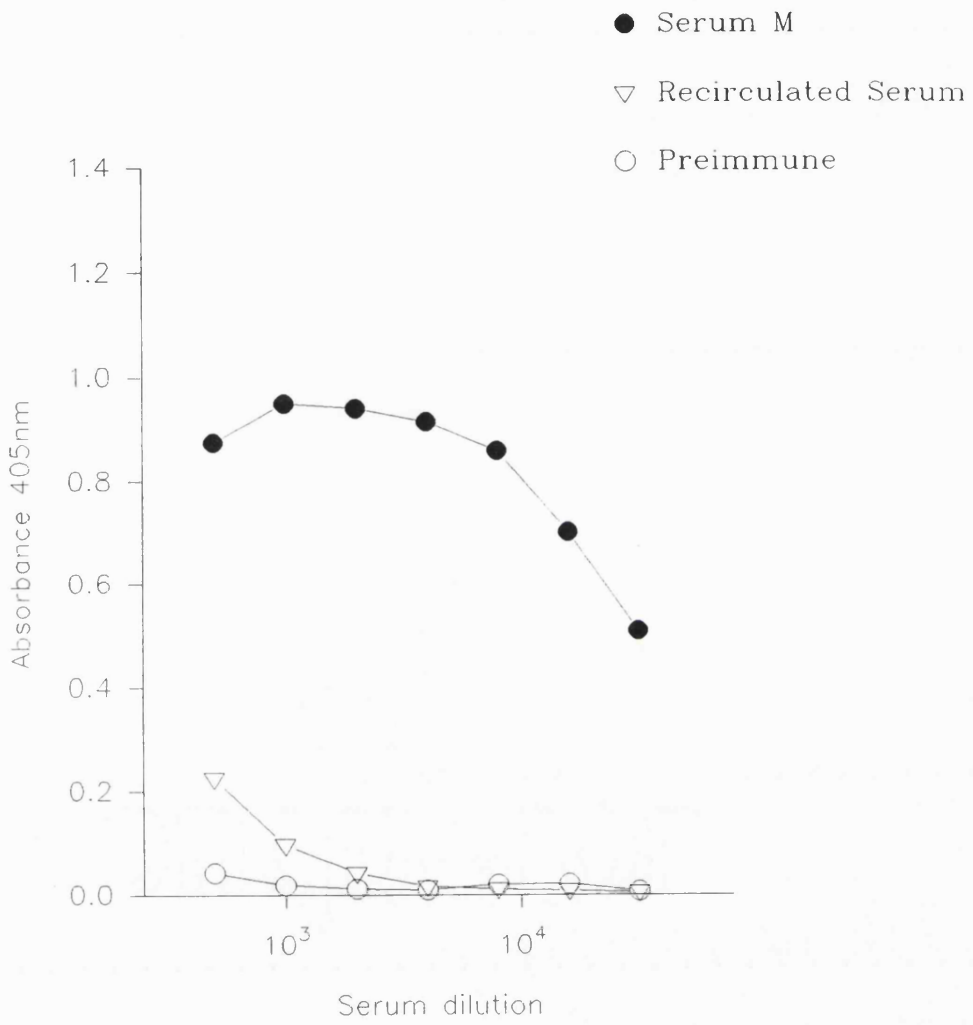

Fig. 4.15 Plot of A_{405} versus serum dilution for preimmune serum, antiserum and recirculated antiserum obtained from Half-Lop rabbit no. 1972 which was immunization using an ovalbumin-conjugate of peptide M. All of the A_{405} values shown have been corrected for background absorbance. The serum was recirculated through a column to which peptide M had been bound. The assay was carried out, using a plate coated with peptide M, as outlined in the legend for Fig. 4.1. Serum dilutions were assayed in triplicate. The error bars representing the SD value for each data point are smaller than the radius of the data point symbols.

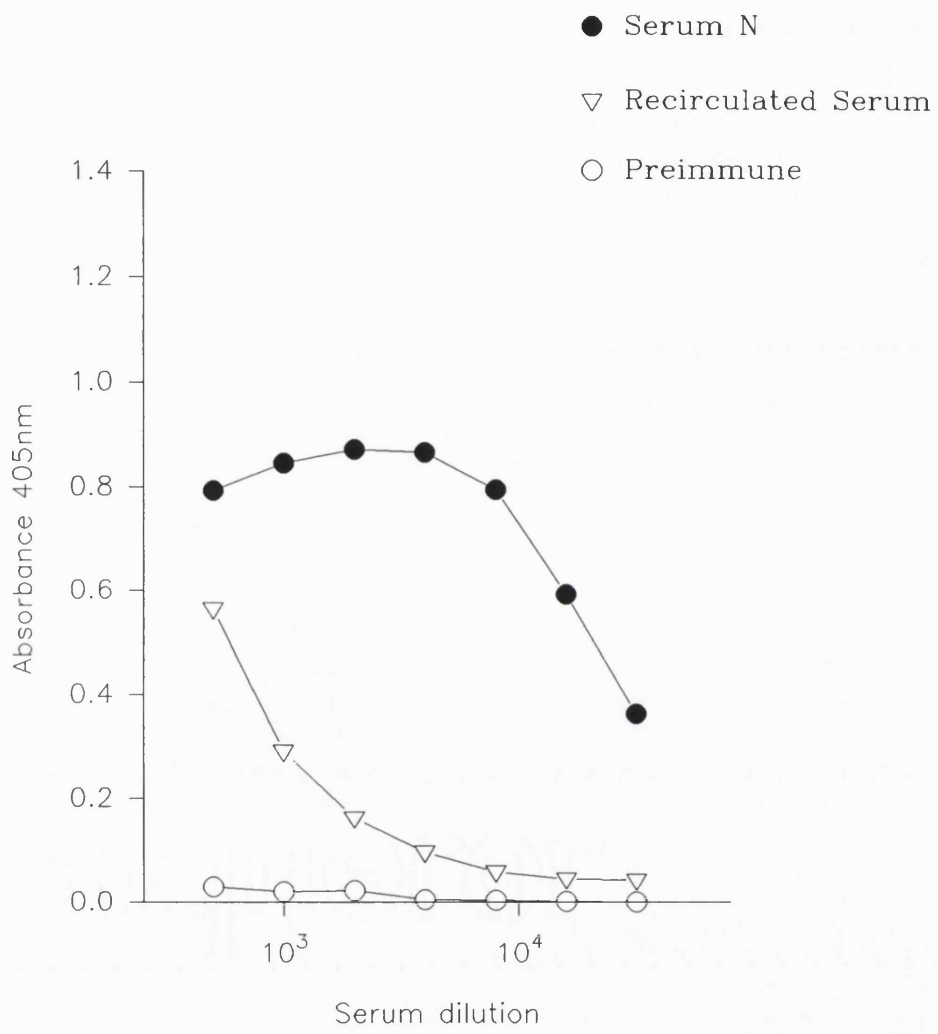

Fig. 4.16 Plot of A_{405} versus serum dilution for preimmune serum, antiserum and recirculated antiserum obtained from Half-Lop rabbit no. 1806 which was immunization using an ovalbumin-conjugate of peptide N. All of the A_{405} values shown have been corrected for background absorbance. The serum was recirculated through a column to which peptide N had been bound. The assay was carried out, using a plate coated with peptide N, as outlined in the legend for Fig. 4.1. Serum dilutions were assayed in triplicate. The error bars representing the SD value for each data point are smaller than the radius of the data point symbols.

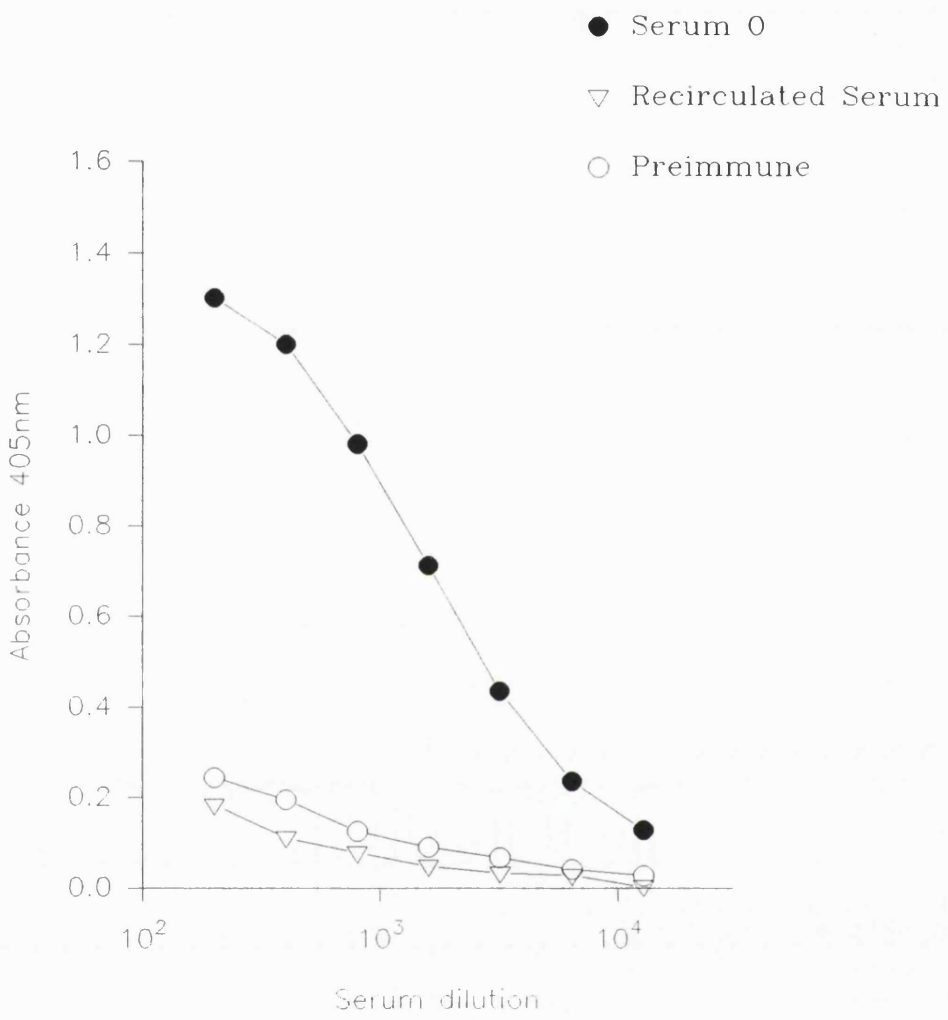

Fig. 4.17 Plot of A_{405} versus serum dilution for preimmune serum, antiserum and recirculated antiserum obtained from Half-Lop rabbit no. 2078 which was immunization using an ovalbumin-conjugate of peptide O. All of the A_{405} values shown have been corrected for background absorbance. The serum was recirculated through a column to which peptide O had been bound. The assay was carried out, using a plate coated with peptide O, as outlined in the legend for Fig. 4.1. Serum dilutions were assayed in triplicate. The error bars representing the SD value for each data point are smaller than the radius of the data point symbols.

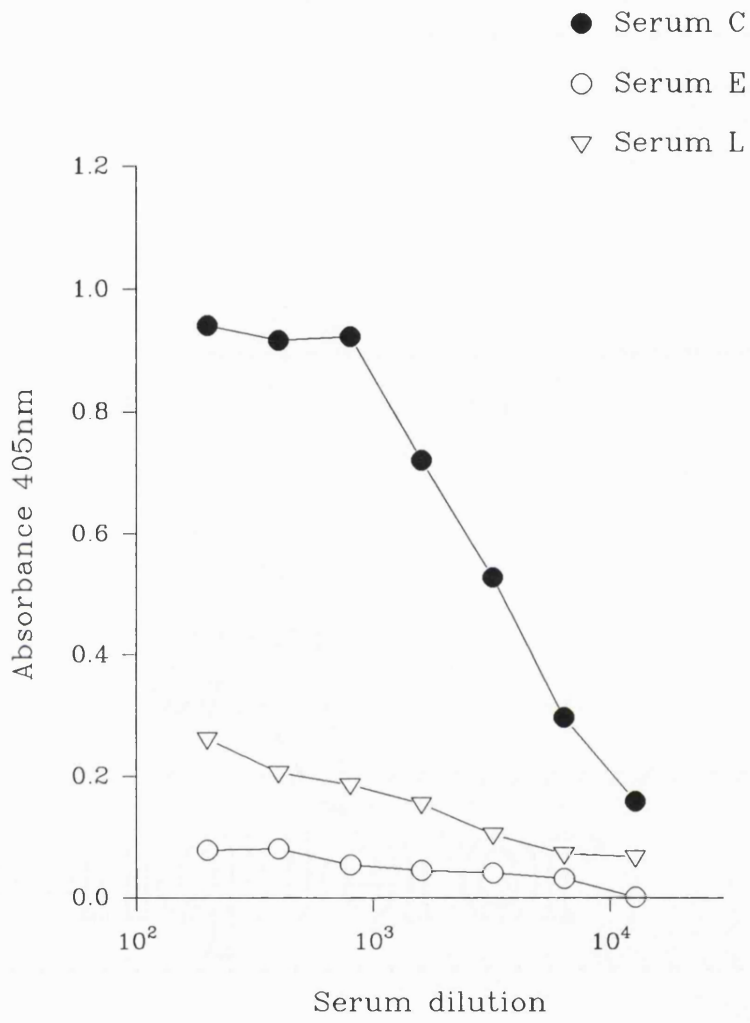

Fig. 4.18 Plot of A_{405} versus serum dilution for serum from rabbits no. 1753, 1805 and 1752 which were immunized using conjugates of peptides C, E, and L, respectively. All of the A_{405} values shown have been corrected for background absorbance. The assay was carried out, using a plate coated with peptide C, as outlined in the legend for Fig. 4.1. Serum dilutions were assayed in triplicate. The error bars representing the SD value for each data point are smaller than the radius of the data point symbols.

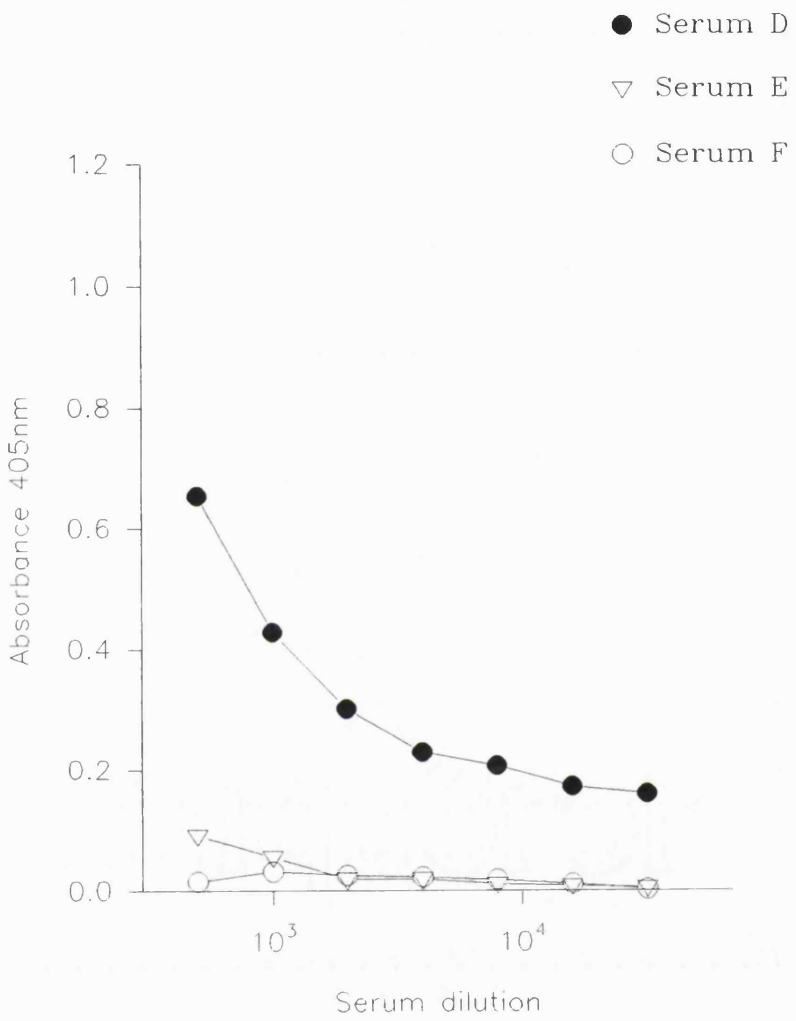

Fig. 4.19 Plot of A_{405} versus serum dilution for serum from rabbits no. 1804, 1805 and 1971 which were immunized using ovalbumin-conjugates of peptides D, E, and F, respectively. All of the A_{405} values shown have been corrected for background absorbance. The assay was carried out, using a plate coated with peptide D, as outlined in the legend for Fig. 4.1. Serum dilutions were assayed in triplicate. The error bars representing the SD value for each data point are smaller than the radius of the data point symbols.

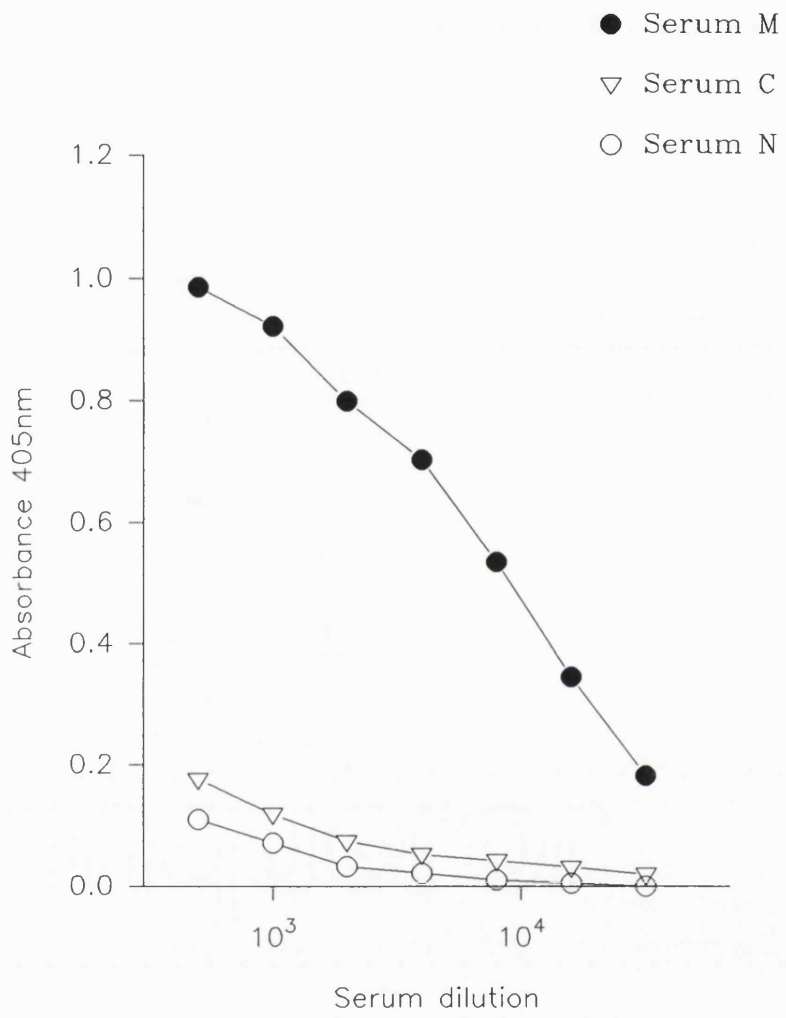

Fig. 4.20 Plot of A_{405} versus serum dilution for serum from rabbits no. 1972, 1753 and 1806 which were immunized using ovalbumin-conjugates of peptides M, C, and N, respectively. All of the A_{405} values shown have been corrected for background absorbance. The assay was carried out, using a plate coated with peptide M, as outlined in the legend for Fig. 4.1. Serum dilutions were assayed in triplicate. The error bars representing the SD value for each data point are smaller than the radius of the data point symbols.

Table 4.1 Table of estimated dilutions of serum, both prior to and following recirculation through a column containing the immunizing peptide, which showed binding to the peptide in ELISA which was half of the maximum value.

Antibody	Peptide carrier	Recirculated Serum Dilution	Antiserum Dilution
A	KLH	400	10,700
C	KLH	3,000	11,000
L	KLH	700	18,000
M	KLH	400	5,700
B	PPD	500	2,900
G	PPD	400	800
A	Ovalbumin	1,400	29,000
D	Ovalbumin	4,000	9,000
E	Ovalbumin	1,000	5,000
F	Ovalbumin	1,100	10,000
H	Ovalbumin	500	4,000
I	Ovalbumin	1,600	11,000
J	Ovalbumin	400	3,300
K	Ovalbumin	3,600	30,000
M	Ovalbumin	900	40,000
N	Ovalbumin	1,100	24,000
O	Ovalbumin	600	1,900

standard deviation (SD) from the mean A_{405} value at each serum dilution in these three plots 4.18-4.20 are within the data point symbol.

With peptide antigens examined, a consistently greater immune response was elicited on immunization of Half Lop rather than New Zealand white rabbits. The specific anti-peptide response elicted by immunization with the various KLH-coupled peptides was good (see Figs. 4.1-4.4 and Table 1). The anti-peptide titres obtained using ovalbumin conjugates were also high (see Figs. 4.7-4.17 and Table 1). However, antisera obtained from animals immunized with PPD conjugated peptides yielded a relatively poor immune response in ELISA versus peptide (Figs. 4.5 and 4.6 and Table 1).

The peptides synthesised show a broad range of immunogenicity estimated by the dilution at which the serum bound to the antigen with half maximum efficiency (see Table 1, column 4). This is most apparent for peptides conjugated to ovalbumin. Of these peptide M showed the greatest, and peptide O the least antigenicity. Peptides conjugated to KLH showed more uniform immunogenicity, with peptide L being the most apparently antigenic of these. Comparatively low immunogenicities were observed for the PPD conjugated peptide B and G. The anti-peptide titres for ovalbumin conjugate of both peptides A and M were much higher than those for their respective KLH conjugates (see Figs. 4.1, 4.4, 4.7, 4.15 and Table 1).

4.2.2 Antibody purification

The amount of peptide coupled to each affinity column was calculated following estimation of free sulfhydryl groups in each peptide solution, both before and after incubation with the column material, using the DTNB assay outlined in Section 2.10. The affinity columns contained peptide quantities in the range (0.3-1.5) μmoles. Assuming that one peptide molecule binds one IgG molecule, this allows individual columns to theoretically bind (45-225)mg IgG.

Peptide-specific antibody purification involving antibody elution using buffer

of either high or low pH resulted in recovery of anti-peptide activity in the range 20-73% (Table. 4.1). This recovery was estimated following ELISA against peptide for various dilutions of samples of the original antiserum and the purified antibody obtained from the purification procedure (see Fig. 4.21). The yield of anti-peptide activity varied greatly for different peptide-specific antibodies eluted under identical conditions (see Table. 4.2). This was also true for individual antibodies eluted at both high and low pH (see Table. 4.2, rows 2, 5 and 11). A combination of low pH and high salt concentration (0.2M glycine/HCl, 3M $MgCl_2$, pH 2.4) did not improve the recovery of anti-peptide activity (results not shown). However, elution of antibody in a more concentrated solution of chaotropic salt, 5M $MgCl_2$, allowed the recovery, in the case of certain antibodies, of more peptide-specific activity than obtained using low or high pH (Table 4.2).

Tables 4.3-4.5 show the observed relative reactivity of each antibody with its peptide and its intact polypeptide in both the denatured and native state, following its purification using elution at high pH, low pH and in 5MMgCl_2, respectively. Reactivity with peptide was estimated from the concentration of each purified antibody at which its binding to the peptide in ELISA with half the maximum value. Relative recognition of the intact denatured polypeptide was estimated from the concentration of each of the antibodies which yielded staining of denatured polypeptide of similar intensity in Western blots. Antibody binding to the native channel was compared in ELISA with purified Ca^{2+} channel for each antibody, at a concentration of 0.01mg/ml.

Antibodies B, D, E, J, K and N, purified in this way, all retained significant reactivity with both their intact native (Fig. 5.6 and 5.7) and denatured (Fig. 4.25) channel polypeptides (see Table. 4.4). Affinity-purified antibodies H and I, eluted in 5M $MgCl_2$, also recognized their intact skeletal muscle polypeptides. Antibody I retained similar reactivity with intact skeletal muscle L-type Ca^{2+} channel α_1 subunit in its native form (result not shown) to that which was evident in antiserum (see Fig. 5.4), while antibody H still reacted following affinity purification with a native (Fig. 7.5) and denatured skeletal muscle polypeptide (see Figs. 7.6 and 7.7). Furthermore,

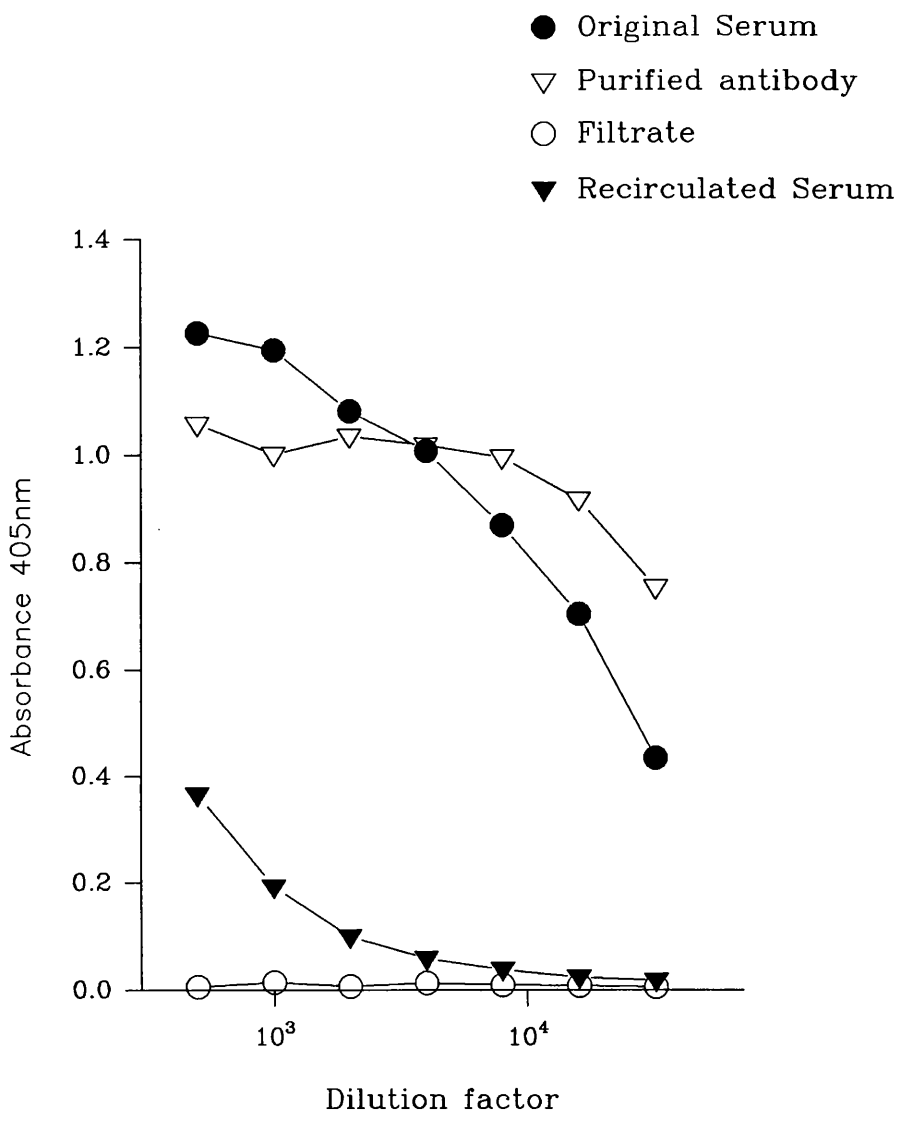

Fig. 4.21 Plot of A_{405} versus dilution factor of various fractions obtained during affinity purification of anti-peptide J antibodies from antiserum. All of the A_{405} values shown have been corrected for background absorbance. Protein concentration of undiluted fractions was as follows; serum (108 mg/ml), recirculated serum (65 mg/ml), filtrate (0.02 mg/ml) and purified antibody (3.8 mg/ml). The assay was carried out, using a plate coated with peptide J, as outlined in the legend for Fig. 4.1. Serum dilutions were assayed in triplicate. The error bars representing the SD value for each data point are smaller than the radius of the data point symbols.

Table 4.2 Table of the % recovery of peptide recognition for each antibody when eluted, during purification, under conditions of either low (0.2M glycine/HCl, pH 2.4) or high pH (50mM diethylamine, pH 11.3) or high salt (5M $MgCl_2$). The elution conditions, for each antibody, resulting in the greatest amount of retention of ability to recognize the intact protein, are given as the optimum elution conditions for that antibody.

Antibody	Low pH	High pH	5M $MgCl_2$	Optimum elution
A	-	36	-	High pH
B	40	30	43	5M $MgCl_2$
C	-	28	44	High pH
D	-	73	20	High pH
E	29	48	72	5M $MgCl_2$
F	48	-	-	Low pH
G	-	69	-	High pH
H	-	-	26	5M $MgCl_2$
I	-	-	45	5M $MgCl_2$
J	-	-	50	5M $MgCl_2$
K	20	24	55	5M $MgCl_2$
L	-	52	-	High pH
M	49	-	66	Low pH
N	-	44	63	5M $MgCl_2$
O	20	-	22	5M $MgCl_2$

Table 4.3 Table of relative reactivity of various purified anti-peptide antibodies eluted at pH 11.3 from their respective peptide columns. Relative reactivity with denatured protein was determined in Western Blots and with both peptide and intact skeletal muscle DHP receptor by ELISA.

Antibody	Peptide	Denatured protein	Native protein
A	+++	-	-
B	++	++	++
C	+++	++	+
D	+++	++++	++++
E	++	-	-
F	++	-	-
G	+++	-	-
K	+++	++++	++++
L	+++	+++++	+++
M	+++	++	-
N	+	-	-

Table 4.4 Table of relative reactivity of various purified anti-peptide antibodies eluted at pH 2.4 from their respective peptide columns. Relative reactivity with denatured protein was determined in Western Blots and with both peptide and intact skeletal muscle DHP receptor by ELISA.

Antibody	Peptide	Denatured protein	Native protein
B	+	+	+++
D	+	-	-
E	+++	++	++
M	++++	++	-
N	+++	++++	+++
O	++	-	-

Table 4.5 Table of relative reactivity of various purified anti-peptide antibodies eluted in 5M $MgCl_2$ from their respective peptide columns. Relative reactivity with denatured protein was determined in Western Blots and with both peptide and intact skeletal muscle DHP receptor was determined in ELISA.

Antibody	Peptide	Denatured protein	Native protein
B	+	++	+++
C	+++	+	+
D	++	+++	+++
E	+++	++	+++
H	+++	+++	-
I	+++	-	+
J	+++	+++	++
K	+++	+++	++++
L	++++	++	++
M	++++	-	-
N	+++	+++	+++
O	+	-	-

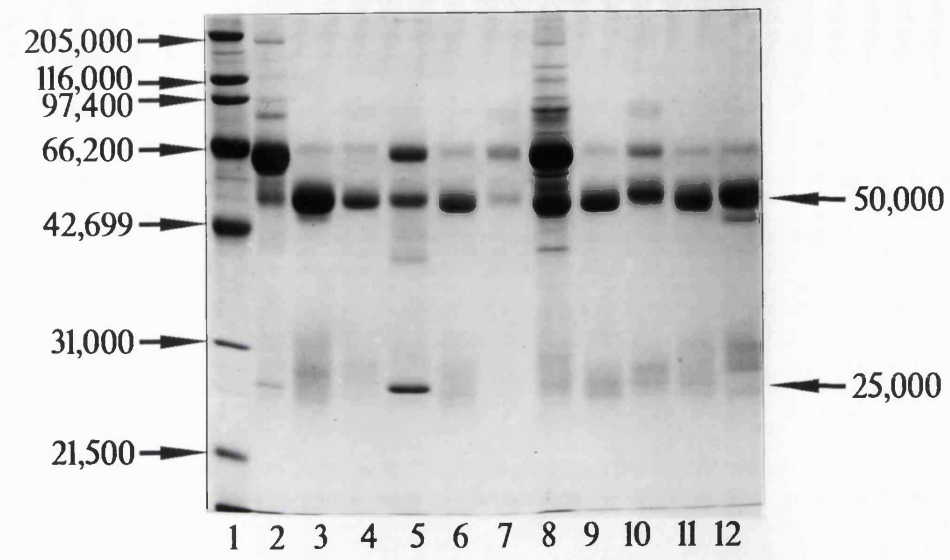

Fig. 4.22 SDS polyacrylamide gel of rabbit serum and antibodies (10-25μg) purified under conditions involving elution in either high or low pH. Samples were loaded onto a 10% (w/v) acrylamide gel as follows; molecular weight markers (BioRad) (lane 1), rabbit serum (lane 2) and purified antibodies A, B, C, D, E, K, J, L, M, and N, respectively, (lanes 3-12). The polypeptides were electrophoresed for 16h. at 12mA (constant current) and stained with Coomassie blue.

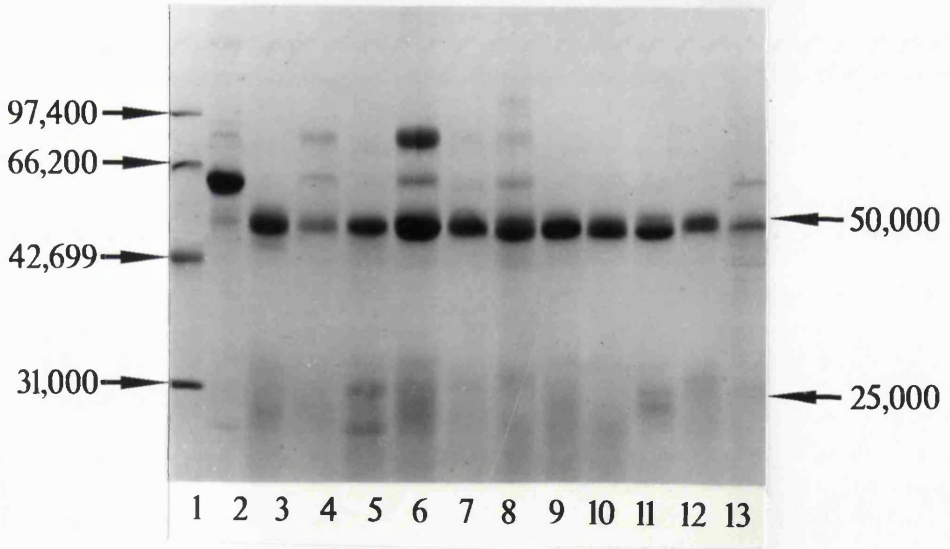

Fig. 4.23 SDS polyacrylamide gel of both rabbit serum and IgG and of antibodies (10-25μg) purified using the optimum elution conditions for each antibody. Samples were loaded onto a 10% (w/v) acrylamide gel as follows; molecular weight markers (BioRad) (lane 1), rabbit serum (lane 2), rabbit IgG (lane 3) and purified antibodies B, C, D, E, K, J, L, M, N and O (lanes 4-13). The polypeptides were electrophoresed for 16h. at 12mA (constant current) and stained with Coomassie blue.

although in some cases elution with 5M $MgCl_2$ yielded less IgG capable of recognizing peptide than did elution at high or low pH, the retention of ability to recognize the intact protein was superior (Tables 4.3-4.5). Indeed, when antibodies E and N were purified using elution at high pH and antibody D was purified using elution at low pH, good reactivity with peptide was recovered but the antibodies failed to bind to their intact denatured polypeptide in Western blots or to the purified DHP receptor in ELISA (Table 4.3 and 4.4).

In initial experiments, the purified antibody obtained, while constituting a large enrichment in IgG relative to serum albumin, still contained significant amounts of this latter protein (Fig. 4.22). During subsequent purifications, the volume of PBS used to wash the column, following both the recirculation of dilute serum and the elution of non-specifically bound protein, and also the volume of 10mM Na_2HPO_4, 800mM NaCl, pH 7.25 used in the latter elution, were increased. The former and latter wash volumes were adjusted from 6 to 16 ml and from 6 to 12 ml, respectively, while optimum elution conditions for each peptide-specific antibody (see Table 4.2) were used. The purity of the specific antibody fraction was thus greatly increased (Fig. 4.23).

4.2.3 Antibody characterization

(Reaction with denatured polypeptide)

T-tubule membranes were prepared from both rabbit and rat skeletal muscle, as outlined in Section 2.5.1, prior to their use in immunoblotting experiments. The specific activity of these t-tubule membranes, with respect to DHP binding, was estimated using Scatchard analysis of binding of PN200-110 to these membranes preparations to be 20.4 $\pm$ 9.0 pmol/mg membrane protein and 19.5 $\pm$ 8.6 pmol/mg membrane protein, respectively for the rabbit and rat t-tubules.

The appearance of a band corresponding to a protein having apparent M_r value of 174,000 in nitrocellulose immunoblots of rabbit skeletal muscle t-tubule membrane

proteins revealed recognition of the denatured 5-6 fold more abundant, truncated Ca^{2+} channel α_1 subunit (M_r value 174,000) by antibodies B, C, D, E, J, K (see Fig. 4.24). Immunoblotting with antibodies M and N produced a band corresponding to a protein of M_r 143,000 in these blots indicating binding of these antibodies to the denatured α_2 polypeptide (Fig. 4.24). Bands also appeared in most of the blot lanes corresponding to proteins having approximate M_r values of 100,000, 50,000 and 25,000. Their intensity is similar in lanes of t-tubules which were blotted together, namely, lanes 1-4, lanes 5-8, lanes 9-12, lane 13-14 and lane 15. However, each of these groups of lanes, which contained immunoblotted membranes from different purifications, reveal a pattern of intensity of staining of these bands.

Amongst the antibodies purified under optimal conditions, those raised against peptide L, corresponding to a region in the α_1 polypeptide C-terminus, were by far the most reactive, showing clear recognition of truncated α_1 in these blots at a concentration of 0.026μg/ml (Fig. 4.24). Most of the remaining antibodies showed binding of similar strength to their polypeptide at concentrations in the range 1.4μg/ml (antibody D) to 6.9μg/ml (antibody M).

The anti-peptide antibodies produced using peptides A, G, F and O as antigen, all showed reactivity with immunizing peptide, which for A and F, was strong (Figs. 4.1, 4.6, 4.10 and 4.17). However, they failed to recognize these peptide sequences in their intact channel polypeptides in Western blots (see Fig. 4.24).

Immunoblots of rabbit and rat t-tubules membrane proteins using purified antibodies and AEC detection (see Fig. 4.25) revealed that all antibodies already shown to recognize the truncated form of rabbit skeletal muscle α_1 subunit (see Fig. 4.24) identified two bands of similar intensity having apparent M_r values of 212,000 and 174,000. This indicates that in addition to binding to truncated α_1, these antibodies also react with the full-length form of the α_1 subunit of rabbit skeletal muscle L-type Ca^{2+} channel. Bands also appeared in each of these blot lanes, which were much more intense in those containing rabbit membranes, corresponding to proteins having approximate M_r values of 50,000 and 25,000. In these blots, similarly strong staining of α_1 was obtained with antibodies D (recognizing a sequence in the

IIS6-IIIS1 loop), L (binding in the α_1 C-terminus) and K (specific for the putative EF-hand domain, C-terminal to the IVS6 domain). J, which recognizes the large domain C-terminal to IVS6, reacted slightly less strongly, while staining with antibody C (specific for the entire IIS4-IIS5 loop) was barely detectable when used at 11μg/ml (Fig. 4.25). Antibody N (recognizing an internal α_2 domain) reacted with similar strength with α_2 (result not shown) as did J with α_1.

The relative reactivities of the various antibodies with the rabbit skeletal muscle channel polypeptides as revealed by immunoblotting using both techniques (i.e. AEC and ECL detection) compare very closely (see Figs. 4.24 and 4.25). A comparison of primary antibody concentrations necessary to produce strongly staining bands in each case revealed that the technique using the ECL detection system is about four times more sensitive than the AEC method (Figs. 4.24 and 4.25) e.g. antibody D (recognizing a region in the II-III loop) incubated with nitrocellulose at 1.4μg/ml and with ProBlott at 6.4μg/ml, yielding bands of comparable intensity. In Fig. 4.25, bands of comparable intensity, having apparent M_r values of 212,000 and 174,000, are obtained with each positive antibody in the lanes containing rat and rabbit membrane proteins. Additionally, the intensity of both the band indicating recognition of truncated α_1 and that indicating binding to its full-length form appeared to be the same within each rat and each rabbit membrane lane.

The apparent M_r values of the rabbit t-tubule polypeptides identified by all of the antibodies specific for sequences in α_1 are approximately 210,000 and 174,000. These antibodies also react with two proteins in rat t-tubule membranes having apparently identical M_r values of 210,000 and 174,000 (Figs. 4.24 and 4.25). The α_2 polypeptides recognized by antibodies M in rabbit (Fig. 4.24) and antibody N in both rat (result not show) and rabbit t-tubules have the same apparent M_r value of 143,000 (Fig. 4.24).

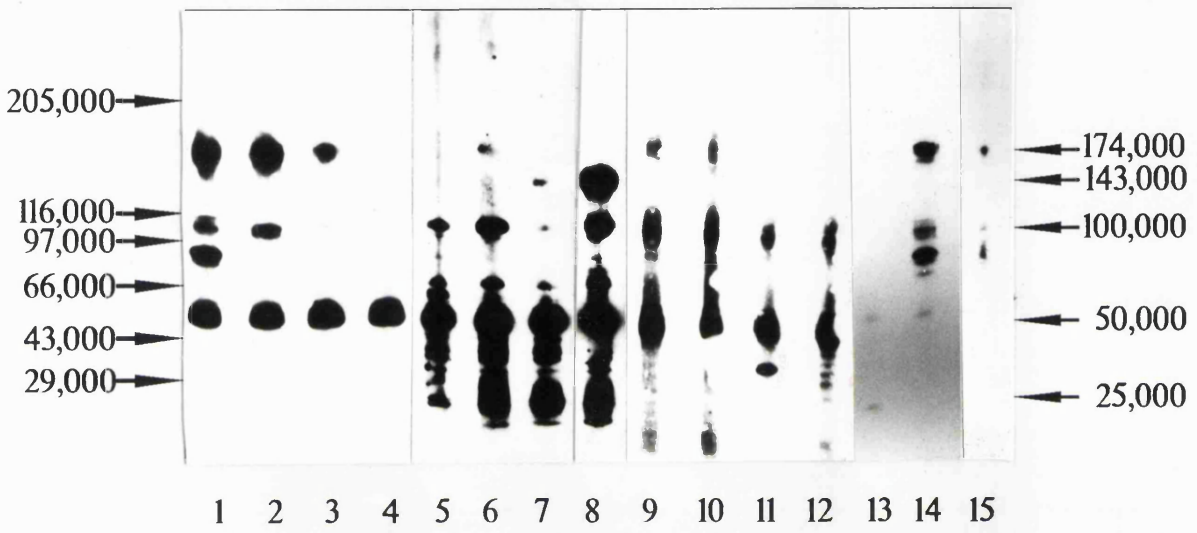

Fig. 4.24 Immunoblots of rabbit skeletal muscle t-tubules membrane proteins using purified antibodies. The protein components of t-tubules (50μg/lane) and molecular weight markers were separated by SDS/PAGE on (4-12)% gels at 50V constant voltage for 16h. Immunoblotting was carried out as described in Section 2.6.4, using ECL detection. Primary antibodies were incubated with blot lanes 1-15, in the following order: D (1.4μg/ml), L (0.03μg/ml), L (0.003μg/ml), A (4μg/ml), G (5μg/ml), B (2μg/ml), M (7μg/ml), N (2μg/ml), C (4μg/ml), E (4μg/ml), F (4μg/ml), control IgG (2μg/ml), O (1μg/ml), K (2μg/ml) and J (4μg/ml). While the blot bands were detected using autoradiography the molecular weight markers were photographed separately. Therefore only marker positions are indicated using arrows.

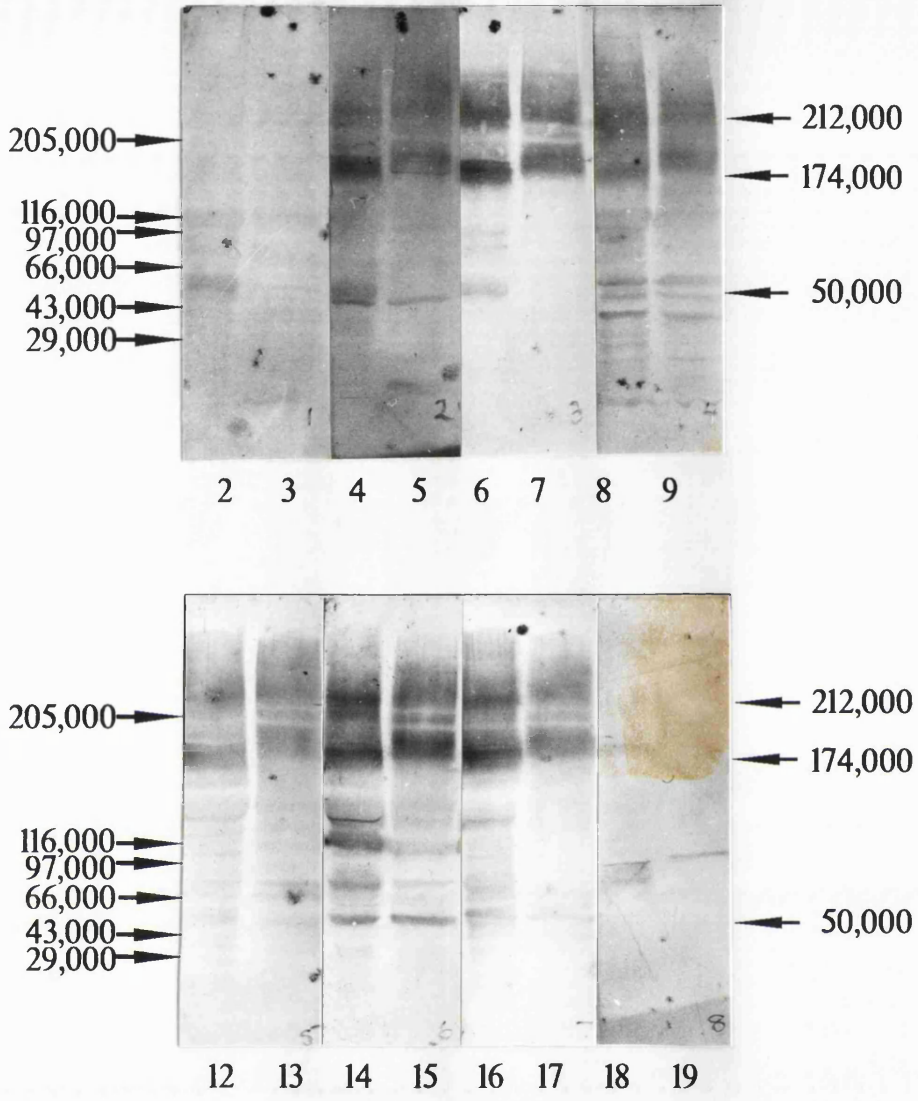

Fig. 4.25 Immunoblots of rabbit and rat t-tubule membrane proteins using purified antibodies. Gel samples were loaded as follows: lanes 1, 10, 11 and 20 molecular weight markers, lanes 2, 4, 6, 8, 12, 14, 16 and 18, rabbit t-tubule membranes (50μg) and lanes 3, 5, 7, 9, 13, 15, 17 and 19, rat t-tubule membranes (50μg). Immunoblotting was carried out using both control and test antibodies, as outlined in Section 2.6.4 using AEC detection. Antibodies were reacted with the blots at the given protein concentrations: control IgG (14μg/ml) (lanes 2 and 3), B (18μg/ml) (lanes 4 and 5), D (6.4μg/ml) (lanes 6 and 7), E (17μg/ml) (lanes 8 and 9), K (13μg/ml) (lanes 12 and 13), J (8.5μg/ml) (lanes 14 and 15), L (5.5μg/ml) (lanes 16 and 17) and C (11μg/ml) (lanes 18 and 19). Because of the different detection system for blot bands and markers these were photographed separately. Therefore only marker positions are indicated using arrows.

4.3 DISCUSSION

4.3.1 Antibody production

ELISA versus peptide revealed that all the immunization procedures outlined above were successful in generating antibodies which recognized the synthetic peptide (see Figs 4.1-4.17). The specificity of recognition of its particular peptide by each antiserum is suggested by the extremely low reactivity with peptide of preimmune serum from each of the immunuzed rabbits. This is also supported by the observation that antibodies produced using any one of the synthetic peptides failed to show reactivity with other peptides synthesized that was greater than that observed for preimmune serum (Figs. 4.18-4.20). However, more convincing evidence for the peptide specificity of the antiserum is provided by the observed removal of the majority of the reactivity of the serum with the peptide following its recirculation through a column containing this peptide (Figs. 4.1-4.17 and Table 1).

It appears that peptides conjugated to ovalbumin in general produced a better immune response to peptide than was obtained when KLH was used as carrier (see Table. 1). This is also supported by the the larger anti-peptide titre observed following immunization of rabbits with peptide A and M which had been coupled to ovalbumin, compared with the anti-peptide titre elicited by the KLH conjugates of these peptides.

The use of ovalbumin conjugates was considered undesirable in the production of the antiserum because the presence of polyclonal antibodies recognizing various regions/domains of this carrier protein was seen to cause cross-reactivity of the antiserum with milk and other proteins which were used to block nonspecific binding sites on the nitrocellulose and Problott membranes. High background was obtained in Western blots using antibodies produced in response to ovalbumin-coupled peptides D, E, J, K and N (see Fig. 4.25). The specific reactivity of the anti-peptide antibodies with the domain on the channel against which they were raised may not be clearly observed using this technique. Therefore, in the case of peptides B and G, the

modified immunization procedure for PPD-peptide conjugates was employed. Despite the low anti-peptide titres elicited by these conjugates, antibody B produced in this way recognized the Ca^{2+} channel α_1 subunit in Western blots (Figs. 4.24 and 4.25) and in immunocytochemistry in unfixed frozen sections of rabbit, rat, mouse and human muscle (see Figs. 5.5, 5.8 and 5.9). These antibodies also reacted with the purified DHP receptor from rabbit skeletal muscle in ELISA (Figs. 5.1 and 5.6).

The procedures for initial immunization and boosting were not modified in any way during the course of this work. However, in the absence of significant immune response to peptide as revealed in ELISA, another identical booster injection was administered, at least 4 weeks subsequent to the first. The success of this step in improving the elicited response generally depended on two factors, the time span between the relevant boost and the initial immunization and the apparent antigenicity of the peptide. The shorter the time span between the boost and the original immunization date the larger the subsequent increase in the anti-peptide antibody titre of the serum (results not shown). Similarly, the more apparently antigenic a peptide, the greater the effect of a boost on the amount of relevant antibody produced by the animal (results not shown). However, the more immunogenic peptides elicited the highest serum anti-peptide titres which therefore did not require frequent boosting (see Figs. 4.1-4.4 and 4.7-4.17 and Table 1), while immunization with peptides of lower antigenicity did not lead to production of significant levels of antipeptide antibodies, even following more than one successive boost. This indicates that the level of the immune response depends on the immunogenicity of the peptide antigen rather than the quantity of the antigen present.

4.3.2 Monitoring antibody production

Antibodies which will react with a peptide in ELISA may be elicited entirely by a region or regions in the peptide, or by domains on both the peptide and the carrier protein. The latter is evidenced by observed reactivity, in immunoblots, of affinity purified anti-peptide antibodies, which were produced using ovalbumin

conjugates, with the ovalbumin molecular weight marker. Thus the low antipeptide titres observed using PPD conjugates may result because the population of antibodies reacting with the peptide consists solely of antibodies in the above, former category. KLH and ovalbumin conjugates were expected to produce antibodies from both categories, thus eliciting a larger anti-peptide response, as monitored in ELISA (Figs 4.1-4.4 and 4.7-4.17).

Immunization using PPD-peptide B conjugate produced a low concentration of peptide-specific antibody as revealed by ELISA versus peptide (Fig. 4.5) and by protein estimation following affinity purification (results not shown). However, a significant proportion of these antibodies recognized the native channel α_1 subunit (see Figs. 5.1 and 5.6). On the other hand, immunization using a KLH-peptide M conjugate caused a much higher anti-peptide response (Fig. 4.4 and Table 1) but only a small fraction of the antibodies produced reacted with the intact α_2 subunit, which was recognized by the antibodies only after its denaturation (Fig. 4.25). Immunization with an ovalbumin-peptide M conjugate elicited an even higher immune response to peptide (Fig. 4.15 and Table 1), but none of these antibodies showed any reactivity with either the denatured or the native intact protein (results not shown). Thus, it is clear that strong recognition of peptide in ELISA, by an antibody, does not necessarily imply strong recognition of the intact protein.

Amongst the most apparently immunogenic peptides, L and K correspond to regions located in the C-terminus of the α_1 polypeptide, while M and N correspond to the N-terminus and a proposed internal domain of α_2, respectively. L and M are therefore likely to have the most conformational freedom of all the peptides synthesized, while N may have similar random structure particularly if the α_2 polypeptide is entirely extracellular. However, K is predicted to have α helical secondary structure. Interestingly, peptide O, corresponding to the N-terminus of the δ polypeptide, which might be expected to possess similar conformational freedom to M and L, appeared to have relatively low immunogenicity (Fig. 4.17 and Table 1). The other peptides, which are located in closer proximity to putative transmembrane domains in the α_1 subunit than K and L (either on extra- or

intracellular loops, or C-terminal to IVS6), have comparable immunogenicities. These were lower than those for L, K, M and N and greater than that of O. This finding may stem from the more stable, ordered secondary structure of these peptides. Both IS4 and IVS4 peptides, B and G, respectively, appeared to be the least immunogenic of the peptides synthesized, possibly because they are amphipathic and have predicted ordered α helical secondary structure.

4.3.3 Antibody purification

A major problem with affinity purification of polyclonal antibodies is the resultant loss of a significant amount of the specific antibody activity. As with antiserum, antibodies were characterized following purification initially using ELISA against the synthetic peptide, indicating the level of peptide recognition present. Antibody purification involving antibody elution using buffer of either high or low pH resulted in recovery of variable amounts of such activity, in the range 20-73% (Table. 4.1). This loss of activity may be due to the fact that the pH elution conditions necessary to disrupt antigen-antibody interactions have an irreversible effect on the tertiary structure of some of the antibody molecules. In support of this hypothesis, insoluble protein material was observed to accumulate near the top of each column, while column flow rates diminished rapidly with subsequent uses. This insoluble protein apparently results from aggregation of IgG molecules, probably via interactions between hydrophobic regions of the proteins, exposed as a result of unfolding. Following elution and rapid neutralization of those protein molecules remaining soluble, some of these may not regain their native structure and hence their affinity. A further contributor to the observed loss of antigen binding activity is the possibility that the antibody molecules with greatest avidity for the antigen, i.e. those binding the peptide on the solid support most tightly, may not be removed under the elution conditions used, and are thus selected out by the procedure. Some protein is also lost during IgG concentration, due to trapping in the Centricon 30 membranes (Amicon) used for this step.

In an attempt to improve recovery of antibody activity the elution conditions were altered. However, a combination of low pH and high salt concentration (0.2M glycine/HCl, 3M $MgCl_2$, pH 2.4) did not improve recovery of anti-peptide activity (results not shown). However, high salt concentrations are known to disrupt protein-protein interactions. This results from the preferential binding, at these high concentrations, of these ions by regions of the protein which at lower salt concentrations are stabilized by binding other proteins. Therefore, elution of antibody in a more concentrated solution of chaotropic salt, 5M $MgCl_2$, was attempted. This allowed the recovery, in the case of certain antibodies, of more peptide-specific activity than was obtained using low or high pH (Table 4.5). Antibodies B, D, E, J, K and N, purified in this way, all retained significant reactivity with both their intact native and denatured channel polypeptides (Table. 4.5). Using the same elution conditions antibodies H and I also retained reactivity with intact skeletal Ca^{2+} channel α_1 polypeptides. H apparently reacted with its polypeptide in both the native (Fig. 7.5) and denatured (see Figs. 7.6 and 7.7) states and I recognized the native form of the skeletal muscle L-type channel α_1 subunit (Fig. 5.4). Furthermore, although in some cases elution with 5M $MgCl_2$ yielded less IgG capable of recognizing the peptide than elution at either high or low pH, the retention of ability to recognize the intact protein as revealed in immunoblots and immunocytochemistry was superior (Tables 4.3-4.5).

This high salt elution, thus appears to have a more reversible effect on the structure of the IgG molecules. Unlike the columns eluted in high or low pH, insoluble protein material did not accumulate at the top of columns eluted with 5M $MgCl_2$. This protein aggregation was either prevented by presence of the salt or does not occur because the IgG molecules were not unfolded fully by the salt solution. Whether one or both of these occur, a greater number of IgG molecules are eluted from the column, under these conditions, which subsequently regain their recognition of the intact protein and therefore, their native conformation.

Good purity was obtained for antibodies following their purification according to the protocol involving use of substantial volumes of PBS and 10mM Na_2HPO_4,

800mM NaCl, pH 7.25 buffers for column washing (16ml) and of optimum elution conditions for each peptide-specific antibody (see Table 4.1).

4.3.4 Antibody characterization (Reaction with denatured polypeptide)

The particular technique of Western blotting using nitrocellulose outlined in Section 2.6.4 only revealed antibody recognition of the 5-6 fold more abundant, truncated α_1 polypeptide (see Fig. 4.25). Therefore, a different blotting technique was necessary to detect both forms of α_1. The variability of the ECL detection method and the frequent presence of high background in nitrocellulose blots, necessitated the development of a different blotting procedure and the use of a different detection system, which were both more reproducible and could detect low amounts of the full length form of the α_1 polypeptide.

Western blotting, carried out as described in Section 2.6.4, using ProBlott membranes with the AEC detection system, allowed detection of the full-length form of the Ca^{2+} channel α_1 subunit. As shown in Fig. 4.26, all antibodies already shown to recognize the truncated form of rabbit skeletal muscle α_1 subunit (see Fig. 4.25) also recognized the 212kDa species of α_1. The relative reactivities of the various antibodies with the rabbit skeletal muscle channel polypeptides as revealed by immunoblotting using both techniques (i.e. AEC and ECL detection) compare very closely (see Figs. 4.25 and 4.26). A comparison of primary antibody concentrations necessary to produce strongly stained bands in each case revealed that the technique using the ECL detection system is about four times more sensitive than the AEC method (Figs. 4.25 and 4.26) e.g. antibody D (recognizing a region in the II-III loop) incubated with nitrocellulose at 1.4μg/ml and with ProBlott at 6.4μg/ml, yielded bands of comparable intensity.

Using AEC, similarly strong staining of α_1 was obtained with antibodies D, L (binding in the α_1 C-terminus) and K (specific for the putative EF-hand domain, C-terminal to the IVS6). J (recognizing the large domain C-terminal the IVS6) reacted

slightly less strongly, while staining with antibody C (specific for the entire IIS4-IIS5 loop) was barely detectable when used at 11μg/ml. Antibody N (recognizing an internal α_2 domain) reacted with similar strength with α_2 (result not shown) as did J with α_1. Interestingly, each of the antibodies exhibited very similar reactivity with both the rat and rabbit proteins at the concentrations used. These results indicate that the L-type channels found in the skeletal muscle of both rat and rabbit have identical or very similar sequences in the regions recognized by the antibodies. The similarities of these particular domains in proteins from two different species which have an identical function suggests that these particular domains are important for the function of this protein.

All the antibodies reaised against intracellular domains of the α_1 polypeptide bind to the intact denatured polypeptide in immunoblots. The failure of antibodies A, G, F and O to recognize their peptide domains in intact denatured channel polypeptides in Western blots (see Fig. 4.24) may arise from a number of factors. The population of antibodies which recognize peptide alone may constitute those elicited by the exposed end of the peptides, but perhaps not against the middle regions of the peptide. It is possible that the failure to produce antibodies that bind to the intact channel using these particular synthetic peptides as antigens is due to the fact that these peptides do not constitute part of epitopes in the intact polypeptides i.e. the peptides are not immunogenic (except for their termini). This may be possible for peptide G is predicted to be located in the membrane having ordered α helical secondary structure. However, the failure of the more apparently antigenic peptides A and F (proposed to be located on extracellular loops of α_1) and O (constituting the predicted exofacial *N*-terminus of δ) to produce antibodies which recognized their denatured channel polypeptides suggests that these domains in the channel corresponding to the sequences of these peptides also have ordered secondary and/or tertiary structure.

With regard to the background observed in both the nitrocellulose and Problott immunoblots, strong bands having apparent M_r values of 50,000 and 25,000 are present in blots probed with purified antibodies whether or not binding of primary

antibody to denatured channel polypeptide is observed. The bands therefore correspond to the heavy and light chains of rabbit IgG present in the rabbit t-tubule membrane preparation, since they result from reactivity of the anti-rabbit secondary antibody with these rabbit IgG polypeptides. The appearance of fainter bands of equivalent M_r values in blot lanes containing rat t-tubule membrane proteins are due to weak reactivity of anti-rabbit IgG second antibody with both the heavy and light chains of endogenous rat IgG (see Fig. 4.25). In the ECL blots, the variable intensity of these bands between lanes of rabbit t-tubules from various purifications, which were immunoblotted on different days may result from different quantities of endogenous IgG in these preparations (see Fig. 4.24). It is also possible that there was some variability in the amount of protein transferred from the gel lanes during the blotting on different days.

Since the rabbit t-tubules were prepared in the absence of protease inhibitors, it was thought possible that failure to detect the 212,000 form of the α_1 subunit in immunoblots using ECL detection (Fig. 4.25) stemmed from its proteolytic degradation. However, the detection of this band in the Western blots for which the AEC detection method was used (Fig. 4.26), indicates that degradation of the 212,000 form of the α_1 subunit did not occur during preparation of the rabbit t-tubules. This conclusion is strengthened by the comparable intensities and staining patterns exhibited by both rabbit and rat t-tubules, the latter having been prepared in the presence of protease inhibitors (Fig. 4.26). Additionally, the proportions of α_1 present in the full length and truncated forms appeared to be the same in both the rat and rabbit membranes. Moreover the two size-forms of α_1 in both species were apparently identical. In comparison to these findings, Brawley and Hosey (1992) reported identification of a single 165,000 polypeptide present in t-tubule membranes, in immunoblots, using an antipeptide antibody which recognizes the same region of the II-III loop of the α_1 polypeptide as antibody D. This polypeptide corresponded to the truncated form of the L-type Ca^{2+} channel α_1 subunit. The differences in sensitivities of the immunoblotting techniques for detection of the large form of α_1 may be due to poorer transfer of this polypeptide onto the nitrocellulose membranes compared to

the ProBlott membranes.

The recognition by each antibody of its domain in the relevant denatured channel polypeptides in both the rat and rabbit skeletal muscle Ca^{2+} channel. It can be concluded from these findings that the α_1 subunit of the L-type Ca^{2+} channels found in both rat and rabbit skeletal muscle t-tubules are very similar in size. They both appear to undergo posttranslational proteolytic modification in the same region in their respective primary structure. Additionally, the ratio of the two size-forms of the polypeptide, present in the t-tubular system, appear to be the same for both species. This demonstration that modification of α_1 occurs in rat as well as rabbit skeletal muscle leads to the proposal that modification of this channel subunit is a more widespread phenomenon, at least, in mammalian species and that it is important for the voltage sensing function of the channel in mammalian muscle.

CHAPTER 5

ANTIBODY RECOGNITION OF THE INTACT PROTEIN

5.1 INTRODUCTION

5.1.1 Location of L-type Ca^{2+} channel in skeletal muscle

In skeletal muscle, both t-tubule Ca^{2+} channels and SR calcium release channels are now known to be concentrated in the junctions between these two membrane systems (Block *et al.*, 1988; Flucher *et al.*, 1990). Freeze-fracture or negatively stained images of the junctions have shown regular chequerboard arrays of junctional "feet" that protrude into the cytosol from the SR membrane (Block *et al.*, 1988). These feet structures have been identified as the SR Ca^{2+} release channels (Wagenknecht *et al.*, 1989), and it is assumed that they represent the cytosolic domain of the SR channel. Intramembranous particles were observed in a similar chequerboard array of square clusters in the t-tubule membrane (Block *et al.*, 1988). This biochemical and morphological evidence suggests that the t-tubule Ca^{2+} channels and SR Ca^{2+} release channels are organized in complementary arrays. The L-type Ca^{2+} channels are thus located in the regularly spaced triads in the invaginating transverse-tubule (t-tubule) system of the plasmalemma, which in mammalian muscle, is located at the interface between the A band and the I band and extends to the cell interior. This system ensures that the Ca^{2+} channels are located throughout the cell interior in a regular pattern in order to mediate uniform contraction throughout the length of the muscle cell.

5.1.2 Binding studies of antibody with the native channel structure

Prior to their use in functional studies it was necessary to establish which antibodies would react with the intact native channel. Therefore, ELISA was carried

out (as described in Section 2.6.3), versus DHP receptor, purified, as outlined in Section 2.5.3, from rabbit skeletal muscle membranes. The receptor complex was adsorbed to the plate, and was maintained at pH 7.2 until after the second antibody was bound to the receptor. Under these conditions, the channel complex is presumed to retain its native conformation. The primary antibody consisted either of dilutions of antiserum or of purified antibody.

Antibody binding to the protein *in situ* was also investigated. This study was performed to confirm the specificity of the antibodies, which had been shown to recognize the relevant channel polypeptide in Western blots and, in some cases, to recognize the purified receptor in ELISA (Section 5.2.1). It was also important to ascertain whether or not the antibodies which failed to recognize a channel subunit in these tests, might nonetheless give a staining pattern typical of the channel when incubated with muscle sections. Species cross reactivity could also be examined using this approach for species where t-tubules for blotting were not available (human and mouse). Antibody binding to the protein *in situ* was examined using the immunofluorescence microscopy technique outlined in Section 2.7., and frozen muscle sections. The latter were fixed by air drying. It is not clear to what extent the air drying of such sections damages membrane proteins. However, it is known that fixation and paraffin processing destroys some cell surface antigens, while this can be avoided by rapid freezing and cryostat sectioning of tissue (as carried out in Section 2.7.1), prior to immunostaining (Jones and Gregory, 1989).

Only antibodies which recognize the native rabbit skeletal muscle protein are useful for tertiary structure and functional studies of this protein. Thus the knowledge that the antibodies produced as described in Section 2.6.1 recognized the rabbit channel and, perhaps more importantly, the channels of other species (rat, mouse and human) was vital to the present study. The latter information was necessary because having been raised in rabbit, complications in immunocytochemical studies of rabbit tissues may result using these antibodies. As previously observed, endogenous rabbit IgG appears in the t-tubule preparations used for Western blotting (see Figs 4.24 and 4.25). The presence of endogenous IgG would cause high background in

immunocytochemical studies of rabbit tissues due to binding of anti-rabbit second antibody. Use of rat or mouse tissue for immunocytochemical, tertiary structural and functional studies may allow this problem to be avoided, while the tissue is more readily available and its use more economical.

A further point of interest concerns the lack of knowledge of the amino acid sequence of any skeletal muscle Ca^{2+} channel α_1 subunit other than those from both rabbit and carp. The fact that these particular sequences are very similar, although they originate from two very diverse species, suggests that this channel polypeptide is highly conserved in all species. This assumption was evaluated for the other mammalian species rat, mouse and human, in the regions of the polypeptide recognized by the anti-peptide antibodies, by probing these domains with the antibodies.

5.2 RESULTS

5.2.1 Reaction with the intact native protein

ELISA versus purified DHP receptor

The specific activity of the DHP receptor preparations were estimated to be 0.91 nmol [^{3}H](+)PN200-110 binding sites per mg protein. Additionally, SDS/PAGE revealed a pentameric subunit composition corresponding to the α_1, α_2, ß, γ and δ polypeptides of the rabbit skeletal muscle L-type Ca^{2+} channel.

Figs. 5.1 to 5.5 show the results obtained from ELISA experiments versus the purified DHP receptor, carried out using dilutions of primary antibody in antiserum and preimmune serum from the immunized rabbit. Immune sera D, E, K, L and to a lesser extent N showed greatest reactivity with the native channel showing significantly more binding than their respective preimmune sera at 1/1000 dilution. Serum B, C and J appear more reactive than their preimmune sera only at 1/100

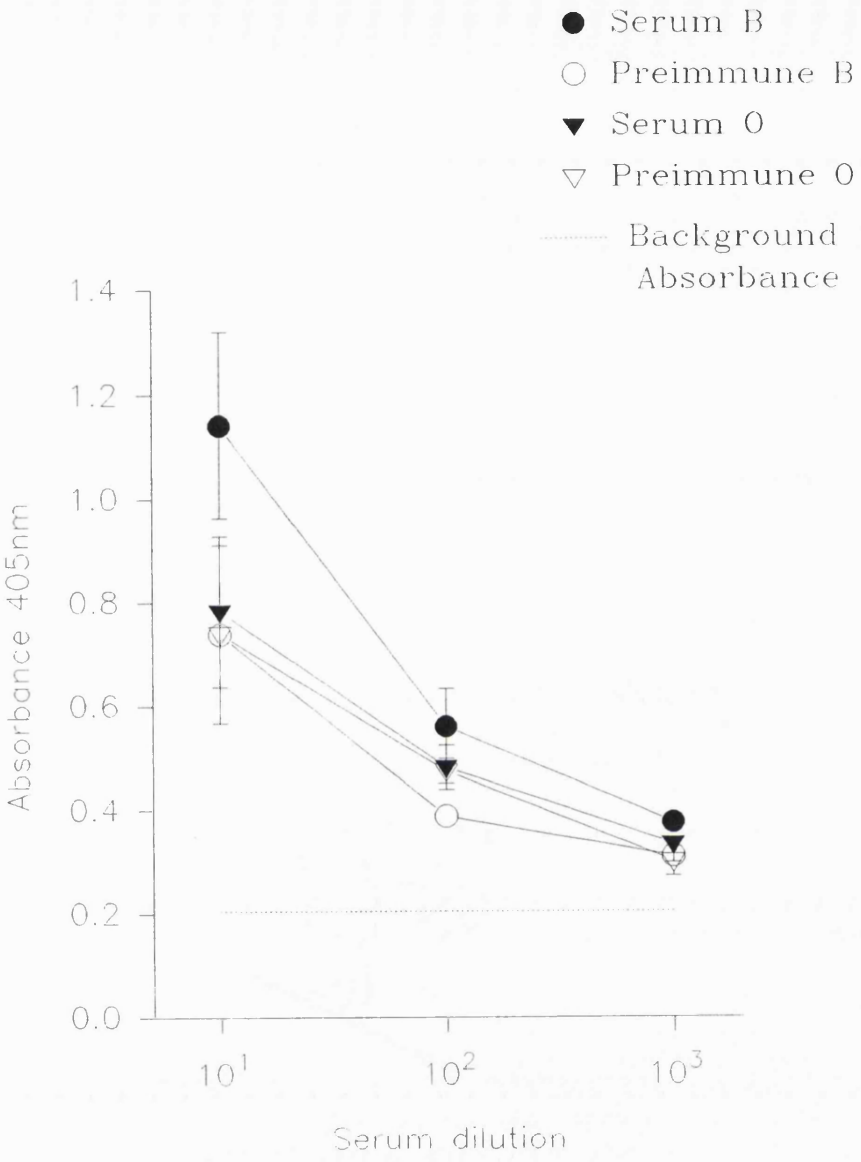

Fig. 5.1 Plot of A_{405} versus serum dilution for preimmune serum obtained from rabbits no. 1501 and 2078 and antiserum obtained following their immunization with ovalbumin-conjugates of peptides B and O, respectively. The background absorbance is also indicated in the plot. Maxisorp microtiter plates were coated with DHP receptor by incubation overnight at 4°C with a solution of purified rabbit skeletal muscle DHP-receptor (140 ng/well) (purified as outlined in Section 2.5.3) in PBS containing 0.0025% (w/v) digitonin. The remaining steps were carried out at 20°C, as outlined for ELISA versus synthetic peptide. Serum dilutions were assayed in triplicate. Error bars representing SD values are shown where they are larger than the radius of the data point symbol.

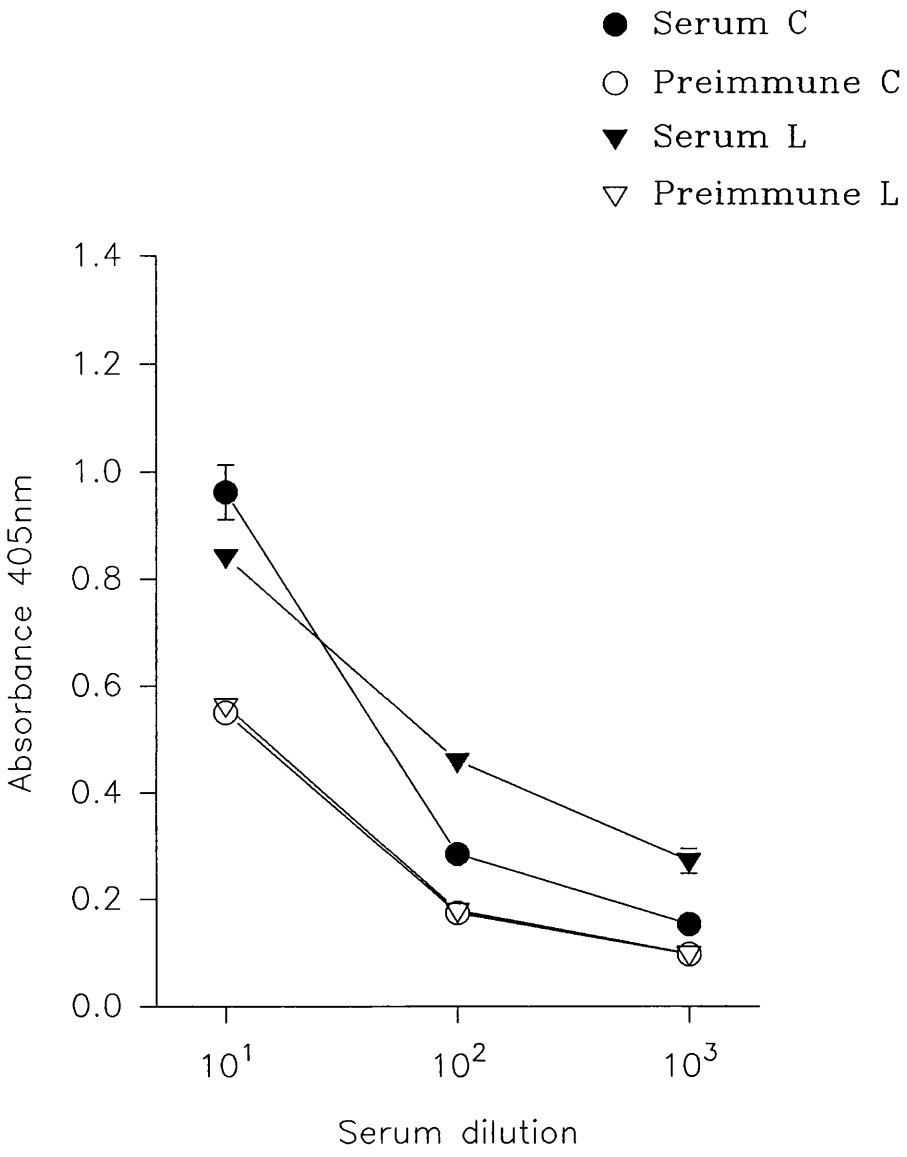

Fig. 5.2 Plot of A_{405} versus serum dilution for preimmune serum obtained from rabbits no. 1753 and 1752 and antiserum obtained following their immunization with KLH-conjugates of peptides C and L, respectively. All the A_{405} values shown have been corrected for background absorbance. Maxisorp microtiter plates were coated with DHP receptor by incubation overnight at 4°C with a solution of purified rabbit skeletal muscle DHP-receptor (140 ng/well) (purified as outlined in Section 2.5.3) in PBS containing 0.0025% (w/v) digitonin. The remaining steps were carried out at 20°C, as outlined for ELISA versus synthetic peptide. Serum dilutions were assayed in triplicate. Error bars representing SD values are shown where they are larger than the radius of the data point symbol.

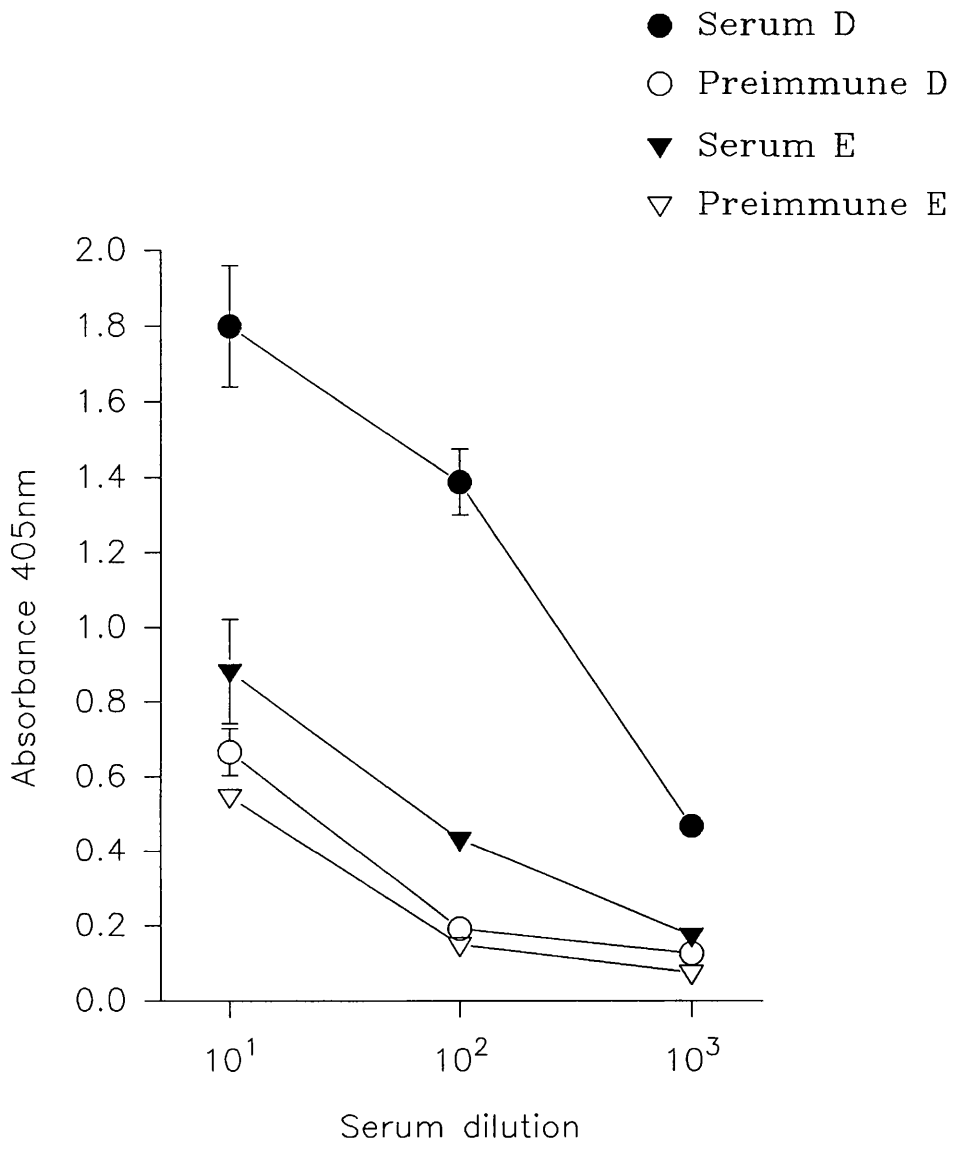

Fig. 5.3 Plot of A_{405} versus serum dilution for preimmune serum obtained from rabbits no. 1804 and 1805 and antiserum obtained following their immunization with ovalbumin-conjugates of peptides D and E, respectively. All the A_{405} values shown have been corrected for background absorbance. Maxisorp microtiter plates were coated with DHP receptor by incubation overnight at 4°C with a solution of purified rabbit skeletal muscle DHP-receptor (140 ng/well) (purified as outlined in Section 2.5.3) in PBS containing 0.0025% (w/v) digitonin. The remaining steps were carried out at 20°C, as outlined for ELISA versus synthetic peptide. Serum dilutions were assayed in triplicate. Error bars representing SD values are shown where they are larger than the radius of the data point symbol.

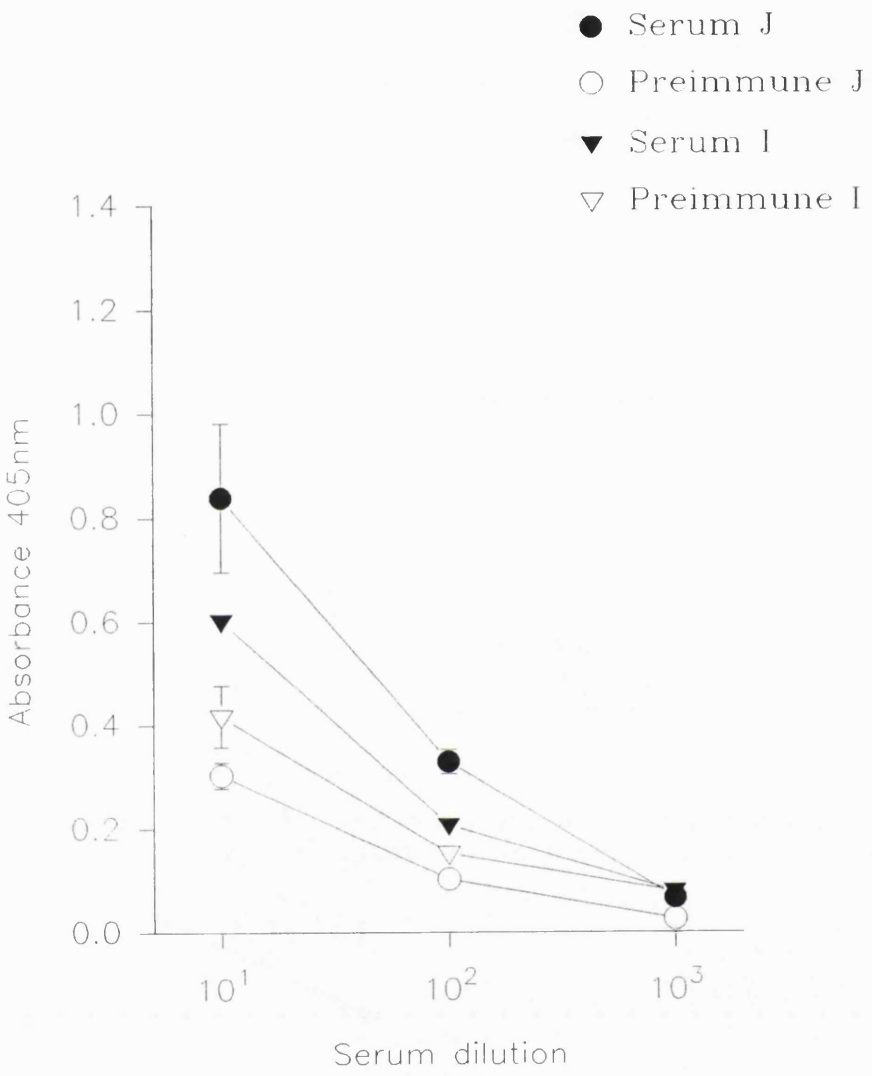

Fig. 5.4 Plot of A_{405} versus serum dilution for preimmune serum obtained from rabbits no. 2192 and 2079 and antiserum obtained following their immunization with peptide J and an ovalbumin-conjugate of peptide I, respectively. All the A_{405} values shown have been corrected for background absorbance. Maxisorp microtiter plates were coated with DHP receptor by incubation overnight at 4°C with a solution of purified rabbit skeletal muscle DHP-receptor (140 ng/well) (purified as outlined in Section 2.5.3) in PBS containing 0.0025% (w/v) digitonin. The remaining steps were carried out at 20°C, as outlined for ELISA versus synthetic peptide. Serum dilutions were assayed in triplicate. Error bars representing SD values are shown where they are larger than the radius of the data point symbol.

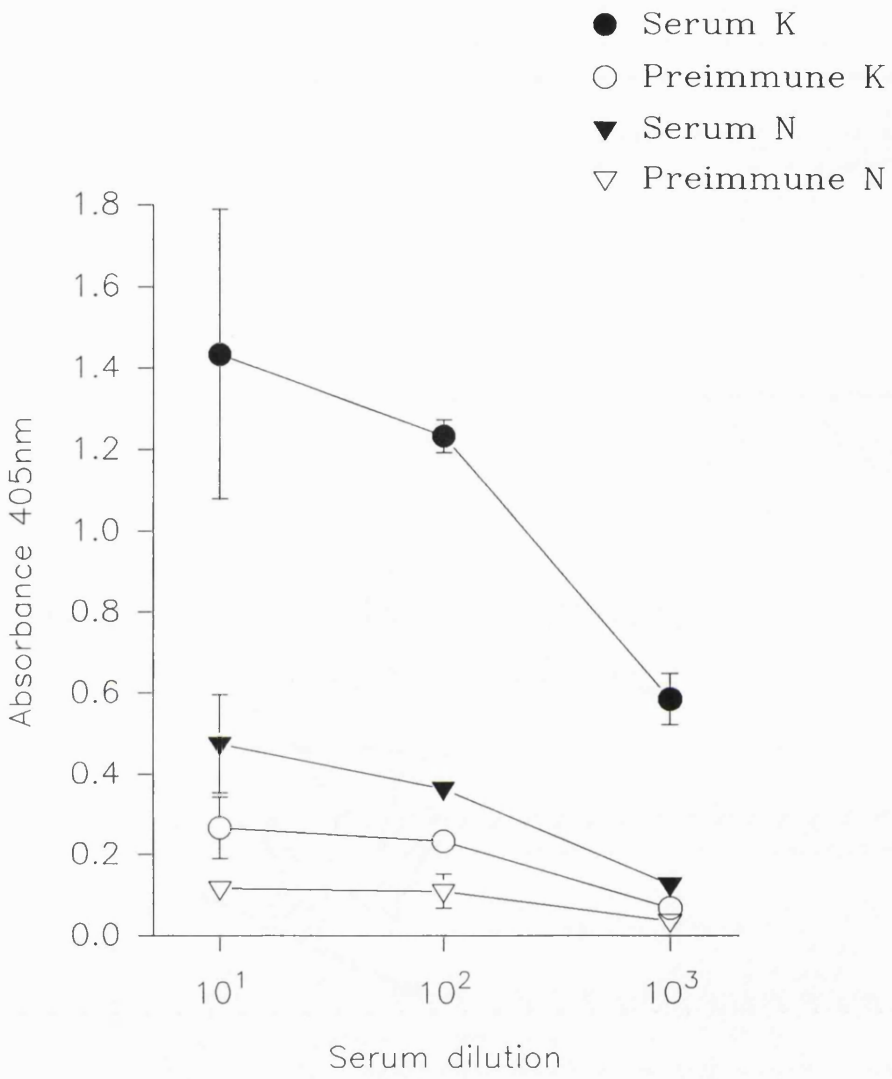

Fig. 5.5 Plot of A_{405} versus serum dilution for preimmune serum obtained from rabbits no. 2077 and 1806 and antiserum obtained following their immunization with ovalbumin-conjugates of peptides K and N, respectively. All the A_{405} values shown have been corrected for background absorbance. Maxisorp microtiter plates were coated with DHP receptor by incubation overnight at 4°C with a solution of purified rabbit skeletal muscle DHP-receptor (140 ng/well) (purified as outlined in Section 2.5.3) in PBS containing 0.0025% (w/v) digitonin. The remaining steps were carried out at 20°C, as outlined for ELISA versus synthetic peptide. Serum dilutions were assayed in triplicate. Error bars representing SD values are shown where they are larger than the radius of the data point symbol.

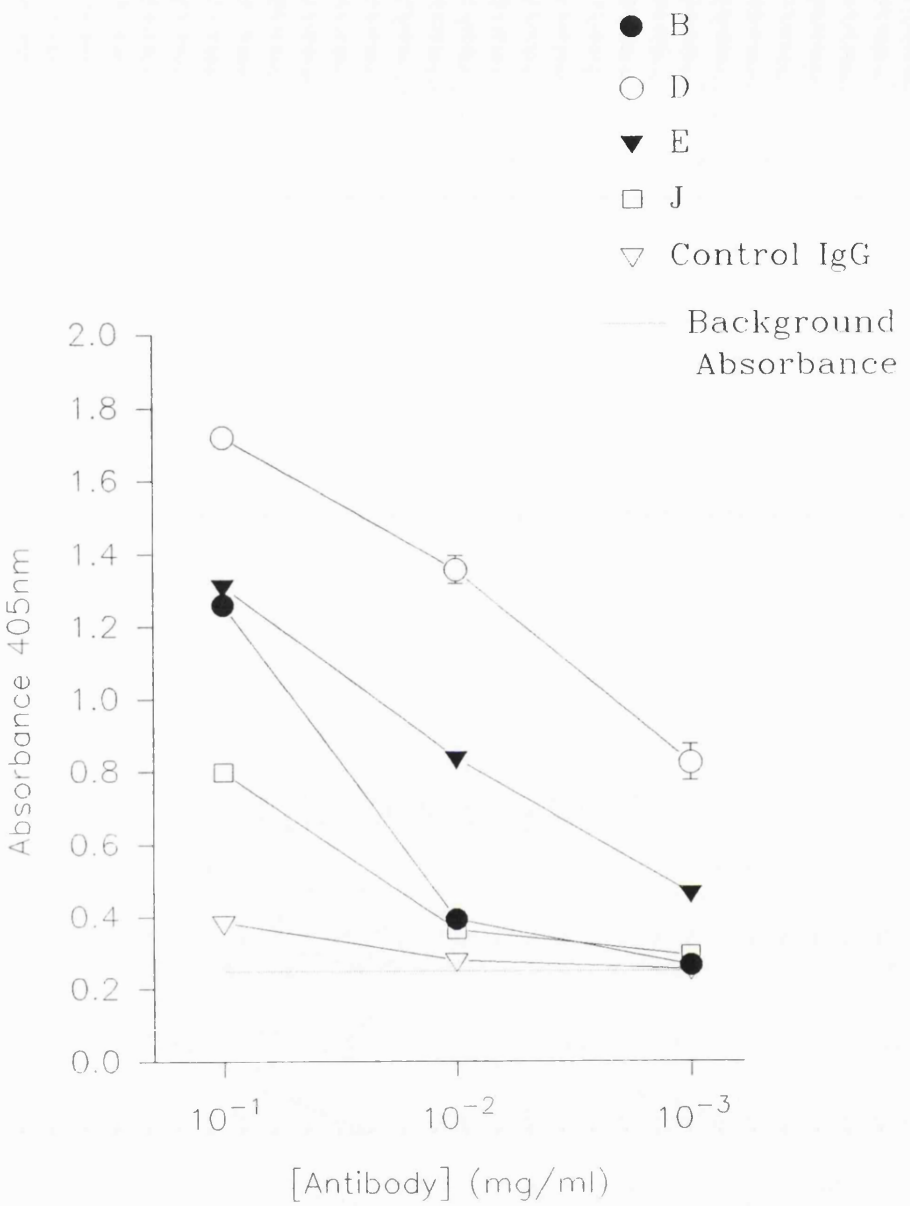

Fig. 5.6 Plot of A_{405} versus concentration of control IgG and purified antibody recognizing peptides B, D, E and J. The background absorbance is also indicated in the plot. The ELISA procedure was as outlined in the legend to Fig 5.1. using maxisorp microtiter plates coated with DHP receptor. Antibody dilutions were assayed in triplicate. Error bars representing SD values are shown where they are larger than the radius of the data point symbol.

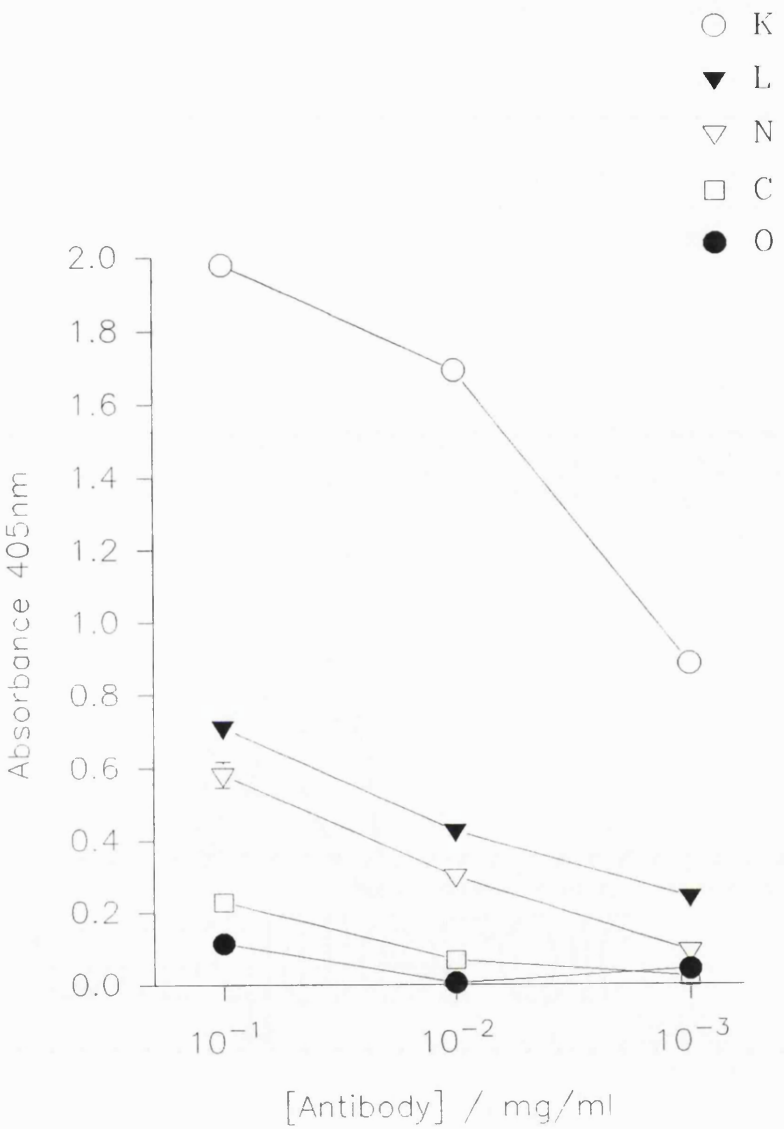

Fig. 5.7 Plot of A_{405} versus concentration of purified antibodies recognizing peptides C, K, L, N and O. All the A_{405} values shown have been corrected for background absorbance. The ELISA procedure was as outlined in the legend to Fig 5.1. using maxisorp microtiter plates coated with DHP receptor. Antibody dilutions were assayed in triplicate. Error bars representing SD values are shown where they are larger than the radius of the data point symbol.

dilution, while serum O did not show better recognition of the channel than its preimmune.

Figs. 5.6 and 5.7 show the results obtained in the same assay, using dilutions of purified antibody which had anti-peptide titres comparable to the serum dilutions assayed in this study. In each case, the particular sample of purified antibody examined was that one which exhibited the greatest reactivity either with its channel polypeptide in immunoblots or with the immunizing peptide in ELISA. In the latter assay the control antibody consisted of rabbit nonimmune IgG (see Figure 5.7). No difference was observed between the binding of this control and of purified antibody O to the channel in this study. Purified antibodies D, E, K and L showed the greatest recognition of the DHP receptor binding significantly more strongly than control IgG and purified antibody O at a protein concentration of 0.001 mg/ml. The next most reactive was antibody N, which along with B and J demonstrated binding to the receptor that was greater than that of the controls at 0.01mg/ml. C apparently only recognized the channel more strongly than the controls at 0.1mg/ml. Thus very good agreement is evident for the observed relative reactivity of each of the different antibodies present in either crude serum or the affinity purified state.

5.2.2 Reaction with the intact protein in situ.

Longitudinal sections of rabbit skeletal muscle were immunolabelled using various anti-peptide antibodies, and their relevant controls. Six of the anti-peptide antibodies raised against peptides corresponding to regions in the skeletal muscle L-type channel α_1 subunit, namely peptides B, C, E, J, K and L, and a single antibody specific for a peptide N corresponding to an internal domain in the α_2 polypeptide, gave a particular staining pattern of varying intensity, which was not observed in the relevant controls. The remaining antibodies gave no discernible pattern of staining different from that obtained when control IgG was used as primary antibody. The pattern of staining observed using these antibodies was characteristic of that seen for

the staining of the L-type Ca^{2+} channel in the skeletal muscle t-tubule membranes (Malouf *et al.*, 1987; Jorgensen *et al.*, 1989; Flucher *et al.*, 1990; Yuan *et al.*, 1990).

Immunocytochemistry was also carried out using transverse sections of rabbit skeletal muscle from each of the four mammalian species. A particular staining pattern was obtained using antibodies B, C, E, J, K, L and N which was not observed with either any of the other purified antibodies or control IgG. The hexagonal pattern of staining obtained correlates with immunostaining of the L-type Ca^{2+} channel previously observed in transverse sections of skeletal muscle (Malouf *et al.*, 1987; Jorgensen *et al.*, 1989; Flucher *et al.*, 1990; Yuan *et al.*, 1990).

Although good staining was obtained in the rabbit tissue, the controls revealed some background staining. The procedure was repeated using rat muscle, in order to confirm the specificity of the antibodies, and subsequently also, using both human and mouse muscle for the purpose of probing the channels present in these three species. The muscle from each of these species yielded an identical pattern of staining with each antibody tested, while the background staining observed when using control antibodies was less than that observed in the sections of rabbit muscle. For this reason the results for rat and human muscle are shown. Figs. 5.8 and 5.9 show longitudinal sections of adult rat skeletal muscle sections, which were immunolabelled using various of the anti-peptide antibodies. Two examples of positive staining and two of control staining, obtained using a non-reactive purified antibody and control IgG are shown in each figure. In the sections shown in Fig. 5.8 primary antibody was labelled with rhodamine conjugated to a secondary antibody while the staining in the sections shown in Fig. 5.9 was enhanced using a biotin-streptavidin amplification step. In Figs. 5.10 and 5.11 similarly, representative sections of adult human skeletal muscle are shown. The sections in Figs. 5.10 and 5.11, respectively, were immunolabelled using the anti-peptide antibodies and their relevant controls in the same way as those sections shown, respectively, in Figs. 5.8 and 5.9. These sections and those from mouse muscle, all revealed an identical pattern of staining to that observed in the rabbit muscle sections with each particular antibody. Again, these anti-peptide

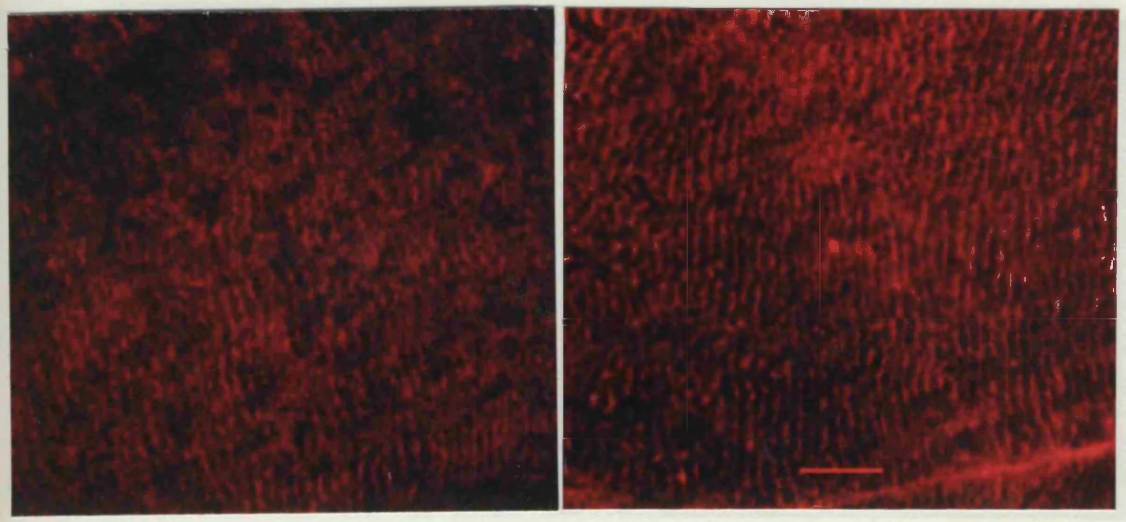

(a)

(b)

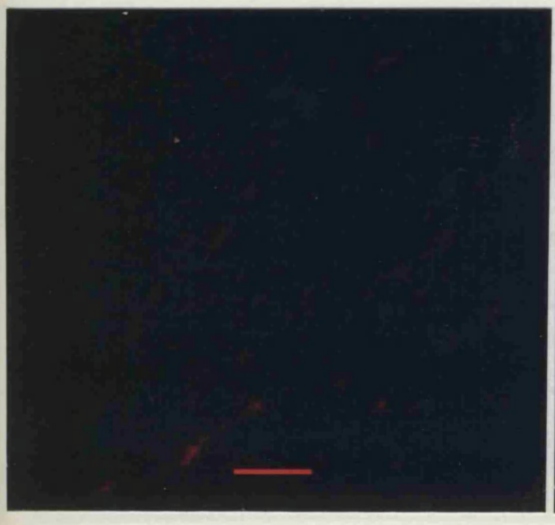

(c)

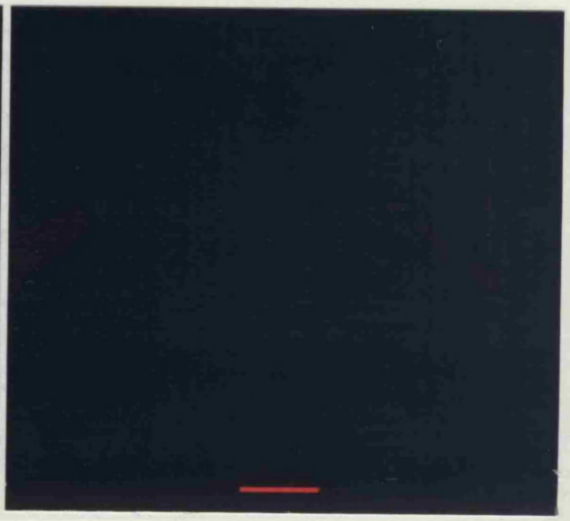

(d)

Fig. 5.8 Immunostaining of adult rat skeletal muscle longitudinal cryosections, prepared as outlined in Section 2.7.1, using purified antibodies. The sections were incubated with the following primary antibodies at the protein concentrations shown; (a) B (20μg/ml), (b) L (40μg/ml), (c) D (30μg/ml) and (d) control rabbit IgG (40 μg/ml). The staining procedure was as outlined in Section 2.7.2, using swine anti-rabbit rhodamine as second antibody. Imaging was performed as outlined in Section 2.7.3. The space bar represents 10μm.

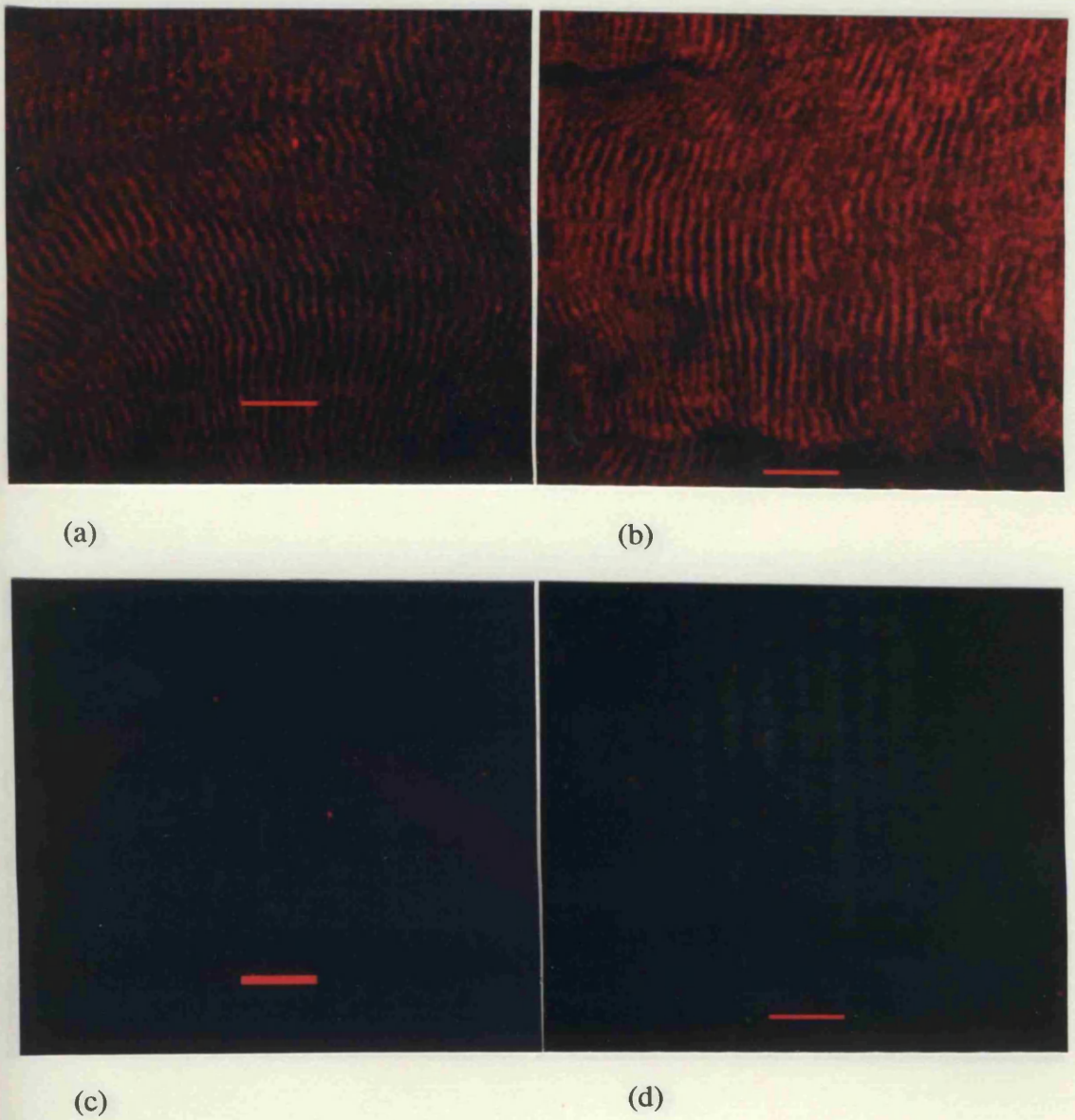

Fig. 5.9 Immunostaining of adult rat skeletal muscle longitudinal sections using purified antibodies. The sections were incubated with the following primary antibodies at a protein concentration of 33μg/ml; (a) C, (b) E, (c) D, (d) control rabbit IgG. The staining procedure was performed as outlined in Section 2.7.2 using Texas Red detection, while imaging was as outlined in Section 2.7.3. The space bar is 10μm.

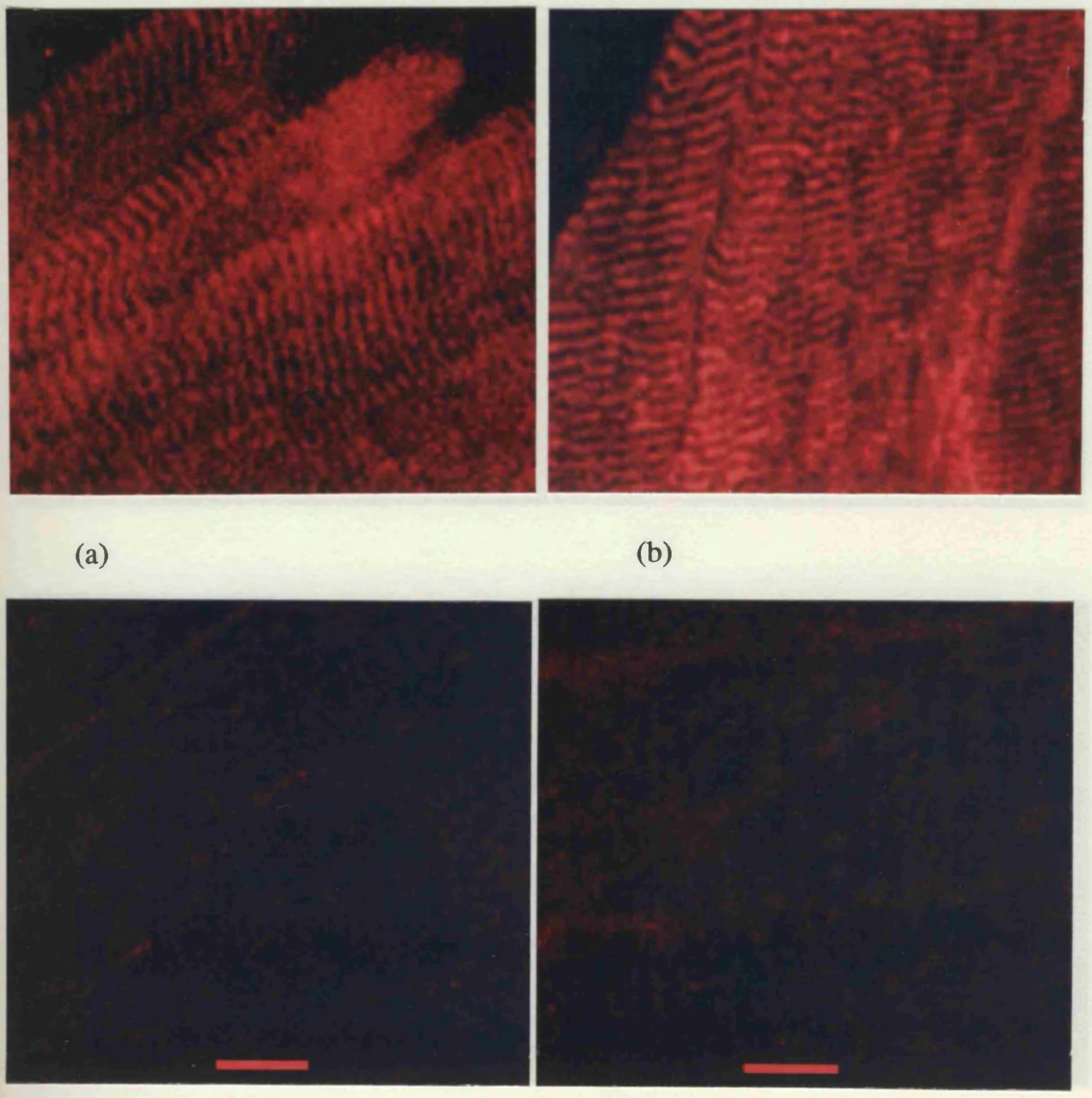

Fig. 5.10 Immunostaining of adult human skeletal muscle longitudinal cryosections, using purified anti-peptide antibodies. The sections were incubated with the following primary antibodies at the protein concentrations given; (a) B (30μg/ml), (b) K (40μg/ml), (c) D (30μg/ml) and (d) control rabbit IgG (40μg/ml). The staining procedure was as outlined in Section 2.7.2, using as second antibody, swine anti-rabbit rhodamine and imaging was performed as outlined in Section 2.7.3. The space bar is 10μm.

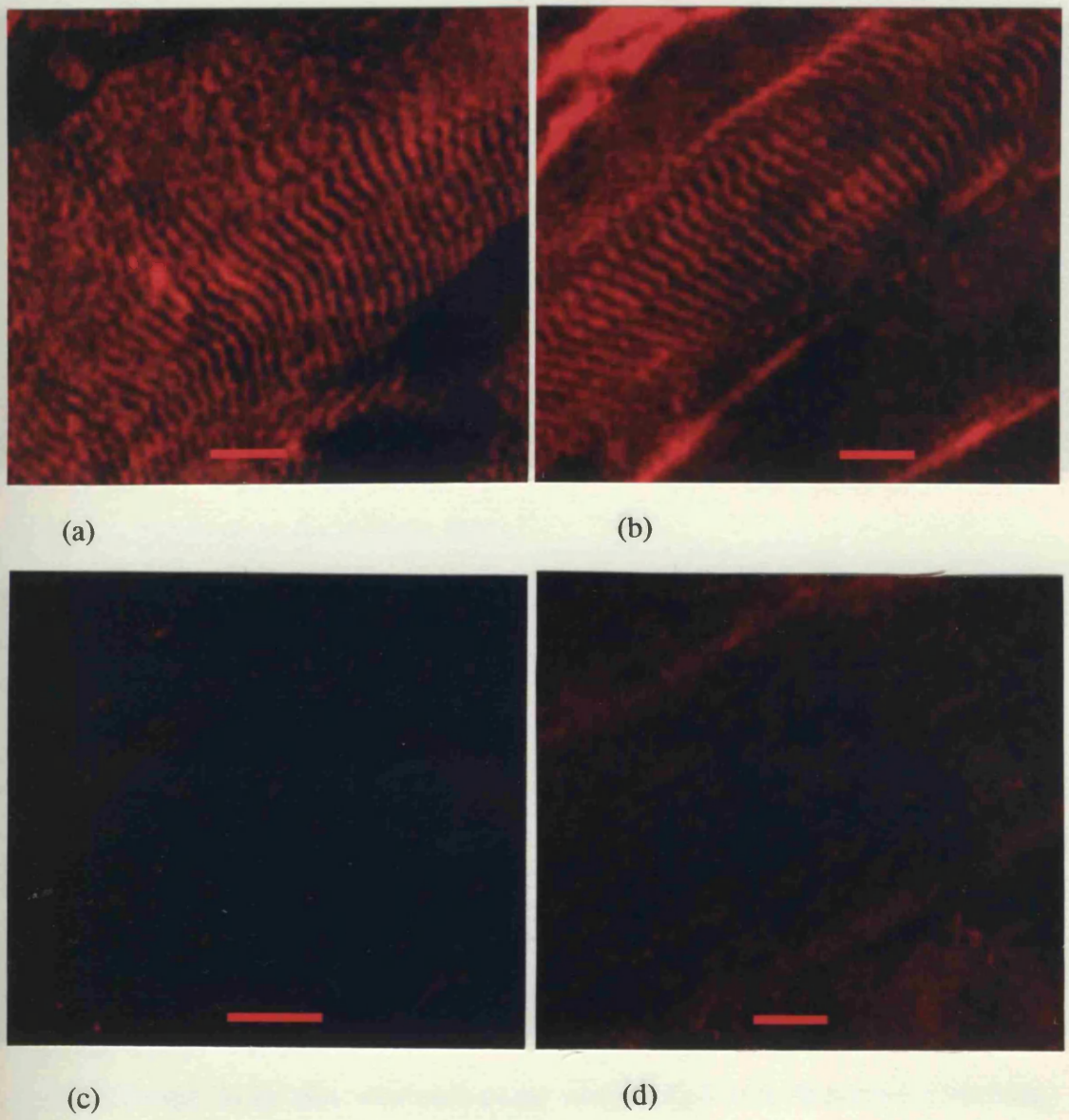

Fig. 5.11 Immunostaining of adult human skeletal muscle longitudinal sections using purified antibodies. The sections were incubated with the following primary antibodies at a protein concentration of 33μg/ml; (a) $\overline{E}$, (b), J, (c) D and (d) control rabbit IgG. The staining procedure was as outlined in Section 2.7.2, using Texas Red, with imaging as outlined in Section 2.7.3. The space bar is 10μm.

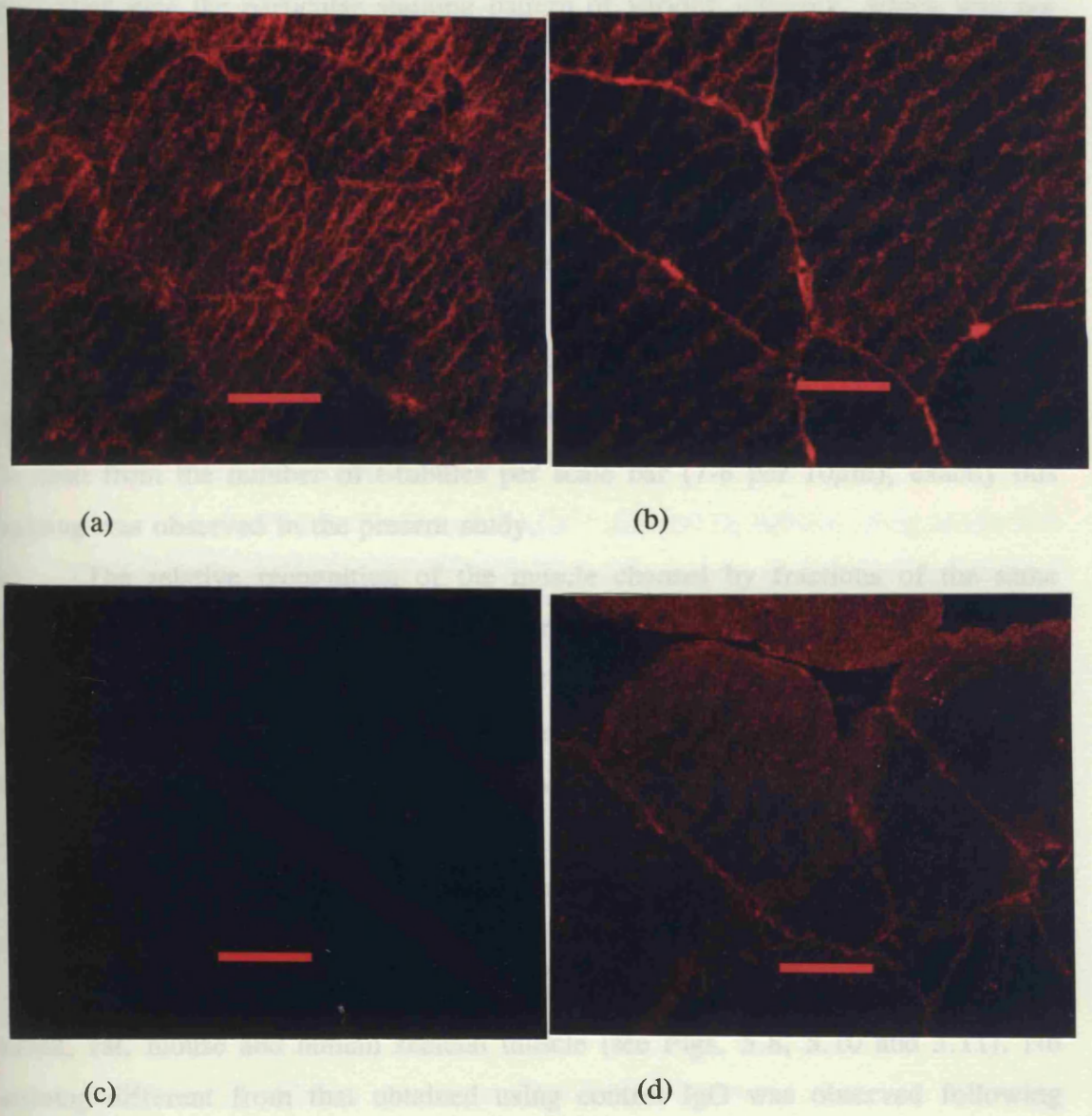

Fig. 5.12 Immunostaining of adult rat skeletal muscle transverse cryosections, using purified anti-peptide antibodies. The sections were incubated with the following primary antibodies at a protein concentration of 33μg/ml; (a) B, (b) E, (c) D and (d) control rabbit IgG. The staining procedure was performed as outlined in Section 2.7.2, using Texas Red, with the imaging procedure as outlined in Section 2.7.3. The space bar represents 25μm.

antibodies give the particular staining pattern of varying intensity, which was not observed in the relevant controls.

In mammalian skeletal muscle the t-tubules are located at each A-I interface and extend parallel to each other to the cell interior (Ogata and Yamasaki, 1991; Sonda et al., 1993). In uncontracted mammalian muscle the distance between each A-I band and hence each t-tubule is approximately 1.4 microns, when the myofibres are viewed longitudinally (reviewed by Landon, 1979). However, in preparing the tissue for freezing the muscle became contracted resulting in the shortening of the sarcomeres and hence the distance between the t-tubules is about 1.3 μm. As can be seen from the number of t-tubules per scale bar (7-8 per 10μm), exactly this spacing was observed in the present study.

The relative recognition of the muscle channel by fractions of the same antibody eluted from the peptide column under different conditions was also examined. This revealed that antibodies B and N, eluted at low pH, stained the muscle sections more intensely than fractions of these antibodies eluted using either high pH or 5M $MgCl_2$. On the other hand antibodies C and L eluted at high pH and antibodies E, J and K eluted in 5M $MgCl_2$ gave stronger staining of the channel in muscle sections than fractions of these channels eluted under the conditions of low pH or 5M $MgCl_2$ and either low or high pH, respectively (results not shown).

Antibody N also bound to the L-type Ca^{2+} in the t-tubules of sections of rabbit, rat, mouse and human skeletal muscle (see Figs. 5.8, 5.10 and 5.11). No staining different from that obtained using control IgG was observed following incubation of the section from any of the four species with antibody M.

Immunostaining by antibodies raised against the α_1 peptides sequences B, C, E, J, K, and L all localized to the t-tubule network in the skeletal muscle sections from each of the four mammalian species (see Figs 5.8-5.12). The staining obtained using antibody C, which bound to the entire loop between domains IIS4 and IIS5, was the faintest obtained. E, which recognized a short sequence on the loop brtween IIIS6 and IVS1 and the staining it reveals, while being stronger than that obtained with C, was still relatively weak. Antibody J, which recognizes the large, highly conserved

peptide located near to IVS6 at the C-terminal side gives staining of a similar intensity to antibody E.

These three antibodies C, E and J required enhancement of their particular staining using the biotin-streptavidin method outlined in Section 2.7.2, in order to make the staining pattern apparent. The remaining three antibodies B (recognizing the IS4 domain of α_1) and K and L (reacting with C-terminal regions of α_1) each produced strong staining patterns. Indeed most intense staining observed by any antibody using this technique was obtained using this antibody in mouse muscle. No staining distict from that obtained using control IgG was obtained with antibodies A, D, F, G and O all failed to bind.

Fig. 5.12 shows localization of the Ca^{2+} channel α_1 subunit using antibodies B, and the α_2 polypeptide using antibody N in transverse sections of rat skeletal muscle. Muscle sections which had been incubated with control IgG and antibody D are also shown.

5.3 DISCUSSION

5.3.1 Reaction with the intact native protein

ELISA versus purified DHP receptor

Previous channel preparations have specific binding of DHP in the range 1.3-2.4 nmoles/mg protein (Flockerzi *et al.*, 1986a; Smith *et al.*, 1987; Hymel *et al.*, 1988; Kanngiesser *et al.*, 1988). If the molecular mass of the entire channel is taken to be 400,000 Da, with each channel containing a single DHP site, a 100% pure preparation of receptor would theoretically bind a maximum of 2.5 nmoles of ligand per mg protein. Indeed, one of the above cited preparations having a measured density of 2 nmoles specific binding sites for DHP / mg protein was shown using

SDS/PAGE to contain primarily α_1 polypeptide and was estimated to be $>80\%$ pure by densitometric scanning of a silver stained SDS/PAGE gel (Smith *et al.*, 1987). Therefore, the specific activity of the purification used in this study indicates that it was approximately 40% pure DHP receptor.

The good agreement between the observed reactivities of each antibody present in either crude serum or the affinity purified state with the receptor indicates that antibodies that were purified as outlined in Section 2.6.2, retained their reactivity with the native protein, when eluted under optimum conditions. All but one of the antibodies which showed recognition of their channel subunit in the denatured state in Western blots (Figs. 4.24 and 4.25), in turn reacted with the channel in ELISA. These two reactivities were similarly strong for five of the antibodies, those specific for peptides D, E, J, K, L and N, indicating a similar recognition of the relevant peptide segments in channels with native structure and in the denatured state. Antibody M recognized the *N*-terminus of the denatured channel α_2 polypeptide (Fig. 4.24), while failing to bind to the receptor in ELISA (results not shown). Since M is a polyclonal antibody it is likely that there are many different IgG molecules which recognize different parts of the peptide sequence in the denatured protein that do not bind to this peptide in the channel in ELISA. This appears to indicate a substantial difference in the structure of the sequence in the channel in immunoblots and ELISA, suggesting that in the latter the channel maintains its native conformation. This is also supported by the observation that, antibody B appears to react weakly with its sequence in the IS4 domain in denatured α_1 (Fig. 4.11 and 4.12) while showing stronger recognition of this domain in the channel in ELISA (Fig. 5.1 and 5.6). Antibody C had stronger reactivity with the channel α_1 in the denatured (Fig. 4.11), rather than the native state (Figs. 5.2 and 5.7). These findings provide some evidence of maintenance of the native conformation of the channel subunits during the course of the ELISA assay.

5.3.2 Reaction with the intact protein in situ.

Antibody M which reacted with the α_2 polypeptide in immunoblots failed to bind to its peptide sequence either in the channel in skeletal muscle cryosections the purified DHP receptor in ELISA. This suggests maintenance of native structure of the channel in air dried sections. The background staining obtained in rabbit muscle sections probably results from the presence of endogenous IgG, which has already observed in immunoblots using t-tubule membranes (see Figs. 4.11 and 4.12). This is supported by the finding that the background staining obtained in the sections of rat, human and mouse skeletal muscle following incubation with control IgG was less than that observed in sections from rabbit.

This study confirmed the specificity of six of the antibodies raised against peptides B, C, E, J, K and L, derived from the rabbit skeletal muscle Ca^{2+} channel α_1 subunit sequence. The ability of these antibodies to recognize their polypeptide in the sections suggests that they can bind to the channel in its native structure. In addition, the reactivity of these antibodies with α_1 in the muscle sections of the other species also revealed that the sequences of the L-type Ca^{2+} channel α_1 subunits present in rabbit, rat, mouse and human skeletal muscle are similar if not identical in the segments of the primary structure recognized by these antibodies. This suggests that the domains including these sequences are important for the structure or function of the channel.

Immunostaining by antibodies raised against the α_1 peptides sequences B, C, E, J, K, and L all localized to the t-tubule network in the skeletal muscle sections from each of the four mammalian species (see Figs 5.5-5.9). All these antibodies with the exception of B were raised against peptide sequences now presumed to have intracellular locations. Antibody C recognized the entire loop between domains IIS4 and IIS5. The staining obtained with this antibody is the faintest obtained. This correlates with the results obtained both in Western blotting (Figs. 4.11 and 4.12) and ELISA with the DHP receptor (Figs. 5.1 and 5.3) where C was also found the least reactive of the anti-L-type Ca^{2+} channel antibodies.

E binds to a short sequence on the loop between IIIS6 and IVS1 and the staining obtained, while stronger than that obtained with C, is still relatively weak. Again this correlated well with its relatively weak reactivity with denatured α_1 in Western blots (Figs. 4.11 and 4.12) and with the native channel in ELISA (Figs. 5.1 and 5.3). Antibody J, which recognizes the large, highly conserved peptide located near to IVS6 at the C-terminal side gives staining of a similar intensity to antibody E (Figs. 5.6 and 5.8).

These three antibodies C, E and J required enhancement of their particular staining using the biotin-streptavidin method outlined in Section 2.7.2, in order to make the staining pattern apparent. The remaining three antibodies B (recognizing the IS4 domain of α_1) and K and L (reacting with C-terminal regions of α_1) each produced strong staining patterns. Similarly strong reactions with the denatured channel α_1 polypeptide were observed with both K and L, while B recognized this subunit with apparently lower efficiency in Western blots (see Figs 4.11 and 4.12). However, all three antibodies reacted very strongly with the purified native protein in ELISA (Figs. 5.1-5.4).

The domain recognized by B, IS4, is proposed to be intramembranous but nonetheless appeared to be highly accessible to this antibody in ELISA with the native protein (Figs 5.1 and 5.3) and in immunocytochemistry of frozen muscle sections (Figs 5.5, 5.8 and 5.9). Indeed the most intense staining observed by any antibody using this technique was obtained using this antibody in mouse muscle (see Fig. 5.9). However, Western blotting did not reveal similarly strong recognition of this domain by its antibody. On examination of the results obtained using these three techniques, it appears possible that the IS4 domain may be exposed and accessible when the protein is in its native form but becomes less accessible to antibody binding upon protein denaturation. However, it is also possible that denaturation causes destruction of the epitope. Since the DHP receptor retains its native conformation during ELISA and the antibody binds in this assay with high efficiency this indicates accessibility of the IS4 region on the native protein surface to antibody molecules.

As mentioned in Section 1.7.1, Meiri *et al.* (1987) observed a functional effect

on the Na^+ channel by an antibody raised against the middle region of its IS4 domain. Since the antibodies mediated their effect when present at the extracellular face of the membrane, this indicated antibody binding to a domain in IS4 which is exposed to the extracellular matrix. Earlier models of voltage-gated ion channel tertiary structure had the S4 sequence located in the membrane bilayer where, it could fulfil its role as the membrane voltage sensor (Noda *et al.*, 1984; Greenblatt et al., 1985; Guy and Seetharamulu, 1986). The model of Noda *et al.*, (1984) had S4 as intramembranous but extending into the extracellular space. Peptide B corresponds to the first 15 residues in the sequence of the putative IS4 domain, some of which would indeed be exposed at the extracellular side of the membrane if the above model was correct. More recent evidence has led to the proposal that the pore of region of voltage-gated ion channels is lined by the loops between the S5 and S6 transmembrane regions with the S2 and S4 domains in close proximity. In this model the S4 domain is in the pore lining, at the surface of the protein and would hence be accessible to antibody B. This finding appear to verify that the part of the IS4 domain, known to be important for channel activation (see Section 1.7.1) is exposed to the extracellular matrix. Therefore the models for the channel tertiary structure either having S4 as a pore lining sequence, or as an intramembranous segment protruding from the membrane, are both supported by this study.

The specificity of a single antibody raised against peptide N corresponding to a sequence found in the α_2 polypeptide has also been confirmed by this study (see Figs. 5.8, 5.10 and 5.11). As is the case for the six anti-α_1 polypeptide antibodies above, it appears that this antibody can also recognize its peptide in the native channel. This antibody binds to its sequence in the L-type Ca^{2+} channel α_2 subunits present in rabbit, rat, mouse and human skeletal muscle. Antibody M which reacted with the α_2 polypeptide in immunoblots failed to bind to its peptide sequence in the channel in the sections.

A further finding of note concerns the peptide sequence on the IIS6-IIIS1 loop of the Ca^{2+} channel α_1 subunit corresponding to peptide D. While the antibody raised against peptide D gave strong reactions with the channel α_1 polypeptide both in

immunoblots (Figs. 4.11 and 4.12) and ELISA with the purified receptor (Figs. 5.1 and 5.3), surprisingly, no staining of t-tubules of any of the four species was observed when muscle sections were incubated with this antibody (results not shown). The failure of the antibody to recognize its peptide sequence on the IIS6-IIIS1 loop of the α_1 polypeptide in frozen muscle sections is therefore most unlikely to be due to the absence of reactivity of the antibody with its domain. A probable explanation for this observation is that the region of the α_1 polypeptide to which the antibody binds in ELISA, is inaccessible to the antibody in the muscle sections. This correlates well with the findings that the IIS6-IIIS1 loop is essential for skeletal-type E-C coupling (Tanabe *et al.*, 1990b). Part of the role of this loop in E-C coupling may be its physical interaction with the ryanodine receptor of the SR via a linker protein. If this was the case, at least part of this loop would be expected to be inaccessible to antibodies in muscle, as this finding suggests.

CHAPTER 6

INHIBITION OF LIGAND BINDING

6.1 GENERAL INTRODUCTION

6.1.1 Allosteric interaction between ligand- and Ca^{2+}-binding sites on the α_1 polypeptide

There is now considerable evidence, as discussed in the Section 1.9.3, that the DHP, PAA and BTA classes of Ca^{2+} channel ligand have distinct, but allosterically related binding sites on the channel α_1 subunit. Each of these sites also appears to be modulated by the binding of Ca^{2+} to this polypeptide.

High affinity binding of DHP (Ebata *et al.*, 1990; Staudinger *et al.*, 1991), BTA and PAA (Schneider *et al.*, 1991; Knaus *et al.*, 1992) ligands to the purified channel requires the presence of Ca^{2+} at different concentrations in the range 30-300 nM (DHP), BTA and 10μM (PAA). However, at higher concentrations $>30\mu$M Ca^{2+}, PAA binding is inhibited (Knaus *et al.*, 1992). Similarly, binding of both verapamil and diltiazem to rat cerebral cortex membranes was inhibited by millimolar Ca^{2+}, while nitrendipine binding was not inhibited at concentrations of Ca^{2+} up to 10mM (Schoemaker and Langer, 1989). Diltiazem was observed to stimulate the binding of [^{3}H]PN200-110 to rabbit heart sarcolemma, skeletal muscle t-tubules and rat cerebral cortex membranes in a temperature-sensitive manner, while verapamil caused inhibition of such [^{3}H]PN200-110 binding (Schoemaker and Langer, 1989; Murphy and Tuana, 1990). The presence of Ca^{2+}, which did not inhibit DHP binding, completely reversed the effects on its binding, both of verapamil, in the cardiac but not skeletal muscle membranes (Murphy and Tuana, 1990) and also diltiazem in rat cerebral cortex membranes (Schoemaker and Langer, 1989). Since these drug interactions are reciprocal, this study reveals tight coupling between these binding sites on the α_1 polypeptide. The binding of [^{3}H]diltiazem was inhibited by Ca^{2+} with

an IC_{50} of 0.31mM. This effect was also evidenced by an increase in the EC_{50} of diltiazem for enhancement of [^{3}H]nitrendipine binding (Schoemaker and Langer, 1989). It was thus proposed that the PAA receptor was stabilized by micromolar Ca^{2+} in a conformation allowing high affinity PAA binding, while millimolar Ca^{2+} induced a low affinity state of the PAA binding site in a stable channel (Schneider *et al.*, 1991).

The voltage sensor function of the α_1 subunit has been shown to have an absolute requirement for extracellular divalent ($Ca^{2+} > Sr^{2+} > Mg^{2+} > Ba^{2+}$) or monovalent ($Li^+ > Na^+ > K^+ > Rb^+ > Cs^+$) metal ions, pointing to an extracellular binding site for Ca^{2+} (Pizarro *et al.*, 1989; Rios and Pizarro, 1991). This essential binding site for E-C coupling is termed the "priming site", having a relative affinity for cations similar to their relative permeability ratios for the L-type cardiac Ca^{2+} channel. The DHP receptor site appears either to be associated with, or to form part of this high affinity Ca^{2+} binding site (Ebata *et al.*, 1990; Staudinger *et al.*, 1991). The PAA binding domain interacts in a similar fashion with a Ca^{2+} binding site (Schoemaker and Langer, 1989; Schneider *et al.*, 1991; Knaus *et al.*, 1992), which is intracellular.

These findings led Rios and Pizarro (1991) to formulate state diagrams to explain inactivation of the Ca^{2+} channel, together with the action of different antagonists and its Ca^{2+}-dependence. The model incorporates state-dependent binding of Ca^{2+} and drugs, with the resting and activated states having affinity for Ca^{2+} but not drugs, while inactivated states have high drug-, but low Ca^{2+}-binding affinity. Knaus *et al.* (1992) have modified this model in which the DHP and PAA binding domains share a common ion binding site having high affinity for Ca^{2+} (Ca^{2+} site I). Ca^{2+} binding to this site is essential for stabilizing these high-affinity drug binding domains (Ebata *et al.*, 1990) and its ion selectivity is similar to that of the priming site (Rios and Pizarro, 1991; Pizarro *et al.*, 1989). Another Ca^{2+} binding site (Ca^{2+} site II) is coupled in a negative fashion to the PAA binding domain. Since voltage sensor function of the α_1 subunit requires bound extracellular Ca^{2+} (Rios and Pizarro, 1991) and DHP antagonists bind to a site exposed to the extracellular matrix (Ebata

et al., 1990; Kass *et al.*, 1991; Striessnig *et al.*, 1991; Nakayama *et al.*, 1991), it seems likely that Ca^{2+} site I is the priming site of the voltage sensor having an extracellular orientation. Ca^{2+} site II appears to have a cytosolic orientation in the light of structural evidence indicating an intracellular orientation for the PAA binding domain of the channel (Hescheler *et al.*, 1982; Striessnig *et al.*, 1990b).

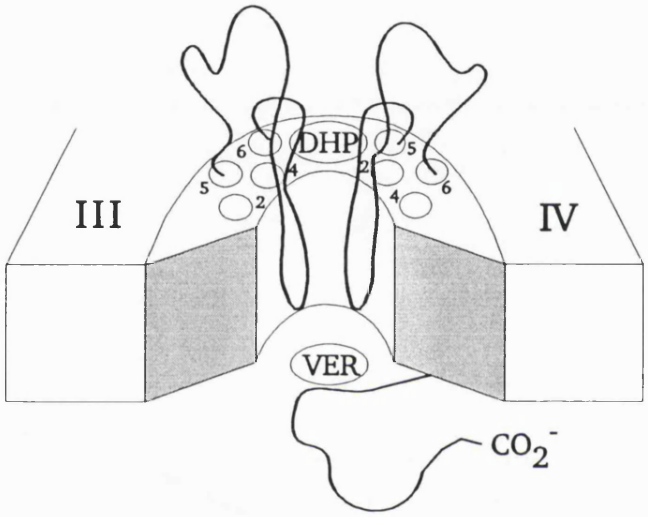

Fig. 6.1 Model of proposed pore region of the channel showing determined sites of binding of both DHP and PAA (verapamil).

6.1.2 Physical location of ligand-binding domains

As outlined in Section 3.2.4, peptide-specific polyclonal antibodies have proved instrumental in the identification of the functionally important binding sites for drugs from the PAA (Striessnig *et al.*, 1990b) and DHP (Striessnig *et al.*, 1991; Nakayama *et al.*, 1991) classes to the Ca^{2+} channel α_1 polypeptide. The site of PAA binding was thus located to the region of the α_1 subunit between Glu-1349 and Trp-1391 using the PAA verapamil derivative ([N-methyl-^{3}H] LU49888). Since the PAA receptor site is only accessible to the cytoplasmic side of the membrane (Hescheler

et al., 1982), this places the binding site of the label at the intracellular end of IVS6 and its adjacent amino acid residues (Striessnig *et al.*, 1990b). This binding domain is situated N-terminal to the domain between residues no. 1390 and 1437 in the rabbit skeletal muscle L-type channel α_1 polypeptide, which is highly conserved in all channel α_1 subunits whose sequences are known. The putative EF hand domain located in this intracellular conserved sequence at α_1(1410-1421), may constitute Ca^{2+} site II.

Striessnig *et al.* (1991) found that the channel was labelled by the DHP PN200-110 in the IIIS6 and IVS6 segments of α_1 and thus, these domains along with their adjacent residues were assumed to comprise the channel DHP binding domain. The IIIS5-IIIS6 loop which was found to be preferentially labelled with azidopine, was thought to contribute to binding of this DHP by interaction with its long side-chain. Nakayama *et al.* (1991) having identified labelling of the α_1 subunit with the DHP, diazipine, suggested that the IIIS5-S6 loop and the extracellular portion of IVS6 form the DHP binding domain. This study failed to confirm the involvement of the IIIS6 segment in DHP binding.

A previous investigation had located the DHP binding domain to the C-terminus of the IVS6 region between residues 1390 and 1437 of α_1 (Regulla *et al.*, 1991). Following either trypsin hydrolysis of channel photolabelled with azidopine, or endoproteinase Asp-N hydrolysis of nitrendipine-labelled channel, labelled fragments were isolated by reverse phase column chromatography, using a linear (0-90)% acetonitrile gradient. The peptides were sequenced following a second chromatography step which involved elution of the pooled azidopine- and nitrendipine-labelled peptides using, respectively, (0-54)% and (18-36)% linear acetonitrile gradients. The peptide 1428-1437 contained the majority of the azidopine with minor labelling of 13-18, while most of the nitrendipine was incorporated into peptide 1390-1399 with some labelling of 1410-1420. Assuming that 13-18 interacts with the long side chain of azidopine this study reveals an intracellular location for the DHP site in the α_1(1390-1437) sequence which is located C-terminal to IVS6.

Despite the different techniques and DHP probes used to physically locate the

DHP-binding domain, all the above studies should have identified common sites of ligand-channel interaction. While all three probes used in the antibody studies identified the IVS6 domain, in addition diazipine and the structurally similar azidopine labelled the IIIS5-IIIS6 loop, while both PN200-110 and azidopine labelled IIIS6, as well. The different physical structures of these probes might be expected to lead to these slightly different findings. However, each ligand appears to interact with homologous domains III and IV, in the vicinity of their S6 peptide segments. The reason for the discrepancies between these results and those of Regulla *et al.*, (1991), using both nitrendipine and azidopine are unclear. However, a possible explanation is that not all of the peptides which were labelled in the latter study eluted from the preparatory column during the second chromatography step. This is likely to occur if some of these labelled peptides required high percentages of acetonitrile for elution in chromatography step I, since strongly hydrophobic conditions were not used in either of the second steps. This would be particularly true for hydrophobic peptide fragments such as those containing the lipophilic transmembrane sequences IIIS6 and IVS6, where Striessnig *et al.* (1991) subsequently identified azidopine-binding.

Originally, single channel recordings revealed that nitrendipine approached the calcium channel through the membrane lipid bilayer (Hess *et al.*, 1984; Reuter *et al.*, 1985). Thus, its blocking effect could have been caused by binding either to the transmembrane or the extracellular region of the channel. More recent studies, using the uncharged DHP PN200-110 (Ebata *et al.*, 1990) and charged membrane-impermeable DHP's amlodipine and SDZ 207-180 have revealed an extracellular location of the DHP binding site (Kass *et al.*, 1991). In light of this it appears that the antibody studies reveal the correct DHP binding domains. However, the precise identification of peptide sequences involved in DHP and PAA binding to the α_1 polypeptide has yet to be achieved.

6.2 INTRODUCTION TO THE PRESENT STUDY

6.2.1 Identification of functionally important ligand-binding domains by examining antibody inhibition of ligand-binding

Recently, a number of successful investigations have been carried out either to identify or confirm the identity of domains of particular polypeptides involved in the binding of a molecular inhibitor, by observing inhibition of binding of the ligand due to the presence of a site-specific antibody. In the case of the α-Scorpion toxin binding site on the rat brain RII Na^+ channel, part of this site had previously been located to the sequence between amino acid residues no. 335 and 378 in the IS5-IS6 loop of the α polypeptide. This was achieved by immunoprecipitation, using peptide-specific antibodies, of a labelled proteolytic fragment obtained following digestion of the channel, prelabelled with toxin, using CNBr (Tejedor and Catterall, 1988). Following this study, inhibition of voltage-dependent binding of α-Scorpion toxin to its site on the Na^+ channel α subunit was examined in the presence of each of six anti-peptide antibodies and each of five monoclonal antibodies. Two of the former antibodies bound on the IS5-IS6 loop and another recognized a domain in the corresponding loop in the fourth homologous domain, while the epitopes on the channel for all the monoclonal antibodies were located on the IS5-IS6 loop. The observed inhibition of ligand binding in the presence of each of the antibodies that recognized the loop in repeat I and by the antibody specific for a sequence in loop IVS5-IVS6 allowed further characterization of the binding domain for this ligand (Thomsen and Catterall, 1989). Identification of sites of phosphorylation on the α polypeptide of the rat brain Na^+ channel has similarly been achieved by observed inhibition of channel phosphorylation in the presence of a site-directed anti-peptide antibody (Nakayama *et al.*, 1992b).

A functionally important site in another membrane protein, the human erythrocyte glucose transporter, involved in the binding of an inhibiting ligand, cytochalasin B, to the polypeptide has also been located, in a study similar to that

carried out by Tejedor and Catterall (1988). In this investigation, the binding of the ligand to the transporter was seen to be inhibited by a maximum of 60% by antibodies raised against two peptides located in the central cytoplasmic loop of the protein. This inhibition was shown to be due to a reduction in the affinity rather than a reduction in the concentration of the binding sites for cytochalasin B (Davies *et al.*, 1990).

This experimental approach can be useful in locating such active sites in proteins. However, in the case of the successful studies on the large Na^+ channel α polypeptide some prior knowledge of potential sites of phosphorylation and ligand-protein interaction was available. Therefore, in both cases polyclonal antibodies were designed to specifically recognize sequences in the channel subunit which were predicted to contain active sites. However, in the absence of such knowledge, the number of peptide specific antibodies required for a comprehensive identification of a binding domain of a ligand restricts the usefulness of this particular approach for identification of ligand binding sites to smaller polypeptides. Hence, the approach taken to identify ligand binding sites on the large Ca^{2+} channel α_1 subunit involved immunoprecipitation of labelled proteolytic fragments of prelabelled polypeptide. Nonetheless, prior knowledge of the location of sites of interaction of ligands with such large polypeptides (e.g. the DHP and PAA binding domains on the L-type Ca^{2+} channel) does allow the approach using observed inhibition of ligand binding due to presence of antibody to be employed to verify these sites. Such studies require antibodies directed against sites in the vicinity of the known binding domain, in order to confirm the location of the ligand binding site by examining inhibition of ligand interaction with the protein using these site-specific antibodies.

6.2.2 Present study of inhibition of [^{3}H]nitrendipine and [^{3}H]D888-binding to the Ca^{2+} channel

The study described in this chapter involved examining the effect of all the anti-peptide antibodies produced, which are known to recognize the L-type Ca^{2+} channel in its native conformation, on the binding of the DHP, nitrendipine to the L-type Ca^{2+} channel in rabbit skeletal muscle t-tubule membranes. The effect of a number of these antibodies on the interaction of the PAA, D888, with the channel in these membranes was also investigated. These binding studies were carried out as outlined in Section 2.8.3.

There are three possible means by which presence of bound antibody can affect binding of a ligand to the α_1 polypeptide. Competitive inhibition will occur if the IgG molecule binds to a peptide which forms part of the binding domain of the ligand. Secondly, the presence of a large antibody molecule, bound to the channel can sterically hinder access of the ligand to its site. This will occur if the ligand binding domain and the binding site of the IgG molecule are in close proximity in the tertiary structure of α_1. Finally, bound antibody can reduce ligand interaction with the channel as a result of allosteric modulation of the ligand binding domain, due to protein-protein interaction between the α_1 polypeptide and the IgG molecule. This will occur if the antibody binds to a site on α_1 in close proximity in the subunit primary structure to part of its site of ligand interaction. PAA and DHP ligands interact allosterically when they occupy their respective sites on opposite sides of the membrane but the DHP site appears to be located in the pore, while PAA's bind at its intracellular entrance. They are therefore quite close in the channel tertiary structure.

6.3 RESULTS

Prior to this study, the specific activity of the t-tubule membrane preparations used for this investigation with regard to both DHP-, and PAA-binding was examined. In order for inhibition of binding of a ligand to a protein to be observed, it is essential that the concentration of the ligand is not saturating for the number of available binding sites present. Therefore, it was first necessary to determine B_{max}, the concentration of specific ligand binding sites present in t-tubule membranes. This was achieved by Scatchard analysis of the data obtained from equilibrium binding assays of [^{3}H]nitrendipine and [^{3}H]D888 to these membranes, carried out as outlined in Section 2.8.2. Figs. 6.3 and 6.5 show Scatchard plot obtained for PN200-110 and D888 binding, respectively, to the t-tubule membrane preparations used in this study. The calculated B_{max} for nitrendipine was 28.3 $\pm$ 9.0 pmol/mg membrane protein, while that for D888 was 21.6 pmol/mg membrane protein.

The calculated K_d for nitrendipine was 1.03 $\pm$ 0.18 nM in the t-tubule preparations used in this study (see Fig 6.3), while the K_d for D888 was determined twice, being 5 nM (see Fig 6.5) and 1.7 nM. The respective quantities of nitrendipine and D888, used in each assay for inhibition of ligand binding to t-tubule membranes, ensured a final concentration of ligand of 2.7nM and 5.4nM, respectively. This is approximately equivalent to the K_d of the receptor for each ligand.

6.3.1 Nitrendipine binding studies

In each of the nitrendipine binding assays individual concentrations of antisera and purified antibody were analysed in duplicate. The results are presented as the graphs (Figs. 6.6-6.10) whose y-axis values represent the specific binding of nitrendipine to the t-tubule membranes as a percentage of that obtained in the absence of primary antibody. No significant inhibition of interaction of nitrendipine with its site in the channel present in the t-tubule membranes was observed as a result of prior

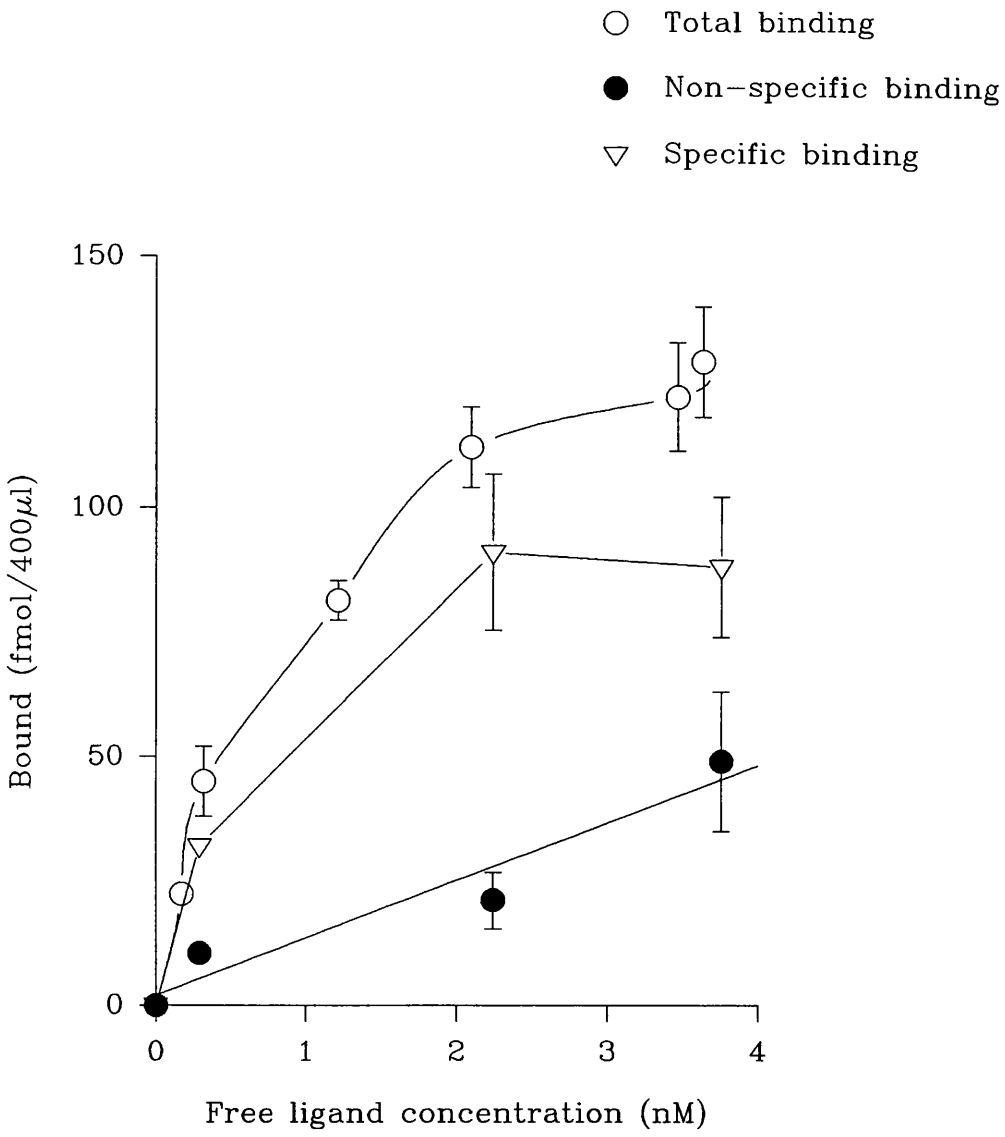

Fig. 6.2 Plot of total, specific and non-specific binding of nitrendipine to t-tubule membranes versus the concentration of ligand present in the assay. Aliquots of t-tubule membranes were incubated with [^{3}H]nitrendipine in 20 mM Tris-HCl, pH 8.0 at final concentrations in the range 0.17-3.6 nM, for 2h. at 4°C. Non-specific binding was determined, in the presence of excess unlabelled nitrendipine. The concentration of t-tubule membrane protein present in the assay was 15μg/ml, while binding at each ligand concentration was examined in duplicate. The error bars represent SEM values (n = 2).

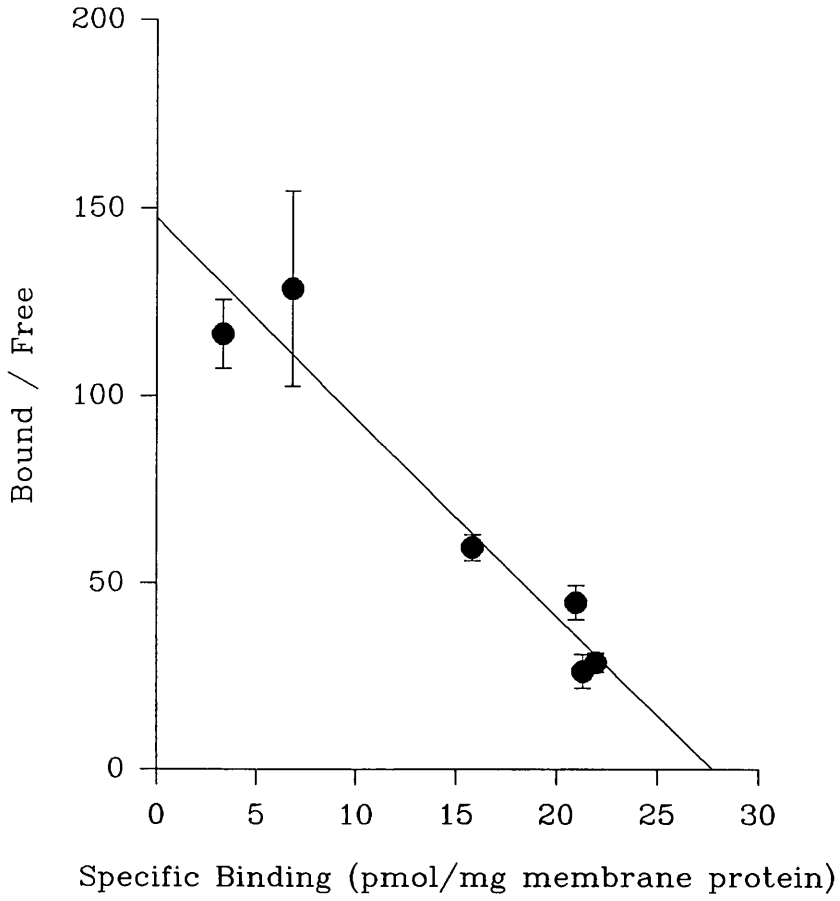

Fig. 6.3 Plot of the amount of bound ligand divided by the amount of free ligand present versus the concentration of bound ligand in the nitrendipine binding assay outlined in the legend to Fig. 6.2. Since the binding at each ligand concentration was examined in duplicate the error bars represent SEM values (n = 2).

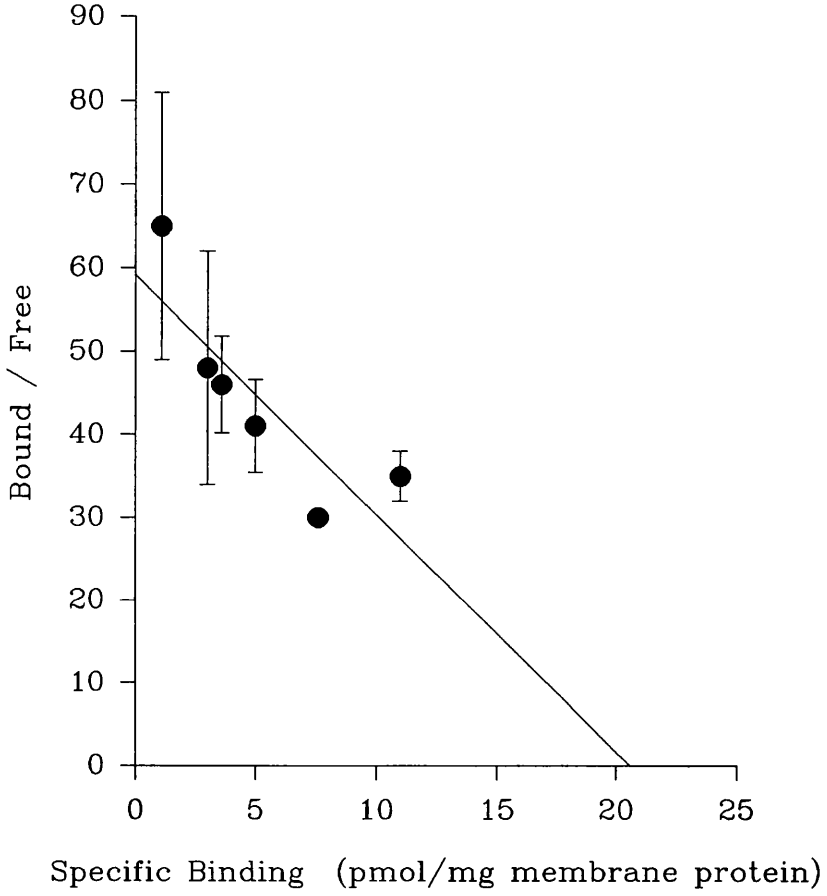

Fig. 6.4 Plot of the amount of total, specific and non-specific binding of D888 to t-tubule membranes versus the concentration of the ligand present. Aliquots of t-tubule membranes were incubated with [^{3}H]D888 in 0.1M Tris-HCl, pH 8.0 at final concentrations in the range 0.17-3.6 nM for 3h. at 20°C. Non-specific binding was determined in the presence of excess cold verapamil. The concentration of t-tubule membrane protein present in the assay was 15μg/ml, while binding at each ligand concentration was examined in duplicate. The error bars represent SEM values (n = 2).

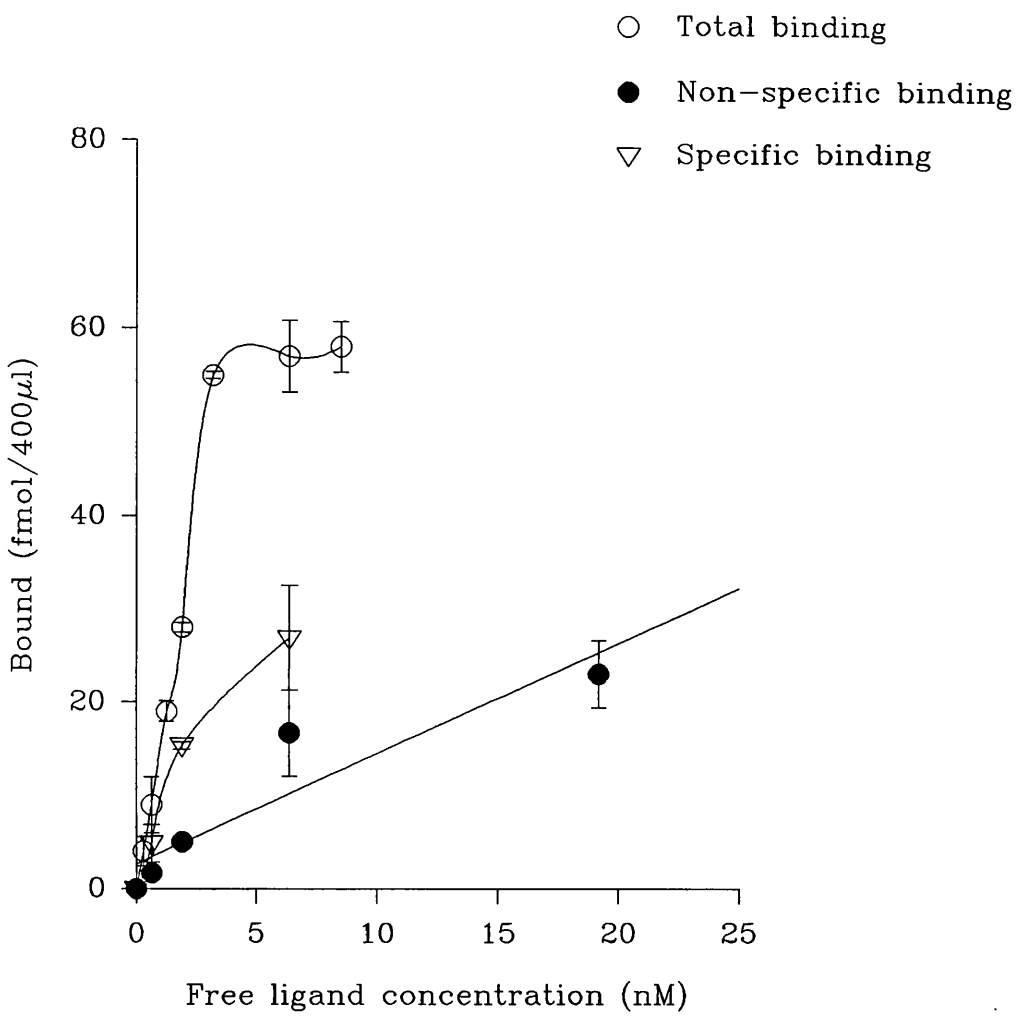

Fig. 6.5 Plot of the amount of bound ligand divided by the amount of free ligand present in the D888 binding assay outlined in the legend to Fig. 6.4, versus the concentration of bound ligand. Since binding at each ligand concentration was examined in duplicate, the error bars represent SEM values (n = 2).

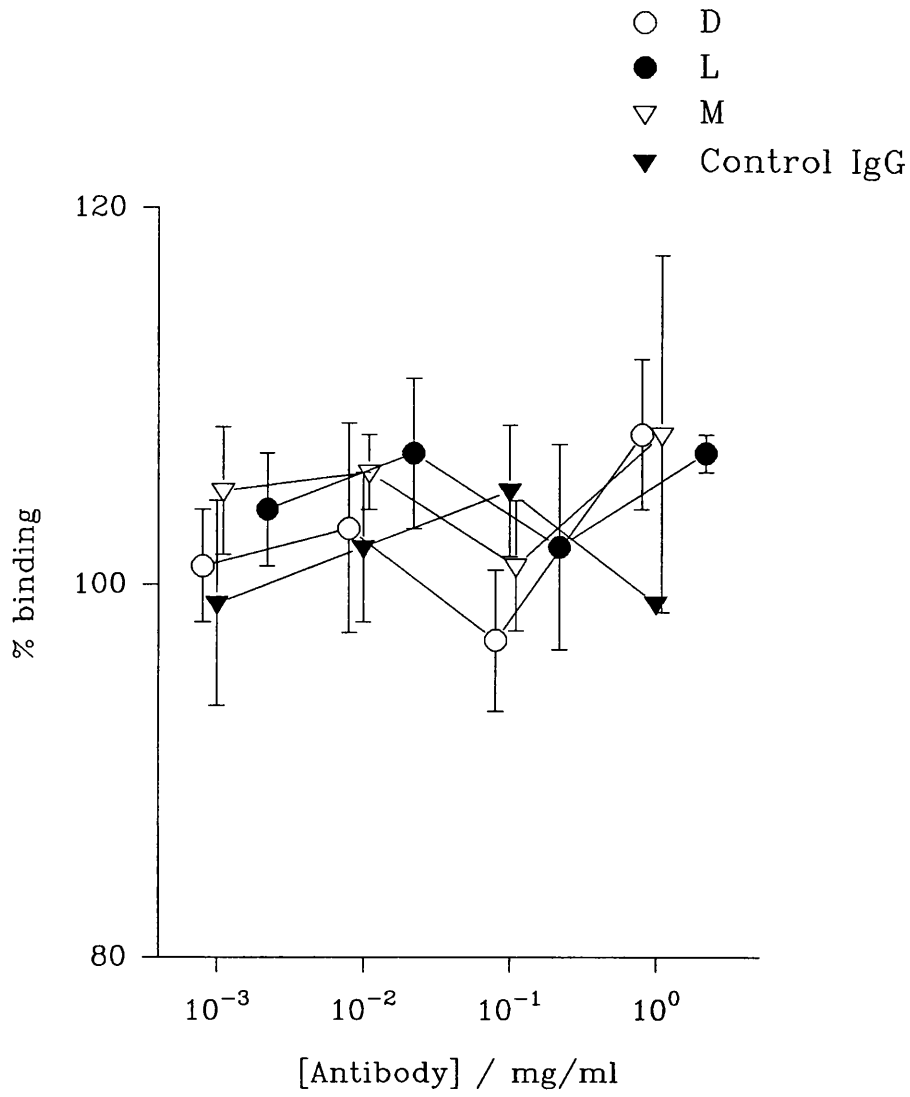

Fig. 6.6 Plot of binding of nitrendipine to t-tubule membranes as a percentage of the binding observed in the absence of antibody versus concentration of control and purified antibodies present. The assay was carried out as outlined in Section 2.8.3. Duplicate samples of control and purified anti-peptide antibodies were incubated at the concentrations indicated, with the membranes (65μg protein) for 16h. at 4°C, in 20mM Tris-HCl, pH 8.0 in a total volume of 0.5ml. The membranes were then incubated with an equal volume of [^{3}H]nitrendipine in 20 mM Tris-HCl, pH 8.0 at a final concentration of 2.7nM, for 2h. at 4°C. Non-specific binding was determined, in the presence of a 370-fold excess of unlabelled nitrendipine (1μM). The error bars represent SD values (n = 4).

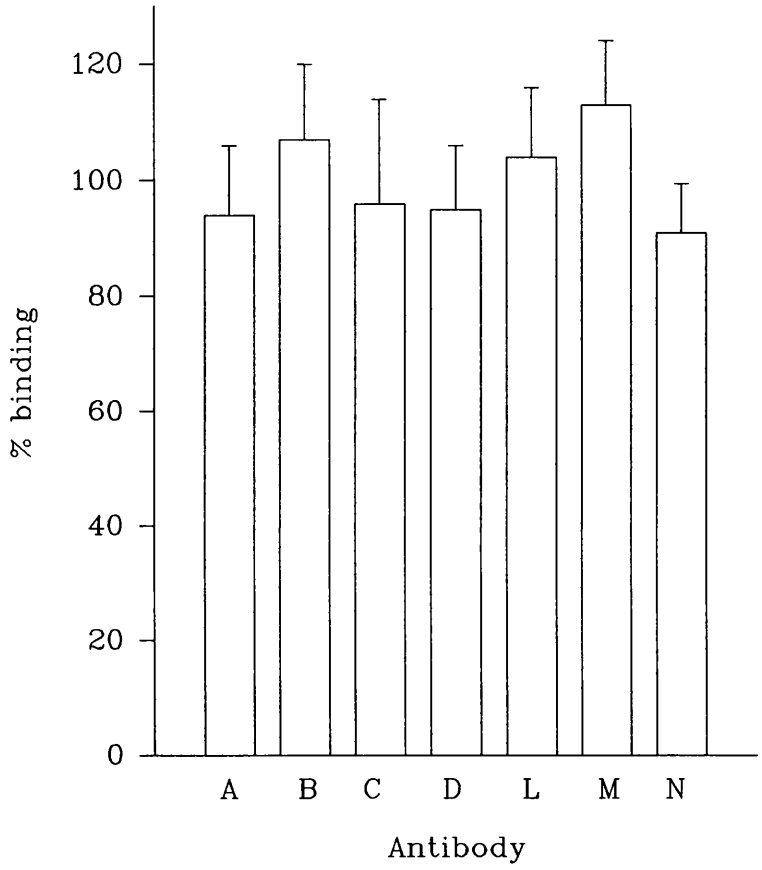

Fig. 6.7 Histogram of binding of nitrendipine to t-tubule membranes in presence of purified antibody given as a percentage of the binding observed in the absence of antibody. The assay was carried out as outlined in Section 2.8.3. Duplicate samples of both control and purified antibodies were incubated at a protein concentration of 0.04mg/ml, with the membranes (65μg protein) for 16h. at 4°C, in 20mM Tris-HCl, pH 8.0 in a total volume of 0.5ml. The membranes were then incubated with an equal volume of [^{3}H]nitrendipine in 20 mM Tris-HCl, pH 8.0 at a final concentration of 2.7nM, for 2h. at 4°C. Non-specific binding was determined, in the presence of a 370-fold excess of unlabelled nitrendipine (1μM). The error bars represent SEM values (n = 4).

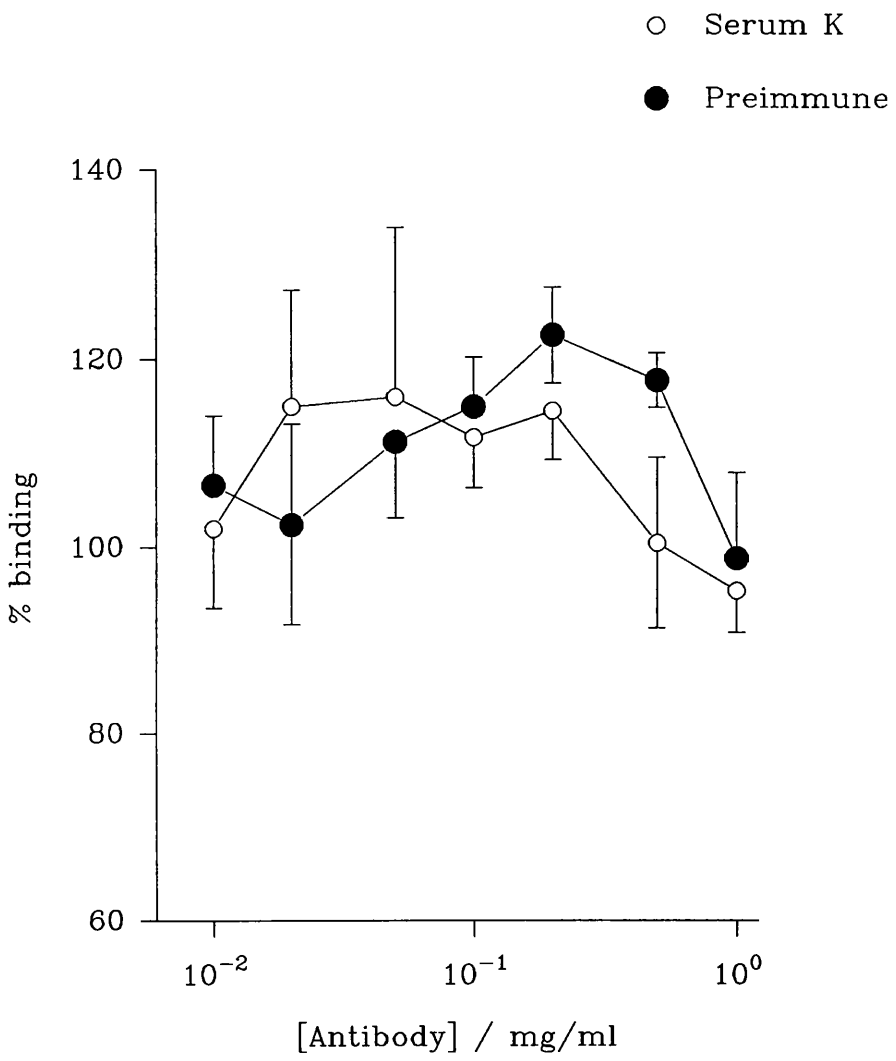

Fig. 6.8 Plot of binding of nitrendipine as a percentage of the binding observed in the absence of antibody versus concentration of preimmune and serum K present. The assay was carried out on seven occasions, as outlined in the legend to Fig. 6.6 using duplicate samples of both preimmune and immune serum at the concentrations indicated. The error bars represent SEM values (n = 7).

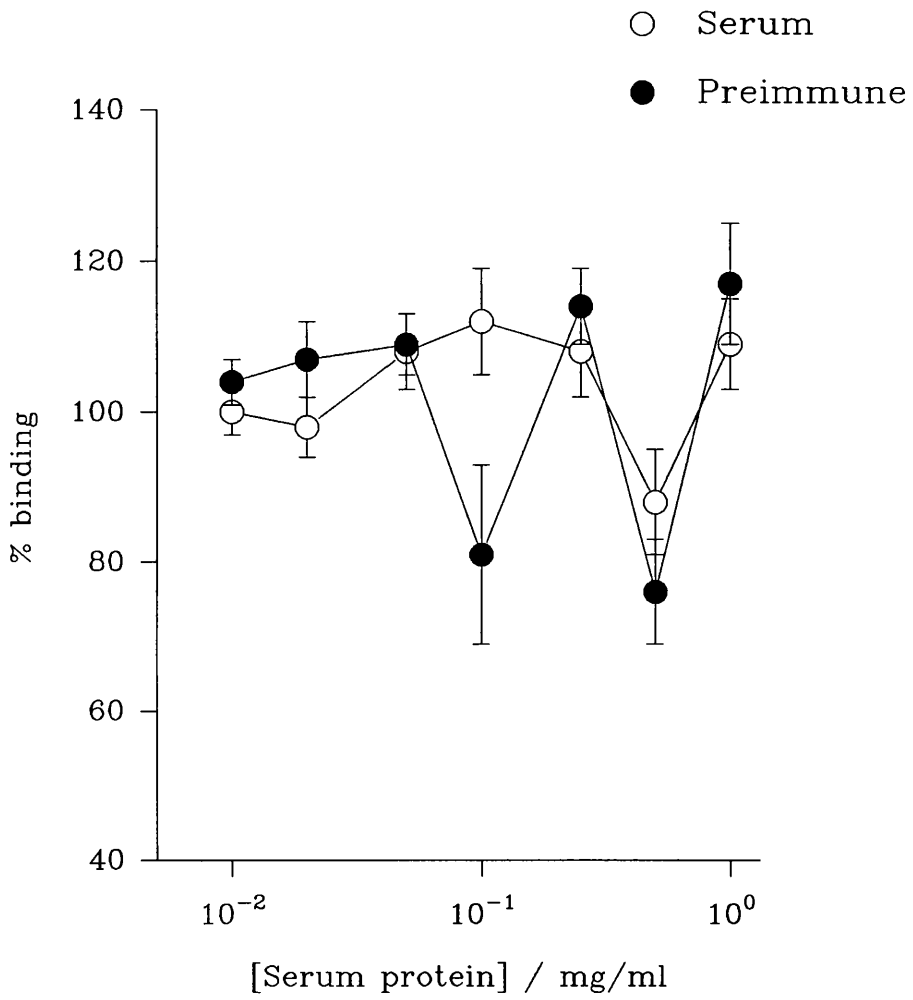

Fig. 6.9 Plot of binding of nitrendipine as a percentage of the binding observed in the absence of antibody versus concentration of preimmune and serum L present in the assay, which was carried out as outlined in the legend to Fig. 6.6 using duplicate samples of both preimmune and immune serum at the concentrations indicated. The error bars represent SEM values (n = 3).

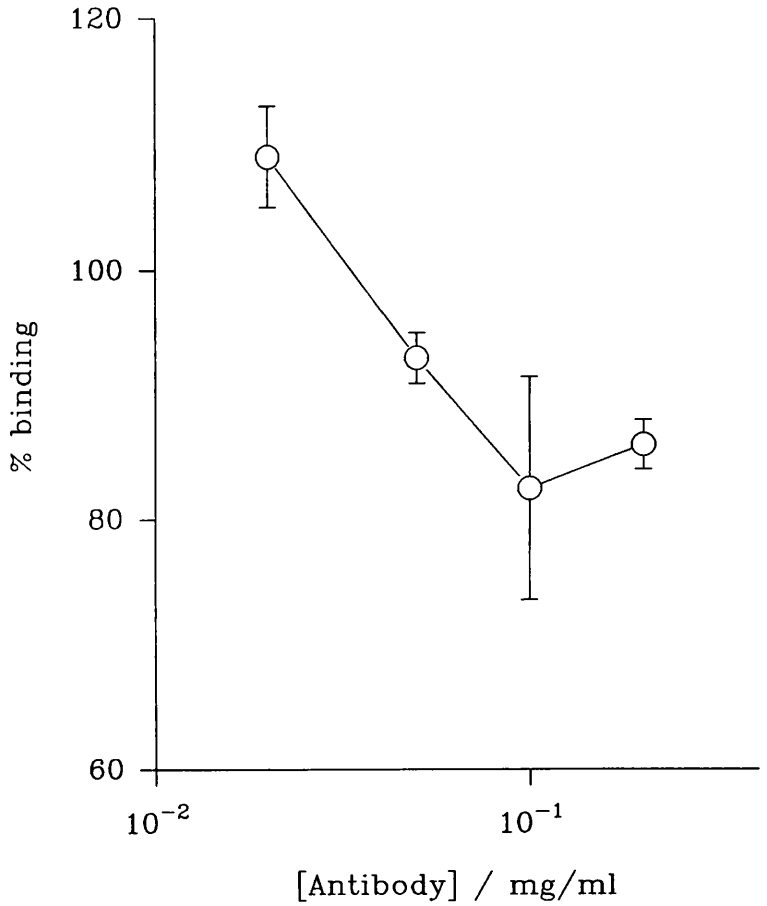

Fig. 6.10 Plot of binding of nitrendipine as a percentage of the binding observed in the absence of antibody versus concentration of purified antibody K present in the assay, carried out as outlined in Section 2.8.3. The assay was carried out as outlined in the legend to Fig. 6.6. The error bars represent the SEM values. Data points for the most and least concentrated antibody dilutions represent the mean of two values, while the second lowest antibody dilution was assayed in triplicate and for the remaining dilution (n = 4).

incubation with affinity-purified antibodies in the concentration range (0.02-20)μg/ml, for antibodies raised against peptides L, M and D (Fig. 6.6). Subsequently, purified antibodies B, C, D, E, L, M, and N, were shown similarly to have no effect on the binding of nitrendipine, even when used at a concentration of 0.04 mg/ml (see Fig. 6.7). Following these findings, another study using a range of antibody concentrations, was undertaken for antibodies K and L, which both bind to α_1 C-terminal to IVS6. Initially, antiserum was used in the concentration range (0.01-1.0)mg/ml. It was estimated that this contained anti-peptide antibodies in the concentration range (0.1-10)μg/ml. Figures 6.8 and 6.9 reveal that nitrendipine binding to the α_1 polypeptide was not affected by presence of either antiserum K or L, respectively. A similar study was undertaken using purified antibody K in the concentration range (0.025-0.2)mg/ml. No inhibition of ligand interaction with α_1 by K, was observed in this concentration range (see Fig. 6.10).

6.3.2 D888 binding studies

In this study no inhibition of D888 binding was observed, following incubation of membranes with these purified antibodies, at a concentration of 0.02mg/ml (Fig. 6.11). Control antibody at the same concentration yielded the same result. Antibody K in the concentration range (0.01-0.08)mg/ml similarly had no effect on the binding of D888 to t-tubules (Fig. 6.12). The PAA D888 is proposed to bind to α_1 at the PAA site located in the C-terminus of the domain between residues 1349 and 1391 in the rabbit skeletal muscle α_1 polypeptide sequence (Striessnig *et al.*, 1990b). Thus, inhibition of binding of D888 to the channel in the presence of either antibody K or antibody J which bind at α_1(1390-1399) and α_1(1399-1418), respectively, would support the above identification of the PAA binding domain.

These antibodies which both bind C-terminal to the IVS6 domain and the previously located PAA site similarly have no effect on binding of D888 to the channel. However, the small D888 ligand molecules may have access to their

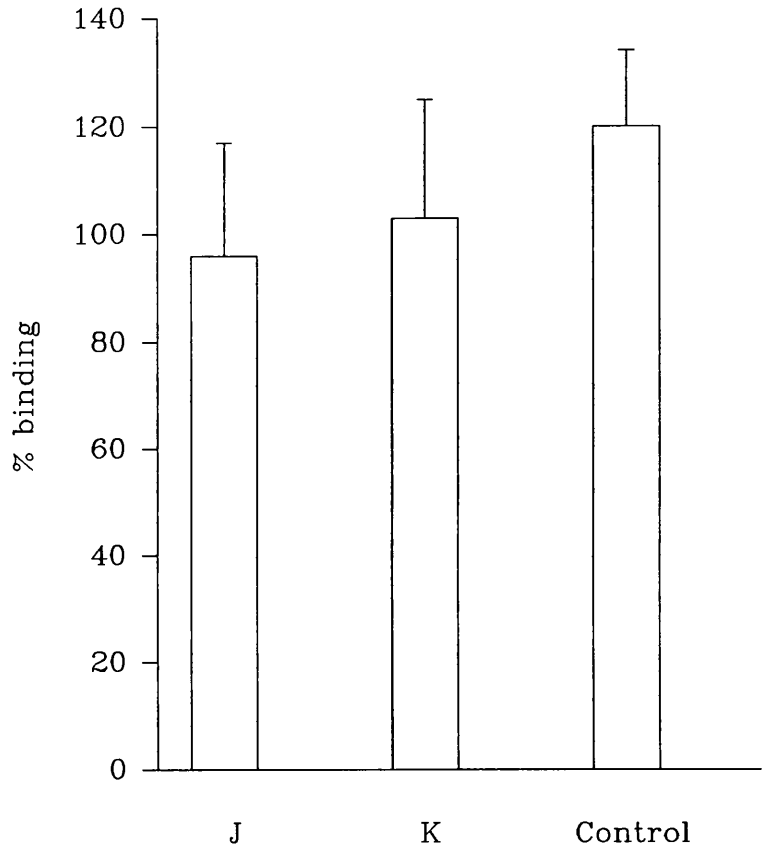

Fig. 6.11 Histogram of binding of D888 to t-tubule membranes in the presence of purified antibody as a percentage of the binding observed in the absence of antibody. Duplicate samples of purified anti-peptide antibody, were incubated at a protein concentration of 0.02mg/ml with the membranes (65μg protein) for 16h. at 4°C, in 0.1M Tris-HCl, pH 8.0 in a total volume of 0.5ml. The membranes were then incubated with an equal volume of [^{3}H]D888 in 0.1M Tris-HCl, pH 8.0 at a final concentration of 5.4nM for 3h. at 20°C. Non-specific binding was determined for D888 in the presence of a 3,700-fold excess of verapamil (200μM). The error bars represent the SEM values (n = 4).

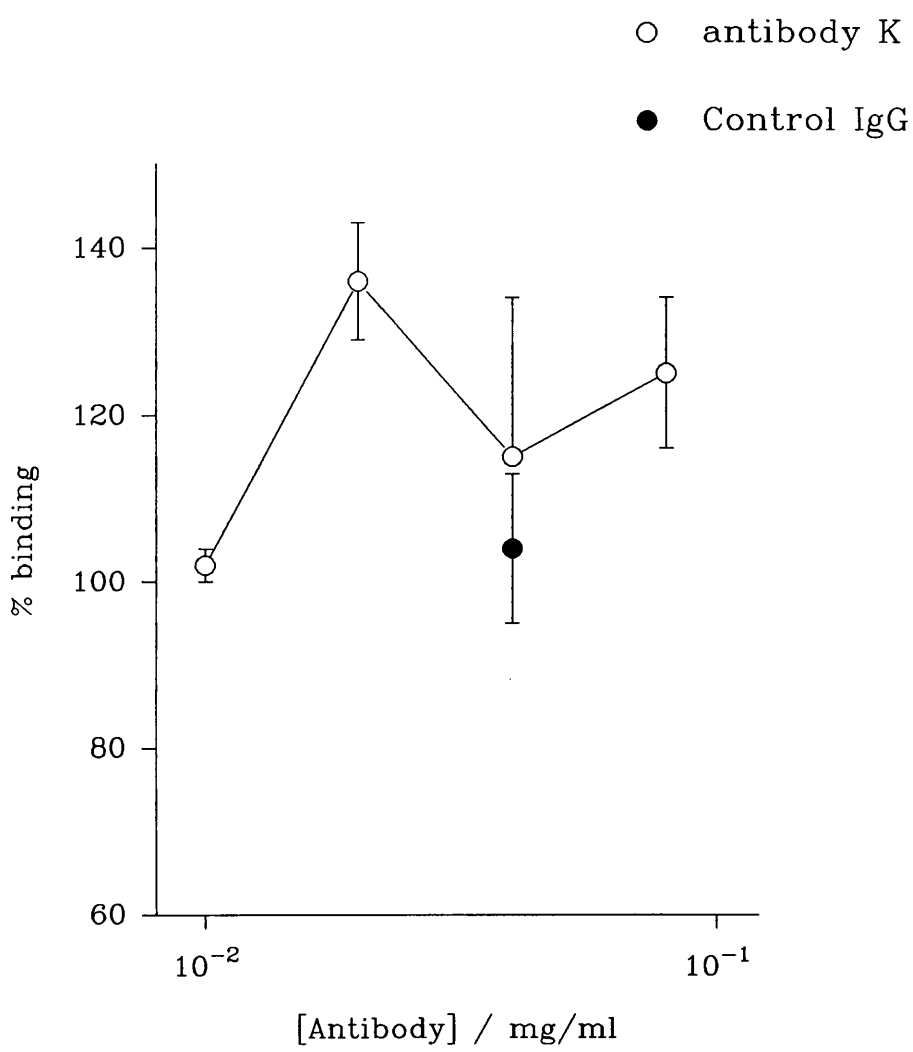

Fig. 6.12 Plot of binding of D888 as a percentage of the binding observed in the absence of antibody versus concentration of purified antibody present in the assay, carried out as outlined in Section 2.8.3. The assay was carried out as outlined in the legend to Fig. 6.11. The error bars represent the SEM values (n = 2).

respective binding domains, in the presence of all channel-bound antibodies, except when the antibodies obscure at least part of the ligand site itself. This may explain the fact that D888 appears to bind to its site on the channel when either antibody K or J are present in close proximity, possibly as little as 20 and 10 amino acids, respectively along the polypeptide primary sequence.

6.3.3 Electrophysiological studies utilizing a number of the peptide-specific antibodies

A further reason for the production of the peptide-specific antibodies was their potential use as probes of functionally important domains of the Ca^{2+} channel. As outlined in Section 3.2.4, studies using anti-peptide antibodies have successfully identified regions in both the Ca^{2+} and Na^{+} channels. Therefore, antibodies A, C, E, L and N were supplied for use as probes of the function of Ca^{2+} channels in NG108-15 cells in whole patch clamp studies. The recordings were carried out on cells following their incubation with either test or control antibody. The results described briefly in this section were generated during the pursuit of a degree of Doctor of Philosophy by Dr. Gary Wilson at the University of Leeds and are published in the thesis of Dr. Wilson (1991).

Some structural and functional information concerning the channels present in the cells, was obtained in the study. Test data obtained in these experiments suggest that antibody C caused a reduction in the inactivation rate of T-type currents. The antibody also appeared to confirm that the IIS4-IIS5 loop is intracellular, since this functional effect was obtained following internal application of antibody and suggests that this domain is involved in channel inactivation. The antibody generated using peptide E α_1(1089-1100) reduced I_{diff} possibly changing the kinetics of one or more of the channel types. E had an intracellular action consistent with the idea that the loop between domains III and IV has an intracellular orientation. The antibody which recognized the intact skeletal muscle channel α_1 polypeptide in the C-terminal peptide

L sequence between residues no. 1555 and 1569 had no effect on channel currents in differentiated NG108-15 cells when applied to the intracellular solution.

The most interesting effect was obtained using the antibody that was raised using peptide A. It caused significant reductions in T-type and N-type channel currents in NG108-15 cells, following 24h. incubation with the cells. This was possibly due to a down-regulation process such as internalization of the channel-antibody complex. This implied that this sequence of the skeletal muscle channel is antigenically and structurally similar to presumably equivalent regions of the T-type and N-type channels. Indeed the sequence of peptide A is now known to be identical in both rabbit skeletal muscle and rat brain N-type α_1 (Tanabe *et al.*, 1987; Dubel *et al.*, 1992). Following intracellular application of the antibody no effect was observed. These findings demonstrate that the sequence corresponding to peptide A recognized by this antibody has an extracellular location in the channel α_1 polypeptide.

This study lends some support to the predicted model for the membrane arrangement of the α_1 subunit shown in Figs. 1.6 and 3.3. The peptides C and E apparently having intracellular orientation, while peptide A seems to be extracellular. A further finding of note was that antibody N which binds to α_2 had no effect following internal application to cells. Its domain was predicted to be intracellular by Ellis *et al.* (1988), while Jay *et al.* (1991) suggest an external orientation for the entire α_2 polypeptide.

6.4 DISCUSSION

6.4.1 Nitrendipine binding studies

The calculated B_{max} of the t-tubule membranes for nitrendipine were 28.3 ± 9.0 pmol / mg membrane protein and the K_d value for the receptor-nitrendipine complex was 1.03 ± 0.18 nM. These compare well with B_{max} values of t-tubule membranes purified by other workers, for nitrendipine. These vary from a value of 8.5 pmol, (Murphy and Tuana, 1990) and 18 pmol, (Goll *et al.*, 1984) binding sites / mg membrane protein to values of the order of 40-50 pmol receptor sites / mg membrane protein (Fosset *et al.*, 1983; Chang and Hosey, 1988). Previously measured K_d values for the nitrendipine-receptor complex were 1.8 ± 0.3 nM (Fosset *et al.*, 1983). Thus the final concentration of nitrendipine used in each assay (2.7nM) was close to the K_d of the receptor for nitrendipine.

The lack of significant inhibition by any of the affinity-purified antibodies B, C, D, E, L, M, and N, compared to control rabbit non-immune IgG, of nitrendipine binding to its site in the channel in the t-tubule membranes following prior incubation of the antibodies at a concentration of 0.04 mg/ml with the membranes (see Fig. 6.7). Following these findings, another study was undertaken using antibodies K and L which both bind to α_1 C-terminal to IVS6. Antiserum was initially used with the view that should an inhibitory effect on nitrendipine interaction with the channel be observed, this would be further investigated by examining the effect of different concentrations of purified antibody. The concentration range of serum protein present in the assay was (0.01-1.0)mg/ml. At concentrations above this value a non-specific protein effect is observed in the assay.

Figures 6.8 and 6.9 reveal that nitrendipine binding to the α_1 polypeptide was not affected by presence of either antiserum K or L which was estimated to contain anti-peptide antibodies in the concentration range (0.1-10)μg/ml. A similar study was undertaken using purified antibody K in the range (0.025-0.2)mg/ml. The results in Fig. 6.10 reveal no inhibition of ligand interaction with α_1 by K, in this concentration

range.

It appears that when bound to the channel antibodies B, C, D, E, K, L and N, fail to inhibit interaction of DHP with its binding site on the channel. This may be because none of the regions recognized by these antibodies are located in close proximity to the DHP binding domain, either in the primary or tertiary structure of the α_1 polypeptide. Since all of these antibodies have predicted intracellular binding sites, this lack of effect is consistent with the finding of an extracellular DHP site in α_1.

As already stated, Regulla *et al.*, (1991) identified a major site in the channel, for nitrendipine binding, in peptide α_1(1390-1399), while that for azidopine was located in α_1(1428-1437). Antibody K is specific for the peptide α_1(1399-1418) and antibody L binds at α_1(1555-1569). If these identified DHP sites form part of the high affinity domain for the ligand, then antibodies K and L could cause inhibition of the interaction of this ligand with the channel. However, it appears that neither of these antibodies bind near the DHP site, suggesting that the high-affinity binding domain for nitrendipine does not include peptide α_1(1390-1399). However, the small lipophilic DHP molecule (300 Da) is thought to approach their site from within the membrane lipid bilayer (Hess *et al.*, 1984; Reuter *et al.*, 1985). Thus, its may in fact be difficult to inhibit access of this ligand using peripherally bound antibodies.

6.4.2 D888 binding studies

The calculated B_{max} and K_d values for D888 were 21.6 pmol/mg membrane protein and 5 nM and 1.7 nM, respectively. The B_{max} value should be the close to that obtained for nitrendipine binding sites in the membrnaes. The lower value indicates that a smaller proportion of the protein present in the t-tubule membranae preparation used in this part of the study is contributed by the L-type Ca^{2+} channel. However, the B_{max} value compares well with those obtained in t-tubules purified by Murphy and Tuana, (1990) and Goll *et al.*, (1984). K_d values for D888 were not available in the literature. However, the K_d of the complex formed by the receptor and the PAA (-)-

[^{3}H]Desmethoxyverapamil previously measured as 2.2 ± 0.1 nM (Goll $_{et\ al.}$, 1984). The final concentration of D888 used in each assay for inhibition of ligand binding to the t-tubules (5.4nM) was close to the K_d of the receptor for the ligand.

The PAA D888 is proposed to bind to α_1 at the PAA site located in the C-terminus of the domain between residues 1349 and 1391 in the rabbit skeletal muscle α_1 polypeptide sequence (Striessnig *et al.*, 1990b). Thus, inhibition of binding of D888 to the channel in the presence of either antibody K or antibody J which bind at α_1(1390-1399) and α_1(1399-1418), respectively, would support the above identification of the PAA binding domain. However, in this study no such inhibition of D888 binding was observed, following incubation of membranes with these purified antibodies, at a concentration of 0.02mg/ml (Fig. 6.11). Control antibody at the same concentration yielded the same result. Antibody K in the concentration range (0.01-0.08)mg/ml similarly had no effect on the binding of D888 to t-tubules (Fig. 6.12).

These antibodies which both bind C-terminal to the IVS6 domain and the previously located PAA site similarly have no effect on binding of D888 to the channel. However, the small D888 ligand molecules may have access to their respective binding domains, in the presence of all channel-bound antibodies, except when the antibodies obscure at least part of the ligand site itself. This may explain the fact that D888 appears to bind to its site on the channel when either antibody K or J are present in close proximity, possibly as little as 20 and 10 amino acids, respectively along the polypeptide primary sequence.

CHAPTER 7

IMMUNOLOGICAL IDENTIFICATION OF NEURONAL AND CARDIAC CALCIUM CHANNEL SUBUNITS IN BRAIN AND MUSCLE

7.1 GENERAL INTRODUCTION

With the exception of the skeletal muscle t-tubule L-type channel, Ca^{2+} channels are present as very low abundance membrane components. As discussed in Section 1.9.5.2, Ca^{2+} channels, purified from brain (Takahashi and Catterall., 1987; Ahlijanian *et al.*, 1990; McEnery *et al.*, 1991; Sakamoto and Campbell, 1991a, 1991b) and cardiac (Cooper *et al.*, 1987; Chang and Hosey., 1988; Schneider and Hofmann, 1988; Haase *et al.*, 1991; Tokumaru *et al.*, 1992) membranes, have been shown to consist of α_1, α_2/δ and ß polypeptides. This has been verified as a result of the elucidation of cDNA sequences for these channel polypeptides from various membrane sources (see Section 1.9.7).

With regard to the $Ca2^{+}$ channel α_1 subunit, the skeletal and cardiac muscle polypeptides were found to be structurally and immunologically distinct (Chang and Hosey., 1988), while the latter was immunologically similar to an ^{125}I-ω-CgTx binding brain α_1 polypeptide (Sakamoto and Campbell, 1991a, 1991b). The diversity of α_1 subunits was verified by elucidation of the cDNA sequences for these polypeptides from various tissues (discussed in section 1.9.10.1). α_1 polypeptides whose sequences have been determined fit structurally into five classes, denoted, A, B, C, D and E (Snutch *et al.*, 1990; Soong *et al.*, 1993). Rat brain contains all five polypeptides, which are possibly associated with a common rat brain α_2 subunit. Rat brain A and B clones are highly homologous to each other but are less closely related to the skeletal and cardiac clones (33% for A) than C and D (Starr *et al.*, 1991; Dubel *et al.*, 1992). The rat brain class C α_1 polypeptides are 95% identical to both the rabbit heart and lung and 70% homologous to the skeletal muscle α_1 subunit

(Snutch *et al.*, 1991). D class α_1 subunits show 71% and 76% similarity, respectively, to the rabbit skeletal and cardiac muscle proteins (Hui *et al.*, 1991). Class E polypeptide is most closely related to class A and class B with 53-54% identity to both polypeptides (Soong *et al.*, 1993).

In contrast, the α_2 subunits from cardiac and skeletal muscle and brain channels were seen to be electrophoretically and immunologically similar (Takahashi and Catterall., 1987; Chang and Hosey., 1988; Hayakawa *et al.*, 1990; Sakamoto and Campbell, 1991a, 1991b; Tokumaru *et al.*, 1992), while the two deduced brain α_2 subunit sequences differ at just 51 and 43 amino acid residues, respectively, from their skeletal muscle counterpart (Ellis *et al.*, 1988; Kim *et al.*, 1992; Williams *et al.*, 1992a).

7.2 INTRODUCTION TO THE STUDY

7.2.1 Cardiac channel polypeptides

Cardiac channel α_1/α_2 complexes have been isolated from porcine (Haase *et al.*, 1991) and chick (Cooper *et al.*, 1987) heart membranes, while individual α_1 and α_2 polypeptides, respectively, have been obtained from bovine (Schneider and Hofmann, 1988) and porcine (Tokumaru *et al.*, 1992) membranes. However, the sole cardiac Ca^{2+} channel polypeptide whose primary structure has been elucidated is the α_1 subunit of the L-type channel in rabbit heart (Mikami *et al.*, 1989). The cardiac channel α_2 subunits are probably highly conserved amongst mammalian species, since the human (Williams *et al.*, 1992a) and rat (Kim *et al.*, 1992) neuronal and rabbit (Ellis *et al.*, 1988) polypeptides are very similar.

As discussed in Section 3.2.2, the various subunits of the L-type Ca^{2+} channel have been co-localized, in both rat and rabbit skeletal muscle, to the t-tubule membranes, by means of either immunogold or immunofluorescence detection using subunit-specific antibodies. However, no such work has been carried out to date in

mammalian cardiac tissue. This is presumably because the cardiac DHP receptor had been estimated to be 50-100-fold less abundant in cardiac membranes compared to its skeletal muscle t-tubule counterpart (Fosset *et al.*, 1983; Glossmann *et al.*, 1983). However, this cardiac channel is now known to be 3-fold more abundant in mammalian cardiac t-tubules than in external sarcolemma (Wibo *et al.*, 1991).

The aim of the study was to localize the channel α_1 and α_2 polypeptides in cardiac muscle by means of similar immunofluorescence studies, using sections of rabbit, rat and porcine cardiac tissue and anti-peptide antibodies which are known to recognize these subunits in the rabbit skeletal muscle L-type channel. Additionally, information on the structure of the rabbit, rat and porcine cardiac channel α_1 and α_2 subunits could also be obtained, by comparing the reactivity of the various site-specific antibodies with their polypeptides in both rat, porcine and rabbit tissue. Since, rabbit ventricular tissue has been seen to have 10 times the quantity of t-tubule membranes that are found in the atrium (Tidball *et al.*, 1991), mammalian ventricular muscle was used in this study.

7.2.2 Neuronal channel polypeptides in brain

Neuronal channels are present in such low abundance in brain membrane preparations that no identification of a Ca^{2+} channel α_1 polypeptide in such preparations using immunoblotting techniques has been reported. It is possible to determine the density of some of the channel α_1 polypeptides which bind radiolabelled ligands with high affinity. In this way, the density of DHP receptors was previously determined to be 112fmol/mg protein in rat brain P2 membranes (Boles *et al.*, 1984) and 80 fmol/mg protein in rat brain lysed P2 membranes (Curtis and Catterall, 1983). Both of these preparations were carried out according to protocols similar to those outlined in Section 2.5.4. However, since the α_2 polypeptide has not been observed to bind ligands this approach cannot be used to estimate the density of this subunit in brain membranes. If all rat brain α_1 subunits are associated with the same α_2 polypeptide this polypeptide would be present in higher concentrations than individual

α_1 polypeptides in brain membrane preparations and therefore, may be detectable, in immunoblots. In order to investigate this a comparative study of the relative abundance of this polypeptide in the various membrane preparations from brain and in the purified t-tubule membranes was carried out.

7.2.3 Neuronal-type channel polypeptides in muscle

Evidence has recently emerged for the presence of at least one other Ca^{2+} channel in skeletal muscle, besides the currently identified L- and T-type. In human skeletal muscle cells, a further Ca^{2+} current, along with the previously described L- and T-type was identified, which resembled an N-type current, but was nevertheless insensitive to ω-CgTx (Rivet *et al.*, 1992). Another study, revealed two polypeptides present in rabbit skeletal muscle, having M_r values of 160,000 and 165,000, which are immunologically related to the L-type Ca^{2+} channel α_1 polypeptide (Brawley and Hosey, 1992). This study employed three antibodies, raised using synthetic peptides corresponding to both the C- and N-terminus and a region in the IIS6-IIIS1 loop of the rabbit skeletal muscle DHP receptor α_1 polypeptide, in immunoblots of various skeletal muscle membrane fractions. The N-terminal and II-III loop, but not the C-terminal, antibodies reacted with the 165,000 polypeptide which was seen to be enriched in t-tubule membranes, while the N- and C-terminal, but not the II-III loop specific anti-peptide antibodies recognized the 160,000 subunit, which was found to be enriched in triad and junctional SR membranes, but was not found in t-tubules. The former polypeptide bound to WGA-Sepharose, while, under the same conditions the latter did not. The 165,000 α_1 polypeptide has tissue localization and also biochemical and immunological properties expected of the truncated DHP receptor α_1 subunit. The smaller, immunologically related, polypeptide had not previously been identified.

Mammalian skeletal muscle thus appears to contain a ω-CgTx-insensitive N-type channel, whose cellular location is unknown and possibly a further channel which appears to be located in the SR at the triad and junctional regions, whose

physiology and pharmacology has not been defined. In light of these findings of diverse skeletal muscle Ca^{2+} channels, it was considered worthwhile to probe both mammalian skeletal muscle sections and membranes, using antibodies H and I which are specific for rat brain class A and D α_1 polypeptides, respectively. The former was employed in the immunocytochemical technique, outlined in Section 2.6, in rabbit skeletal muscle sections and also in immunoblotting with t-tubule membranes. Antibody I had previously been shown to react weakly with the intact rabbit skeletal muscle DHP receptor α_1 subunit in both its denatured (in immunoblots) and native (ELISA with purified channel) conformations (results not shown).

7.3 RESULTS

7.3.1 Cardiac Ca^{2+} channel polypeptides

Antibodies B, C, E, J and K are specific for peptide sequences which are either identical or very similar in both rabbit skeletal and cardiac muscle L-type channel α_1 subunits. These antibodies, along with antibody N which is specific for an internal domain in the L-type Ca^{2+} channel α_2 polypeptide, which each reacted with their intact rabbit skeletal muscle Ca^{2+} channel polypeptide in immunoblots (Figs. 4.24 and 4.25), ELISA with purified receptor (Figs. 5.1-5.7) and immunocytochemistry in muscle cryosections were used to examine the distribution of these channel subunits in rabbit, rat and porcine cardiac muscle. This was carried out according to the method for immunostaining outlined in Section 2.7.2, using biotinylated second antibody and Streptavidin-Texas Red detection, in unfixed cryosections of rabbit, rat and porcine cardiac muscle.

A identical pattern of staining of varying intensity was also obtained in both rabbit and rat sections, using each of the antibodies B, C, E, K and N, which was not obtained using control primary antibody. Fig. 7.1 shows the staining obtained using

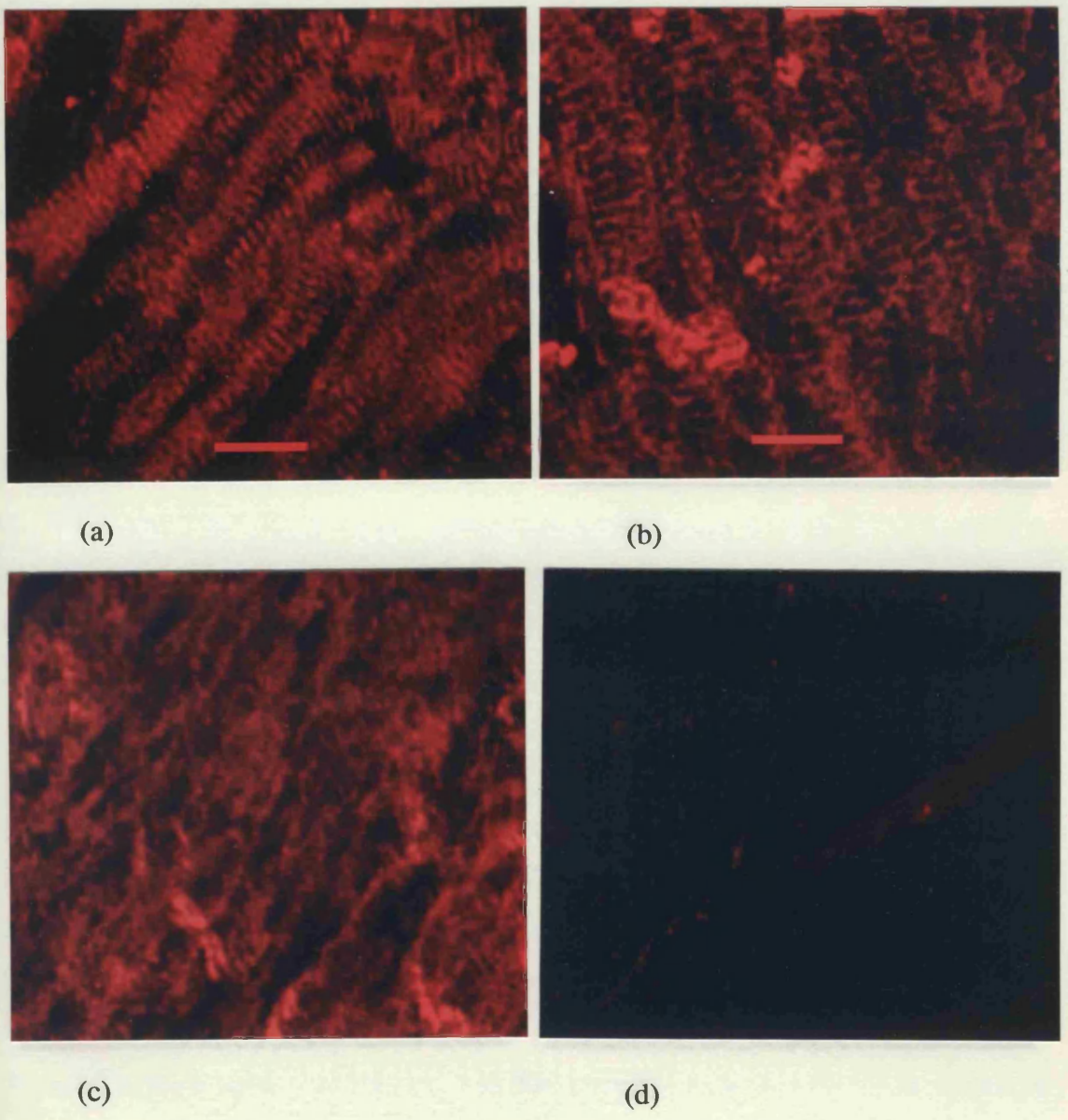

Fig. 7.1 Immunostaining of rabbit cardiac ventricular muscle longitudinal cryosections incubated with primary antibodies (a) B, (b) E, (c) N and (d) control rabbit IgG, each at concentrations of 40μg/ml. The magnification is 40x and the scale bar 10μm.

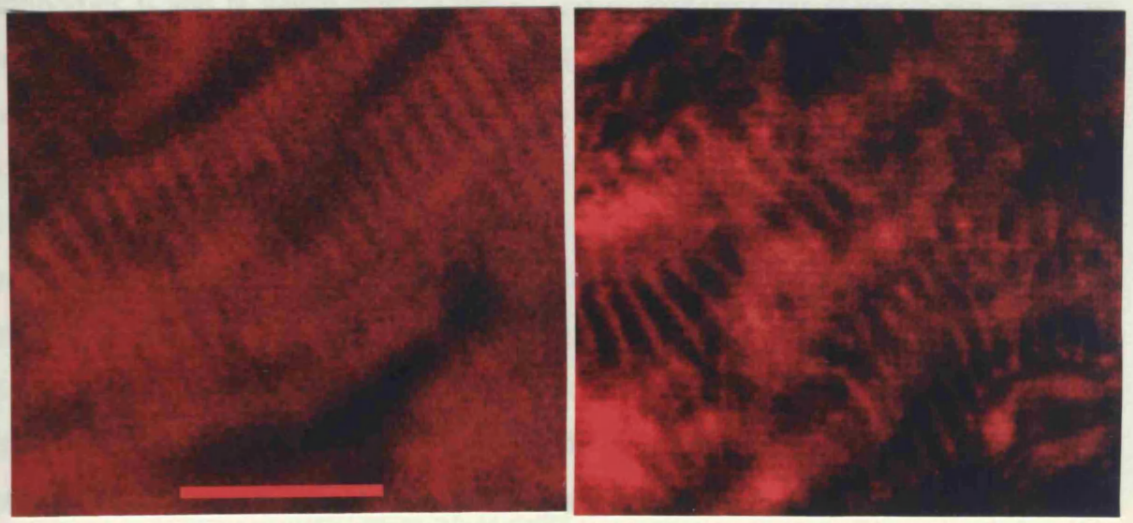

(a)

(b)

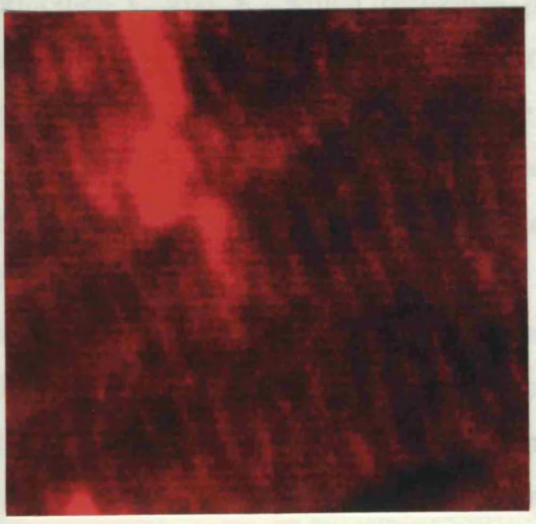

(c)

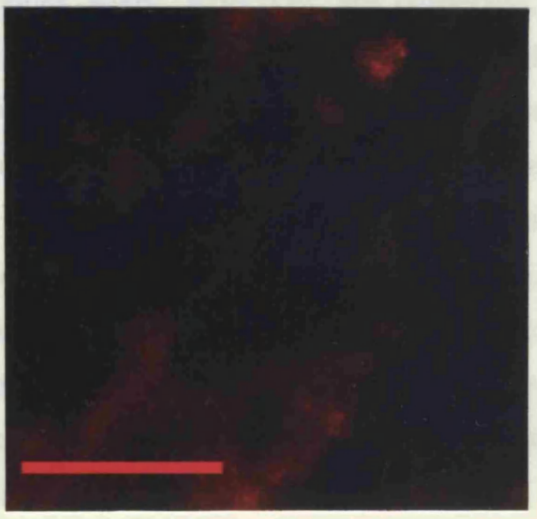

(d)

Fig. 7.2 Longitudinal sections of rabbit cardiac ventricular muscle cryosections, prepared, immunostained, using streptavidin-Texas Red, and examined, as outlined in Section 2.6. The primary antibody incubated with each section was as follows (a) B, (b) E, (c) N and (d) control rabbit IgG at concentrations of 40μg/ml. Each print shows 100x magnification of the relevant section. The scale bar corresponds to 10μm.

antibodies B and N which bind to the α_1 and α_2 polypeptides respectively. Sections which had been incubated with antibody L and control IgG are also shown. The pattern locates the channel to the t-tubule system of the cardiac tissue, which in longitudinal sections of rat ventricular muscle reveals a separation of approximately 1.4μm between individual tubules (Ogata and Yamasaki, 1990). There is a spacing of 1.1-1.4μm between each of these parallel membranes as is revealed by the number of membranes (7-9) per space bar of 10μm (see Figs 7.1).

The most intense staining of α_1 was obtained using antibody B. This antibody is specific for the IS4 peptide domain which is identical in the L-type channel α_1 of both rabbit skeletal and cardiac muscle α_1 subunits (Tanabe *et al.*, 1987; Mikami *et al.*, 1989) (see Fig 3.2). The least intense detectable staining was observed using both antibodies C and K, which recognize peptides whose sequences are conserved, respectively, at 17 out of 19 and 19 out of 20 of their residues, in rabbit heart and skeletal muscle. Antibody E identified the cardiac channel with greater intensity than C and K, binding to a 10 amino acid sequence differing in just a single residue between both channels. Staining of greater intensity to E but less intense than that obtained using antibody B was observed with antibody N, which is specific for α_2 subunit. The staining obtained using antibodies B, E, N and control IgG is shown at 100x magnification in Figure 7.2 (space bar 10μm) and at 40x magnification in Figure 7.1. At greater magnification a spacing between the labelled membranes of (1.3-1.4)μm is also revealed since (7-9) membranes occur per 10μm.

The same pattern of staining was obtained for antibodies B, C, E, K and N in rat and B, C, E, K and N in porcine cardiac ventricular cryosections (results not shown). In rat tissue, the most intense staining was observed using antibodies B and E, while that obtained using C and N was fainter, while antibody K reacted with the least intensity. Differences in staining intensity between rat and rabbit were observed, for antibodies C and E (stronger than in rabbit) and for antibody K and N (fainter than in rabbit). In porcine cardiac muscle, theintensity of staining obtained using antibodies B, E, and N was similar to that obtained using rabbit tissue, while antibodies C and K apparently reacted more strongly with the porcine compared to

the rabbit channel α_1 subunit.

7.3.2 Brain Ca^{2+} channel α_1 polypeptides

The α_1 polypeptide of the rabbit skeletal muscle L-type channel were detectable in this study, using the Western blotting techniques outlined in Section 2.6.4, when 10μg t-tubule membrane proteins were loaded on the gel (results not shown). However, antibodies H and I failed to recognize the Class A and Class D α_1 polypeptides, respectively, when 500μg whole rat brain or rat cerebellar P2 membranes (prepared as outlined in Section 2.5.4) were used. Antibodies recognizing peptides B, J and K, which are known to bind to intact denatured (see Figs. 4.11 and 4.12) and native (see Figs. 5.1-5.9) channel α_1 polypeptide from skeletal muscle, at domains conserved in all channels, similarly failed to identify this subunit in rat brain membranes.

7.3.3 Brain Ca^{2+} channel α_2 polypeptides

Staining of a band corresponding to a protein of apparent M_r value 143,000 was observed in immunoblots of both rat whole brain lysed and unlysed P2, cerebellar P2 and skeletal muscle t-tubule, membranes using antibody H (see Figs. 7.3 and 7.4). The specificity of this staining is indicated by its absence when rabbit nonimmune IgG control primary antibody was used (Figs. 7.3 and 7.4). A polypeptide of corresponding size was previously identified in immunoblots of rabbit skeletal muscle t-tubules using both purified antibodies M and N as the α_2 subunit of the Ca^{2+} channel. The identification of a polypeptide having the same apparent M_r value in both lysed and unlysed rat whole brain P2 membranes and in rat cerebellar P2 membranes indicates binding of antibody N to the rat brain Ca^{2+} channel α_2 subunit, since the size of the rat brain Ca^{2+} channel α_2 polypeptides is very close to that of the rabbit skeletal muscle isoform. The intensity of these particular bands in each of the blot lanes which contain protein from one of the three brain membrane

fractions appears to be proportional to the amount of membrane protein present that particular blot lane.

In Fig. 7.4, background staining of similar pattern was obtained in the lanes immunoblotted using both control IgG and antibody H. In Fig. 7.3, the lanes containing brain

membranes contained more background when probed using antibody H compared to control IgG. A single intense background band corresponding to a protein having apparent M_r value 85,000 was obtained using control IgG in the blot lanes containing brain proteins which was not apparent in the equivalent lanes immunoblotted with antibody H (see Fig 7.3). This band was not evident in blot lanes containing 153μg or less of brain proteins (see Fig 7.4) which were probed using control IgG. However, a band of similar intensity was obtained when similar quantities of brain membrane proteins to those immunoblotted in Fig. 7.3 were again probed using control IgG (results not shown).

In the blots shown in Fig. 7.3, where the gel samples of whole brain membranes (lanes 3 and 7) contained a 27-fold excess of protein over the t-tubule samples (lanes 2 and 6) and the band corresponding to the channel α_2 subunit is stained more intensely in the lane containing brain membrane rather than that containing t-tubules. However, α_2 is stained less intensely in the whole brain P2, compared to the t-tubule membranes in Fig. 7.4, when an 8.7-fold excess of brain over t-tubule membrane protein is present in the gel samples for lanes 3 and 7 and 2 and 6, respectively. More intense staining of α_2 polypeptide is evident in the cerebellar P2 fraction compared to the t-tubule membrane sample, when the gel samples of the former purification contain a 35-fold excess of protein over the t-tubule membrane purification in the gel samples for lanes 5 and 9 and lanes 2 and 6, respectively (Fig. 7.3). In Fig. 7.4, when a 7.1-fold excess of the brain over the t-tubule membrane proteins in gel samples for lanes 4 and 8 and 2 and 6, respective a less intense band corresponding to the channel α_2 subunit is observed in the lane containing cerebellar membrane.

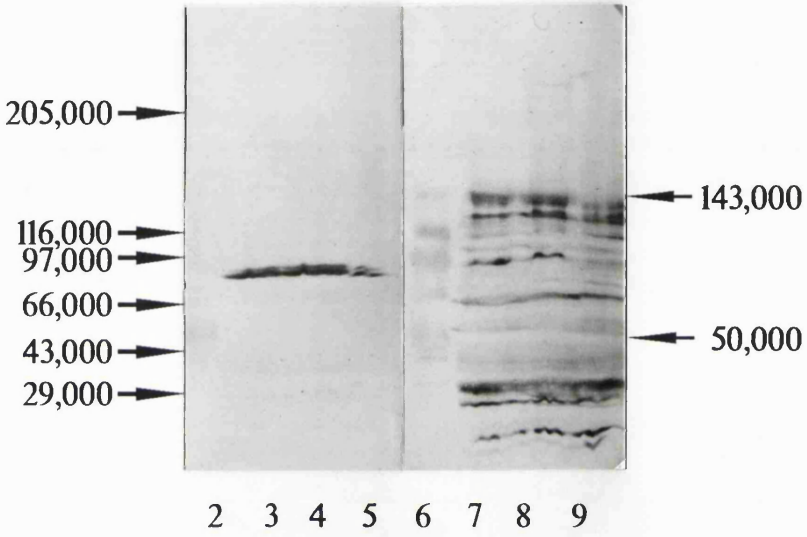

Fig. 7.3 Western blot of rabbit muscle and rat brain membranes using antibody N. Gel samples were loaded as follows: lanes 1 and 10 molecular weight markers (Sigma); lanes 2 and 6, rabbit skeletal muscle t-tubule membranes (10μg); lanes 3 and 7, rat whole brain P2 membranes (270μg); lanes 4 and 8, lysed rat whole brain P2 membranes (600μg) and lanes 5 and 9, rat cerebellar P2 membranes (350μg). Immunoblotting was carried out using both control (lanes 2-5) and test (lanes 6-9) antibodies, at concentrations of 14μg/ml, using ProBlott membranes and AEC detection. Because of the different detection system for blot bands and markers these were photographed separately. Therefore marker positions are indicated using arrows.

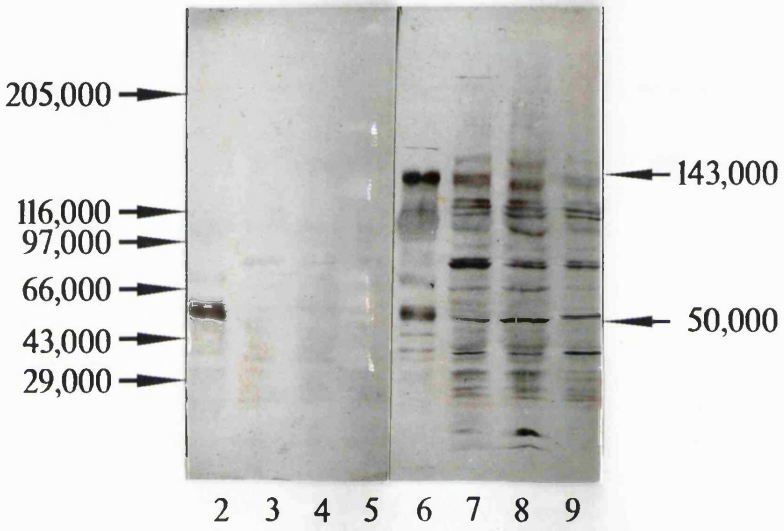

Fig. 7.4 Western blot of rabbit muscle and rat brain membranes using antibody N. Gel samples were loaded as follows: lanes 1 and 10 molecular weight markers; lanes 2 and 6, rabbit skeletal muscle t-tubule membranes (17.6μg); lanes 3 and 7, rat whole brain P2 membranes (153μg); lanes 4 and 8, rat cerebellar P2 membranes (125μg); and lanes 5 and 9, rat whole brain lysed P2 membranes (100μg). Immunoblotting was carried out using both control (lanes 2-5) and test (lanes 6-9) antibodies at concentrations of 10μg/ml, using ProBlott membranes and AEC detection. Because of the different detection system for blot bands and markers these were photographed separately. Therefore marker positions are indicated using arrows.

7.3.4 P-type α_1 polypeptide

T-tubule membranes were prepared from both rabbit and rat skeletal muscle, as outlined in Section 2.5.1, prior to their use in immunoblotting experiments. The specific activity of these t-tubule membranes, with respect to DHP binding, was estimated using Scatchard analysis of binding of PN200-110 to these membranes preparations to be 20.4 $\pm$ 9.0 pmol/mg membrane protein and 19.5 $\pm$ 8.6 pmol/mg membrane protein, respectively for the rabbit and rat t-tubules.

When the antibody raised against peptide H, which is specific for rat brain class A α_1, was used in immunocytochemical studies of rabbit skeletal muscle cryosections a staining pattern was obtained which was identical, but less intense than that obtained with the majority of the antibodies specific for the t-tubular L-type Ca^{2+} channel (revealed in Figs. 7.5 and 5.8-5.12, respectively). This antibody which was raised using a peptide corresponing to a region on the proposed extracellular loop between domains IIIS5 and IIIS6, to the N-terminal side of the SS1-SS2 region in the rat brain class A Ca^{2+} channel α_1 polypeptide, produced staining of similar intensity to that obtained using antibodies E and J in rabbit skeletal muscle sections (see Figs. 5.8 and 5.9). Immunoblotting of t-tubule membranes from rat skeletal muscle, using antibody H, according to the protocol using AEC detection (outline in Section 2.6.4), identified two polypeptides, having apparent M_r values of 255,000 and 195,000 (see Fig. 7.6). Talk about 100,000 M_r band. These are clearly structurally different from the 173,000 and 212,000 forms of the L-type channel α_1 subunit, identified by antibodies B, C, D, E, J and K using the same immunoblotting method (see Fig. 4.12). This difference was confirmed by immunoblotting antibody H against both t-tubule membranes and DHP receptor which were purified from rabbit skeletal muscle. While antibody H reacted with t-tubular polypeptides of apparent M_r 250,000 and 190,000, it failed to recognize the α_1 polypeptide of the purified DHP receptor (see Fig. 7.7). On the other hand, antibodies D and L reacted with the purified DHP receptor α_1 subunit as well as the 212,000 and 173,000 isoforms of this polypeptide in the t-tubule membranes (Fig. 7.7).

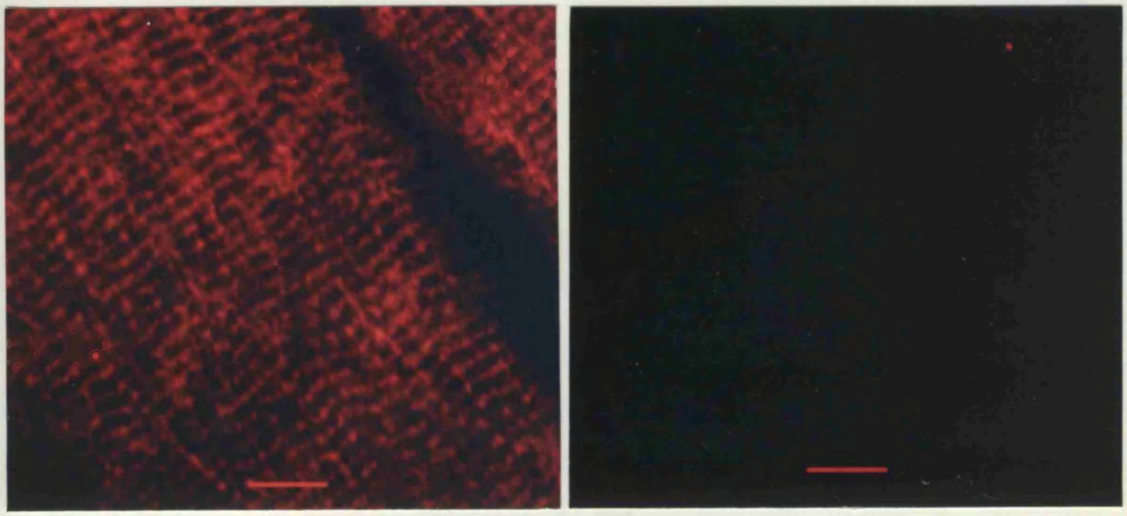

(a) (b)

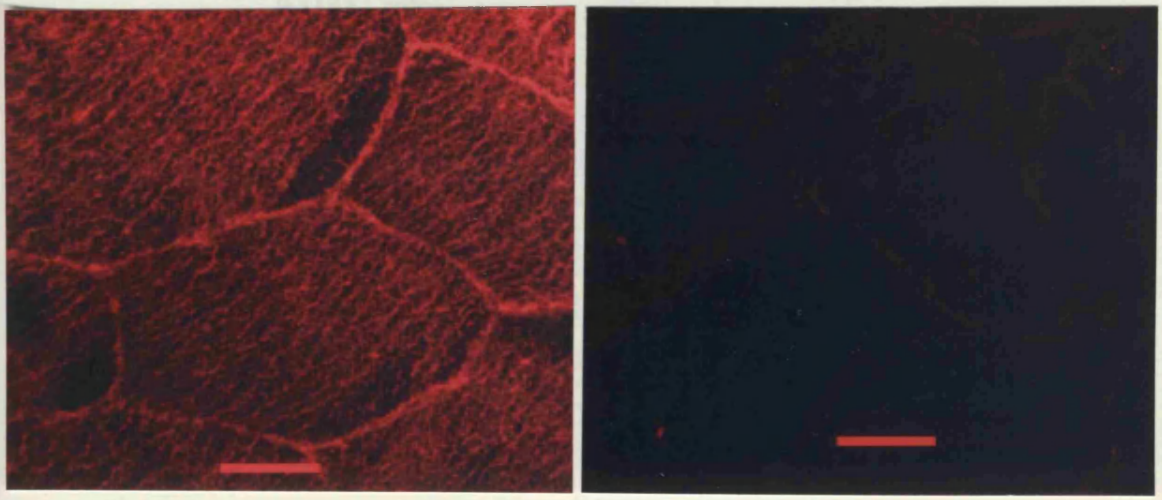

(c) (d)

Fig. 7.5 Immunostaining of adult rabbit skeletal muscle longitudinal [(a) and (b)], and transverse [(c) and (d)], cryosections, using both control and purified anti-peptide H antibody, at a protein concentration of 35μg/ml. The labelled prints identify the staining obtained using the following primary antibodies; (a) H, (b) control IgG (c) H and (d) control IgG. Immunostaining was carried out as outlined in Section 2.7.2, using Texas Red, while the imaging procedure as outlined in Section 2.7.3. The scale bar is 10μm in (a) and (b) and 25μm in (c) and (d).

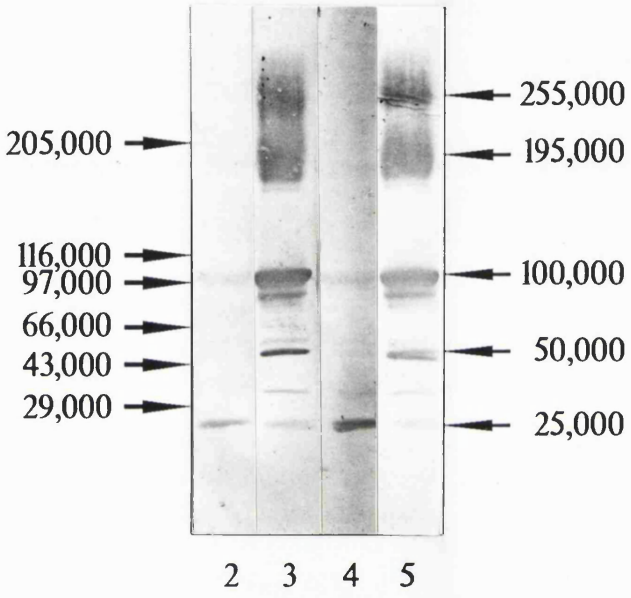

Fig. 7.6 Western blot of rat skeletal muscle t-tubule membranes using control and anti-peptide H antibody. Gel samples consisted of molecular weight markers and rabbit t-tubule membranes (40μg/lane). Immunoblotting was carried out using preimmune serum diluted 1/500 (lane 1), antiserum H diluted 1/500 (lane 2), preimmune serum diluted 1/1000 (lane 3) and antiserum H diluted 1/1000 (lane 4), using ProBlott membranes and AEC detection. Because of the different detection system for blot bands and markers these were photographed separately. Therefore marker positions are indicated using arrows.

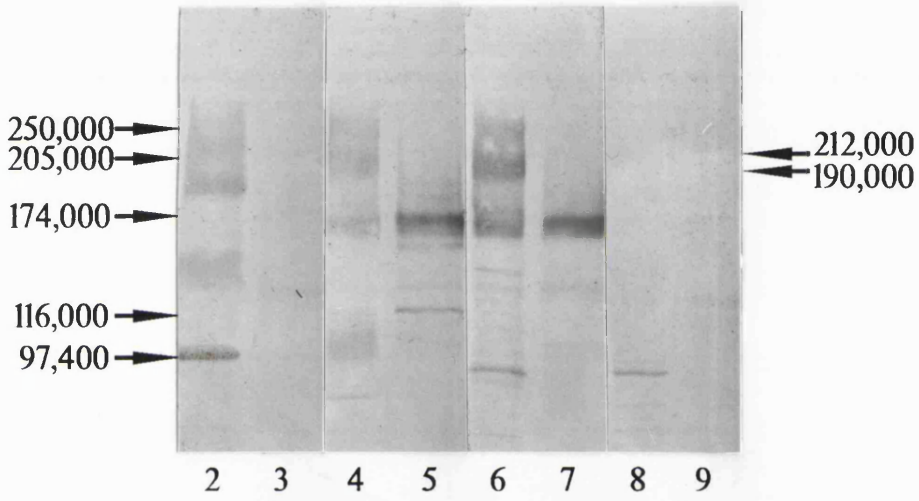

Fig. 7.7 Western blot of rabbit skeletal muscle t-tubule membranes and DHP receptor, purified as outlined in Section 2.7 using control and anti-peptide H antibody. The gel lanes were loaded with the following: lanes 1 and 10 molecular weight markers; lane 2, 4, 6 and 8 rabbit t-tubule membranes (40μg); lane 3, 5, 7, and 9 DHP receptor (3μg). Immunoblotting was carried out using anti-peptide H (lanes 2 and 3), D (lanes 4 and 5), and L (lanes 6 and 7) antibodies and control IgG (lanes 8 and 9) at a protein concentration of 4μg/ml, as outlined in Section 2.6.4, using ProBlott membranes and AEC detection. Because of the different detection system for blot bands and markers these were photographed separately. Therefore marker positions are indicated using arrows.

7.4 DISCUSSION

7.4.1 Cardiac Ca^{2+} channel polypeptides

Antibodies B, C, E, J and K are specific for peptide sequences which are either identical or very similar in both rabbit skeletal and cardiac muscle L-type channel α_1 subunits. The pattern locates the channel to the t-tubule system of the cardiac tissue, which in transverse sections of rat ventricular muscle reveals a separation of approximately 1.4μm between individual tubules (Ogata and Yamasaki, 1990). There is a spacing of 1.1-1.4μm between each of these parallel membranes as is revealed by the number of membranes (7-9) per space bar of 10μm (see Fig. 7.1).

The IS4 domain the L-type channel of both rabbit skeletal and cardiac muscle α_1 subunits (Tanabe *et al.*, 1987; Mikami *et al.*, 1989) (see Fig. 3.1). The least intense detectable staining was observed using both antibodies C and K, which recognize peptides whose sequences are conserved, respectively, at 17 out of 19 and 19 out of 20 of their residues, in rabbit heart and skeletal muscle. Antibody E identified the cardiac channel with greater intensity than C and K, binding to a 10 amino acid sequence differing in just a single residue between both channels. Staining of similar intensity to that obtained using antibody B was observed with antibody N, which is specific for α_2 subunit. The staining obtained using antibodies B, E, N and control IgG is shown at 40x magnification in Figure 7.2 (space bar 10μm) and at 100x magnification in Figure 7.1. The latter magnification reveals a spacing between the labelled membranes of (1.3-1.4)μm since (7-9) membranes occur per 10μm.

The same pattern of staining was obtained for antibodies B, C, E, K and N in rat and B, C, E, K and N in porcine cardiac ventricular cryosections (results not shown). In rat tissue, the most intense staining was observed using antibodies B and E, while that obtained using C and N was fainter, with antibody K reacted with the least intensity. Differences in staining intensity between rat and rabbit were observed, for antibodies C and E (stronger than in rabbit) and for antibody K and N (fainter than in rabbit). In porcine cardiac muscle, the intensity of staining obtained using

antibodies B, E, and N was similar to that obtained using rabbit tissue, while antibodies C and K apparently reacted more strongly with the porcine compared to the rabbit channel α_1 subunit.

The recognition of the rabbit, porcine and rat cardiac L-type channel α_1 polypeptide with antibodies B, C, E indicates that these channels are immunologically similar in the regions recognized by these antibodies. It seems likely that the rat and porcine α_1 polypeptides, whose sequences are as yet unknown, are identical or very similar in this peptide region to the rabbit cardiac and rabbit skeletal muscle channel sequenced α_1 polypeptides (Tanabe *et al.*, 1987; Mikami *et al.*, 1989). The 10 aa peptide region recognized by antibody E differs at a single residue in the rabbit muscle and cardiac α_1 polypeptides. The corresponding sequence found in both the rat and porcine cardiac α_1 subunits again appears to be very similar to the known sequence in the rabbit muscle α_1 polypeptides. The 19 aa peptide sequence identified by antibody C differs at 2 residues between rabbit cardiac and skeletal α_1. In both the rat and porcine channel polypeptides the corresponding peptide region appears to contain very similar sequences. Regarding the sequence of peptide K all but one of its 20 aa residues are conserved between the two rabbit muscle channels α_1 subunits. Strong reactivity of antibody K with porcine cardiac α_1, revealed an apparently highly similar sequence for the corresponding domain in this polypeptide. However, this sequence in rat cardiac muscle α_1 appears to be less similar than the equivalent sequence in the porcine channel to those found in both rabbit muscle α_1 polypeptides.

The primary structures of the α_2 polypeptides from rat, rabbit and porcine cardiac tissue are unknown. The same pattern of staining was obtained for antibody N in rat, rabbit and porcine cardiac ventricular cryosections. Staining with N was faintest in rat tissue, while in porcine cardiac muscle, the intensity of staining obtained using antibody N was similar to that obtained using rabbit tissue. The recognition of the porcine and rabbit cardiac L-type channel α_2 polypeptide with antibody N indicates that these channels are also immunologically similar in the region recognized by antibody N, to the rabbit skeletal muscle L-type channel α_2 subunit, whose sequence is known (Ellis *et al.*, 1988) (see Fig. 3.2). Poorer

identification of its domain in rat cardiac tissue by antibody N suggests that in the rat channel the sequence recognized by antibody N may be less similar than the corresponding sequences in both the porcine and rabbit α_2, to the sequence in rabbit skeletal muscle channel subunit.

For most of the antibodies which reacted with the channel in cardiac tissue the intensity of labelling of the cryosections of cardiac muscle from each of the three mammalian species was quite similar. While the staining was less intense than that obtained in skeletal muscle cryosections (see Figs. 5.5-5.9), using the same antibodies, it was nevertheless detectible. This study therefore constitutes the first reported localization of a subunit of the L-type Ca^{2+} in cardiac tissue and implies that this approach is available for further study of the cardiac channel.

7.4.2 Brain Ca^{2+} channel α_1 polypeptides

The lack of observed reactivity of antibodies H and I with rat brain membranes in immunoblots could be due, either to the lack of availability of antigen in sufficient quantity, or to either very poor or complete lack of reactivity of these antibodies with their antigen. Antibodies J and K also failed to identify a Ca^{2+} channel α_1 subunit in immunoblots of rat brain membranes. Antibodies J and K both recognize their respective domains in the intact denatured channel α_1 polypeptide from both rabbit and rat skeketal muscle (see Figs. 4.24 and 4.25). Since all Ca^{2+} channel α_1 polypeptides, including those from the five rat brain classes, whose sequences are known are conserved in this region, these antibodies ought to react with each of the brain channel α_1 polypeptides in immunoblots carried out according to the protocol outlined in Section (2.6.4). Their observed failed to do so suggests that the difficulty in detecting these ploypeptides arises from lack of availability of sufficient antigen in the gel samples of brain membrane used in the blots rather resulting from the lack of reactivity of the antibodies with their intact α_1 polypeptides.

7.4.3 Brain Ca^{2+} channel α_2 polypeptides

The Ca^{2+} channel α_2 subunit was detected in rat brain and rabbit t-tubule membranes in immunoblots using antibody N [see Figs. 7.3 and 7.4]. It is presumed that antibody N recognizes the muscle and brain polypeptides with equal avidity, since the peptide sequence against which it was raised is identical in the polypeptide present in both tissue (Ellis *et al.*, 1988; Kim *et al.*, 1992). Thus, an examination of the relative intensity of the staining obtained using antibody N in each lane was used to compare the total amounts of α_2 polypeptide present in the gel samples immunoblotted in each lane. When whole brain P2 membrane protein were present in the blots in a 26-fold excess over t-tubule membrane protein there appeared to be more α_2 in the former samples, as revealed by stronger reactivity of antibody N (Fig. 7.3). However, an 8.7-fold excess of brain over t-tubule membrane protein contained apparently less of the α_2 polypeptide than the t-tubules, since the staining intensity obtained using antibody N was lower in the brain compared to the t-tubule membranes. It is presumed that antibody N recognizes the muscle and brain polypeptides with equal avidity, since the peptide sequence it against which it was raised is conserved in the polypeptide present in both tissue (Ellis *et al.*, 1988; Kim *et al.*, 1992). Thus, the relative abundance of the brain α_2 in the rat whole brain P2 membranes (i.e. the amount of the total membrane protein which is contributed by α_2) is between 8.7 and 26 times less than that for the muscle α_2 polypeptide in rabbit t-tubule membranes. se staining of α_2 was observed in the blot lane containing whole brain P2 than in the lane containing t-tubule membrane proteins.

The α_2 polypeptide in the lysed whole brain P2 fraction is stained less intensely than the subunit in the t-tubule membranes, despite the presence of a 7.1-fold excess of membrane protein in the gel (Fig. 7.4), while 33.3-fold excess of cerebellar P2 over t-tubule membrane protein, apparently contained more Ca^{2+} channel α_2 subunit. Thus, the relative abundance of α_2 is 7.1-33.3-fold less in cerebellar P2 membranes than in t-tubule membranes.

All three brain membrane fractions appear to contain similar amounts of α_2

as a proportion of total membrane protein, indicating that the levels of α_2 appear to be similar in the membranes isolated from homogenized whole brain and cerebellum. The lysis of whole brain P2 membranes does not appear to make a significant contribution to the partial purification of rat brain Ca^{2+} channels. This latter finding is in agreement with the DHP binding results cited in Section 7.2.2 (Curtis and Catterall, 1983; Boles *et al.*, 1984).

Background staining was most intense in the blot lanes containing brain membrane proteins in Fig. 7.3. Because of the relatively low abundance of the α_2 polypeptide in brain the amount of protein present in these lanes is very high, between 270μg and 600μg compared to the amount in the lanes containing t-tubule membrane proteins (10μg). Hence, the background staining obtained following probing with antibody H was much higher in the brain, compared to the t-tubule membrane protein containing lanes. The identity of the brain polypeptide of apparent M_r value 85,000 by control IgG occurs only in blot lanes containing large amounts of protein. However its identity remains obscure.

Successful identification of the intact denatured rabbit skeletal muscle L-type Ca^{2+} channel α_2 subunit has been achieved, using antibody N and also antibody M, recognizing the N-terminus of α_2 (see Figs. 4.24), in immunoblots, using the protocol involving ECL detection (outlined in Section 2.6.4). Antibodies J and K also both recognize their respective domains in the intact denatured channel α_1 polypeptide from both rabbit and rat skeketal muscle (see Figs. 4.24 and 4.25). The observed recognition in immunoblots of rat brain membranes of Ca^{2+} channel α_2 subunit by antibody N, coupled with the observed failure of antibodies J and K to identify any Ca^{2+} channel α_1 polypeptide in these membranes suggests that α_2 is present in large excess over any α_1 polypeptide in the brain membrane preparations used during this study.

7.4.4 P-type α_1 polypeptide

When the antibody raised using peptide H, which is specific for rat brain class A α_1, was used in immunocytochemical studies of rabbit skeletal muscle cryosections a staining pattern was obtained which was identical, but more faint than that obtained with the majority of the antibodies specific for the t-tubular L-type Ca^{2+} channel (revealed in Figs. 7.5 and 5.5-5.9, respectively). This antibody was raised against the extracellular peptide domain between IIIS5 and IIIS6, to the N-terminal side of the SS1-SS2 of rat brain A channel, produced staining of similar intensity to that obtained using antibodies E and J in rabbit skeletal muscle sections (see Figs. 5.5 and 5.6). Immunoblotting of t-tubule membranes from both rabbit and rat skeletal muscle, using antibody H, according to the protocol using AEC detection (outline in Section 2.6.4), identified two polypeptides, having apparent M_r values of 255,000 and 195,000 (see Fig. 7.6). These are clearly structurally different from the 173 and 212K forms of the L-type channel α_1 subunit, identified by antibodies B, C, D, E, J and K using the same immunoblotting method (see fig. 4.12). This difference was confirmed by immunoblotting antibody H against both t-tubule membranes and DHP receptor which were purified from rabbit skeletal muscle. While antibody H reacted with t-tubular polypeptides of apparent M_r 250,000 and 190,000, it failed to recognize the α_1 polypeptide of the purified DHP receptor (see Fig. 7.7). On the other hand, antibodies D and L reacted with the purified DHP receptor α_1 subunit as well as the 212,000 and 173,000 isoforms of this polypeptide in the t-tubule membranes (Fig. 7.7).

These findings are possibly due to the appearance of a peptide sequence in two t-tubular polypeptides which is identical or similar to the peptide sequence in the rat brain class A Ca^{2+} channel α_1 polypeptide, against which the antibody was raised. This polypeptide is as yet unidentified. However, it is clear that it is structurally and immunologically distinct from the L-type channel in the regions recognized by antibodies B, C, D, E, I, J, K and L, (since none of these antibodies identified this protein in immunoblots) (Figs. 4.11 and 4.12), and structurally and immunologically

similar to the rat brain class A channel, in the region recognized by antibody H. It seems likely that the two t-tubular polypeptides, identified by antibody H, represent products of the same mRNA transcript, with the smaller polypeptide being a truncated version of the larger. This protein is therefore posttranslationally modified in a similar way to the t-tubular L-type channel α_1 subunit, with the truncated polypeptide present in comparably larger quantities (as revealed by Fig. 7.7). Taken together, this finding and the observed reactivity of this polypeptide with an antibody specific for rat brain class A Ca^{2+} channel α_1 suggest that this polypeptide could be a novel skeletal muscle class A Ca^{2+} channel α_1 subunit. The presence of such a channel would be compatible with the observations of Rivet *et al.*, (1992) of a ω-CgTx-insensitive Ca^{2+} current, resembling N-type, in human skeletal muscle cells.

7.5 FUTURE WORK

The successful production of site-specific antibodies which recognize their particular Ca^{2+} channel polypeptides in their intact denatured and native conformations has made available immunological probes for further investigations of the Ca^{2+} channels, particularly concerning their structure.

7.5.1 Investigation of membrane orientation of channel α polypeptides

With regard to the structure of the channel, the membrane arrangement of the Ca^{2+} channel α_1 polypeptide has not as yet been experimentally established. While α_1 is presumed to have similar topology to the Na^+ channel α subunit (see Section 1.5.2), unlike the latter membrane polypeptide no study published to date has experimetally determined the membrane orientation of any of the hydrophilic loops or of the termini of the Ca^{2+} α_1 subunit.

As outlined in Section 1.9.7.2.2, the precise location of the Ca^{2+} channel α_2 polypeptide with respect to the membrane is also unknown. A Kyte-Dolittle hydrophathy plot, was used to predict two membrane spanning sequences in the polypeptide with an extracellular orientation assigned to the termini (Ellis *et al.*, 1988). However, physical evidence suggests that α_2 is extracellular and peripheral to the membrane (Jay *et al.*, 1991).

During the course of this thesis attempts were made to establish the membrane orientation of domains on the rabbit skeletal muscle t-tubular L-type Ca^{2+} α polypeptides using those peptide-specific antibodies which bound to exposed domains of the channel. The protocol used attempted to label the t-tubule membrane extracellular face with WGA conjugated to 10nm colloidal gold particles. Following binding of the antibody to its epitope, the antibody was labelled with anti-rabbit IgG conjugated to colloidal gold (5nm). The membranes were to be viewed using a scanning electron microscopy.

The initial method involved incubation of the membranes, following permeabilization, with primary or control antibody followed by removal of unbound antibody by sedimentation at 100,000g for 30 min. The membranes were then incubated with anti-rabbit IgG conjugated to colloidal gold particles (5nm). It was intended to wash the membranes free of unbound second antibody, followed by incubation with 10nm colloidal gold-labelled WGA, prior to washing and preparation of the membranes for electron microscopy (EM). However, the t-tubule membranes sedimented along with the colloidal gold particles making removal of unbound secondary antibody impossible using this technique.

As a result, it was attempted to adsorb t-tubule membranes on to the polylysine-coated base of plastic microtitre plates wells by sedimentation of t-tubule suspension (50μl/well) at 9,000g for 20 min. It was hoped that the membranes would remain adsorbed to the plastic during incubation with antibody and subsequent washing. However, much of the membrane appeared to be washed from the plate during washing following incubation with antibody and in preparation for EM.

The topology of the channel polypeptides was also investigated using both

permeabilized and unpermeabilized fixed, cultured, chick skeletal muscle myotubes. However, it was not possible to detect immunostaining of these cells using the peptide-specific antibodies. However, it is possible to separate right-side out from inside-out t-tubule membranes by virtue of the fact that the former are glycosylated on the outside, using lectin affinity chromatography (Ebata *et al.*, 1990). By passing the t-tubules through a WGA-Sepharose column only the right-side out membranes become bound. Immobilization of these membranes on this solid support would allow incubation with both primary and gold-labelled secondary antibody, with subsequent washes to be carried out. These steps can be carried out on both permeabilized and unpermeabilized membranes. The membranes can then be eluted from the column under the same conditions outlined in Section 2.5.3 for elution of the purified DHP receptor and prepared for viewing using EM. Unpermeabilized membranes have extracellular epitopes exposed to the primary antibody while, following permeabilization the intracellular domains of the Ca^{2+} channel also become accessible. In this way antibodies which bound to the non-permeabilized membranes would identify extracellular domains of the channel, while those which only bind to permeabilized membranes would reveal intracellular orientation for their epitopes in the channel. Thus this protocol has the advantages of a simple procedure for washing unbound antibody from the column, which unlike washing by sedimentation does not damage the membranes. Additionally a probe for the extracellular membrane face is not required.

7.5.2 Characterization of the polypeptides identified by antibody H in t-tubules

In order to further characterize the polypeptides which are identified by antibody H in t-tubule membranes, their further purification would be necessary. A possible approach would be to simultaneously purify both the DHP receptor and these polypeptides from solubilized rabbit microsomal membranes by a modification of the procedure outlined in Section 2.5.3. Using this protocol the DHP receptor can be

isolated using WGA-sepharose chromatography. The putative neuronal-type channel may subsequently be isolated using an immunoaffinity column of antibody H. If this polypeptide is a channel component the channel subunit profile may be compared to that of the DHP receptor using SDS/PAGE, following their isolation.

7.5.3 Developmental expression of both L-type Ca^{2+} channel α polypeptides in cardiac tissue

The level of expression of both L-type Ca^{2+} channel α_1 and α_2 subunits has been examined at different stages during the development of skeletal muscle tissue (see Section 3.2.2). However, to date no such study has been carried out using cardiac tissue. A possible reason due to the lower level of these polypeptides found in cardiac compared to skeletal muscle their detection may not have been thought possible in the former tissue. However, identification of both α subunits of the L-type Ca^{2+} channel has been achieved in this study using detection of immunofluorescently-labelled subunits in ventricular muscle cyrosections. Thus a study of the distribution of both channel polypeptides could be carried out for cardiac muscle during its development using tissue obtained from animals of different ages.

CHAPTER 8

GENERAL DISCUSSION

8.1 Anti-peptide antibody production

In this study, the use of synthetic peptides in the production of antibodies which recognize the intact Ca^{2+} channel subunits in both their native conformation and in the denatured state, was successful, in most cases. The majority of the 13 anti-peptide antibodies (i.e. those generated against synthetic peptides B, C, D, E, J, K, L, M and N, corresponding to regions of the subunits of the rabbit skeletal muscle L-type Ca^{2+} channel) recognized the intact denatured polypeptides in immunoblots and in skeletal muscle cryosections. These antibodies, with the exception of M, also reacted with their intact native polypeptides in ELISA with the purified skeletal muscle DHP receptor (see Table 8.1).

As stated in Section 7.3.2, it appears that rat brain membranes did not contain a sufficiently high concentration of the relevant rat brain class A and D Ca^{2+} channel α_1 subunits to allow their detection using antibodies H and I, respectively. It was therefore not possible to characterize antibodies H and I, using either membranes, cryosections or purified receptor from rat brain. However, both H and I reacted in immunoblots with different polypeptides present in t-tubule membranes. The latter antibody also weakly recognized the intact native α_1 subunit of the purified skeletal muscle L-type Ca^{2+} channel, which contains a peptide corresponding to peptide I which is different at 2 out of 17 aa residues. It thus seems likely that both H and I react with rat brain class A and D α_1 polypeptides, respectively, even though this has not been experimentally established.

Only the antibodies specific for the extracellular peptides A, F, G and O failed to show any reactivity with the intact channel polypeptides. However, antibody A has been seen to reduce T-type and N-type Ca^{2+} currents in NG108-15 cells, following extracellular incubation with these cells (Wilson, 1991). This sequence is conserved

Table 8.1 Table showing the relative reactivities of the antibodies in Western blots with rabbit and rat t-tubules, in immunocytochemistry in skeletal muscle, in ELISA with purified DHP receptor.

Antibody	Western Blot	Immunocytochemistry	ELISA	DHP binding
A	-	-	-	
B	+	+++	+	-
C	+	+	+	-
D	+++	-	+++	_
E	+	+	+	_
F	-	-	-	
G	-	-	-	
H	+++	+	-	
I	+		+	
J	+	+	+	_
K	+++	+++	+++	-
L	+++	+++	+++	-
M	+	-	-	-
N	+++	+++	+	-
O	-	-	-	-

in rat brain N-type channel sequence published by Dubel *et al.* (1992). This implies reactivity of A with an external domain of the α_1 polypeptide. Peptide G is amphipathic and has a predicted α helical secondary structure which would render the

peptide non-immunogenic. However, the external peptides F and O are hydrophilic and predicted to be immunogenic and yet fail to elicit antibodies that recognize their peptides in the native channel.

8.2 Structural information on Ca^{2+} channel polypeptides

8.2.1 Primary Structure

Particular Ca^{2+} channel subunits present in various tissues of different species appear to be homologous. This homology is apparent from the alignments of all the α_1 (see Fig. 3.1), α_2 (see Fig. 3.2) and ß polypeptides (not shown), whose sequences have been deduced to date. Specifically, each α_1 polypeptide contains the same pattern of putative membrane spanning domains, indicating that this is part of the structural requirement for function of α_1 as the channel pore. The α_2 subunit is much more highly homologous amongst the three sequences determined (rat and human neuronal and rabbit skeletal muscle) than is α_1. This identity between tissues and species suggests that this conserved structure of the polypeptide is very important to its function in the channel complex and hence that this polypeptide indeed has an important role in the channel complex.

Information on the structure of mammalian muscle channel polypeptides whose sequences are not known was deduced using the peptide-specific antibodies. This study supports the supposition that the skeletal muscle L-type channel α_1 and α_2 polypeptides are very highly conserved amongst mammalian species. The same appears to be true for the corresponding channel subunits of mammalian cardiac muscle from rabbit, rat and pig. This study shows that sequences corresponding to peptides B, C, D, E, J, K and L are very similar if not identical in rat, mouse and human skeletal muscle Ca^{2+} channel α_1 to the known peptides in the rabbit muscle channel polypeptide. Peptides homologous to B, C, E and K were also identified in the cardiac muscle α_1 polypeptide in rat, rabbit and pig, whose sequences are unknown.

Regarding the α_2 polypeptide, the sequence of peptide N appears to be similar or identical in the channels from each of both skeletal and cardiac tissue from the species examined.

8.2.2 Secondary Structure

These antibodies also yielded some information on the secondary structure of the channel subunits. As expected the strength of recognition of its polypeptide varied with each particular antibody. Antibodies C, D, E, K, L and N showed similarly strong reactivity with their intact native and denatured channel subunits. Of these, antibody C specific for the entire, small intracellular loop IIS4-IIS5 shows the weakest reactivity with intact α_1, while the recognition of this polypeptide by E, binding to a peptide in the larger IIIS6-IVS1 loop, is slightly stronger. It thus appears that the peptides located in these smaller putative intracellular loops resemble but have slightly different conformation to those of the synthetic peptides and thus, these loops apparently have some ordered secondary structure in the native polypeptide. Interestingly, antibodies specific for peptides A and F fain to react with these sequences in either the denatured or native form of α^1. this suggests that the extracellular loops IS3-IS4 and IVS3-IVS4 on which these peptides located are also conformational. On the other hand, D, K, L and N show relatively strong recognition of their polypeptides. Their domains in the channel, located on the loop between domains II and III (D), C-terminal to IVS6 (K and L) in α_1 and on the proposed intracellular loop in α_2 (N), thus probably have less stable and/or random coil secondary structure.

Other antibodies evidently recognize their specific epitopes more strongly in either the native or denatured intact channel polypeptide. Antibody J shows relatively strong recognition of the denatured α_1, and has relatively weak reactivity with the native channel. Antibody B, reacts strongly compared to other antibodies with the native form of α_1, while its reactivity is relatively weak with the denatured polypeptide. Additionally, M only recognizes α_2 when this polypeptide is denatured.

It appears that the N-terminus of α_2 is only accessible to its antibody following denaturation. A probable explanation for this, is that this peptide region is inaccessible to antibody in the native polypeptide, becoming accessible as a result of denaturation. However, this is surprising in light of the apparent hydrophilicity of the peptide.

J reacts less strongly than D, K, L and N, but more strongly than E with the denatured α_1 polypeptide. Some ordered secondary structure in the native channel of the large domain targetted by J in the C-terminal region of α_1, may result in antibody J showing relatively strong reactivity with its peptide domain in the denatured, and relatively weak reactivity with the peptide in the native channel, compared to other antibodies. This supports a predicted secondary structure including two α-helical regions as part of a putative EF-hand domain. However, FTIR and CD studies of the secondary structure of a synthetic polypeptide corresponding to the domain recognized by antibody J revealed some ß-sheet but no α helical structure in this region of α_1.

Similar to the domain recognized by antibody J, the IS4 domain of α_1, recognized by antibody B, also appears to have different secondary structure in both the denatured and native channel. In this case, the native rather than the denatured peptide appears to more closely resemble the synthetic peptide. It appears that an ordered secondary structure is lost by this domain upon denaturation, resulting in reduced recognition of this peptide by its antibody. This is in agreement with a predicted ordered α-helical secondary structure for the S4 putative membrane spanning domains of all voltage-gated ion channels. This α-helical secondary structure has been verified for a synthetic K^+ channel S4 peptide by means of FTIR (see Section 3.3.2) (Ben-Efraim *et al.*, 1993).

8.3 Tertiary structure and structural/functional information on channel polypeptides

Some information on the tertiary structure of both channel α subunits was also obtained from the reactivity of the antibodies with their polypeptides. The binding of antibodies B, C, D, E, J, K and L to intact native α_1 indicate that these peptides are exposed on the surface of the polypeptide. This supports the currently proposed model for the arrangement of the channel in the membrane, having four homologous domains each containing six membrane spanning sequences, which requires that domains C, D and E are located on intracellular loops, while J, K and L are situated on the C-terminal end of the polypeptide. Antibodies bound to these exposed peptide domains failed to inhibit binding of either nitrendipine or D888 to the channel. This suggests that the DHP binding site is not in the region α_1(1390-1437), as suggested by Regulla *et al.* (1991), but is compatible with a location at the extracellular side of the IIIS6 and IVS6 domains (Nakayama *et al.*, 1991). Despite binding to the α_1 polypeptide C-terminal and in close proximity to the PAA binding domain identified by Striessnig *et al.* (1990b), antibodies J and K do not inhibit D888 binding. It is possible that conformational changes in these regions, due to presence of antibody, do not significantly alter the PAA binding. It is more likely, however, that the antibodies bound even in close proximity to the drug binding domains do not inhibit access of the ligands to the channel because of the small size of the latter.

In the native channel the IS4 domain, which is proposed to be transmembrane, is highly accessible to its antibody and therefore exposed at the protein surface. The corresponding domain in a native Na^+ channel is also accessible to antibodies (Meiri *et al.*, 1987). However, the IVS4 region in the latter channel appears to be inaccessible for antibody binding (Nakayama et al., 1993). The finding of an exposed IS4 supports the proposed model for the arrangement of the pore structure of voltage-gated ion channels proposed by Sato and Matsumoto, (1992) (see Fig.1.3). This model has S4, along with S2, acting as the channel-forming domains, interacting with the SS1-SS2 region which actually lines the pore. This arrangement would give the

antibody access to S4 from close to, or inside the pore itself.

Part of the II-III loop of the L-type channel α_1 subunit was inaccessible to antibody D when the channel was probed in skeletal muscle cryosections. All other antibodies which, like D, showed reactivity with the DHP receptor in ELISA bound to the channel in muscle sections. Binding of antibody D to the DHP receptor in ELISA show that its domain is exposed at the surface of the native protein. Thus, the inaccessibility to antibody of this site in the channel suggests that this region of α_1 is interacting with another molecule or protein in the cell. The Ca^{2+} channel is believed to interact with the SR ryanodine receptor via triadin or another linker polypeptide (see Section 1.9.9.3) and it is thus possible that this polypeptide binds to the II-III loop of α_1. This is supported by the previous finding that this loop is essential for skeletal E-C coupling (Tanabe *et al.*, 1990b).

8.4 Distribution of cardiac and neuronal channel polypeptides in brain and muscle

The availability of antibodies which recognized regions that were highly similar or identical in rabbit cardiac and skeletal muscle α_1 polypeptide facilitated the first reported *in situ* localization this polypeptide to the t-tubules membranes of this tissue in rat and rabbit muscle. The α_2 polypeptide was also similarly localized for the first time. Since the level of cardiac channel was estimated, using radiolabelled DHP's, to be 100-fold lower in cardiac compared to skeletal muscle (Fosset *et al.*, 1983; Glossmann *et al.*, 1983) it is surprising that the channel polypeptides were detectible following immunofluorescence labelling in light of failure to detect these polypeptides in cultured chick skeltal muscle myotubes and rat DRG cells, using the same procedure.

Simultaneous imunoblotting of various rat brain and rabbit t-tubule membranes, using antibody N, has also allowed the estimation of the relative abundance of this channel polypeptide in rat whole brain and cerebellar P2 membrane preparations. A similar proportion of the total P2 membrane protein from both whole

brain and cerebellum was evidently contributed by α_2. The level of α_2 relative to total membrane protein was 10-25-fold and 10-30-fold lower, in whole brain and cerebellum, than in rabbit t-tubules. This value was much higher than expected for a brain Ca^{2+} channel polypeptide. Along with antibodies H and I, which are specific for class A and D channel α_1 polypeptides, none of the antibodies B, C, E, J, K, which bind to sequences which are very highly conserved in all classes of rat brain channel, identified an α_1 polypeptide in immunoblots using similar quantities of brain membranes. These findings indicate that brain α_2 recognized by antibody N is much more abundant than any of the brain α_1 polypeptides. A possible explanation for this apparent excess of α_2 over brain α_1 is that the same α_2 polypeptide may interact with each of the classes of brain α_1 subunit. However, if the domain on α_2, recognized by antibody N, is highly homologous between a number of brain α_2 polypeptides, then different α_2 polypeptides can may interact with α_1 polypeptides of the different brain classes. What is clear is that the level of expression of brain Ca^{2+} channel α_2 is much higher than the level for individual classes of α_1 and also possibly higher than the collective expression of all brain Ca^{2+} channel α_1 subunits. If this is true α_2 may have at least one other role in the brain other than stabilization of Ca^{2+} channel α_1 polypeptides.

The reaction of antibody H with a polypeptide present in both rat and rabbit t-tubule membranes which is distinct from the L-type Ca^{2+} channel, indicates the presence of a protein in these membranes which is immunologically similar to the rat brain class A channel. This suggests the possibility that the polypeptide is a neuronal type channel subunit. Interestingly, a neuronal Ca^{2+} channel present in human skeletal muscle cells which is insensitive to ω-CgTx has been identified (Rivet *et al.*, 1992). Additionally, similar to skeletal muscle L-type α_1, two size forms of the protein identified by antibody H appear to occur in the t-tubule. However, the specificity of antibody H for the peptide against which it was raised in the rat brain class A channel α_1 subunit has yet to be established.

CHAPTER 9

REFERENCES

Abe, T., Koyano, K., Saisu, H., Nishiuchi, Y., Sakakibara, S., 1986, Neurosci. Lett., 71: 203-208.

Adams, B.A., Tanabe, T., Mikami, A., Numa, S. and Beam, K.G., 1990, Nature, 346: 569-572.

Adams, T.C., Dupont, A.C., Carter, J.P., Kachur, J.F., Guzewska, M.E., Rzeszotarski, W.J., Farmer, S.G., Noronha-Blob, L. and Kaiser C., 1991, J. Med. Chem., 34: 1585-1593.

Ahlijanian, M.K., Westenbroek, R.E. and Catterall, W.A., 1990, Neuron, 4: 819-832.

Ahlijanian, M.K., Striessnig, J. and Catterall, W.A., 1991, J. Biol. Chem., 266: 20192-20197.

Aldrich, R.W. and Stevens, C.F., 1983, Cold Spring Harbor Symp. Quant. Biol., 48: 147-153.

Almers, W., 1978, Rev. Physiol. Biochem. Pharmacol., 82: 96-190.

Armstrong, C.M. and Binstock, L., 1965, J. Gen. Physiol., 48: 859-872.

Armstrong, C.M., 1969, J. Gen. Physiol., 54: 553-575.

Armstrong, C.M., Bezanilla, K.M. and Horowicz, P., 1972, Biochim. Biophys. Acta., 267: 605-608.

Armstrong, C.M., Benzanilla, F. and Rojas, E., 1973, J. Gen. Physiol., 62: 375-391.

Armstrong, C.M. and Benzanilla, F., 1973, Nature, 242: 459-461.

Armstrong, C.M., 1981, Physiol. Rev., 61: 644-683.

Arreola, J., Calvo, J., Garcia, M.C. and Sanchez, J.A., 1987, J. Physiol., 393: 307-330.

Artymiuk, P.J., Blake, C.C.F., Grace, D.E.P., Oatley, S.J., Phillips, D.C. and

Sternberg, M.J.E., 1979, Nature, 280: 563-568.

Atherton, E. and Sheppard, R.C. 1985, J. Chem. Soc. Chem. Commun., 165-166.

Augustine, G.J., Charlton, M.P. and Smith, S.J., 1987, Ann. Rev. Neurosci., 10: 633-693.

Auld, V.J., Marshall, J., Goldin, A.L., Dowsett, A., Catterall, W.A., Davidson, N. and Dunn R.J., 1985, J. Gen. Physiol. 86: 10a (abstr.).

Auld, V.J., Goldin, A.L., Krafte, D.S., Marshall, J., Dunn, J.M., Catterall, W.A., Lester, H.A., Davidson, N. and Dunn R.J., 1988, Neuron, 1: 449-461.

Auld, V.J., Goldin, A.L., Krafte, D.S., Catterall, W.A., Lester, H.A., Davidson, N. and Dunn R.J., 1989, Proc. Natl. Acad. Sci. USA., 87: 323-327.

Babitch, J.A., 1990, Nature, 346: 321-322.

Babu, Y.S., Sack, J.S., Greenhough, T.J., Bugg, C.E., Means, A.R. and Cook, W.J., 1985, Nature, 315: 37-40.

Babu, Y.S., Bugg, C.E. and Cook, W.J., 1987, Methods Enzymol., 139: 632-642.

Backx, P.H., Yue, D.T., Lawrence, J.H., Marban, E. and Tomaselli, G.F., 1992, Science, 257: 248-251.

Baldwin, T.J., Tsaur, M.-L., Lopez, L.A., Jan, Y.N. and Jan, L.Y., 1991, Neuron, 7: 471-483.

Balwierczak, J.L., Johnson, L. and Schwartz, A., 1987, Mol. Pharmacol., 31: 175-179.

Barchi, R.L., 1988, Ann. Rev. Neurosci., 11: 455-495.

Barhanin, J., Coppola, T., Schmid, A., Borsotto, M. and Lazdunski, M., 1987, Eur. J. Biochem., 164: 525-531.

Barhanin, J., Schmid, A. and Lazdunski, M., 1988, Biochem. Biophys. Res. Commun., 150: 1051-1062.

Baumann, A., Grupe, A., Ackermann, A. and Pongs, O., 1988, EMBO J., 7: 2457-2463.

Beam, K.G., Adams, B.A., Niidome, T., Numa, S. and Tanabe, T., 1992, Nature, 360: 169-171.

Bean, B.P., 1984, Proc. Natl. Acad. Sci. USA., 81: 6388-6392.

Bean, B.P., 1989, Ann. Rev. Physiol., 51: 367-384.

Beaty and Stefani, 1976, Proc. R. Soc. B. 194: 141-150.

Belleman, P., Schade, A. and Toward, R., 1983, Proc. Natl. Acad. Sci. USA., 80: 2356-2360.

Ben-Efraim, I., Bach, D. and Shai, Y., 1993, Biochem., 32: 2371-2377.

Betsholtz, C., Baumann, A., Kenna, S., Ashcroft, F.M., Ashcroft, S.J.H., Berggren, P.-O., Grupe, A., Pongs, O., Rorsman, P., Sandblom, J. and Welsh, M., 1990, FEBS Lett., 263: 121-126.

Beuckelmann, D.J. and Wier, W.G., 1988, J. Physiol., 405: 233-255.

Bianchi and Shanes, 1959, J. Gen. Physiol., 42: 803-815.

Biel, M., Ruth, P., Hullin,R., Stuhmer, W., Flockerzi, V. and Hofmann, F., 1990, FEBS Lett., 269: 409-412.

Block, B.A., Imagawa, T., Campbell, K.P. and Franzini-Armstrong, C., 1988, J. Cell Biol., 107: 2587-2600.

Boles, R.G., Yamamura, H.I., Schoemaker, H. and Roeske, W.R., 1984, J. Pharmacol. Exper. Ther., 229: 333-339.

Bolger, G.T., Gengo, P.J., Luchowski, E.M., Siegel, H., Triggle, D.J. and Janis, R.A., 1982, Biochem. Biophys. Res. Commun., 104: 1604-1609.

Bolger, G.T., Gengo, P.J., Klockowski, R., Luchowski, E.M., Siegel, H., Janis, R.A., Triggle, A.M. and Triggle, D.J., 1983, J. Pharmacol. Exper. Ther., 225: 291-309.

Boll, W. and Lux, H.D., 1985, Neuroscience Lett., 56: 335-339.

Borsotto, M., Barhanin, J., Norman, R.I. and Lazdunski, M., 1984, Biochem. Biophys. Res. Commun., 122: 1357-1366.

Bosse, E., Regulla, S., Biel, M., Ruth, P., Meyer, H.E., Flockerzi, V. and Hofmann F., 1990, FEBS Lett., 267: 153-156.

Botfield, M.C. and Wilson, T.H., 1989, J. Biol. Chem., 264: 11649-11652.

Brady, A.J. and Woodbury, J.W., 1960, J. Physiol., 154: 385-407.

Brandolin, G., Boulay, F., Dolbon, P. and Vignais, P.V., 1989, Biochemistry, 28: 1093-1100.

Brandt, N.R., Caswell, A.H., Wen, S.-R., and Talvenheimo, J.A., 1990, J. Memb. Biol., 113: 237-251.

Brandt, N.R., Caswell, A.H., Brunschwig,J.-P., Kang, J.-J., Antoniu, B. and Ikemoto, N., 1992, FEBS Lett., 299: 57-59.

Brawley, R.M. and Hosey, M.M., 1992, J. Biol. Chem., 267: 18218-18223.

Burgess A.J. and Norman, R.I., 1988, Eur. J. Biochem., 178: 527-533.

Campbell, K.P., Leung, A.T. and Sharp, A.H., 1988, T.I.N.S., 11: 425-430.

Carbone, E. and Lux, H.D., 1987, J. Physiol., 386: 547-570.

Carrasco, N., Herzlinger, D., Danho, W. and Kabach, H.R., 1986, Methods Enzymol., 125: 453-467.

Castellano, A., Wei, X., Birnbaumer, L. and Perez-Reyes, E., 1993a, J. Biol Chem., 268: 3450-3455.

Castellano, A., Wei, X., Birnbaumer, L. and Perez-Reyes, E., 1993b, J. Biol Chem., 268: 12359-12366.

Caswell, A.H. and Brandt, N.R., 1989, T.I.B.S., 14: 161-165.

Caswell, A.H., Brandt, N.R., Brunschwig, J.-P. and Purkerson, S., 1991, Biochemistry, 30: 7507-7513.

Catterall, W.A., 1986, Annu. Rev. Biochem., 55: 953-985.

Catterall, W.A., 1988, Science, 242: 50-61.

Catterall, W.A., Seagar, M.J., Takahashi, M., 1988; J. Biol. Chem., 263: 3535-3538.

Catterall, W.A., Seagar, M.J., Takahashi, M. and Nunoki, K., 1989, Ann. New York Acad. Sci., 560: 1-14.

Cazalis, M., Dayanithi, G. and Nordmann, J.J., 1987, J. Physiol., 390: 55-70.

Cena, V., Nicolas, G.P., Sanchez Garcia, P., Kirpekar, S.M. and Garcia, A.G., 1983, Neuroscience, 10: 1455-1462.

Chang, F.C. and Hosey, M.M., 1988, J. Biol. Chem., 263: 18929-18937.

Chang, C.F., Gutierrez, L.M., Mundina-Wielenmann, C. and Hosey, M.M., 1991, J. Biol. Chem., 266: 16395-16400.

Chen, L.-Q., Chahine, M., Kallen, R.G., Barchi, R.L. and Horn, R., 1992, FEBS Letters, 309: 253-257.

Cherksey, B.D., Sugimori, M. and Llinas, R.R., 1991, Ann. N. Y. Acad. Sci., 635: 80-89.

Chin, H., Smith, M.A., Kim, H.-L. and Kim, H., 1992, FEBS Lett., 299: 69-74.

Choi, K.L., Aldrich, R.W. and Yellen, G., 1991, Proc. Natl. Acad. Sci. USA., 88: 5092-5095.

Chou, P.Y. and Fasman, G.D., 1978, Advances Enzymol., 47: 45-148.

Clark-Lewis, I., Aebersold, R., Ziltener, H., Schrader, J.W., Hood, L.E. and Kent, S.B.H., 1986, Science, 231: 136-139.

Closset, J. and Gerday, C., 1975. Biochim. Biophys. Acta, 405: 228-235.

Cohen, C.J., Ertel, E.A., Smith, M.M., Venema, V.J., Adams, M.E. and Leibowitz, M.D., 1992, Mol. Pharm., 42: 947-951.

Collin, T., Wang, J.-J., Nargeot, J. and Schwartz, A., 1993, Circ. Res., 72: 1337-1344.

Connor, J.A. and Stevens, C.F., 1971, J. Physiol., 213: 31-53.

Coombs, J., Scheuer, T., Rossie, S.R. and Catterall, W.A., 1988, Biophys. J., 53: 542a.

Cooper, C.L., Vandaele, S., Barhanin, J., Fosset, M., Lazdunski, M. and Hosey, M., 1987, J. Biol. Chem., 262: 509-512.

Coraboeuf, E. and Otsuka, M., 1956, C. R. Hebd. Seanc. Acad. Sci. Paris, 243: 441-444.

Costa, M.R.C., Casnellie, J. and Catterall, W.A., 1982, J. Biol. Chem., 257: 7918-7921.

Costa, M.R.C. and Catterall, W.A., 1984, J. Biol. Chem., 259: 8210-8218.

Cota, G. and Stefani, E., 1986, J. Physiol., 370: 151-163.

Cruz, L.J. and Olivera, B., 1986, J. Biol. Chem., 261: 6230-6233.

Curtis, B.M. and Catterall, W.A., 1983, J. Biol. Chem., 258: 7280-7283.

Curtis, B.M. and Catterall, W.A., 1984, Biochemistry, 23: 2113-2118.

Curtis, B.M. and Catterall, W.A., 1985, Proc. Natl. Acad. Sci. USA., 82: 2528-2532.

Curtis, B.M. and Catterall, W.A., 1986, Biochemistry, 25: 3077-3083.

Davies, A., Meeran, K., Cairns, M.T. and Baldwin, S.A., 1987, J. Biol. Chem., 262: 9347-9352.

Davies, A., Ciardelli, T.L., Lienhard, E., Boyle, J.M., Whetton, A.D. and Baldwin, S.A., 1990a, Biochem. J., 266: 799-808.

Davies, A., 1990b, Ph.D Thesis, University of London, London, U.K.

De Jongh, K.S., Merrick. D.K. and Catterall, W.A., 1989, Proc. Natl. Acad. Sci. USA., 86: 8585-8589.

De Jongh, K.S., Warner, C. and Catterall, W.A., 1990, J. Biol. Chem., 265: 14738-14741.

De Jongh, K.S., Warner, C., Colvin, A.A. and Catterall, W.A., 1991, Proc. Natl. Acad. Sci. USA., 88: 10778-10782.

DePover, A., Matlib, M.A., Lee, S.W., Dube, G.P., Grupp, I.L., Grupp, G. and Schwartz, A., 1982, Biochem. Biophys. Res. Commun., 108: 110-117.

Dubel, S.J., Starr, T.V.B., Hell, J., Ahlijanian, M.K., Enyeart, J.J., Catterall, W.A. and Snutch, T.P., 1992, Proc. Natl. Acad. Sci. USA., 89: 5058-5062.

Duch, D.S. and Levinson, S.R., 1987, J. Memb. Biol., 98: 43-55.

Durell, S.R. and Guy, H.R., 1992, Biophys. J., 62: 238-247.

Dyson, H.J., Cross, K.J., Houghten, R.A., Wilson, I.A., Wright, P.E. and Lerner, R.A., 1985, Nature, 318: 480-483.

Dyson, H.J., Rance, M., Houghten, R.A., Wright, P.E. and Lerner, R.A., 1988, J. Mol. Biol., 201: 161-200.

Ebata, H., Mills, J.S., Nemcek, K. and Johnson, J.D., 1990, J. Biol. Chem., 265: 177-182.

Ehrlert, F.J., Roeske, W.R., Itoga, E. and Yamamura, H.I., 1982, Life Sci., 30: 2192-2202.

Ellis, S.B., Williams, M.E., Ways, N.R., Brenner, R., Sharp, A.H., Leung, A.T., Campbell, K.P., McKenna, E., Koch, W.J., Hui, A., Schwartz, A. and Harpold M.M., 1988, Science, 241: 1661-1664.

Ellman, G.L., 1959, Arch. Biochem. Biophys., 82: 70-77.

Emerick, M.C. and Agnew, W.S., 1989, Biochem., 28: 8367-8380.

Fabiato, A., 1985, J. Gen. Physiol., 85: 189-320.

Fatt, P. and Katz, B., 1953, J. Physiol., 120: 171-204.

Fatt, P. and Ginsborg, B.L., 1958, J. Physiol., 142: 516-543.

Fedulova, S.A., Kostyuk, P.G. and Veselovsky, N.S., 1985, J. Physiol., 359: 431-446.

Ferry, D.R. and Glossmann, H., 1982, Naunyn-Schmiedeberg's Arch. Pharmacol., 321: 80-83.

Ferry, D.R., Goll, A. and Glossmann, H., 1987, Biochem. J., 243: 127-135.

Fields, G.B. and Noble, R.L., 1990, Int. J. Peptide Protein Res., 35: 161-214.

Fitzpatrick, L.A., Chin, H., Nirenberg, M. and Aurbach, G.D., 1988, Proc. Natl. Acad. Sci. USA., 85: 2115-2119.

Fleckenstein, A., 1964, Verh. Dtsch. Ges. Inn. Med., 70: 81-99.

Fleckenstein, A., Kammermeier, H., Doring, H.J. and Freund, H.J., 1967, Z. Kreislaufforsch, 56: 716-744, 839-853.

Flockerzi, V., Oeken, H.-J., Hofmann, F., Pelzer, D., Cavalie, A. and Trautwein, W., 1986a, Nature, 323: 66-68.

Flockerzi, V., Oeken, H.J. and Hofmann, F., 1986b, Eur. J. Biochem., 161: 217-

222.

Flucher, B.E., Morton, M.E., Froehner, S.C. and Daniels, M.P., 1990, Neuron, 5: 339-351.

Flucher, B.E., Phillips, J.L. and Powell, J.A., 1991a, J. Cell Biol., 115: 1345-1356.

Flucher, B.E., Terasaki, M., Chin, H., Beeler, T. and Daniels, M.P., 1991b, Dev. Biol., 145: 77-90.

Fosset, M., Jaimovich, E., Delpont, E. and Lazdunski, M., 1983, J. Biol. Chem., 258: 6086-6092.

Fox, A.P., Nowycky, M.C. and Tsien, R.W, 1987a, J. Physiol., 394: 149-172.

Fox, A.P., Nowycky, M.C. and Tsien, R.W, 1987b, J. Physiol., 394: 173-200.

Frankenhaeuser, B. and Huxley, A.F., 1964, J. Physiol., 171: 302-315.

Frech, G.C., Vandongen, A.M.J., Schuster, G., Brown, A.M. and Joho, R.H., 1989, Nature, 340: 643-645.

Fujita, Y., Mynlieff, M., Dirksen, R.T., Kim, M.-S., Niidome, T., Nakai, J., Friedrich, T., Iwabe, N., Miyata, T., Furuichi, T., Furutama, D., Mikoshiba, K., Mori, Y. and Beam, K.G., 1993, Neuron, 10: 585-598.

Fukushima, Y. and Hagiwara, S., 1983, Proc. Natl. Acad. Sci. USA., 80:2240-2242.

Furman, R., Tanaka, J., Mueller, P. and Barchi, R., 1986, Proc. Natl. Acad. Sci. USA., 83: 488-492.

Galizzi, J.P., Fosset, M. and Lazdunski, M., 1984, Eur. J. Biochem., 144: 211-215.

Galizzi, J.P., Fosset, M., Romey, G., Laduron, P. and Lazdunski, M., 1986, Proc. Natl. Acad. Sci. USA., 83: 7513-7517.

Galizzi, J.P., Borsotto, M., Barhanin, J., Fosset, M. and Lazdunski, M., 1986, J. Biol. Chem., 261: 1393-1397.

Garcia, M., King, V., Siegl, P., Reuben, J. and Kaczorowski, G., 1986, J. Biol. Chem., 261: 8146-8157.

Garcia, J. and Stefani, E., 1987, Pflugers Archiv., 408: 646-648.

Garnier, J., Osguthorpe, D.J. and Robson, B., 1978, J. Mol. Biol., 120: 97-120.

Geduldig, D. and Gruener, R., 1970, J. Physiol., 211: 217-244.

Ghanshani, S., Pak, M., McPherson, J.D., Strong, M., Dethlefs, B., Wasmuth, J.J., Salkoff, L., Gutman, G.A. and Chandy, K.G., 1992, Genomics, 12: 190-196.

Glossmann, H. and Ferry, D.R., 1983, Naunyn Schmiedebergs Arch. Pharmacol., 323: 279-291.

Glossmann, H., Ferry, D.R. and Boshcek, C.B., 1983, Naunyn-Schmiedeberg's Arch. Pharmacol., 323: 1-11.

Glossmann, H., Ferry, D.R., Goll, A., Striessnig, J. and Schober, M., 1985, J. Cardiovasc. Pharmacol., 7: 520-530.

Glossmann, H. and Striessnig, J., 1990, Rev. Physiol. Biochem. Pharmacol., 114: 1-105.

Goll, A., Ferry, D.R., Striessnig, J., Schober, M. and Glossmann, H., 1984, FEBS Lett., 176: 371-377.

Goll, A., Glossmann, H. and Mannhold, R., 1986, Naunyn-Schmiedeberg's Arch. Pharmacol., 334: 303-312.

Gordon, R.D., Fieles, W.E., Schotland, D.L., Hogne-Angelett, R. and Barchi, R.L., 1987, Proc. Natl. Acad. Sci. USA., 84: 308-312.

Gordon, D., Merrick, D., Wollner, D. and Catterall, W.A., 1988a, Biochemistry, 27: 7032-7038.

Gordon, R.D., Li, Y., Fieles, W.E., Schotland, D.L. and Barchi, R.L., 1988b, J. Neurosci., 8: 3742-3749.

Grabner., M., Friedrich, K., Knaus., H.G., Striessnig, J., Scheffauer, F., Staudinger, R., Koch, W.J., Schwartz, A. and Glossmann, H., 1991, Proc. Natl. Acad. Sci. USA., 88: 727-731.

Greenblatt, R.E., Blatt, Y. and Montal, M. 1985, FEBS Lett., 193: 125-134.

Grissmer, S., Dethlefs, B., Wasmuth, J., Goldin, A.L., Gutman, G.A., Cahalan, M.D. and Chandy, K.G., 1990, Proc. Natl. Acad. Sci. USA., 87: 9411-9415.

Grupe, A., 1991, Ph. D. Thesis, Ruhr Univ., Bochum, Germany.

Gutierrez, L.M., Brawley, R.M. and Hosey, M.M., 1991, J. Biol. Chem., 266: 16387-16394.

Guy, H.R. and Seetharamulu, P., 1986, Proc. Natl. Acad. Sci. USA., 83: 508-512.

Haase, H., Striessnig, J., Holtzhauer, M., Vetter, R. and Glossmann, H., 1991, Eur. J. Pharmacol- Molecul. Pharmacol. Section, 207: 51-59.

Hagiwara, S., Kusano, K. and Siato, N., 1961, J. Physiol., 155: 470-489.

Hagiwara, S. and Naka, K., 1964, J. Gen. Physiol., 48: 141-162.

Hagiwara, S. and Nakagima, S., 1965, Science N. Y., 149: 1254-1255.

Hagiwara, S., Hayashi, H. and Takahashi, K., 1969, J. Physiol., 205: 115-129.

Hamill, O.P., Marty, A., Neher, E., Sakmann, B. and Sigworth, F.J., 1981, Pflugers Archiv., 391: 85-100.

Haris, P.I., Lee, D.C., Gabriella, S. and Chapman, D., 1987, British Biophysical Society Meeting, Cambridge, Abstract no. 4.

Haris, P.I. and Chapman, D., 1992, T.I.B.S., 17: 328-333.

Haris, P.I., Ramesh, B., Srai, K.S. and Chapman, D., 1993, Biochem. Soc. Transactions., 21: 81S.

Hartmann, H.A., Kirsch, G.E., Drewe, J.A., Taglialatela, M., Joho, R.H. and Brown, A.M., 1991, Science, 251: 942-944.

Hartshorne, R., Keller, B., Talvenheimo, J., Catterall, W.A. and Montal, M., 1985, Proc. Natl. Acad. Sci. USA., 82: 240-244.

Hayakawa, N., Morita, T., Yamaguchi, T., Mitsui, H., Mori, K.J., Saisu, H. and Abe, T., 1990, Biochem. Biophys. Res. Commun., 173: 483-490.

Heinemann, S.H., Terlau, H., Stuhmer, W, Imoto, K. and Numa, S., 1992, Nature, 356: 441-443.

Hering, S., Savchenko, A., Strubing, C., Lakitsch, M., Striessnig, J., 1993, Mol. Pharm., 43: 820-826.

Hertzberg, O. and James, M.N.G., 1985, Nature, 313: 653-659.

Hescheler, D., Pelzer, D., Trube, G. and Trautwein, W., 1982, Pflugers Archiv., 393: 287-291.

Hess, P., Lansman, J.B. and Tsien, R.W., 1984, Nature, 311: 538-544.

Hess, P., 1990, Annu. Rev. Neurosci., 13: 337-356.

Hille, B., 1984, Ionic Channels of Excitable Membranes, (Sanderland, M.A., Sinauer Associates).

Hirayama, A., Takagaki, Y. and Karush, F., 1985, J. Immunol., 134: 3241-3244.

Hirning, L.D., Fox, A.P., McCleskey, E.W., Olivera, B.M., Thayer, S.A., Miller, R.J. and Tsien, R.W., 1988, Science, 239: 57-61.

Hodgkin, A.L. and Huxley, A.F., 1952a, J. Physiol., 116: 449-472.

Hodgkin, A.L. and Huxley, A.F., 1952b, J. Physiol., 117: 500-544.

Hofmann, F., Oeken, H,J., Schneider, T. and Sieber M., 1988, J. Cardiovasc. Pharmacol., 12(Suppl.1): S25-S30.

Hopp, T.P. and Woods, K.R., 1981, Proc. Natl. Acad. Sci. USA., 78: 3824-3828.

Hopp, T.P., 1985, In "Synthetic Peptides in Biology and Medicine", eds. Alitalo, K., Partanen, P. and Vaheri, A., Elsevier Science Publishers B.V., North-Holland, 3-11.

Horne, A.L. and Kemp, J.A., 1991, Br. J. Pharmacol., 103: 1733-1739.

Horne, W.A., Abdel-Ghany, M., Racker, E., Weiland, G.A., Oswald, R.E. and Cerione, R.A., 1988, Proc. Natl. Acad. Sci. USA., 85: 3718-3722.

Hosey, M.M., Barhanin, J., Schmid, A., Vandaele, S., Ptasienski, J., O,Callahan, C., Cooper, C. and Lazdunski, M., 1987, Biochem. Biophys. Res. Commun., 147: 1137-1145.

Hosey, M. and Lazdunski, M., 1988, J. Memb. Biol., 104: 81-105.

Hoshi, T., Zagotta, W.N. and Aldrich, R.W., 1990, Science, 250: 533-538.

Hoshi, T., Zagotta, W.N. and Aldrich, R.W., 1991, Neuron, 7: 547-556.

Hui, A., Ellinor, P.T., Krizanova, O., Wang, J.-J., Diebold, R.J. and Schwartz, A., 1991, Neuron, 7: 35-44.

Hullin, R., Singer-Lahat, D., Freichel, M., Biel, M., Dascal, N., Hofmann, F. and Flockerzi, V., 1992, EMBO J., 11: 885-890.

Hwang, P.M., Glatt, C.D., Bredth, D.S., Yellen, G. and Snyder, S.H., 1992,

Neuron, 8: 473-481.

Hymel, L., Striessnig, J., Glossmann, H. and Schindler, H., 1988, Proc. Natl. Acad. Sci. USA., 85: 4290-4294.

Ikemoto, N., Antoniu, B. and Kim, D.H., 1984, J. Biol. Chem., 259: 13151-13158.

Isacoff, E.Y., Jan, Y.N. and Jan, L.Y., 1990, Nature, 345: 530-534.

Isacoff, E.Y., Jan, Y.N. and Jan, L.Y., 1991, Nature, 353: 86-90.

Itagaki, K., Koch, W.J., Bodi, I., Klockner, U., Slish. D.F. and Schwartz. A., 1992, FEBS Lett., 297: 221-225.

Iverson, L.E., Tanouye, M.A., Lester, H.A., Davidson, N. and Rudy, B., 1988, Proc. Natl. Acad. Sci. USA., 85: 5723-5727.

Jahnsen, H. and Llinas, R., 1984, J. Physiol., 349: 227-247.

Jay, S.D., Ellis, S.B., McCue, A.F., Williams, M.E., Vedvick, T.S., Harpold, M.M. and Campbell, K.P., 1990, Science, 248: 490-492.

Jay, S.D., Sharp, A.H., Kahl, S.D., Vedvick, T.S., Harpold, M.M. and Campbell, K.P., 1991, J. Biol. Chem., 266: 3287-3293.

Johnston, P.A., Jahn, R. and Sudhof, T.C., 1989, J. Biol. Chem., 264: 1268-1273.

Jones, E.L. and Gregory, J., 1989, In 'Antibodies Vol. II, a practical approach,' eds. Rickwood D. and Hanes, B.D., IRL Press, 155-177.

Jorgensen, A.O., Shen, A. C.-Y., Arnold, W., Leung, A.T and Campbell, K.P., 1989, J. Cell Biol., 109: 135-147.

Josephson, I.R., Sanchez-Chapula, J. and Brown, A.M., 1984, Circ. Res., 54: 157-162.

Kamb, A., Tseng-Crank, J. and Tanouye, M.A., 1988, Neuron, 1: 421-430.

Kanngiesser, U., Nalik, P. and Pongs, O., 1988, Proc. Natl. Acad. Sci. USA., 85: 2969-2973.

Karplus, P.A. and Schulz, G.E., 1985, Naturwissenschaften, 72: 212-213.

Kasai, H., Aosaki, T. and Fukuda, J., 1987, Neurosci. Res., 4: 228-235.

Kass, R.S., Arena, J.P. and Chin, S., 1991, J. Gen. Physiol., 98: 63-75.

Katz, B., 1969, The Release of Neurotransmitter Substances. Liverpool Univ. Press, Liverpool, U.K.

Kawai, T. and Watanabe, M., 1986, Br. J. Pharmacol., 87: 225-232.

Kayano, T., Noda, M., Flockerzi, V., Takahashi, H. and Numa, S., 1988, FEBS Letters, 228: 187-194.

Kazazoglou, T., Schackmann, R.W., Fosset, M. and Shapiro, B.M., 1985, Proc. Natl. Acad. Sci. USA., 82: 1460-1464.

Kerr, L.M. and Yoshikami, D., 1984, Nature, 308: 282-284.

Keynes, R.D., Rojas, E., Taylor, R.E. and Vergara J., 1973, J. Physiol. 229: 409-455.

Kim, K.C., Caswell, A.H., Talvenheimo, J.A. and Brandt, N.R., 1990a, Biochemistry, 29: 9281-9289.

Kim, H.S., Wei, X., Ruth, P., Perez-Reyes, E., Flockerzi, V., Hofmann, F. and Birnbaumer, L., 1990b, J. Biol. Chem., 265: 11858-11863.

Kim, H.-L., Kim, H., Lee, P., King, R.G. and Chin, H., 1992, Proc. Natl. Acad. Sci. USA., 89: 3251-3255.

Kirsch, G.E., Taglialatela, M. and Brown, A.M., 1991, Am. J. Physiol., 261: C583-C590.

Klockner, U., Itagaki, K., Bodi, I. and Schwartz, A., 1992, Pflugers Archiv., 420: 413-415.

Knaus, H.-G., Moshammer, T., Kang, H.C., Haugland, R.P. and Glossmann, H., 1992, J. Biol. Chem., 267: 2179-2189.

Koch, W.J., Ellinor, P.T. and Schwartz, A., 1990, J. Biol. Chem., 265: 17786-17791.

Kosower, E.M., 1985, FEBS Lett., 182: 234-242.

Kraner, S., Tanaka, J. and Barchi, R., 1985, J. Biol. Chem., 260: 6341-6347.

Kretsinger, R.H. and Nockolds, C.E., 1973, J. Biol. Chem., 248: 3313-3321.

Kyte, J. and Dolittle, R.F., 1982, J. Mol. Biol., 157: 105-132.

Lacerda, A.E., Kim, H.S., Ruth, P., Perez-Reyes E., Flockerzi, V., Hofmann, F., Birnbaumer, L. and Brown, A.M., 1991, Nature, 352: 527-530.

Lachmann, P.J., Strangeways, L., Vyakarnam, A. and Evan, G., 1986, Ciba Foundation Symposium, 119: 25-57.

Laemmli, U.K., 1970, Nature, 227: 680-685.

Lai, Y., Seagar, M.J., Takahashi, M. and Catterall, W.A., 1990, J. Biol. Chem., 265: 20839-20848.

Landon, D.L., 1979, In 'Skeletal Muscle Pathology', ed. Mastaglia, F.L. and Walton, J., Churchill Livingston, 1-87.

Landschulz, W.H., Johnson, P.F. and McKnight, S.L., 1988, Science, 240: 1759-1764.

Langs, D.A., Kwon, Y.W., Strong, P.D. and Triggle, D.J., 1990, J. Computer-Aided Mol. Design, 5: 95-106.

LaRochelle, W.J., Wray, B.E., Sealock, R. and Froehner, S.C., 1985, J. Cell Biol., 100: 684-691.

Lerner, R.A., 1982, Nature, 299: 592-596.

Lerner, R.A., 1984, Adv. Immunol., 36: 1-44.

Leung, A.T., Imagawa, T. and Campbell, K.P., 1987, J. Biol. Chem., 262: 7943-7946.

Leung, A.T., Imagawa, T., Block, B., Franzini-Armstrong, C. and Campbell, K.P., 1988, J. Biol. Chem., 263: 994-1001.

Liman, E.R., Hess, P., Weaver, F. and Koren, G., 1991, Nature, 353: 752-756.

Lindgren, C.A. and Moore, J.W., 1989, J. Physiol., 414: 201-222.

Lipscombe, D., Madison, D.V., Poenie, M., Reuter, H., Tsien, R.Y. and Tsien R.W., 1988, Proc. Natl. Acad. Sci. USA., 85: 2398-2402.

Llinas, R. and Sugimori, M., 1980, J. Physiol., 305: 171-195.

Llinas, R. and Yarom, Y., 1981, J. Physiol., 315: 569-584.

Llinas, R., Sugimori, M., Lin, J.-W. and Cherksey, B., 1989, Proc. Natl. Acad. Sci. USA., 86: 1689-1693.

Llinas, R.R., 1991, Ann. N.Y. Acad. Sci., 635: 3-17.

Logothetis, D,E., Movahedi, S., Satler, C., Lindpaintner, K. and Nadal-Ginard, G., 1992, Neuron, 8: 531-540.

Lowry, O.H., Rosebrough, N.J., Farr, A.L. and Randall, R.J., 1951, J. Biol. Chem., 193: 265-275.

Lopez, G.A., Jan, Y.N. and Jan, L.Y., 1991, Neuron, 7: 327-336.

Luneau, C.J., Wiedmann, R., Smith, S.J. and Williams, J.B., 1991a FEBS Lett., 288: 163-167.

Luneau, C.J., Williams, J.B., Marshall, J., Levitan, E.S., Oliva, C., Smith, J.S., Antanavage, J., Folander, K., Stein, R.B., Swanson, R., Kaczmarek, L.K. and Bushrow, S., 1991b, Proc. Natl. Acad. Sci. USA., 88: 3932-3936.

Ma, J., Mundina-Weilenmann, C., Hosey, M.M. and Rios, E., 1991, Biophys. J., 60: 890-901.

Ma, W.-J., Holz, R.W. and Uhler, M.D., 1992, J. Biol. Chem., 267: 22728-22732.

MacKinnon, R. and Miller, C., 1989, Science, 245: 1382-1385.

MacKinnon, R., Heginbotham, L. and Abramson, T., 1990, Neuron, 5: 767-771.

MacKinnon, R. and Yellen, G., 1990, Science, 250: 276-279.

MacKinnon, R., 1991a, Curr. Opin. Neurobiol., 1:14-19.

MacKinnon, R., 1991b, Nature, 350: 232-235.

Malouf, N.N., Coronado, R., McMahon, D., Meissner, G. and Gillespie, G.Y., 1987, Proc. Natl. Acad. Sci. USA., 84: 5019-5023.

Marty, A., 1981, Nature, 291: 497-500.

Marty, A. and Neher, E., 1982, J. Physiol., 326: 36P-37P.

Matterson, D.R. and Carmeliet, P., 1988, Biophys. J., 53: 641-645.

McCleskey, E.W., 1985, J. Physiol., 361: 231-249.

McCleskey, E.W., Fox, A.P., Feldman, D.H., Cruz, L.J., Olivera, B.M., Tsien, R.W. and Yoshikami, D., 1987, Proc. Natl. Acad. Sci. USA., 84: 4327-4331.

McCormack, K., Lin, J.W., Iverson, L.E. and Rudy, B., 1990a, Biochem. Biophys. Res. Commun., 171: 1361-1371.

McCormack, T., Vega-Sandez De Miera, E.C. and Rudy, B., 1990b, Proc. Natl. Acad. Sci. USA., 87:5227-5231.

McCormack, T., Tanouye, M.A., Iverson, L.E., Lin, J.-W., Tamaswami, M., McCormack, T., Pampanelle, J.T., Mathew, M.K. and Rudy, B., 1991, Proc. Natl. Acad. Sci. USA., 88: 2931-2935.

McEnery, M.W., Snowman, A.M., Sharp, A.H., Adams, M.E. and Snyder, S.H., 1991, Proc. Natl. Acad. Sci. USA., 88: 11095-11099.

Meiri, H., Spira, G., Sammar, M., Namir, M., Schwartz, A., Komoriya, A., Kosower, E.M. and Palti, Y., 1987, Proc. Natl. Acad. Sci. USA., 84: 5058-5062.

Mikami, A., Imoto, K., Tanabe, T., Niidome, T., Mori, Y., Takeshima, H., Narumiya S. and Numa, S., 1989, Nature, 340: 230-233.

Miller, C., 1990, Science, 252: 1092-1096.

Mintz, I.M., Venema, V.J., Adams, M.E. and Bean, B.P., 1991, Proc. Natl. Acad. Sci. USA., 88: 6628-6631.

Mintz., I.M., Venema, V.J., Swiderek, K.M., Lee, T.D., Bean, B.P. and Adams, M.E., 1992, Nature, 355: 827-829.

Moews, P.C. and Kretsinger, R.H., 1975, J. Mol. Biol., 91: 201-228.

Moore, G.R. and Williams, R.J.P., 1980, Eur. J. Biochem., 103: 543-550.

Moorman, J.R., Kirsch, G.E., Brown, A.M. and Joho, R.H., 1990, Science, 250: 688-691.

Mori, Y., Friedrich, T., Kim, M.S., Mikami, A., Nakai, J., Ruth, P., Bosse, E., Hofmann, F., Flockerzi, V., Furuichi, T., Mikoshiba, K., Imoto, K., Tanabe, T. and Numa, S., 1991, Nature, 350: 398-402.

Morton, M.E. and Froehner, S.C., 1987, J. Biol. Chem., 262: 11904-11907.

Morton, M.E. and Froehner, S.C., 1989, Neuron, 2: 1499-1506.

Mundina-Weilenmann, C., Chang, C.F., Gutierrez, L.M. and Hosey, M.M., 1991, J. Biol. Chem., 266: 4067-4073.

Murphy, K.M.M., Gould, R.J., Largent, B.L. and Snyder, S.H., 1983, Proc. Natl. Acad. Sci. USA., 80: 860-864.

Murphy, B.J. and Tuana, B.S., 1990, Can. J. Physiol. Pharmacol., 68: 1389-1395.

Nabauer, M., Callewaert, G., Cleemann, L. and Morad, M., 1989, Science, 244: 800-803.

Nakajima, H., Hoshiyama, M., Yamashita, K. and Kiyomoto, A., 1975, Jpn. J. Pharmacol., 25: 383-392.

Nakayama, H., Taki, M., Striessnig, J., Glossmann, I.T., Catterall, W.A. and Kanaoka, Y., 1991, Proc. Natl. Acad. Sci. USA., 88: 9203-9207.

Nakayama, H., Hatanaka, Y., Yoshida, E., Oka, K., Takanohashi, M., Amano, Y. and Kanaoka, Y., 1992a, Biochem. Biophys. Res. Commun., 184: 900-907.

Nakayama, H., Shikano, H. and Kanaoka, Y., 1992b, Biochim. Biophys. Acta., 1175: 67-72.

Nakayama, H., Nakayama, K., Nonomura, Y., Kobayashi, M., Kangawa, K., Matsuo, H. and Kanaoka, Y., 1993, Biochem. Biophys. Acta., 1145: 134-140.

Neher, E., 1971, J. Gen. Physiol., 61: 385-399.

Niidome, T., Kim, M.-S., Friedrich, T. and Mori, Y., 1992, FEBS Lett., 308: 7-13.

Niman, H.L., Houghten, R.A., Walker, L.E., Reisfeld, R.A., Wilson, I.A., Hogle, J.M. and Lerner, R.A., 1983, Proc. Natl. Acad. Sci. USA., 80: 4949-4953.

Noda, M., Shimizu, S., Tanabe, T., Takai, T., Kayano, T., Ikeda, T., Takahashi, H., Nakayama, H., Kanaoka, Y., Minamino, N., Kangawa, K., Matsu, H., Raftery, M.A., Hirose, T., Inayama, S., Hayashida, H., Miyata, T. and Numa, S., 1984, Nature, 312: 121-127.

Noda, M., Ikeda, T., Kayano, T., Suzuki, H., Takeshima, H., Kurasaki, M., Takahashi, H. and Numa, S., 1986a, Nature, 320: 188-192.

Noda, M., Ikeda, T., Suzuki, H., Takeshima, H., Takahashi, T., Kuno, M. and Numa, S., 1986b, Nature, 322: 826-828.

Noda, M., Suzuki, H., Numa, S. and Stuhmer, W., 1989, FEBS Lett., 259: 213-216.

Norman, R.I., Burgess, A.J., Allen, E. and Harrison, T.M., 1987, FEBS Lett., 212: 127-132.

Nowycky, M.C., Fox, A.P. and Tsien, R.W, 1985, Nature, 316: 440-443.

Nunoki, N., Florio, V. and Catterall, W.A., 1989, Proc. Natl. Acad. Sci. USA., 86: 6816-6820.

Ogata and Yamasaki, 1990, Anatomical Record, 228: 277-287.

Ogata, T. and Yamasaki, Y., 1991, Archives of Histology and Cytology, 54: 471-490.

Ohkusa, T., Smilowitz, H.M. and Ikemoto, N., 1990, Biophys. J., 57: 498a.

Ohkusa, T., Carlos, A.D., Kang, J.-J., Smilowitz, H. and Ikemoto, N., 1991a, Biochem. Biophys. Res. Commun., 175: 271-276.

Ohkusa, T., Kang, J.-J., Antoniu, B., Rosemblatt, M.S., Jay, S.D., Campbell, K.P. and Ikemoto, N., 1991b, Biophys J., 59: 44a.

Okamoto, H., Takahashi, K. and Yoshii, M., 1976, J. Physiol. 255: 527-561.

Olivera, B.M., McIntosh, J.M., Cruz, L.J., Luque, F.A. and Gray, W.R., 1984, Biochemistry, 23: 5087-5090.

Olivera, B.M., Gray, W.R., Zeikus, R., McIntosh, J.M., Varga, J., Rivier, J., De Santos, V. and Cruz, L.J., 1985, Science, 230: 1338-1343.

Orkand, R.K. and Niedergerke, R., 1964, Science N.Y., 146: 1176-1177.

Pak, M.D., Covarrubias, M., Ratcliffe, A. and Salkoff, L., 1991, J. Neurosci., 11: 869-880.

Palfreyman, J.W., Aitcheson, T.C. and Taylor, P., 1984, J. Immunol. Methods, 75: 383-393.

Papazian, D.M., Timpe, L.C., Jan, Y.N. and Jan, L.Y., 1991, Nature, 349: 305-310.

Pennefather, P., Lancaster, B., Adams, P.R. and Nicoll, R.A., 1985, Proc. Natl. Acad. Sci. USA., 82: 3040-3044.

Perez-Reyes, E., Kim, H. S., Lacerda, A.E., Horne, W., Wei, X., Rampe, D., Campbell, K.P., Brown, A.M. and Birnbaumer, L., 1989, Nature, 340: 233-236.

Perez-Reyes, E., Castellano, A., Kim, H.S., Bertrand, P., Baggstrom, E., Lacerda, A.E., Wei, X. and Birnbaumer, L., 1992, J. Biol. Chem., 267: 1792-1797.

Perney, T.M., Hirning, L.D., Leeman, S.E. and Miller, R.L., 1986, Proc. Natl. Acad. Sci. USA., 83: 6656-6659.

Pizarro, G., Fitts, R., Uribe, I. and Rios, E., 1989, J. Gen. Physiol., 94: 405-428.

Plummer, M.R., Logothetis, D.E. and Hess, P., 1989, Neuron, 2: 1453-1463.

Pongs, O., Kecskemethy, N., Mueller, R., Krah-Jentzens, I., Baumann, A., Kiltz, H.H., Canal,I., Llamazares, S. and Ferrus, A., 1988, EMBO. J., 7: 1087-1096.

Powers, P.A., Liu, S., Hogan, K. and Gregg, R.G., 1992, J. Biol. Chem., 267: 22967-22972.

Pragnell, M., Sakamoto, J., Jay, S.D. and Campbell, K.P., 1991, FEBS Lett., 291: 253-258.

Prentki, M. and Matschinsky, F., 1987, Physiol. Rev., 67: 1185-1248.

Pusch, M., Noda, M., Stuhmer, W., Numa, S. and Conti, F., 1991, Eur. Biophys. J., 20: 127-133.

Ratnam, M., Sargent, P.B., Sarin, V., Fox, J.L., Le Nguyen, D., Rivier, J., Criado, M. and Lindstrom, J., 1986, Biochemistry, 25: 2621-2632.

Recio-Pinto, E., Duch, D.S., Levinson, S.R. and Urban, B.W., 1987, J. Gen. Physiol., 90: 375-395.

Regan, L.J., 1991, J. Neurosci., 11: 2259-2260.

Regan, L.J., Sah, D.W. and Bean, B.P., 1991, Neuron, 6: 259-280.

Regulla, S., Schneider, T., Nastainczyk, W., Meyer, H.E. and Hymann, F., 1991, EMBO J., 10: 45-49.

Rettig, J., Wunder, F., Stocker, M., Lichting-Hagen, R., Mstiaux, F., Beckh, S., Kues, W., Pedarzani, P., Schroter, K.H., Ruppersberg, J.P., Veh, R. and Pongs, O., 1992, EMBO J., 11: 2473-2486.

Reuter, H., 1968, J. Physiol., 197: 233-253.

Reuter, H. and Scholz, H., 1977, J. Physiol. 264: 17-47.

Reuter, H., Porzig, H. and Kokubun, S., 1985, Trends in Neuro..???. Sci., 8: 396-400.

Reynolds, I.J., Wagner, J.A., Snyder, S.H., Thayer, S.A., Olivera, B.M. and Miller, R.J., 1986, Proc. Natl. Acad. Sci. USA., 83: 8804-8807.

Rios, E. and Brum, G., 1987, Nature, 325: 717-720.

Rios, E. and Pizarro, G., 1991, Physiol. Rev., 71: 849-908.

Rivet, M., Cognard, C., Imbert, N., Rideau, Y., Duport, G. and Raymond, G., 1992, Neurosci. Lett., 138: 97-102.

Rivier, J., Gayiean, R., Gray, W.R., Azimi-Zonooz, A., McIntosh, M., Cruz, L. and Olivera, B.M., 1987, J. Biol. Chem., 262: 1194-1198.

Roberds, S.L. and Tamkum, M.M., 1991, Proc. Natl. Acad. Sci. USA., 88: 1798-1802.

Rojas, E. and Keynes, R.D., 1975, Phil. Trans. of the Royal Soc. of London, Series B. (Biol. Sci.), 270: 459-482.

Rojas, E. and Rudy, B., 1976, Lolijo J. Physiol., 262: 501-531.

Romey, G., Garcia, L., Rieger, F. and Lazdunski, M., 1988, Biochem. Biophys Res. Commun., 156: 1324-1332.

Rosemblatt, N., Hidalgo, C., Verago, C. and Ikemoto, N., 1981, J. Biol. Chem., 256: 8140-8148.

Rosenberg, R., Isaacson, J. and Tsien, R., 1989, Annals New York Acad. Sci., 560: 39-52.

Rossie, S., Gordon, D. and Catterall, W. A., 1987, J. Biol. Chem., 262: 17530-17535.

Rossie, S. and Catterall, W.A., 1987, J. Biol. Chem., 262: 12735-12744.

Rossie, S. and Catterall, W.A., 1989, J. Biol. Chem., 264: 14220-14224.

Rossier, J.R., Cox, J.A., Niesor, E.J. and Bentzen, C.L., 1989, J. Biol. Chem., 264: 16598-16607.

Ruppersberg, J.P., Schroter, K.H., Sakmann, B., Stocker, M. Sewing, S., Pongs, O., 1990, Nature, 345: 535-537.

Ruth, P., Rohrkasten, A., Biel, M., Bosse, E., Regulla, S., Meyer, H.E., Flockerzi, V. and Hofmann, F., 1989, Science, 245: 1115-1118.

Sakamoto, J. and Campbell, K.P., 1991a, Physiologist, 34: 109 (abstr.)

Sakamoto, J. and Campbell, K.P., 1991b, J. Biol. Chem., 266: 18914-18919.

Sakmann, B. and Neher, E., 1984, Annu. Rev. Physiol., 46: 455-472.

Sanchez, J.A. and Stefani, E., 1978, J. Physiol. 283: 197-209.

Sanguinetti, M.C. and Jurkiewicz, N.K., 1990, J. Gen. Physiol., 96: 195-215.

Sanguinetti, M.C. and Kass, R.S., 1984, Circ. Res., 55: 336-348.

Sato, C. and Matsumoto, G., 1992, Biochem. Biophys Res. Commun., 186: 1158-1167.

Schagger, H. and Von Jagow, G., 1987, Anal. Biochem., 166: 368-379.

Schmid, A., Barhanin, J., Coppola, T., Borsotto, M. and Lazdunski, M., 1986a, Biochemistry, 25: 3492-3495.

Schmid, A., Barhanin, J., Mourre, C., Coppola, T., Borsotto, M. and Lazdunski, M., 1986b, Biochem. Biophys. Res. Commun., 139: 996-1002.

Schneider, T. and Hofmann, F., 1988, Eur. J. Biochem., 174: 369-375.

Schneider, T., Regulla, S. and Hofmann, F., 1991, Eur. J. Biochem., 200: 245-253.

Schoemaker, H., Hicks, P.E. and Langer, S.Z., 1987, J. Cardiovasc. Pharmacol., 9: 173-180.

Schoemaker, H. and Langer, S.Z., 1989, J. Pharmacol. Exper. Therapeutics, 248: 710-715.

Schroter, K.-H., Ruppersberg, J.P., Wunder, F., Rettig, J., Stocker, M. and Pongs, O., 1991, FEBS Lett., 278: 211-216.

Schwartz, L.M., McCleskey, E.W. and Almers, W., 1985, Nature, 314: 747-751.

Schwarz, T.L., Tempel, B.L., Papazian, D.M., Jan Y.N. and Jan, L.Y., 1988, Nature, 331: 137-142.

Seckler, R., Wright, J.K. and Overath, P., 1983, J. Biol. Chem., 258: 10817-10820.

Seckler, R., Moroy, T., Wright, J.K. and Overath, P., 1986, Biochemistry, 25: 2403-2409.

Seino, S., Chen, L., Seino, M., Blondel, O., Takeda, J., Johnson, J.H. and Bell, G.I., 1992, Proc. Nalt. Acad. Sci. USA., 89: 584-588.

Sharp, A.H., Imagawa, T., Leung, A.T. and Campbell, K.P., 1987, J. Biol. Chem., 262: 12309-12315.

Sharp, A.H. and Campbell, K.P., 1989, J. Biol. Chem., 264: 2816-2825.

Sheng, M., Liao, Y.J., Jan, Y.N. and Jan, L.Y., 1993, Nature, 365: 72-75.

Singer, D., Biel, M., Lotan, I., Flockerzi, V., Hofmann, F. and Dascal, N., 1991, Science, 253: 1553-1557.

Smith, J.S., McKenna, E.J., Ma, J., Vilven, J., Vaghy, P.L., Schwartz, A. and Coronado, R., 1987, Biochemistry, 26: 7182-7188.

Snutch, T.P., Leonard, J.P., Gilbert, M.M., Lester, H.A. and Davidson, N., 1990, Proc. Natl. Acad. Sci. USA., 87: 3391-3395.

Snutch, T.P., Tomlinson, W.J., Leonard, J.P. and Gilbert, M.M., 1991, Neuron, 7: 45-59.

Sonda, M., Moriya, H. and Shimada, Y., 1993, Microscopy Res. Tech., 24: 423-428.

Soong, T.W., Stea, A., Hodson, C.D., Dubel, S.J., Vincent, S.R. and Snutch, T.P., 1993, Science, 260: 1133-1136.

Starr, T.V.B., Prystay, W. and Snutch, T.P., 1991, Proc. Natl. Acad. Sci. USA., 88: 5621-5625.

Staudinger, R., Knaus, H.-G. and Glossmann, H., 1991, J. Biol. Chem., 266: 10787-10795.

Steck, T.L. and Yu, J. 1973, J. Supramolecular Structure, 1: 220-232.

Stefani, E. and Uchitel, O.D., 1976, J. Physiol. 255: 435-448.
Stevens, V.C., Chou, W-S., Powell, J.E., Lee, A.C. and Smoot, J., 1986, Immunol. Lett., 12: 11-15.

Striessnig, J., Moosburger, K., Goll, A., Ferry, D.R. and Glossmann, H., 1986, Eur. J. Biochem., 261: 603-609.

Striessnig, J., Knaus, H.G., Grabner, M., Mossburger, K., Seitz, W., Lietz, H. and Glossmann, H., 1987, FEBS Lett., 212: 247-253.

Striessnig, J., Knaus, H.G., and Glossmann, H., 1988, Biochem. J., 253: 39-47.

Striessnig, J., Scheffauer, F., Mitterdorfer, J., Schirmer, M. and Glossmann, H., 1990a, J. Biol. Chem., 265: 363-370.

Striessnig, J., Glossmann, H. and Catterall, W.A., 1990b, Proc. Natl. Acad. Sci. USA., 87: 9108-9112.

Striessnig, J., Murphy, B.J. and Catterall, W.A., 1991, Proc. Natl. Acad. Sci. USA., 88: 10769-10773.

Stuhmer, W., Stocker, M., Sakmann, B., Seeburg, P., Baumann, A., Grupe, A. and Pongs, O., 1988, FEBS Lett., 242: 199-206.

Stuhmer, W., Ruppersberg, J.P., Schroter, K.H., Sakmann, B., Stocker, M., Giese, K.P., Perschke, A., Baumann, A. and Pongs, O., 1989, EMBO J., 8: 3235-3244.

Sugimori, M. amd Llinas, R., 1987, Soc. Neurosci. Abstr., 13.

Suzuki, H., Beckh, S., Kubo, H., Yahagi, N., Ishida, H., Kayano, T., Noda, M. and Numa, S., 1988, FEBS Lett., 228: 195-200.

Swandulla, D. and Armstrong, C.M., 1988, J. Gen. Physiol., 92: 197-218.

Taglialatela, M., VanDongen, A.M.J., Drewe, J.A., Joho, R.H., Brown, A.M., Kirsch, G.E., 1992, Mol. Pharm., 40: 299-307.

Tainer, J.A., Getzoff, E.D., Alexander, H., Houghten, R.A., Olson, A.J. and Lerner, R.A., 1984, Nature, 312: 127-134.

Tainer, J.A., Getzoff, E.D., Paterson, Y., Olson, A.J. and Lerner, R.A., 1985, Annu. Rev. Immunol., 3: 501-535.

Takahashi, M., Seagar, M.J., Jones, J.F., Reber, B.F. and Catterall, W.A., 1987, Proc. Natl. Acad. Sci., 84: 5478-5482.

Takahashi, M. and Catterall, W.A., 1987a, Biochem., 26: 5518-5526.

Takahashi, M. and Catterall, W.A., 1987b, Science, 236: 88-91.

Talvenheimo, J.A., Worley, J.F. and Nelson, M.T., 1987, Biophys. J., 52: 891-899.

Tamkun, M., Talvenheimo, J. and Catterall, W.A., 1984, J. Biol. Chem., 259: 1676-1688.

Tanabe, T., Takeshima, H., Mikami, A., Flockerzi, V., Takahashi, H., Kangawa, K., Kojima, M., Matsuo, H., Hirose, T. and Numa, S., 1987, Nature, 328: 313-318.

Tanabe, T., Beam, K.G., Powell, J.A. and Numa, S., 1988, Nature, 336: 134-139.

Tanabe, T., Mikami, A., Numa, S. and Beam, K.G., 1990a, Nature, 344: 451-453.

Tanabe, T., Beam, K.G., Adams, B.A., Niidome, T. and Numa, S., 1990b, Nature, 346: 567-569.

Tejedor, F.J. and Caterall, W.A., 1988, Proc. Natl. Acad. Sci. USA., 85: 8742-8746.

Tempel, B.L., Papazian, D.M., Schwarz, T.L., Jan, Y.N. and Jan, L.Y., 1987, Science, 237: 770-775.

Terlau, H., Heinemann, S.H., Stuhmer, W., Pusch, M., Conti, F., Imoto, K. and Numa, S., 1991, FEBS Letters, 293: 93-96.

Thomsen, W. and Catterall, W.A., 1989, Proc. Natl. Acad. Sci. USA., 86: 10161-10165.

Tidball, J.G., Cederdahl, J.E., Bers, D.M., 1991, Cell Tissue Research, 264: 293-298.

Timpe, L.C., Schwarz, T.L., Tempel, B.L., Papazian, D.M., Jan, Y.N. and Jan, L.Y., 1988a, Nature, 331: 143-145.

Timpe, L.C., Jan, Y.N. and Jan, L.Y., 1988b, Neuron, 1: 659-667.

Tokumaru, H., Anzai, K., Abe, T. and Kirino, Y., 1992, Eur. J. Pharmacol. (Mol. Pharmacol. Section), 227: 363-370.

Trewhella, J., Liddle, W.K., Heidorn, D.B. and Strynadka, N., 1989, Biochem., 28: 1294-1301.

Trimmer, J.S., Cooperman, S.S., Tomiko, S.A., Zhou, J.Y., Crean, S.M., Boyle, M.B., Kallen, R., Sheng, Z., Barchi, R.L., Sigworth, F.J., Goodman, R.H., Agnew, W.S. and Mandel, G., 1989, Neuron, 3: 33-49.

Tscharner, V. von., Prod'hom, B., Baggiolini, M. and Reuter, H., 1986, Nature, 324: 369-372.

Tsien, R.W., Lipscombe, D., Madison, D.V., Bley, K.R. and Fox, A.P., 1988, T.I.N.S., 11: 431-438.

Tsien, R.W. and Tsien, R.Y., 1990, Ann. Rev. Cell Biol., 6: 715-760.

Tufty, R.M. and Kretsinger, R.H., Science, 1975, 187: 167-169.

Turner, T.J. and Goldin, S.M., 1989, Biochemistry, 28: 586-593.

Turner, T.J., Adams, M.E. and Dunlap, K., 1992, Science, 258: 310-313.

Uchitel, O.D., Protti, D.A., Sanchez, V., Cherksey, B.D., Sugimori, M. and Llinas, R., 1992, Proc Natl. Acad. Sci. USA., 89: 3330-3333.

Umbach, J.A. and Gundersen, C.B., 1987, Proc Natl. Acad. Sci. USA., 84: 5464-5468.

Vaghy, P.L., Striessnig, J., Miwa, K., Knaus, H.-G., Itagaki, K., McKenna, E., Glossmann, H. and Schwartz, A., 1987, J. Biol. Chem., 262: 14337-14342.

Vaghy, P.L., McKenna, E., Itagaki, K. and Schwartz, A., 1988, T.I.P.S., 9: 398-402.

Vandaele, S., Fosset, M., Galizzi, J.-P. and Lazdunski, M., 1987, Biochemistry, 26: 5-9.

VanDongen, A.M.J., Frech, G.C., Drewe, J.A., Joho, R.H. and Brown, A.M., 1990, Neuron, 5: 433-443.

Varadi, G., Lory, P., Schultz, D., Varadi, M. and Schwartz, A., 1991, Nature, 352: 159-162.

Vassilev, P.M., Scheuer, T. and Catterall, W.A., 1988, Science, 241: 1658-1661.

Vassilev, P.M., Scheuer, T. and Catterall, W.A., 1989, Proc Natl. Acad. Sci. USA., 86: 8147-8151.

Vassort, G., Rougier, O., Garnier, D., Sauviat, M.P., Coraboeuf, E. and Gargouil, Y.M., 1969, Pflug. Arch., 309: 70-81.

Venema, V.J., Swiderek, K.M., Lee, T.D., Hathaway, G.M. and Adams, M.E., 1992, J. Biol. Chem., 267: 2610-2616.

Wagenknecht, T., Grassucci, R., Frank, J., Saito,A., Inui, M. and Fleischer, S., 1989, Nature, 338: 167-170.

Walter, G., 1986, J Immunological Methods, 88: 149-161.

Wang, H.-Y., Lipfert, L., Malbon, G.C. and Bahouth, S., 1989, J. Biol. Chem., 264: 14424-14431.

Wang, H., Kunkel, D.D., Martin, T.M., Schwartzkroin, P.A. and Tempel, B.L., 1993, Mature, 365: 75-79.

Wei, A., Covarrubias,M., Butler, A., Baker, K., Pak, M. and Salkoff, L., 1990, Science, 248: 599-603.

Wei, X.Y., Perez-Reyes, E., Lacerda, A.E., Schuster, G., Brown, A.M. and Birnbaumer, L., 1991, J. Biol. Chem., 266: 21943-21947.

West, J.W., Numann, R., Murphy, B.J., Scheuer, T. and Catterall, W.A., 1991, Science, 254: 866-868.

Westhof, E., Altschuh, D., Moras, D., Bloomer, A.C., Mondragon, A., Klug, A. and Van Regenmortel, M.H.V., 1984, Nature, 311: 123-126.

White, R.G., 1976, Ann. Rev. Microbiol., 30: 579-600.

Wibo, M., Bravo, G. and Godfraind, T., 1991, Circ. Res., 68: 662-673.

Williams, M.E., Feldman, D.H., Mc Cue, A.F., Brenner, R., Velicelebi, G., Ellis, S.B. and Harpold, M.M., 1992a, Neuron, 8: 71-84.

Williams, M.E., Brust, P.F., Feldman, D.H., Patthi, S., Simerson, S., Maroufi, A., Mc Cue, A.F., Velicelebi, G., Ellis, S.B. and Harpold, M.M., 1992b, Science, 257: 389-395.

Williams, R.J.P. and Moore, G.R., 1985, Trends Biochem. Sci., 10: 96-97.

Wilson, G.G., 1991, Ph.D., University of Leeds, Leeds, U.K.

Wong, B.S., Lecar, H. and Adler, M., 1982, Biophys. J., 39: 313-317.

Wright, P.E., Dyson, H.J. and Lerner, R.A., 1988, Biochemistry, 27: 7167-7175.

Yaney, G.C., Wheeler, M.B., Wei, X.Y., Perez-Reyes, E., Birnbaumer, L., Boyd, A.E. and Moss, L.G., 1992, Molecular Endocrinology, 6: 2143-2152.

Yellen, G., Jurman, M.E., Abramson, T. and MacKinnon, R., 1991, Science, 251: 939-942.

Yokoyama, S., Imoto, K., Kawamura, T., Higashida, H., Iwabe, N., Miyata, T. and Numa, S., 1989, FEBS Lett., 259: 37-42.

Yool, A.J. and Schwartz, T.L., 1991, Nature, 349: 700-704.

Yoshida, A., Takahashi, M., Fujimoto, Y., Takisawa, H. and Nakamura, T., 1990, J. Biochem., 107: 608-612.

Yoshida, A., Takahashi, M., Nishimura, S., Takeshima, H. and Kokubun, S., 1992, FEBS Lett., 309: 343-349.

Yuan, S., Arnold, W. and Jorgensen, A.O., 1990, J. Cell. Biol., 110: 1187-1198.

Zagotta, W.N., Brainard, M.S. and Aldrich, R.W., 1988, J.Neuroscience, 8: 4765-4779.

Zagotta, W.N., Hoshi, T. and Aldrich, R.W., 1990, Science, 250: 568-571.

Zagotta, W.N., Hoshi, T. and Aldrich, R.W., 1991, Biophys. J. 59: 2a.